



DECEMBER 8TH 2022 – AACHEN

POWERSKIN CONFERENCE

PROCEEDINGS

DECEMBER 8TH 2022 – AACHEN
POWERSKIN CONFERENCE

Editors

Thomas Auer, TUM
Ulrich Knaack, TU Delft
Jens Schneider, TU Darmstadt
Linda Hildebrand, RWTH Aachen
Daniele Santucci, RWTH Aachen

Editorial office

Uta Stettner, TUM
Bilge Kobas, TUM
Laura Franke, TUM

Layout & typesetting

Usch Engelmann

Cover image

Photo by Laura Franke

Print

Druckzentrum Neumünster

Contents

CONFERENCE HOSTS

SCIENTIFIC COMMITTEE

KEYNOTES

PART 1 // ENERGY

- 013 **The Potential of Static and Thermochromic Window Films for Energy Efficient Building Renovations**
A.J.J. Kragt, E.R. van den Ham, H. Sentjens, A.P.H.J. Schenning, T. Klein
- 015 **Determining the Infiltration and Exfiltration in Super-Tall and Mega-Tall Buildings**
Peter Simmonds, Duncan Phillips
- 027 **FACA-DE-LIT: Façade Optimisation for Visual Comfort by Controlled Daylight Distribution in High-Rise Office Buildings**
Akash Changlani, Michela Turin, Alejandro Prieto Hoces
- 043 **Photovoltaics Potential for Façade Renovations**
Eleonora Nicoletti
- 053 **Suntex: Weaving Solar Energy – Into the Building Skin**
Pauline van Dongen, Ellen Britton, Anna Wetzels, Rogier Houtman, Ahmed Mohamed Ahmed, Stephanie Ramos
- 055 **The “Invisible-Solar-Panel” – Coloured Photovoltaic Panels with High Efficiency**
Christof Erban

PART 2 // ENVELOPE

- 073 **Visions for a Paradigm Shift – Based on AM for Façade Application**
Holger Strauß
- 083 **CoolSkin**
Andreas Greiner, Olaf Böckmann, Simon Weber, Martin Ostermann, Micha Schaefer
- 085 **Renovating Modern Heritage – The Upgraded Façade of Commerzbank Düsseldorf**
Rouven S. Grom, Andreas W. Putz

- 087 **Active, Passive and Cyber-Physical Adaptive Façade Strategies: a Comparative Analysis Through Case Studies**
Jens Böke, Paul-Rouven Denz, Natchai Suwannapruk, Puttakhun Vongsingha
- 089 **Scrolling Screen: A Responsive Building Envelope for Energetic Adaptations**
Erik Hegre, Angie Müller-Puch, Randa Omar, David Horvarth, Ryan Maruyama, Avril Te
- 103 **Adobe Cavity Wall Envelopes with High Thermal Performance: the Middle-Eastern Scenario**
Claudio Marini, Alessandro D'Ambrosio, Erolcan Erdogan
- 119 **6dTEX – Lightweight Building Components made of 3D Textiles in Combination with 3D Printing**
Claudia Lüling, Sascha Biehl, Roxana Tennert, Gözdem Dittel, Marina Chernyshova, Thomas Gries
- 135 **Interactive Façade Impact Tool for Evolutional Trade-off Analysis**
Xiaofei Shen, Aman Singhvi, Nick Novelli, PHD, Maria Aiolova, Kieran Rice, Jason Vollen
- 153 **Generative Design as a Technique for Creating Energy-Efficient Building Envelopes**
Venus Kashyap, Bhavya Jain
- 171 **Adaptive Building Skins Inspired by Lizards in the Hot Desert Climate of Egypt**
Mina Ishac
- 191 **Influence of Automated Façades on Occupants: A Review**
Pedro de la Barra, Alessandra Luna-Navarro, Ulrick Knaack, Claudio Vásquez, Alejandro Prieto
- PART 3 // ENVIRONMENT**
- 195 **Digital Imperfection**
Christian Schmitt, Federico Garrido, Rodrigo Brum
- 205 **Establishing Benchmarks for Low-Carbon, Circular Façade Design on Refurbishment Projects**
Laura Craft, Christina Koukelli, Melissa Tanuharja
- 235 **Additively Manufactured Urban Multispecies Façades for Building Renovation**
Iuliia Larikova, Julia Fleckenstein, Ata Chokhachian, Thomas Auer, Wolfgang Weisser, Kathrin Dörfler
- 237 **Timber-Based Façades with Different Connections and Claddings: Assessing Materials' Reusability, Water Use and Global Warming Potential**
Miren Juaristi Gutierrez
- 239 **Mapping and Evaluating External Wall Material Stock in Terms of Circularity: a Case Study in Istanbul**
Sühan Artuğ

251 **Retrospective Façade LCA: Lessons Learned from a Newly Completed Case Study**

Montemayor Javier, Li Florence, McGilveray Hugh

269 **Retrofitting Potential of Building Envelopes Based on Semantic Surface Models Derived From Point Clouds**

Edina Selimovic, Florian Noichl, Kasimir Forth, André Borrmann

PREFACE

Environmental aspects have shaped façades in various ways over the last decades. The decreased demand for operational energy and the growing share of renewable energy lowered the amount of greenhouse gas emissions during this phase. Based on this improvement, the building fabric becomes the relevant parameter with environmental potential to unlock. Buildings in stock store energy and greenhouse gas emissions linked to their production and can provide spatial quality with low environmental impact. Keeping the buildings as an active part of the built environment requires technical solutions as well as adaption in the design and fabrication process. PowerSKIN 2022, titled “Build in stock – renovation strategies: inorganic, circular materials vs organic, compostable materials”, presents different approaches grouped into the themes “Energy”, “Envelope”, and “Environment”. As an international scientific event, the PowerSKIN Conference builds a bridge between science and practice, between research and construction, and between the latest developments and innovations for the façade of the future.

The Technical University of Munich, Prof. Dipl.-Ing. Thomas Auer, TU Darmstadt, Prof. Dr.-Ing. Jens Schneider and TU Delft, Prof. Dr.-Ing. Ulrich Knaack, are hosting the PowerSKIN Conference this year together with the local hosts from RWTH Aachen, Prof. Dr.-Ing. Linda Hildebrand and Prof. Dr.-Ing. Daniele Santucci. It is the fourth event of a biennial series. Architects, engineers, and scientists present their latest developments and research projects for public discussion and reflection. The conference will be held in person and be virtually accessible.

Thomas Auer,
Ulrich Knaack,
Jens Schneider,
Linda Hildebrand,
Daniele Santucci

the conference hosts.

CONFERENCE HOSTS



Prof. Dipl.-Ing. Thomas Auer

Trained as a Process Engineer at the Technical University in Stuttgart, Thomas is a partner and managing director of Transsolar GmbH, a German engineering firm specialized in energy efficient building design and environmental quality with offices in Stuttgart, Munich, Paris and New York. In January of 2014 Thomas became Professor for building technology and climate responsive design at TUM. Thomas collaborated with world known architecture firms on numerous international design projects and competitions. A specialist in the fields of integrated building systems and energy efficiency in buildings as well as sustainable urban design, Thomas has developed concepts for projects around the world noted for their innovative design and energy performance – an integral part of signature architecture. The office tower for Manitoba Hydro in downtown Winnipeg, Canada, is considered one of the most energy efficient high-rise buildings in North America. Outside of Transsolar, Thomas taught at Yale University and was a visiting professor at the ESA in Paris and other Universities. He speaks frequently at conferences and symposia. In 2010 Thomas received the Treehugger “best of green” award as “best engineer”.



Prof. Dr.-Ing. Ulrich Knaack

Ulrich was trained as an architect at the RWTH Aachen University, Germany. After earning his degree he worked at the university as a researcher in the field of structural use of glass and completed his studies with a PhD. In his professional career Ulrich worked as an architect and general planner in Düsseldorf, Germany, succeeding in national and international competitions. His projects include high-rise and office buildings, commercial buildings and stadiums. In his academic career Ulrich was professor for Design and Construction at the Hochschule OWL, Germany. He also was and still is appointed professor for Design of Construction at the Delft University of Technology / Faculty of Architecture, Netherlands, where he developed the Façade Research Group. In parallel Ulrich is professor for Façade Technology at the TU Darmstadt / Faculty of Civil engineering in Germany where he participates in the Institute of Structural Mechanics + Design. Ulrich organises interdisciplinary design workshops and symposiums in the field of façades and is author of several well-known reference books, articles and lectures.



Prof. Dr.-Ing. Jens Schneider

Jens is a full professor for structural engineering at the Institute of Structural Mechanics and Design, TU Darmstadt, Germany. After his studies in civil engineering in Darmstadt and Coimbra, Portugal, Jens received his PhD from TU Darmstadt in 2001 in a topic about structural glass design and impact loading. From 2001-2005, Jens worked at the engineering office Schlaich, Bergemann and Partner where he was involved in the structural design of complex steel, glass and concrete structures. In 2006, Jens was appointed as an authorized sworn expert on glass structures, in 2007 to the position of a professor for structural engineering in Frankfurt. and in 2009 to his current position at TU Darmstadt, where Jens is currently Vice President for Transfer and International Affairs. Since 2011, Jens is also partner in his engineering office SGS GmbH in Heusenstamm in Frankfurt, Germany. Since 2015, he leads the European project group for the preparation of the new Eurocode 11 „Structural Glass“. From October 2023, he will serve as the new rector of TU Wien in Vienna, Austria. Jens is specialized in structural mechanics of glass & polymers, façade structures, structural design and synergetic, energy-efficient design of façades and buildings.

CONFERENCE HOSTS (CONT.)



Prof. Dr.-Ing. Linda Hildebrand

Linda studied Architecture at the Detmolder School for Architecture and Interior Design. After graduating, she started working on Green Building Certificates and became a self-employed consultant for environmental aspects in architectural design at c u b e, circularity in the built environment. She was a researcher and teacher at the Detmolder School and TU Delft, where she wrote her PhD thesis on Embodied energy in architecture. She was assigned as Junior professor for Reuse in Architecture 2014 at RWTH Aachen and co-founded the Start-up Concular, a platform for digital services to facilitate circularity in the built environment in 2020. Due to different visiting professorships, such as at the University of California Los Angeles or the University of Mitrovica, she gained insight into different international approaches and strategies for sustainability. Linda's work is focused on the reciprocal interchange between research and application, reflected in her projects at the university as well as in her practice. Clients are architects and engineering companies as well as tech companies, the building industry and communities. She is an expert on the sustainability of buildings and building materials, specialising in resources throughout a building's life cycle. Publications include scientific articles, literature for students and architecture books. .



Prof. Dr.-Ing. Daniele Santucci

Daniele is a scientist, educator, and entrepreneur. He is deputy head of the Chair for Building Technology at RWTH Aachen University and managing director at Climateflux, a company that consults architecture firms, public institutions, and private companies on strategies and design solutions to increase public health. His professional expertise is in environmental engineering, low-carbon design, and computational transscalar workflows targeted to achieve carbon neutrality in the built environment.

KEYNOTE SPEAKERS



Caro van de Venne

Caro van de Venne is partner and co-founder of Barcode Architects. Her strength lies in combining progressive designs with her specific knowledge and experience in leading complex, multidisciplinary projects, in which specialists, clients, and users are involved in the design process.

As partner architect, Caro is responsible for, among other things, the design of the iconic residential tower The Muse and the adjacent triangular tower CasaNova, together forming an ensemble in the Rotterdam Wijnhaven; the master plan and three educational buildings for the new Fontys University of Applied Sciences campus in Eindhoven; the urban plan for the new Utrecht Science Park; and the design for a new Matrix Innovation Center at the Zuidas focusing on med-tech and life sciences.

Caro is also a supervisor for the Sloterdijk I Zuid transformation project in Amsterdam, a board member of the Stichting Hoogbouw (high-rise foundation), and a member of the Commissie Welstand en Monumenten (aesthetics and monuments committee) of the municipality of Utrecht. She was a visiting professor at the Delft University of Technology, the Eindhoven University of Technology, the Academy of Architecture in Amsterdam, and Fontys University of Applied Sciences in Tilburg.

Caro studied at the Technical University Eindhoven and the Technische Universität Berlin. Before her partnership at Barcode Architects, she worked for Herzog & de Meuron in Basel and Foster + Partners in London.



Ingemar Vollenweider

Ingemar Vollenweider studied at the ETH Zurich and at Columbia University in New York. He then worked for Kollhoff & Timmermann in Berlin. In 1999, he founded the architecture firm jessenvollenweider in Basel together with Anna Jessen. 2006-2018 he was professor for urban architecture and design at the TU Kaiserslautern. Since 2018, together with Anna Jessen, he has headed the Chair of Urban Design at TU Dortmund University.

The firm jessenvollenweider has distinguished itself in dealing with challenging urban situations as well as with new buildings and extensions of existing buildings and ensembles. The projects realized are almost always based on winning competitions for public buildings as well as for residential and commercial buildings, such as the extension of the Lange & Söhne watch factory in Glashütte near Dresden or the expansion of the headquarters of the Zürcher Kantonalbank on Bahnhofstrasse in Zurich. Most recently, jessenvollenweider won the Swiss Steel Construction Award 2021 with the extension of the Auen school complex in Frauenfeld. In addition to regular jury activities, Ingemar Vollenweider is currently a member of the Building Committee of the City of Zurich.



Jaap Wiedenhoff

Jaap Wiedenhoff started his career as an MEP engineer. He distinguished himself by a thorough open-minded first principles approach. This rapidly evolved leading large multi-disciplinary design teams on complex projects across the world with some of the most renowned architects of our time. Today, his passion is still finding elegant solutions for complex issues, both for business and design. His understanding of human needs, physics and appreciation for nature has helped shape some of the most healthy, comfortable and sustainable buildings and built environments. His ultimate driver has been and still is the simple question asked to him 20 years ago by Alvaro Siza, 'What is wrong with the indoor environment in buildings. Why cannot they simply feel like a fresh, pleasant spring forest?'

Today he leads the engineering design of the new Terminal for Schiphol with KAAAN, the Museum for Contemporary Art Amsterdam with Rem Koolhaas (OMA) as well as the Oosterhoff group innovation center. The innovation center develops tools and strategies to deal with the challenges of energy transition, climate change and adaptation and material shortages on a building, district and infrastructural level. After nearly 30 years of enjoying doing having fun doing this, he now realizes that we need more than just some exemplary projects to be able to stay happy and healthy in a sustainable built environment; we need a mind shift.

PART 1 // ENERGY

The Potential of Static and Thermochromic Window Films for Energy Efficient Building Renovations



A.J.J. Kragt ^{1,2*}, **E.R. van den Ham** ¹, **H. Sentjens** ³, **A.P.H.J. Schenning** ³, **T. Klein** ¹

* Corresponding author, a.j.j.kragt@tudelft.nl

¹ Delft University of Technology, Netherlands

² ClimAd Technology

³ Eindhoven University of Technology, Netherlands

Abstract

The type of glazing implemented in a building plays an important role in the heat management of a building. Solar heat entering through glazing causes overheating of interior spaces and increases building's cooling load. In this work, the energy saving potential of window films based on Cholesteric Liquid Crystals (CLC) is explored. This emerging technology allows for the fabrication of static and thermochromic solar heat rejecting window films and can provide a simple renovation solution towards energy efficient buildings. Simulations on a model office showed that static CLC-based window films can save up to 29% on a building's annual energy use in warm climates. In climates with distinct summer and winter seasons, static solar heat rejecting windows films cause an additional heating demand during winters, which reduces the annual energy savings. In these climates, the benefit of thermochromic CLC-based window films becomes evident and an annual energy saving up to 22% can be achieved.

Keywords

Glazing, solar heat rejection, window films, thermochromic, energy savings

DOI [10.47982/jfde.2022.powerskin.3](https://doi.org/10.47982/jfde.2022.powerskin.3)

Determining the Infiltration and Exfiltration in Super-Tall and Mega-Tall Buildings

Peter Simmonds¹, PhD, Fellow Life Member ASHRAE, FIBPSA, Duncan Phillips², PhD, MASHRAE

* Corresponding author

1 Building and Systems Analytics, Los Angeles and Bergen, the Netherlands

2 RWDI, Guelph, Ontario, Canada N1G 4P6

Abstract

Most traditional heating and cooling load calculations are based on weather conditions measured at a height of 10 m. But how appropriate is this in super-tall buildings 300m+ and mega-tall buildings 600m+? This paper will present some specifics of evaluating building designs and performance in tall buildings.

Previous designs and research show that outdoor conditions vary with height. And the outside climate can have both a positive and a negative effect on the space conditions within the building. This paper illustrates the fluctuation of pressure differentials on the heating and cooling loads of spaces across the height of the building.

Rarely does the design of the upper level of the building capitalize on this phenomenon. Furthermore, wind, temperature, and pressure conditions at the top of a tall building are considerably different; therefore, façade leakage rates and the buildings stack effect must be carefully assessed. This difference can be incorporated to optimize the overall building design if sufficient data is known.

This novel paper explores the nuances of the ambient climate on tall buildings and the effects on the performance of the building.

Keywords

Mega-tall buildings, stack effect, energy consumption

1 INTRODUCTION

Stack effect is a phenomenon that causes challenges in tall building design and subsequent operation. Temperature and air density differences between the indoors and outdoors cause stack effect driven pressure differences that drive airflows through the building envelope. The pressure differences are created because the air density inside the building is less than that outside. This results in the weight of the column of air inside being lighter than that outside in winter months. The weight difference results in inward flow at lower levels in winter and outward flow out at the top. Somewhere up the height of the building, the inward flow transitions to being outward. This transition is typically where the indoor-outdoor pressure difference is zero. During cooling months (for example, the summer), the pressure differences are typically less as the temperature difference is not as severe as during winter conditions. This results in a lower pressure differential between the shaft and the outside compared to those under winter temperature differences.

2 BACKGROUND INFORMATION

In most tall buildings, there are shafts/risers that run from top to bottom in the building. The floorplan layouts used in this and previous papers include two emergency exit stairways and two freight elevators. There are also other risers, such as plumbing chases and electrical chases, but these are not considered in this exercise.

The dimensions of the stairs and elevator shaft openings, such as doors and cracks, are provided in the NPL calculations provided in previous papers.

3 CALCULATING THE LOCATION OF NEUTRAL PLANE LEVEL (NPL)

A resistance formula is used to calculate the sum of the effective crack area openings:

$$ECA = \frac{1}{\frac{1}{\sum AF} + \frac{1}{\sum S+E}} \quad (1)$$

Where: $\sum AF$ is the crack opening areas such as:

- entrance doors
- exterior wall leakage cracks

And $\sum S+E$ is the crack opening areas such as:

- stair shaft wall
- stair shaft doors
- elevator shaft wall
- elevator doors

The crack opening areas effectively act as a passage for airflow with resistance in place. In a manner analogous to electrical circuits, the flow network established by these resistances across doors, through walls, façades, up and down ducts etc., creates a resistance network. Hence the objective is to calculate an effective crack area on each floor and then calculate a height-weighted average and turn that into an estimate of the NPL (Simmonds and Phillips, 2022).

The design engineer will determine the number of elevators, transfer floors, refuge floors, and other such elements as shown on the architectural drawings.

In this case, the exterior wall leakage rate is $1.96 \text{ cm}^2/\text{m}^2$. The area of the exterior walls is 756 m^2 . The crack area is $1.96 \times 756 = 1481.76 \text{ cm}^2$ or 0.148 m^2 . This term is called AF, $1/\text{AF} = 6.7$

The leakage rate of the stairs shaft is $0.4 \text{ cm}^2/\text{m}^2$, the area of the stairwell = 62.1 m^2 and the crack area = 25.5 cm^2 or 0.0025 m^2 .

The leakage of the elevator doors = 187.5 cm^2 per elevator, there are 6 elevators giving a total crack area of 1125 cm^2 or 0.1125 m^2 .

The leakage rate of the elevator wall is $1.57 \text{ cm}^2/\text{m}^2$, the elevator wall area = 100.8 m^2 giving a total crack area of 158.25 cm^2 or 0.0158 m^2 .

The total stairwell and elevator (S+E) area is $0.0025+0.1125+0.0158 = 0.128 \text{ m}^2$. This term is called S+E, $1/\text{S+E} = 7.792$.

The sum of the crack areas = $1/ (1/\text{AF} + 1/\text{S+E}) = 0.0687$ (at the highest level)

For details of areas and leakage rates, see ASHRAE Fundamentals (2021) Chapters 16 and 24, also ASHRAE Applications Handbook (2019) Chapter 4 and Chapter 54.

4 STACK EFFECTS

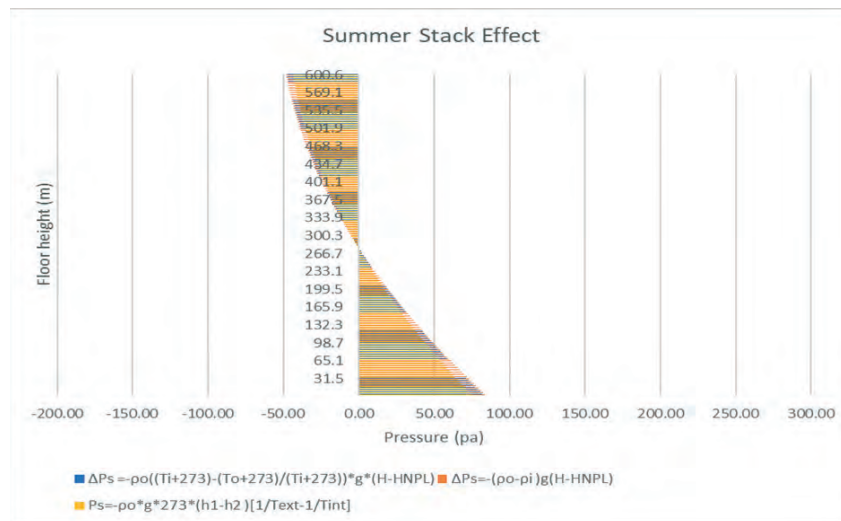


FIG. 1 Stack effect driven indoor-outdoor pressure difference as a function of height in summer given the position of the neutral plane assuming the building is a single zone.

Figure 1 presents the reference building's indoor/outdoor pressure difference for summer conditions with an outside temperature of 32°C and an indoor temperature of 24°C . This pressure difference is created exclusively because of the temperature difference between the indoors and outdoors.

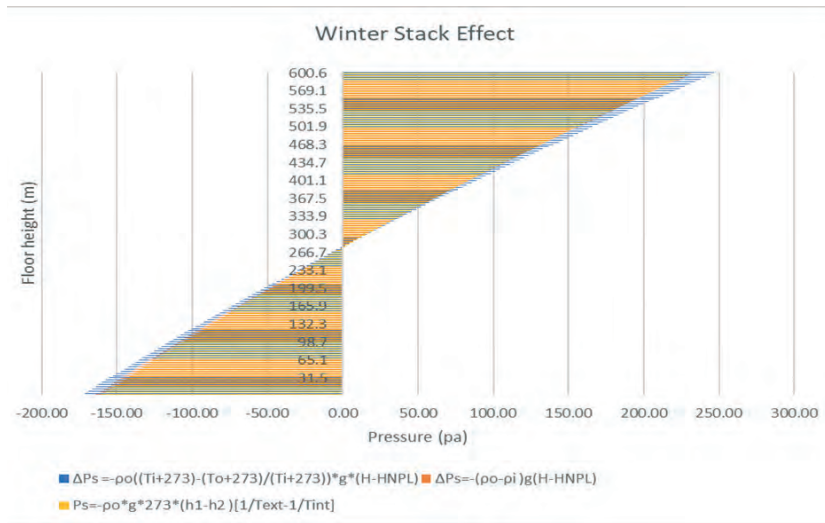


FIG. 2 Stack effect driven indoor-outdoor pressure difference as a function of height in summer given the position of the neutral plane assuming the building is a single zone.

Figure 2 presents the indoor/outdoor pressure difference for winter conditions: the outdoor temperature is 6°C and the indoor temperature 20°C. The total delta P for the building is approximately 330 Pa. Clearly, the slope here is less steep, indicating a higher temperature difference: a vertical plot would mean zero temperature difference, and a more horizontal slope would reflect a very high temperature difference.

5 STATIC AIR PRESSURE IN THE SHAFTS

Static pressure, or hydrostatic pressure as it is sometimes called, is the pressure exerted by a fluid at rest. A fluid is any substance that does not conform to a fixed shape. This can be a liquid or a gas. Since the fluid is not moving, static pressure is the result of the fluid's weight or the force of gravity acting on the particles in the fluid.

Static pressure is the weight of the fluid above the point being examined. The pressure difference between two elevations can be calculated using the following equation:

$$P = \rho \times g \times \Delta h \tag{2}$$

Where:

P = hydrostatic pressure (Pa)

ρ = density of the air at height h

Δh = height difference between the two points being examined

For this paper, we assume the building to be 600m tall and calculate the hydrostatic pressure on each floor starting at the top of the building. As we go down the building, the air pressure on the floor above is integrated with the hydrostatic pressure on the floor being considered. At the bottom of the building, a height of 600m creates the hydrostatic pressure difference.

6 CALCULATING STATIC PRESSURE DIFFERENCES

Using the data shown in Tables 1 through 4, we can calculate the static pressure of the air in a shaft.

TABLE 1 Summer conditions in the stair shaft

SUMMER TEMPERATURE °C	SUMMER DENSITY (KG/M ³)
18	1.212

TABLE 2 Winter conditions in the stair shaft

WINTER TEMPERATURE °C	WINTER DENSITY (KG/M ³)
14	1.229

TABLE 3 Summer conditions in the elevator shaft

SUMMER TEMPERATURE °C	SUMMER DENSITY (KG/M ³)
28	1.172

TABLE 4 Winter conditions in the elevator shaft

WINTER TEMPERATURE °C	WINTER DENSITY (KG/M ³)
18	1.212

The pressures in the shafts are calculated using the above temperatures and resultant densities.

7 CALCULATING FLOW DRIVEN BY PREDICTED PRESSURE DIFFERENTIAL ON EACH LEVEL

To calculate the air movement either from the shaft to the outside or vice versa, the following formula is used:

$$Q = C_p A \sqrt{2 \Delta P_{tot} / \rho} \quad (3)$$

Where:

Q = airflow, m³/s

C_p = flow coefficient (0.61 was used for these calculations)

A = cross-sectional area of opening (e.g., the cracks in the case of infiltration), m²

ΔP_{tot} = total pressure difference between the vertical shaft and outdoors at the elevation of interest {Pa}

ρ = air density, kg/m³

The following formula is used to express the total pressure differential between a shaft and the outside:

$$\frac{1}{c_p^2} \left(\frac{Q}{A} \right)^2 \frac{\rho}{2} = \Delta P_{tot} \quad (4)$$

If we work with just the elevator shafts and assume the stair shafts are not participating in the stack effect:

$$\Delta P_{tot} = \Delta P_F + \Delta P_E \quad (5)$$

The total pressure is the pressure differential across the façade and the pressure differential across the elevator doors.

$$\Delta P = \frac{\rho}{2} \frac{1}{c_p^2} \left(\frac{Q_F}{A_F} \right)^2 + \frac{\rho}{2} \frac{1}{c_p^2} \left(\frac{Q_E}{A_E} \right)^2 \quad (6)$$

Where:

Q_F = air flow through the façade

Q_E = airflow through doors and cracks

A_F = area of the façade

A_E = area of doors and cracks

Formula 4 is derived from expanding formula 3 with formula 2.

Simplifying formula 4, we get:

$$\Delta P = \frac{\rho}{2c_p^2} \left(\frac{Q_F}{A_F} + \frac{Q_E}{A_E} \right)^2 \quad (7)$$

As the airflows through the two sets of cracks (for example, elevator and façade) are equal, we get:

$$Q_F = Q_E \quad (8)$$

The next step is to assess the infiltration or exfiltration through the elevator shaft and the infiltration or exfiltration through the façade:

$$\Delta P = \frac{\rho}{2c_p^2} (Q_F A_E + Q_E A_F / A_F A_E)^2 \quad (9)$$

Simplifying Formula 7, we get:

$$\Delta P = \frac{\rho}{2c_p^2} (2Q(A_E + A_F) / A_F A_E)^2 \quad (10)$$

Further simplifying Formula 8, we get:

$$Q = \sqrt{2 \Delta P / \rho} \frac{c_p}{2} (A_E A_F) / (A_E + A_F) \quad (11)$$

To identify the pressure differential across the façade, we get:

$$\Delta P_F = \Delta P_{tot} - \frac{\rho}{2C_p^2} \left(\frac{Q}{A_E} \right)^2 \quad (12)$$

This equation permits one to split the total pressure difference at any elevation into that across the façade and elevator doors based on the relative leakiness of the elements. To use this approach, the designer needs to acquire the following information:

- Equivalent façade leakage areas (at a known pressure difference) over the height of the building.
- Emergency exit stair shafts (these are usually the height of the building).
- Openings in stairs shafts that lead to leakage, including gaps underneath the doors.
- All elevator shafts, including goods and firefighter's elevators, as well as the height of each elevator shaft.
- Openings in elevator shafts that lead to leakage, including the gaps around the elevator doors.
- Any required building sections, such as refuge floors.

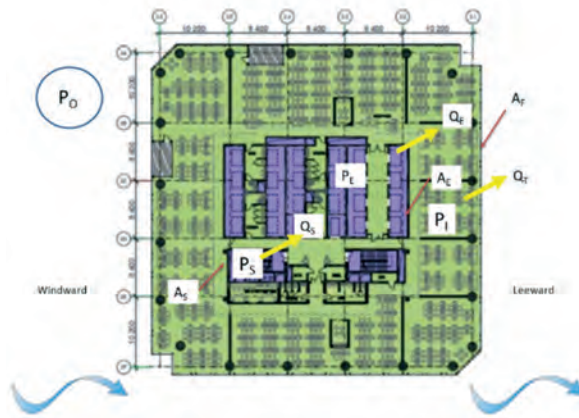


FIG. 3 Typical floorplan of the building under consideration. There are two emergency staircases and two freight elevators.

Leakage performance data is sometimes specified as a flow at a given pressure difference – this is typically used for the façade. For other components, for example, operable windows, the leakage performance data is specified as a leakage area per linear distance of component. Finally, the leakage area could be specified per unit (for example, per door). To perform the calculation, the equivalent leakage areas should be calculated for all components, which removes the pressure-based relationship of flow vs pressure difference.

8 PRESSURE PREDICTIONS

Due to the dynamics of the interaction between outside conditions and temperatures in unconditioned spaces, the study was conducted using three steps. The first step was to assume the outside temperature was constant over the height of the building, the second step was to assume a variable temperature over the height of the building, and the third step was to assume a variable temperature and pressure over the height of the building.

The pressure in the stair shaft and elevator shaft was calculated for each floor, and then the pressure in the floor above was integrated with the pressure from the floor below to provide a pressure head at that point.

The following figures show the results of comparing the pressure differential between the stairs shaft and outside and the pressure differential between the elevator shaft and the outside.

From Figures 1 and 2, we can see the building has different characteristics for the summer and the winter. During the summer, the pressure flow is from the outside to the inside above the neutral plane. This means outside air will infiltrate the building and will add an extra cooling load to the conditioning system. In the winter, the pressure flow is from the outside to the inside below the neutral plane. This results in outside air infiltrating the building and increases the heating load.

The goal of this research is to quantify the energy effects of the outside air infiltration due to the pressure differential between shafts and the outside.

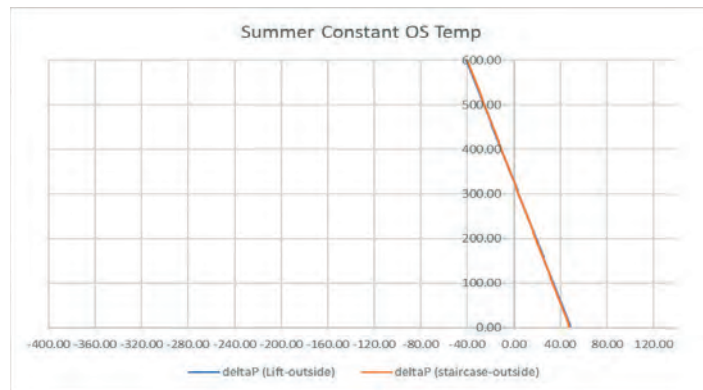


FIG. 4 Pressure differential between the shafts and the outside when the outside temperature is assumed to be constant across the height of the building.

The pressure differential is from -40 Pa at the top of the building to +40 Pa at the bottom of the building. The temperature differentials between shafts and outside are relatively small, namely 80 Pa.

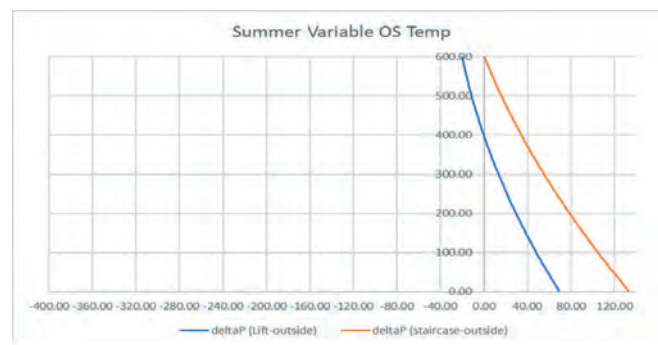


FIG. 5 Pressure differential between the shafts and the outside when the outside temperature is assumed to be variable across the height of the building.

Figure 5 shows a curved relationship due to the temperatures in the shafts being constant, but the outside temperature reduces across the height of the building. The pressure differential between the elevator shaft and outside is from -40 Pa at the top of the building to +80 Pa at the bottom of the building. The pressure differential between the stairs shaft and outside is from 0 Pa at the top of the building to +130 Pa at the bottom of the building.

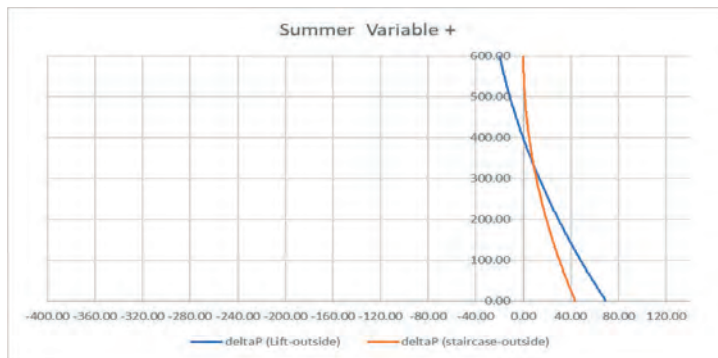


FIG. 6 Pressure differential between the shafts and the outside when the outside temperature and pressure is assumed to be variable across the height of the building.

Figure 6 shows the sensitivity of the pressure relationships. The pressure differential between the elevator shaft and outside is from -20 Pa at the top of the building to +70 Pa at the bottom of the building. The pressure differential between the stairs shaft and outside is from 0 Pa at the top of the building to +40 Pa at the bottom of the building.

Both stair and elevator shafts to outside pressure differentials are lower than the pressure differentials shown in Figure 5.

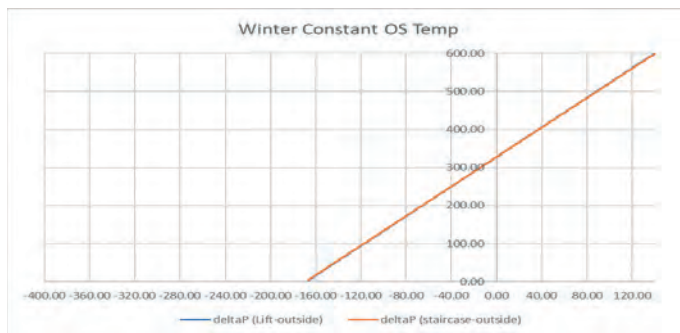


FIG. 7 Pressure differential between the shafts and the outside when the outside temperature is assumed to be constant across the height of the building.

The pressure differential is from +130 Pa at the top of the building to -160 Pa at the bottom of the building. The temperature differentials between shafts and outside are large, namely 290 Pa.

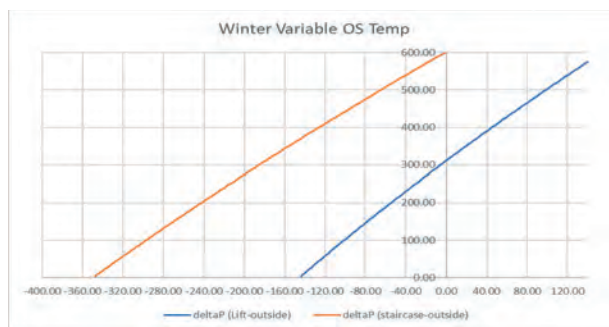


FIG. 8 Pressure differential between the shafts and the outside when the outside temperature is assumed to be variable across the height of the building.

Figure 8 shows a curved relationship due to the temperatures in the shafts being constant, but the outside temperature reduces across the height of the building. The pressure differential between the elevator shaft and outside is from +130 Pa at the top of the building to -140 Pa at the bottom of the building. The pressure differential between the stairs shaft and outside is from 0 Pa at the top of the building to -350 Pa at the bottom of the building. Both pressure differentials are much higher than the summer calculation, which is due to the larger temperature differential between the shafts and the outside.

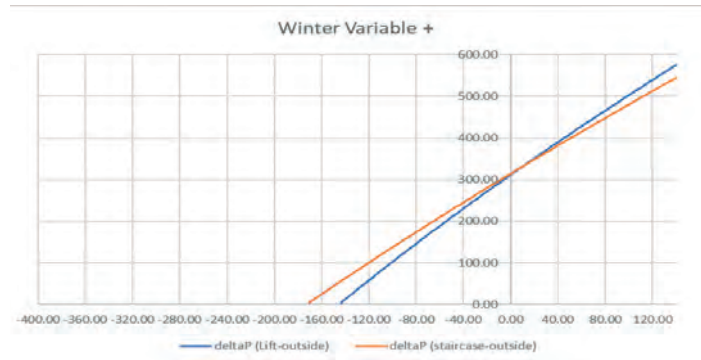


FIG. 9 Pressure differential between the shafts and the outside when the outside temperature and pressure is assumed to be variable across the height of the building.

Figure 9 shows the sensitivity of the pressure relationships. The pressure differential between the elevator shaft and outside is from +130 Pa at the top of the building to -140 Pa at the bottom of the building, resulting in 270 Pa. The pressure differential between the stairs shaft and outside is from +130 Pa at the top of the building to -170 Pa at the bottom of the building, which is 300 Pa.

9 FLOW PREDICTIONS

The following results are for a single stair shaft and a single elevator shaft. For combinations of multiple stair and elevator shafts, we refer to a future paper that will include these complicated calculations.

Using the following data from the preliminary analysis:

- ρ stair
- ρ elevator
- ΔP_s stair to outside
- ΔP_e elevator to outside
- A_s = area of the stair openings
- A_e = area of the elevator openings
- A_f = area of the façade

Using Formula 13 results in the following:

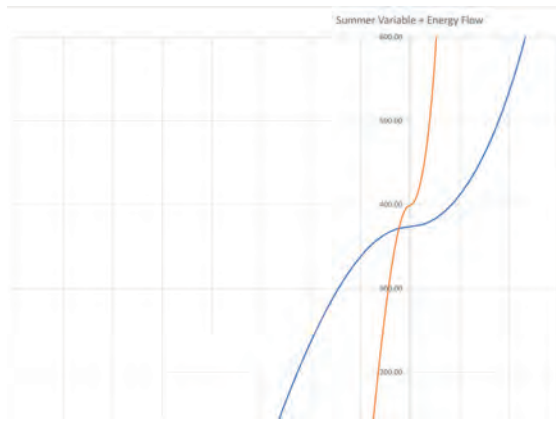


FIG. 10 Volume of airflow infiltrating and exfiltrating the building in the summer.

When the flow is positive, outside air will infiltrate the building. In summer, the infiltration of outside air will increase the space cooling load. The increase in cooling load is estimated at $149 \times 1 \times 1.172 \times (30 - 24) = 1,047.7 \text{ kW}$ on the design day.

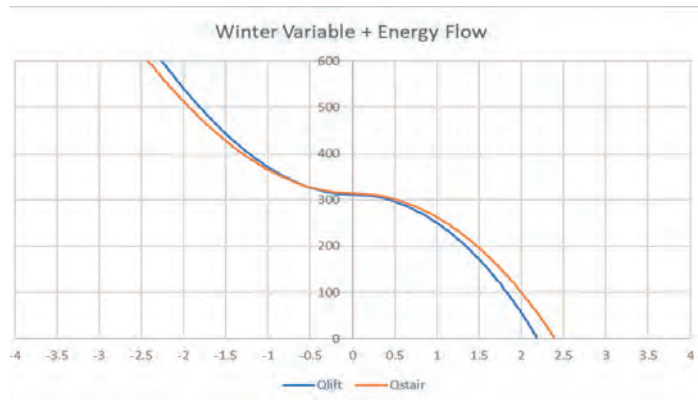


FIG. 11 Volume of airflow infiltrating and exfiltrating the building in the winter at 6° C outside temperature.

When the flow is negative, outside air will infiltrate the building. In winter, the infiltration of outside air will increase the space cooling load. The increase in cooling load is estimated at $110 \times 1 \times 1.172 \times (20 - 6) = 1,804 \text{ kW}$ on the design day.

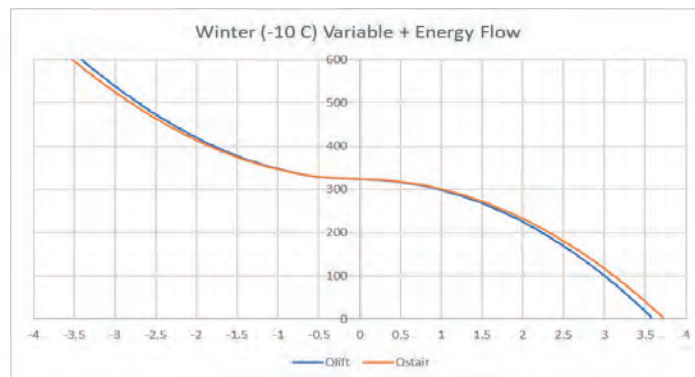


FIG. 12 Volume of airflow infiltrating and exfiltrating the building in the winter at -10° C outside temperature.

When the flow is negative, outside air will infiltrate the building. In winter, the infiltration of outside air will increase the space cooling load. The increase in cooling load is estimated at $121 \times 1 \times 1.19 \times (20 - -10) = 4,319.7$ kW on the design day.

10 CONCLUSIONS

The results clearly show that when calculating heating and cooling loads for tall, super-tall and mega-tall buildings, the actual outside temperature differentials at different building heights need to be incorporated into the calculations.

The critical period is winter as the temperature differential between internal shafts and the outside are largest, and the infiltrating outside air is at a lower temperature. The actual outside air infiltration will be much higher than specified will be responsible for the increase in infiltration. At what pressure should the façade be tested? Which outside air infiltration rate has been included in the heating and cooling load calculations?

At present, there are no commercially available load calculation programs that use a variable outside temperature in the calculations. This paper shows how the variable outside temperature can be used when calculating a building's heating and cooling loads in a spreadsheet. These manual calculations should be recommended for tall, super-tall and mega-tall buildings. It is, of course, essential that the vertical weather data is available for such calculations. The façade air infiltration rate specified by the architect should be appropriate for the overall height of the building.

References

- ASHRAE. (2019). Standard 62.1-2019. Ventilation for Acceptable Indoor Air Quality, ASHRAE: Atlanta, Ga 30329.
- ASHRAE. (2021). Chapter 16 and Chapter 24 Fundamentals Handbook 2021. ASHRAE: Atlanta, Ga 30329.
- ASHRAE. (2019). Chapter 4 and Chapter 54, Applications Handbook 2019. ASHRAE: Atlanta, Ga 30329.
- Lovatt, J. E. and Wilson, A. G. (1994). Stack effect in tall buildings. ASHRAE Transactions 100(2), pp. 420-431.
- Nylund, P.O. 1980. Infiltration and ventilation. Report D22:1980. Swedish Council for Building Research, Stockholm.
- Raymond, W. H. (2000). Estimating Moisture Profiles Using a Modified Power Law, Journal of Applied Meteorology 39(7), pp. 1059-1070.
- Ross, D. (2004). An HVAC design guide for tall commercial buildings, ASHRAE.
- Persily, A.K., and R.A. Grot. 1986. Pressurization testing of federal buildings. In Measured air leakage of buildings, STP 904, p. 184. H.R. Trechsel and P.L. Lagus, eds. American Society for Testing and Materials, West Conshohocken, PA.
- Phillips, D. (2014) Personal Correspondence.
- Phillips, Duncan A. (2021), Managing Infiltration in Tall Buildings to Control Energy Loss, Minimize Pathogen Transport and Enhance Air Quality, Presented at the ASHRAE January 2021 Conference, Seminar 75.
- Simmonds, P., and Zhu, R., Stack Effect Guidelines for Tall, Mega Tall and Super Tall Buildings, International Journal of High-Rise Buildings, December 2013, Vol 2, No 4, 1-8
- Simmonds, P., The new ASHRAE Design Guide for Tall, Supertall and Megatall Building Systems, ASHRAE 2015 and second edition 2020
- Simmonds, P., and Phillips, D., A unique way to determine the Neutral Plane height in Stack Effect calculations. ASHRAE Journal, 2022
- Tamblyn, R. T. (1991). Coping with air pressure problems in tall buildings. ASHRAE Transactions 97(1), pp. 824-827.
- Tamura, G.T., and C.Y. Shaw. 1976a. Studies on exterior wall air tightness and air infiltration of tall buildings. ASHRAE Transactions 82(1):122. Paper DA-2388.
- Tamura, G.T., and C.Y. Shaw. 1976b. Air leakage data for the design of elevator and stair shaft pressurization system. ASHRAE Transactions 82(2):179. Paper SE-2413.
- Tamura, G.T., and A.G. Wilson. 1966. Pressure differences for a nine-story building as a result of chimney effect and ventilation system operation. ASHRAE Transactions 72(1):180.
- Tamura, G.T., and A.G. Wilson. 1967a. Pressure differences caused by chimney effect in three high buildings. ASHRAE Transactions 73(2): II.1.1.
- Tamura, G.T., and A.G. Wilson. 1967b. Building pressures caused by chimney action and mechanical ventilation. ASHRAE Transactions 73(2): II.2.1.

FACA-DE-LIT: Façade Optimisation for Visual Comfort by Controlled Daylight Distribution in High-Rise Office Buildings

Ar. Ir. Akash Changlani¹ , Dr. Michela Turin² , Dr. Alejandro Prieto Hoces³

- 1 Delft University of Technology (TU Delft), Mekelweg 5, 2628 CD, Delft, akash.changlani93@gmail.com
- 2 Delft University of Technology (TU Delft), Mekelweg 5, 2628 CD, Delft, M.Turrin@tudelft.nl
- 3 Delft University of Technology (TU Delft), Mekelweg 5, 2628 CD, Delft, A.I.PrietoHoces@tudelft.nl

Abstract

The evolution of high-rises creates a greater challenge for achieving indoor visual comfort because natural light can only penetrate the building through the sidewalls. This is especially true for deep floorplans like those in office buildings, where visual discomfort is very commonly experienced. Without any measures taken, such a scenario causes glare near the windows and demands the use of artificial light at depth. The illuminance decreases in a gradient along the depth and creates an uncontrolled and non-uniform distribution of daylight. Moreover, daylight is very dynamic in nature, continuously changing over time, which adds complexity to the design. This research aims to improve the visual comfort efficiency of deep office spaces by developing a dynamic façade system that (i) adapts to various external factors that are responsible for dynamic daylight behaviour throughout the year; (ii) distributes the daylight more uniformly and homogeneously along the depth, and (iii) results in a controlled distribution of daylight to a visually comfortable range (daylit range) of 300-2000 lux. The strategies applied for the design development were using computational methods workflows by means of parametric modelling, daylight simulation and optimisation. As the final outcome, an average of 88% of the work area is found to be within the daylit range featuring an average illuminance of 561 lux, which is distributed with an average uniformity ratio of 0.57 with minimal risk of glare and contrast; validating that a visually comfortable environment is achieved (NEN-EN 17037 and BREEAM 2016). It further indicates that the use of artificial light can be reduced by 88%, saving equivalent energy consumption concerning artificial lighting. PV modules are used for energy offsetting, which covers 30% of the envelope surface. The study also covers the constructability and feasibility aspects of the proposed scheme. The façade scheme is designed for disassembly as a circular product, and the choice of material is made with recycled content in mind. Overall, 98% of the whole façade by mass weight is demountable, recyclable and directly reusable. The façade complies with the circular economy and energy-neutrality guidelines given by the Dutch government for 2030 and 2050.

Keywords

Dynamic façade, high-rise, office building, daylight, visual comfort, computation design, optimisation

1 INTRODUCTION

The evolution of high-rises creates a greater challenge for achieving indoor visual comfort because natural light can only enter the building through the sidewalls, especially in deep floorplans like office buildings, where visual discomfort is very commonly experienced. Without any measures taken, the illuminance exceeds the comfort requirements in the vicinity of windows by creating over-lit areas causing glare issues. Furthermore, the illuminance decreases in a gradient along the depth, leaving illuminance below comfort requirements towards the end of the rooms by creating under-lit areas that demand the use of artificial lighting. This creates an uncontrolled and non-uniform distribution of daylight along the room depth. Moreover, daylight is very dynamic in nature, continuously changing over time, which adds complexity to the design and leads to the use of computational design methods.

This research aims to improve visual comfort efficiency for office spaces with the help of computational methods by developing a dynamic façade system. This system adapts to various external factors that are responsible for dynamic daylight behaviour, results in a controlled distribution of daylight throughout the depth of the space, and homogeneously distributes the daylight to the indoor space, balancing the light intensity of under-lit and over-lit areas into a visually comfortable range or daylit range.

Responsive façades can be made with several components and technologies (mechanical, electrical, ICT, etc.). These technologies have been experimented, studied and tested in their specific industrial sectors, but there are no studies about the reliability of these technologies in buildings. Thus, managing and carrying out maintenance on these skins is increasingly complicated and the solutions that are usually pursued in new designs involve the reduction of mechanical devices in favor of chemical technologies and digital technologies. In general, passive technologies are preferred over active ones, in order to reduce operational energy as well as maintenance costs. These aspects and the incidence of innovative and emerging technologies have been investigated in this research.

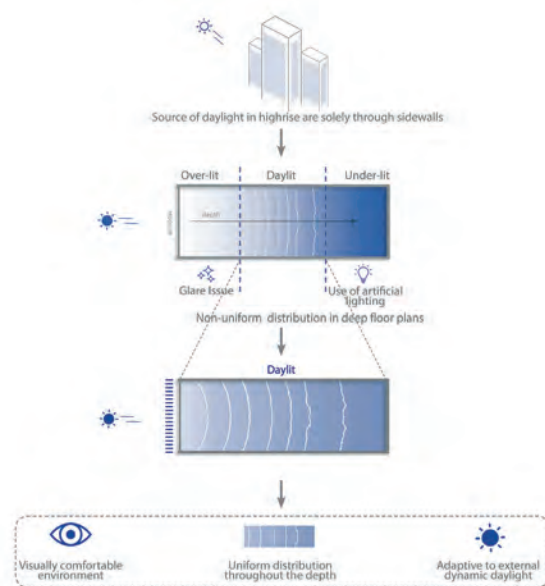


FIG. 13 Formulation of objectives for the research study

2 METHODOLOGY

The literature study was carried out to determine the design requirements for façade design. A geometry was selected and modified, and the first design proposal for the façade was made. This model was fed into Rhino and Grasshopper for parametric modelling, and the most crucial parameters of the façade were developed. This façade is formulated by fixing one location, weather type, and the room's dimension with appropriate depth. The model was further analysed for daylight simulation using the plugin Honeybee-Ladybug plus and was then optimised using the plugin Wallacei. The optimisation method is applied to bring a near-optimal solution for the façade's performance on daylight quality and its uniform distribution for indoor spaces by reducing over-lit and under-lit areas to gain maximum daylit area.

The solution obtained from the optimisation process was tested for the evaluation criteria to validate the façade for the visual comfort criteria of the space. The gathered knowledge from the optimisation process was used to formulate a full-scope workflow that can help to optimise and evaluate a façade solution that deals with the dynamic behaviour of daylight to provide visual comfort indoors. However, this research uses a limited scope of the same workflow. Furthermore, the final design of the façade was detailed for its constructability and feasibility with its dynamic motion.

3 EXPERIMENT / RESEARCH

3.1 VISUAL COMFORT CRITERIA

The evaluation process of this research is based on the criteria that will help to achieve visual comfort inside the building, along with uniform distribution of daylight intensity. The analysis will focus on these three factors – the distribution of daylight, the presence of glare and contrast. The metrics corresponding to these three factors are considered the foremost focus for the visual comfort criteria to validate the proposed façade for visual comfort in this research. None of the annual metrics is considered for the daylight analysis study.

The standards for daylight provided by NEN-EN 17037 (2018) are based on annual calculations, wherein the analysis performed in this study is for a specific hour. Also, NEN-EN does not mention uniformity ratio and contrast ratio, whereas BREEAM (2016) has guidelines on these metrics. Furthermore, CIBSE (2015) recommends a specific illuminance value of 500 lux for an office workplace, while Chauvel (1982) recommends using a range of daylight for validating a room as daylight's intensity varies with the depth of the room.

Hence, all the values for the visual comfort criteria are based on NEN-EN 17037, BREEAM (2016) and Design guidelines. The required values for evaluation criteria are formulated below:

TABLE 5 Selected visual comfort criteria and their required metrics and target values

FACTORS	DAYLIGHT METRICS	TARGET VALUES
Distribution of daylight	Average illuminance	300-750 lux
	Daylit area	300-2000 lux for >95% Minimum lux >100
	Uniformity ratio	>0.3
Glare	Daylight Glare Probability (DGP)	0.45-0.35 (Perceptible glare)
		<0.35 (Imperceptible glare)
Contrast	Contrast ratio	<3.0

However, the limit values of the range are not standardised values, for various literature studies on different values for the useful range have been proposed by researchers based on their study's priority (Suk, 2016). Taking into consideration the above-mentioned cases, a range of 300-2000 lux was identified to be a common value. Hence, the three ranges of UDI (Useful Daylight Illuminance) for the proposed study were considered as follows:

UDI under-lit = 0-300 lux

UDI day-lit = 300-2000 lux (useful or ambient light range)

UDI over-lit = >2000 lux.

3.2 INSTANCES

The quality, as well as the quantity of daylight in a building annually or diurnally, is highly dependent on its geographical location and climate. The sun's position for any specific location is a variable which depends on the earth's revolution around the sun annually and its rotation around its axis daily. Moreover, the prevailing climatic condition affects the luminous intensity and visibility of the sun and the luminous distribution of the sky. Thus, after fixing the location and orientation, three main external factors influence the behaviour of light that reaches the building and affects daylight performance; the sun's altitude, the sun's azimuth and the luminous distribution in the sky.

A part of the objective is to develop a façade that can perform effectively by adapting to changes in external factors that influences the change of daylight levels. The selection of different cases within these factors was made by considering the extremities possible in all factors of an outdoor environment.

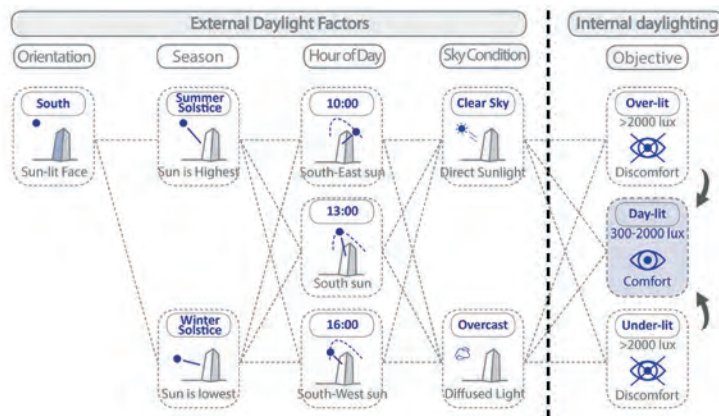


FIG. 14 Selected instances for the proposed research

3.3 FAÇADE LOCATION

The location for the proposed study was Rotterdam, The Netherlands. The climate experienced in Rotterdam is temperate oceanic as per the Köppen Climate Classification (cfb). The space subject

of this research is an office space in a high-rise office building. The activities in the office space selected for this research are tasks that require the use of computer screens.

An office space can be as small as a single-occupancy cabin to an open office plan where the whole floor space is open without any partition. To restrict the limit and to study the nature of the distribution of light levels in a space with respect to its depth, a tube-shaped modular room is proposed as a fraction of a typical floor plan. The proposed room is 3 m wide, 9 m deep (Figure 3.4) and has a 3 m clear height from floor to ceiling. The proposed room is aligned to the north-south axis, and a south-facing opening in the façade is used for daylight analysis. The specified Visible Transmitted (VT) value for the window glazing is 0.65, which means only 65% of the light will be transmitted inside the building.

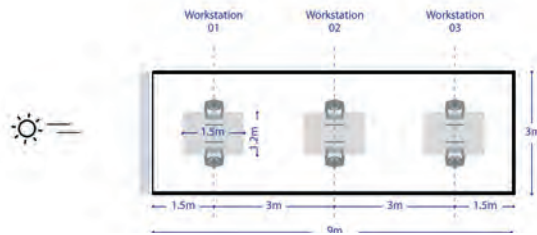


FIG. 15 Plan of selected room with its dimensions

3.4 GEOMETRY

3.4.1 Geometry Selection

The approach towards developing the final geometry began with understanding an 8-connection Kaleidocycle, made with the paper-folding technique. The Kaleidocycle was then broken down into parts, and a pair of mirrored disphenoids was selected as the base geometry for one module of this façade study.

As the sole purpose behind the choice of Kaleidocycle was to use a multi-surfaced geometry to treat different surfaces with different material properties, the purpose is still being fulfilled because the disphenoids also represent a multi-surface geometry, but with a more flexible approach.

3.4.2 Geometry modification

Taking the base geometry – a pair of disphenoids – where the module is motionless and has a static shape, the module is modified in three steps to make it dynamic to adapt to dynamic daylighting. The idea behind the modification process was to make the module as flexible as possible to achieve the optimal result in performance.

1 Folding/Unfolding

The first modification of the geometry is made by adding a half-cut at the centre of the geometry along the XY-plane, with a folding feature (Figure.4.4). The module is now capable of folding and unfolding dynamically to achieve several variations. Furthermore, the folding/unfolding is separated for both tetragonal disphenoids, resulting in four different variations obtained from one single module.

2 Rotation

Rotation is a major parameter that can greatly influence the performance of daylight, as stated by Samadi (2019). The rotational motion can be executed in various ways; along the x, y, or z-axis or along a non-axial direction. To keep the dynamism of the proposed façade as simple as possible while considering practical application and automation, the module features rotation along the axis that is formed on its longest length from the centroid point.

3 Material set

The module is provided with different material properties on different surfaces, which was the foremost reason behind selecting this geometry. The number of material variations can vary from having the same material on each surface to all surfaces with different materials or different materials on different groups of surfaces. In the proposed study, two sets of materials were chosen for each module.

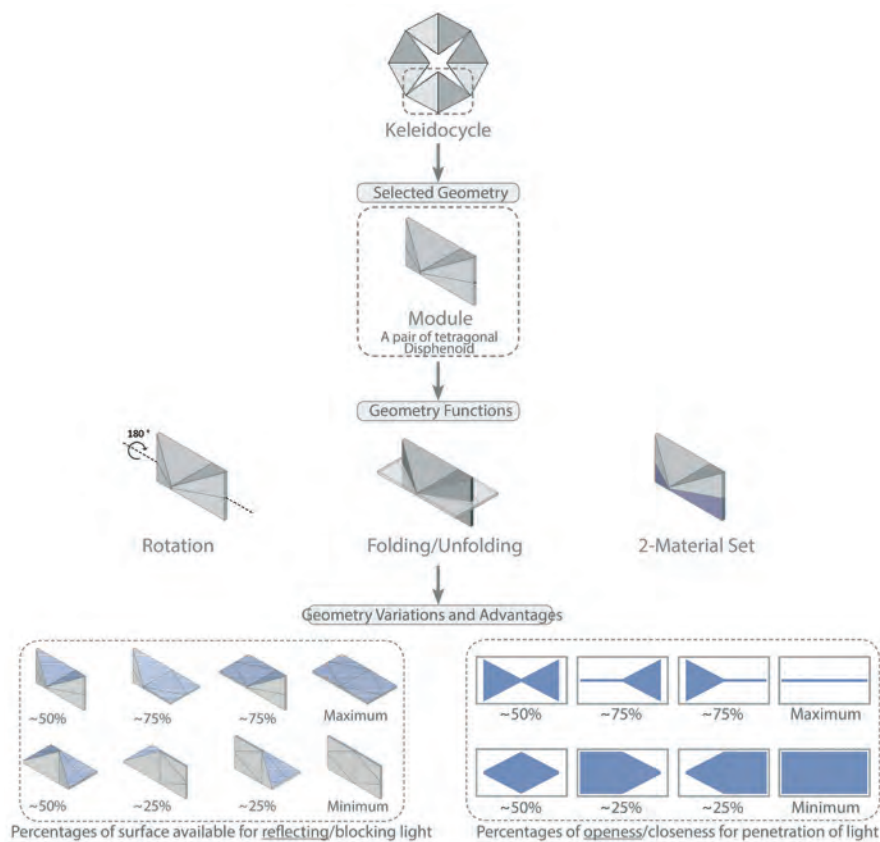


FIG. 16 The process showing the evolution of the selected geometry and its advantages

3.4.3 Geometry variations and advantages

1 Reflecting surface

Another advantage of using a modified module is the potential to control the amount of direct light to be redirected or blocked from the inside using the surface available on the module. As shown in Figure 4.8, a high percentage of the available surface is obtained by looking at the top. Again, this wide variation of the range is believed to help control two factors, the amount of light redirected inside and the amount of light blocked by the adjacent surface.

2 Openness/closeness

One of the advantages of using the modified module with the selected geometry is the potential to control the amount of openness and closeness when configured in a façade. As shown in Figure 4.7, a large percentage of openness is obtained by utilising different variations of the modified module by looking at its elevation. This wide variation of the range is believed to help control two factors, the amount of light penetrating the room and the amount of visual connectivity with the outside. The penetration of light can be increased by folding more modules, which increases the openness of the façade. Similarly, to increase the visual connection to the outdoors, more modules need to be folded and vice versa.

3.5 COMPUTATION DESIGN

The façade geometry was developed further to find an optimal façade design solution that provides visual comfort indoors with high efficiency, dealing with all of the different external daylight conditions. The computational design method allows us to deal with complex challenges; however, a computational workflow is developed, which is applied for this study to find a façade design solution with high-performance efficiency in achieving visual comfort.

The workflow is divided into several steps that include parameterisation of the façade geometry through parametric modelling using Grasshopper (GH) and Rhino, then performing daylight simulation using the Honeybee and Ladybug plugins used within GH, conducting an optimisation process using the Wallacei plugin used within GH, and finalising the design solutions by going through an evaluation process to fulfil visual comfort criteria developed in this study. The solutions that do not fulfil all required criteria will be sent back for changes, and the process is continued until all the required criteria relating to visual comfort are met.

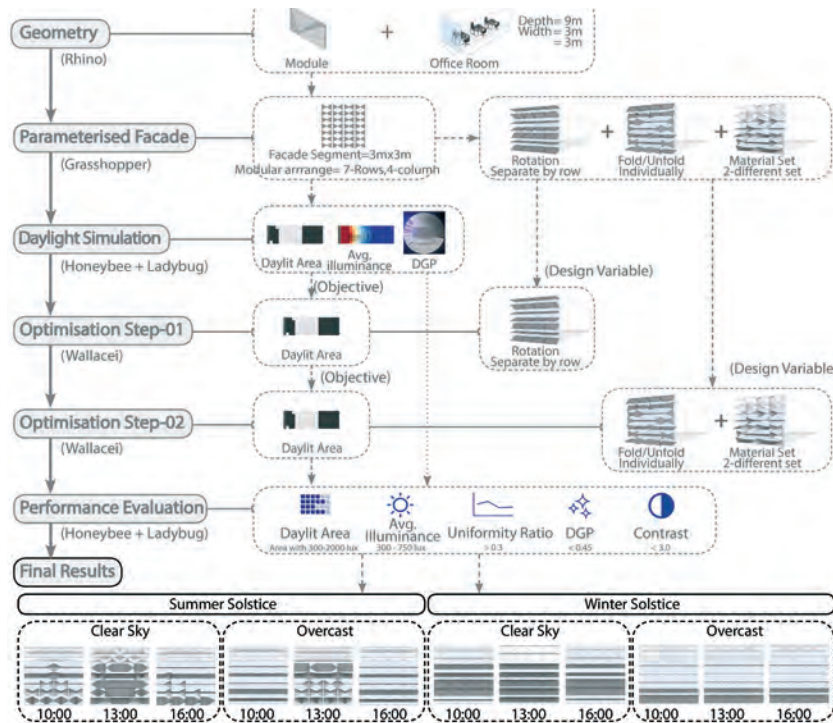


FIG. 17 Computation design workflow used

3.5.1 Parametric Modelling

A setup of the room is made in Grasshopper to study daylight performance. The dimensions of the room remain fixed. The room created is made to integrate the façade geometry.

Façade Parameters:

Three parameters are developed for this study – Rotation of modules, Folding/unfolding of modules (perceived as configuration) and Material on modules.

- 1 Rotation of Modules: The rotation parameter of modules is separated by rows; each panel is kept independent, and all modules within the same panel will have the same rotation.
- 2 Folding/Unfolding of Module: The folding/unfolding parameter for each module is kept independent; each module within the panel can change independently too.
- 3 Material on Module: The material parameter is based on the number of applied materials on each module. The change of material is basically linked to the first parameter – rotation. A module, with two materials on opposite faces, will be rotated 180° to flip the other material on the effective side for daylight performance by facing towards incoming light.

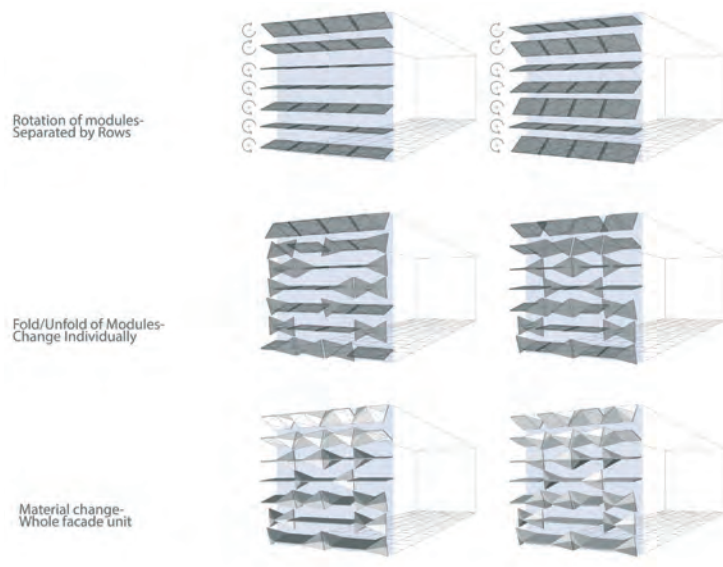


FIG. 18 Model set in Grasshopper with required objectives as the parameters

3.5.2 Daylight Simulation

The simulations are made assuming that the proposed office space is located in Rotterdam. For climate data, a weather file of Rotterdam is used ("Climate.OneBuilding.Org", n.d) in EnergyPlus Weather Format (EPW).

The simulations are performed using Ladybug Tools (Roudsari, n.d). For illuminance simulations, LB legacy (Version 0.0.68- 01 Jan, 2020) and HB+ (Version 0.0.04- 06 Oct, 2018) is used, and LB Legacy (Version 0.0.68- 01 Jan, 2020) and HB Legacy (Version 0.0.65- 01 Jan, 2020) are used for simulation of glare analysis.

Analysis Method

Three different analysis methods are used to calculate different metrics from the evaluation criteria:

- 1 Grid-based Illuminance for Average Illuminance, Day-lit Area and Uniformity Ratio. This method provides the lux values on each grid cell on a working plane. All the lux values are averaged to gain the resultant value for average illuminance in lux. A threshold upper and lower limit of 300-2000 lux is inputted, and the percentage is calculated for the number of grids with their lux values that fall within inputted range to gain the result for day-lit area in %. Furthermore, a division is applied between the lowest lux value on the reference grid to the previously calculated average illuminance value; the resultant value is the uniformity ratio.
- 2 Image-based Luminance for DGP. This method quantifies the spread of brightness within the selected field of view. The value of DGR is calculated using an inbuilt component 'Glare Analysis' in HB+.
- 3 Grid-based Luminance for Contrast Ratio. This method calculates the value of luminance on each grid's cells of the working plane. The working plane is divided into three equal parts as per the requirement of evaluation criteria for contrast ratio, and the obtained values of luminance for each division are averaged separately. The value for the contrast ratio is obtained by dividing the average luminance of one division by the adjacent division. The working plane is considered at the height of 0.70 m, a standard height for a workstation. The same working plane is divided into a number of 0.5x0.5 m grid cells for GB simulations.

Analysis Visualisation

The results obtained from HB+ is visualised differently for different analysis method.

The representation of GB-illuminance is a gradient of colour on a grid mesh. Two different grid meshes are used. One represents the gradient of light intensity in lux used for average illuminance, and the other represents the useful (300-2000 lux) and non-useful (>2000 lux and <300 lux) illuminance used for the day-lit area.

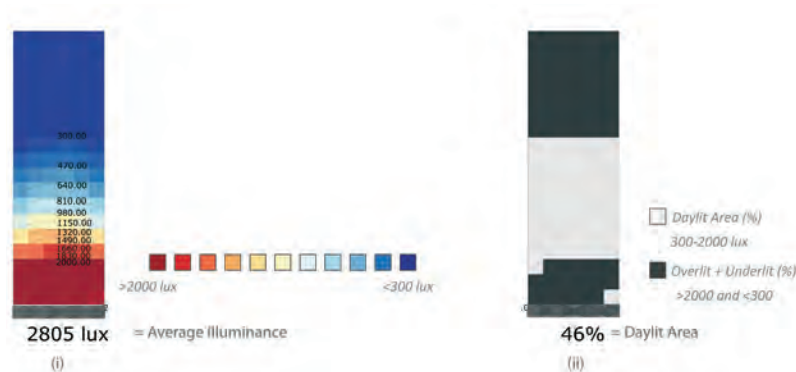


FIG. 19 Daylight simulation visualisation

3.5.3 Optimisation

All the attempts of optimisation made in this study are using Wallacei (Version V2.55- 29 March, 2020) (Makki,n.d). A workflow within the scope of Wallacei is applied to perform optimisation and to gain an optimal solution for the proposed façade for visual comfort.

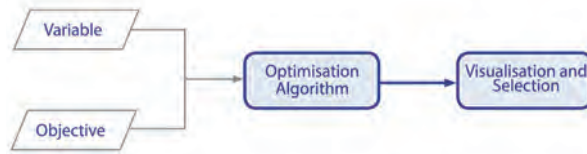


FIG. 20 Optimisation workflow

Design Variables

The three-developed parameters on façade geometry through the parameterisation process are taken further as design variables to attempt the process of optimisation as follows:

- 1 Rotation – The rotation parameter provided is separated by row; each module on the same row is given a similar rotation. However, all rows are treated independently, having individual variables. The considered rotation angle for the optimisation process is limited to 0-90°, where the diffusing modules are given a rotation outside (0 to 90°) and the diffusing modules are given a rotation towards the inside (-0 to -90°).
- 2 Folding/Unfolding – A module is considered for the optimisation process with the folding/unfolding parameter as a variable. Each module with this parameter is a separate variable.
- 3 Material – Two sets of material as variables that apply the same for each module on the façade segment.

Objective Functions

This choice of objective functions for the optimisation process is made with the idea of achieving the maximum area on the working plane between 300-2000 lux by reducing over-lit and under-lit areas. This will solve major issues related to glare and light reaching into the depth of a room, as well.

Three objective functions are developed for the optimisation:

- 1 Maximise % of day-lit area
- 2 Minimise illuminance (lux) where lux values are >2000 lux on the working plane (over-lit area)
- 3 Maximise illuminance (lux) where lux values are < 300 lux on the working plane (under-lit area)

3.5.4 Performance Evaluation

The performance evaluation is run using developed scripts in Grasshopper using the daylight simulation tools HB+ and HB Legacy. Performance evaluation is made based on the set visual comfort criteria.

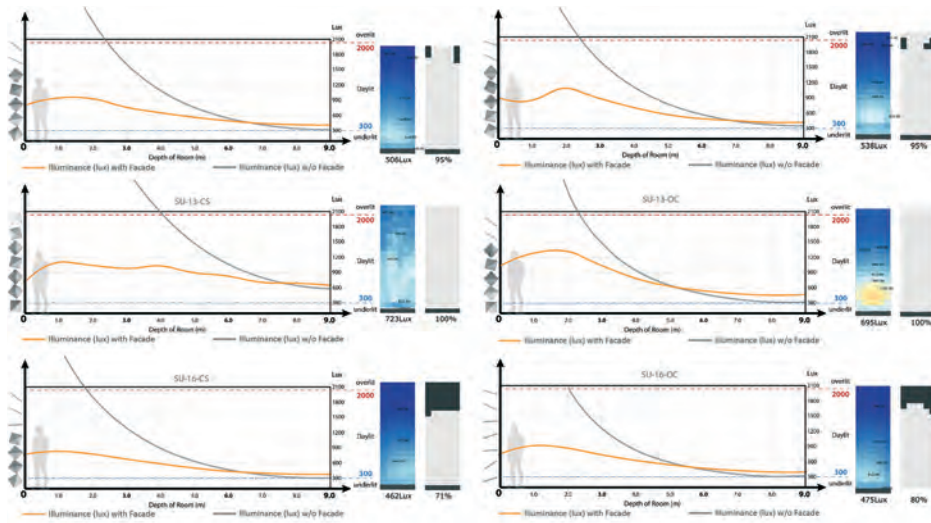


FIG. 21 Graph showing daylight illuminance distribution along the depth of the room for all summer instances

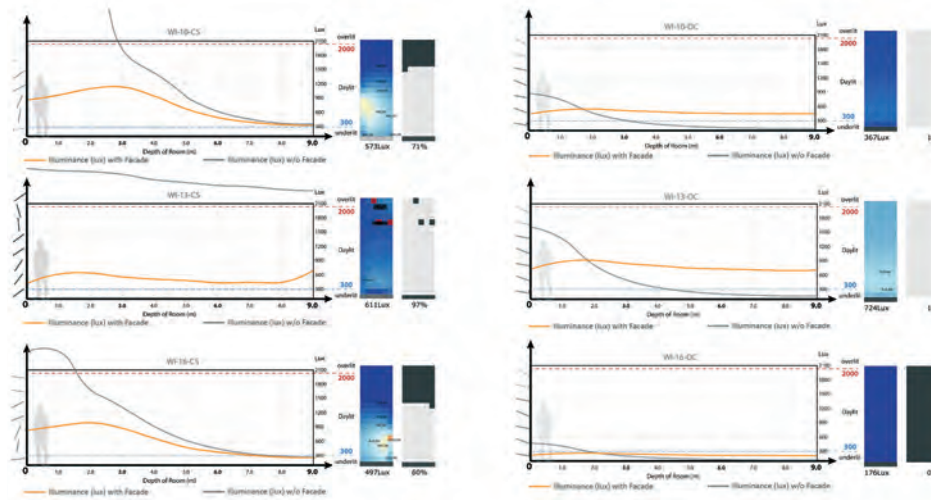


FIG. 22 Graph showing daylight illuminance distribution along the depth of the room for all winter instances

TABLE 6 All results of final optimised solution for all instances that fulfil all evaluation criteria

Instances	Distribution of Daylight			DGP		Contrast		Highest lux	lowest lux	Avg lux/mt.	Overlit	Underlit	Material Set
	Avg Lux	Daylit%	Uniformity Ratio	O11	O12	C1	C2						
SU-10-CS	506	95	0.56	0.25	0.26	2.3	2	915	284	59	0	5	M11
SU-13-CS	723	100	0.62	0.24	0.23	2.59	0.96	1002	447	50	0	0	M11
SU-16-CS	462	71	0.55	0.23	0.25	2	2.5	807	252	52	0	29	M11
SU-10-OC	538	95	0.53	0.23	0.23	2	2	979	286	75	0	5	M11
SU-13-OC	695	100	0.51	0.23	0.23	1.86	2	1336	353	98	0	0	M22
SU-16-OC	475	80	0.54	0.22	0.23	1.9	2	846	258	57	0	20	M11
WI-10-CS	573	71	0.35	0.2	0.22	1.98	2.24	1137	200	62	0	29	M22
WI-13-CS	611	97	0.5	0.2	0.21	0.85	0.37	607	305	4	3	0	M11
WI-16-CS	497	60	0.3	0.21	0.2	2.98	1.97	1483	147	40	0	60	M22
WI-10-OC	367	100	0.89	0.12	0.12	1.89	1.56	441	326	12	0	0	Higher reflectivity
WI-13-OC	724	100	0.88	0.19	0.19	2.12	2.1	863	640	24	0	0	Higher reflectivity
WI-16-OC	176	0	0.89	0.03	0.03	1.4	1.21	211	156	6	0	100	Higher reflectivity
Average**	561	88	0.57	0.21	0.22	2.04	1.79	946	318	48	0	13	-

3.6 CONSTRUCTION AND FEASIBILITY

After validating the design based on its performance, which showed the promising potential of the designed façade by meeting all the required criteria for visual comfort indoors, the next step is to realise the same façade in the practical world. Henceforth, the façade is explored and detailed with an approach to integrate within available material and technology in the market for construction.

3.6.1 Façade Scheme

The final façade scheme comprises three different modules. PV modules are provided in front of the ceiling, slab and floor depth.

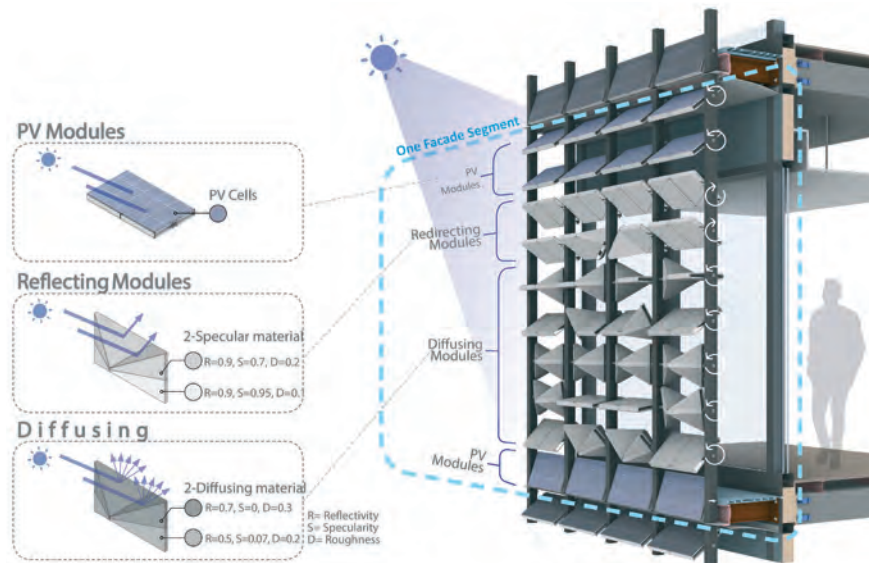


FIG. 23 Façade scheme and its components

3.6.2 Mechanism

Folding Mechanism: The linear actuator provides the mechanical pull and push within the provided stretch length in connection to a sliding bar to achieve desired motion as per the requirement.

Rotational Mechanism: This rotary actuator is installed within the vertical mullion I-section of the façade inside a gearbox.

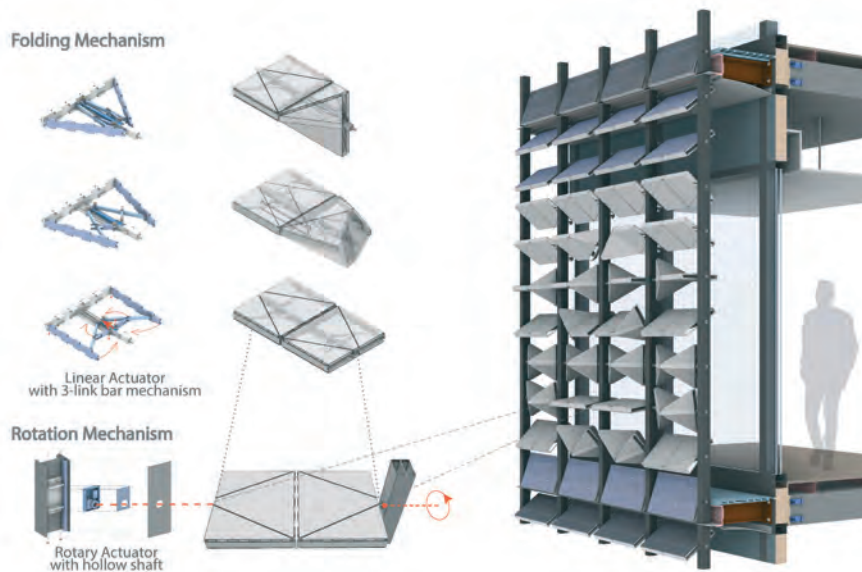


FIG. 24 Folding and rotation mechanism for dynamic movement that helps adapt to different daylight conditions

3.6.3 Automation

To allow for the motion, the automation consists of four main components:

- 1 Sun sensors: read the external condition and send the signal to the processing unit.
- 2 Processing unit: generates a response by calculating the required rotation and fold/unfold as per visual comfort requirement.
- 3 Data transfer unit: receives the calculated data and sends the signal to operate actuators.
- 4 Actuators: provide mechanical motion – rotation and folding, after receiving a signal.

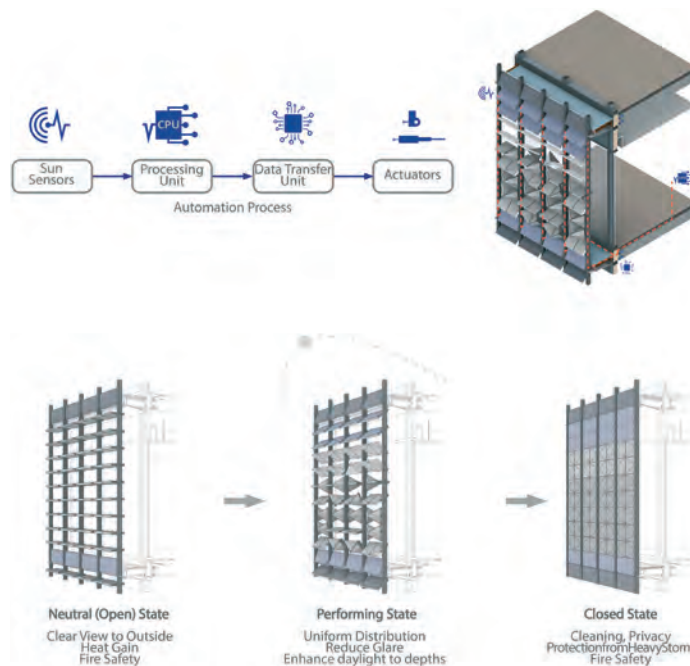


FIG. 25 Automation system integrated within façade

4 RESULTS

As the final outcome, an average of 88% of the working plane is found to be within the daylit range with an average illuminance of 561 lux, which is distributed with an average uniformity ratio of 0.57 with minimal risk of glare and contrast; validating that a visually comfortable environment is achieved (NEN-EN 17037 and BREEAM 2016). This further indicates that the use of artificial light can be reduced by 88%, saving equivalent energy consumption concerning artificial lighting. PV modules are used for energy offsetting, which covers 30% surface of the envelope.



The selected features and external factors each play an important role in aiding to control the indoor environment. More elaboratively, the individual roles are:

- 1 Rotation – This feature was found to have a major impact in terms of the changing Sun's altitude and minor impact with Sun's azimuth and sky condition as an external factor; it was found to be responsible for controlling the daylight to reach the depth of the indoor environment.
- 2 Folding – (or change of module types) This feature had a major impact in terms of the changing Sun's azimuth and minor impact with the Sun's altitude and sky condition as an external factor. It was found to be responsible for controlling the uniformity of light intensity along the depth of the indoor environment.
- 3 Material set – This feature had a major impact in terms of changing sky conditions and minor impact with the Sun's altitude and azimuth as an external factor. It was found to be responsible for controlling the enhancement of light intensity in the indoor environment.

These features are correlated and together influence the external factors; hence, the process of this study showed that each feature contributes to delivering the final result. Furthermore, the combination of the three features showed the potential to deal with diverse external daylight factors and control daylight distribution indoors.

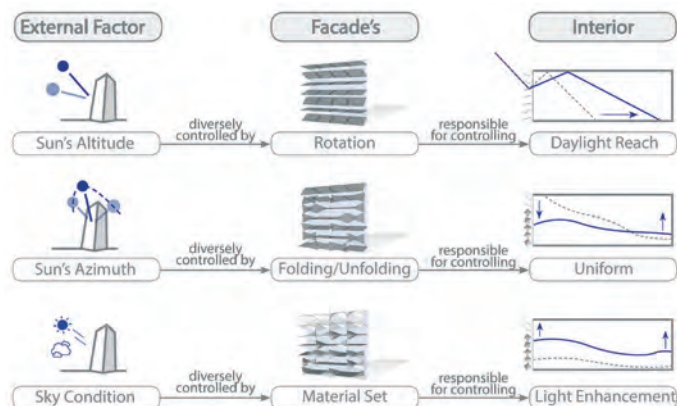


FIG. 26 Façade's performance with three façade features/objectives

The study also covers constructability and feasibility aspects of the proposed scheme. The façade scheme is designed for disassembly as a circular product, and the choice of material is made with recycled content in mind. Overall, 98% of the whole façade scheme by mass weight is demountable, recyclable and directly reusable. The façade complies with circular economy and energy-neutrality guidelines articulated by the Dutch government for 2030 and 2050. Furthermore, the choice of material with maximum recycled content for steel and aluminium contributes towards reducing embodied carbon content for the whole façade system.

5 CONCLUSIONS

The outcome of this study is a dynamic façade for an office space that adheres to visual comfort criteria of a high-rise building, allowing for controlled distribution of daylight throughout the depth of the space by adapting to diverse external daylight conditions. The applied computational design method is found to be a reliable medium to explore a design solution for a façade that has increased performance efficiency while achieving visual comfort. This is explored specifically through parametric modelling, daylight simulation and optimisation.

The façade scheme allows visual comfort with controlled distribution based on three features provided for each module – rotation, folding/unfolding and different material sets. However, with the help of computational methods, the final sets of configurations in combination with previously mentioned features were achieved for each instance using a developed digital workflow. By optimising the process with daylight simulations, a near-optimal solution was found.

References

- NEN-EN 17037". (2018). Daylight in buildings, Dutch standards.
- BREEAM, 2016. Hea 01 Visual Comfort. Retrieved from https://www.breeam.com/BREEAMUK2014SchemeDocument/content/05_health/hea01_nc.htm
- Chauvel, P., Collins J., Dogniaux R., & Longmore J. (1982). Glare from windows: current views of the problem, *Lighting Research & Technology* 14 (1)
- Suk, J., Schiler, M., & Kensek K. (2016). Absolute glare factor and relative glare factor based metric: predicting and quantifying levels of daylight glare in office space. Syed, A. (2012). 30 St Mary Axe. (H. John Wiley & Sons, Inc., Ed.). New Jersey
- "Climate.OneBuilding.Org", n.d. NLD_ZH_Rotterdam.The.Hague.AP.063440_TMYx.2004-2018.epw. Retrieved from http://climate.onebuilding.org/WMO_Region_6_Europe/NLD_Netherlands/index.html
- Roudsari, M., S. (2018). Daylight simulation with Honeybee[+] vs Honeybee Legacy. Retrieved from <https://github.com/ladybug-tools/honeybee/wiki/Daylight-simulation-with-Honeybee%5B-%5D-vs-Honeybee-Legacy>
- Makki, M., Showkatbakhsh, M. & Song, Y. (n.d). Wallacei (Version V2.55 - 29 March, 2020) [Computer Software]. Retrieved from <https://www.food4rhino.com/app/wallacei-0#>

Photovoltaics Potential for Façade Renovations

Eleonora Nicoletti¹

- 1 University of the West of England, Coldharbour Ln, Bristol BS16 1QY, United Kingdom, tel.: +4411732 81276, e-mail: Eleonora.Nicoletti@uwe.ac.uk

Abstract

As urgent action is needed to tackle the climate crisis by lowering greenhouse gas emissions, façade renovations can improve the performance and reduce the environmental impact of the existing building stock. Integrating photovoltaics into the envelope can supply buildings with electrical energy generated from a renewable resource, limiting energy-related costs and reliance on fossil fuels. Embedding photovoltaics into façades can impact buildings' appearance and environmental performance differently depending on the solar technology used. From crystalline silicon to organic solar cells, first-, second-, and third-generation photovoltaics present varying characteristics such as energy conversion efficiency and visual qualities as well as embodied energy, durability, and recyclability. Additionally, methods ranging from solar concentration to cooling techniques may improve energy generation while reducing the amount of photovoltaic material needed. This study aims to identify the potential of photovoltaic-based technologies for integration into the building envelope, with a particular focus on façade renovation projects and improving the overall performance of existing buildings while considering the environmental impact of photovoltaics. It reviews interdisciplinary literature, design examples, and products by focusing on photovoltaics for building integration and façade renovation approaches, with attention to the whole life-cycle carbon as well as the experiential quality of solar façades. The paper proposes a framework of potential design strategies for holistically enhancing the performance of façades with integrated photovoltaics in building renovation projects and highlights possible avenues for future research on the topic.

Keywords

Building-integrated photovoltaics, solar façades, façade design, façade renovation

1 INTRODUCTION

Recently, the Glasgow Climate Pact (UNFCCC, 2021) confirmed the need for urgent action to reduce global green-house gas emissions and tackle the climate emergency. Given the large impact of the building sector on the world's energy use (International Energy Agency, 2013), solutions have been implemented to improve the energy efficiency of existing building stocks through façade renovations, and solar technologies have been deployed to supply built environments with energy generated from solar radiation which is a renewable resource. In particular, photovoltaic technologies can provide buildings with electrical energy generated from sunlight on-site by reducing energy costs for building users as well as the reliance on electricity produced from fossil fuels. Photovoltaics can be deployed in different ways on the building envelope, which has been explored for decades. Already in the 1990s, Sick & Erge (1995) examined possibilities for photovoltaic installations on roofs and external walls and shading systems, noting the similarities in assembly methods between conventional envelopes and photovoltaic façades. They stressed the importance of suitable exposure to sunlight and buildings' energy efficiency to the effectiveness of photovoltaic energy generation. While considering the development stages of photovoltaic installations for building projects, they highlighted how the earlier design phase involves dealing with issues of size, orientation, form, and colour, while later stages focus more on functional, mechanical, electrical and operational issues (Sick & Erge, 1995). Although the vertical arrangement of photovoltaics may not be optimal for absorbing sunlight, Freitas & Brito (2019) highlighted the benefit of combined energy generation from both roof and façade surfaces in urban environments. When photovoltaic technologies are embedded in the building skin by replacing conventional materials, they are identified as BIPVs, or Building Integrated Photovoltaics (Shukla, Sudhakar, & Baredar, 2016, p. 100), and their impact on the architectural image as well as on the environmental performance can vary according to the photovoltaic technology used.

With different visual and efficiency characteristics, photovoltaics are generally distinguished as first-, second- and third-generation solar cells. Crystalline silicon solar cells represent the most established technology, thus belonging to the first generation. The second generation refers to established thin-film solar cell materials like amorphous silicon, copper indium gallium diselenide (CIGS) and cadmium telluride (CdTe). On the other hand, the third-generation group involves more recent technologies that are still being improved, such as organic solar cells (Sampaio and González, 2017). There may also be strategies that are worth exploring for enhancing the performance and appearance of BIPVs, such as solar concentration, spectral conversion, the cooling of photovoltaic modules and employing high-efficiency photovoltaic cells as well as optimising and adapting geometries to local environmental conditions (Nicoletti, 2020, pp. 87-102). Photovoltaic technologies in development include dye-sensitised and perovskite solar cells, among others, as well as systems using solar concentrators. While integrating photovoltaics into the building envelope appears overall advantageous for improving buildings' energy performance with aesthetically acceptable outcomes, more needs to be understood about the life-cycle environmental impacts of BIPVs (Zhang, Wang, & Yang, 2018).

By conducting an interdisciplinary review of relevant literature, including examples of façade designs and BIPV products, this study aims to shed light on the potential of photovoltaics for façade designs within envelope renovations directed at improving building performance, with attention to the environmental impact of photovoltaics.

2 METHODOLOGY

This study explores the integration of photovoltaics into façades with a focus on envelope renovation strategies by conducting an interdisciplinary review on the topic in two stages, based on different key term searches on Google Scholar, Scopus, and Science Direct.

An initial broader review was directed at providing an overview of strategies for visually integrating photovoltaics into building envelopes, particularly in retrofit contexts. The key terms searched included "building-integrated photovoltaics" or "BIPV" or "solar façades" and "renovation" or "retrofit". Sources were selected among scholarly publications, as well as web sources where appropriate, that were found to have a focus on proposing approaches to solar façade design or exemplifying them through cases of buildings and products.

A later review concentrated on examining the environmental impact of photovoltaic technologies for façade integration, which was based on the search of the key terms including "photovoltaic" and "embodied carbon" or "embodied energy", "end-of-life", and "durability". To retrieve up-to-date information on the topic, the researcher selected scholarly sources published predominantly since 2018, with a primary focus on academic journal articles.

The following sections present and then discuss the findings of the reviews by relating reflections on solar façade design approaches in retrofit contexts to observations on the environmental impact of photovoltaic technologies for building integration towards identifying potential strategies for sustainable façade renovations with photovoltaics.

3 DESIGN AND LIFE-CYCLE CONSIDERATIONS FOR INTEGRATING PHOTOVOLTAICS INTO THE BUILDING ENVELOPE

3.1 BUILDING-INTEGRATED PHOTOVOLTAICS IN FAÇADE RENOVATIONS

The design of building-integrated photovoltaic systems is informed by multiple factors affecting the functioning and the appearance of solar architectural installations, including the angle of PV modules and shading on them as well as their temperature, which can be simulated computationally (Biyik et al., 2017). Features of the PV system that impact its performance include the overall extent of the photovoltaic surface, the solar cell type and its efficiency, the geometry of the installation, and shading and soiling of the PV modules, which can be exacerbated by unfavourable environmental conditions such as limited solar radiation and high temperatures. There may be a need for cleaning and maintenance of PV modules, with associated economic costs, while characteristics of other system components, such as energy storage devices, also need considering ((Fouad, Shihata, & Morgan 2017)). Given the complexity of the problem, there has been extensive research on designing solar façades, which has led to proposing a range of design principles that may be followed by architects.

Solar products for building integration include solutions for 'opaque' or 'transparent' and 'semi-transparent' façades within a broad range of technologies, including solar thermal and hybrid photovoltaic-thermal systems as well as adaptive 'smart windows' (Lai & Hokoi, 2015). Available solar skin products usually embed either crystalline or thin-film, amorphous silicon cells. Photovoltaic cladding components can vary in weight and flexibility from 'foil' to 'tile' products or can replace conventional weather skin modules. On the other hand, photovoltaic glazing products can vary not only in colour but also in transparency level to fulfil daylighting, shading, and electricity generation

functions (Shukla, Sudhakar, & Baredar, 2016, p.105). To achieve semi-transparency, glazing products are characterised by lower solar cell coverage, which reduces the generated energy output (Robinson, Athienitis, & Tzempelikos, 2008).



FIG. 1 Photovoltaic glass façade integrating crystalline silicon solar cells. Note. From Balenciaga Miami Design District. Photograph by Phillip Pessar, 2018, Flickr, (<https://www.flickr.com/photos/25955895@N03/46276576481>). CC BY 2.0.



FIG. 2 Thin film photovoltaic modules. Note. From Thin Film Flexible Solar PV Installation 2. Photograph by Ken Fields, 2008, Flickr, (<https://www.flickr.com/photos/51925339@N05/4783039248>). CC BY-SA 2.0.

Previous studies outlined principles for the architectural integration of photovoltaics. Schoen et al. (2001) suggested a set of criteria ranging from a seamless integration of photovoltaics and 'harmony' with the local context to unconventional designs that stand out. Similarly, Kaan & Reijenga (2004) proposed that photovoltaics may be part of architectural designs in different ways, from 'invisibly' to installations that can enhance and produce the architectural appearance or even convey novel concepts.

Guidance provided by Farkas (2013) for developing building-integrated photovoltaic systems, which refers to commercially available solar technologies, distinguishes more technical issues of 'functional' and 'constructive' nature from aesthetic aspects that need considering. Besides fulfilling building envelope functions of security, views, sound and thermal insulation, comfort, providing protection from the weather protection such as weather protection, security, thermal and sound insulation, security, ventilation and comfort, as well as energy generation, building-integrated

photovoltaic systems need to be designed with attention to their appearance by considering the overall size of the solar installation as well as the shape, size, colour, texture, the type of connections characterising the photovoltaic modules. Adaptability in the visual composition of the solar installation may be achieved by using non-active elements identified as 'dummies' and coloured photovoltaic products (Farkas, 2013). Photovoltaic modules may also be integrated unnoticeably by seemingly 'blending' photovoltaic cells with the building skin, as highlighted by Corti et al. (2018, p. 93) by presenting a case study located in Zurich, although this type of solution reduces the efficiency of photovoltaic modules. Nonetheless, as Scognamiglio (2021) pointed out, the 'visual performance' is not to be overlooked, as it determines people's acceptance of solar installations. Kuhn et al. (2021) highlighted two alternative avenues for integrating photovoltaics into the visual design of façades: either to make the solar cells distinguishable within the façade design and use them as modular elements to compose patterns or to make the solar cells invisible by applying front covers that produce a coloured effect but also reduce the energy generation efficiency (Kuhn et al., 2021, p. 14). As noted by Scognamiglio (2017), 'preservation laws' may pose obstacles to the integration of photovoltaics into buildings within certain settings (Scognamiglio, 2017, p. 192), where their visual contrast with the context might need to be minimised. Xu and Wittkopf (2014) pointed out that the visual impact of building-integrated photovoltaics may not be easily predictable if evaluated according to qualitative indicators and proposed the use of saliency maps for measuring the visual impact of photovoltaics integrated into the envelopes of historical buildings. Thus, the invisible integration of photovoltaics may be particularly suitable for renovations in historical contexts.

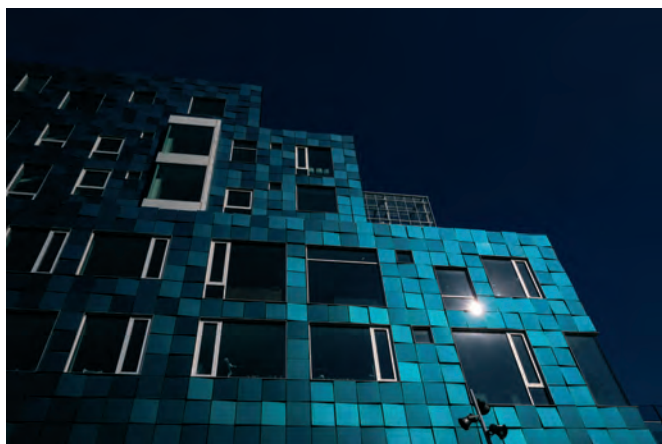


FIG. 3 Photovoltaic cladding of the Copenhagen International School designed by C.F. Møller Architects. Note. From Copenhagen International School. Photograph by Stig Nygaard, 2019, Flickr, (<https://www.flickr.com/photos/10259776@N00/48338691067>). CC BY 2.0.

Polo López, Troia & Nocera (2021) explored the integration of photovoltaics into heritage buildings, noting that new interventions should be easy to distinguish and remove from the pre-existing artefacts without damaging them, and they should also be minimally invasive as well as compatible with the original buildings in terms of construction and aesthetics. Within their study, two Swiss case studies also exemplified the integration of photovoltaics into heritage buildings: a farmhouse from the 19th century, presenting roof-integrated, anti-reflective solar modules resembling traditional terracotta tiles, and a family villa from the late 1930s, where the roof was instead fully replaced by highly reflective solar panels of blue colour. It was shown that a design choice can be made between visually blending photovoltaic installations with the existing building and replacing entire parts of the envelope with new materials to prioritise the energy performance enhancement.

Building renovations do not always involve intervening in protected areas on artefacts with historical and cultural value. Evola & Margani (2014) showed that using photovoltaics in renovating the façade

of a poorly energy-efficient block of flats built during the second half of the 20th century can improve its performance towards zero-energy standards, enhance its architectural image and increase its commercial value. Martín-Chivelet et al. (2018) showed how replacing an existing polymer concrete skin with a BIPV ventilated façade system can improve a building's energy efficiency and appearance while providing it with a source of electrical energy. It can be observed that there may be renovation cases in which the building energy upgrade becomes the priority, and more freedom may be given to the designer on how to transform the architectural image through façade integrated photovoltaics.

In a study on designing solar façades for visual engagement, Nicoletti (2020) proposed a framework for conceiving solar architectural skins capable of attracting attention and interest, involving strategies inspired by media façades for producing motion impressions in various ways through static solar envelopes. The framework considered the architectural potential of photovoltaics that are still in development, highlighting strategies for increasing the efficiency of photovoltaics, such as improved geometries, spectral conversion, using optical devices with low-concentration ratios, and ventilated systems for cooling solar modules. These strategies may even be used to display contents like images or patterns and add visual qualities to the building envelope, such as colour, reflectivity, refractivity, or luminescence. Existing façade designs with similar visual properties may serve as references for developing innovative designs integrating more efficient photovoltaic-based technologies (Nicoletti, 2020). However, while new photovoltaic solutions for their building integration are being explored, the environmental impact of the technologies used needs to be taken into account.

3.2 ENVIRONMENTAL IMPACT OF PHOTOVOLTAICS

Photovoltaic technologies continue to be developed. While silicon solar cells currently prevail among commercial products, other photovoltaics are being improved in terms of efficiency, stability, durability, stability material composition and costs (Ontiri & Amuhaya, 2022). While the energy generation efficiency needs to increase and cost needs to be reduced, it is important to understand the environmental impact of photovoltaics in the long run (Zhang, Wang, & Yang, 2018). The durability and operational performance of photovoltaics may be improved by superhydrophobic coatings facilitating the cleaning of solar modules and preventing the accumulation of dust or ice (Wu et al., 2021), potentially avoiding the breakage of glass covers or solar cells that are, according to Kim et al. (2021), among known causes of solar panel degradation, along with the penetration of moisture (Segbefia, Imenes, & Saetre, 2021), which is likely to stimulate research on high-performance encapsulants for better protecting solar cells (Gaddam, Pothu & Boddula (2021). However, more research is needed on how the whole life cycle of BIPVs affects the environment (Yan, 2019).

Bartie et al. (2022) suggested that the spread of photovoltaics contributes to depleting the planet's natural resources, as the technology involves the use of valuable materials such as precious metals. By analysing the life-cycle and cost of rooftop photovoltaic systems in the European context, Martinopoulos (2020) questioned their sustainability which may vary according to factors such as the geographic area and its climate, the local energy supply, the impact of transportation and cleaner energy generation systems that may be introduced in the future. According to Ludin et al. (2018), mono-crystalline silicon products have the worst impact among photovoltaic technologies in terms of energy use, energy payback time and greenhouse gas emissions. Nonetheless, as highlighted by Muteri et al. (2020), the results of evaluations on the life-cycle of photovoltaics can vary depending on the scope and methods of each assessment.

As highlighted by Piasecka (2020), the negative environmental impacts of photovoltaic systems are those of production and end-of-life processes that are energy- and material-intensive. The disposal

of PV systems can be harmful due to the presence of materials such as lead and cadmium, among others, thus, requiring careful recycling (Piasecka, 2020). End-of-life processes in the life-cycle of photovoltaics can produce dangerous waste which may contaminate potable water if dispersed in the environment, so there is an urgent need for accelerated implementation of recycling solutions through rapid developments in technologies and policies (Chowdhury et al., 2020). The inadequate disposal of photovoltaic system elements can cause the leaching of carcinogenic materials, including lead, cadmium, and arsenic (Nain & Kumar, 2020).

Lamnatou & Chemisana (2019) conducted a review on different photovoltaic technologies with a focus on their life cycle assessment, noting that existing studies on the topic are predominantly on crystalline silicon photovoltaics, and more is to be researched about less established solar cell types. While it was suggested that the environmental impact of façade-integrated photovoltaics is comparable to that of optimally oriented solar panels installed on roofs, the benefits depend on local conditions. Instead, known negative impacts of thin-film photovoltaic technologies include the human and environmental toxicity of some of the materials used, e.g., cadmium in CdTe solar cells or lead in the otherwise very promising perovskite solar cells. Third-generation photovoltaics, such as organic solar cells, are much less durable and efficient in generating electricity but may offer potentially lower environmental impacts, including a reduction in life-cycle greenhouse gas emissions, in comparison to conventional silicon photovoltaics. On the other hand, concentrating photovoltaics can replace large amounts of solar cell material with optical devices that direct sunlight onto smaller photovoltaic areas, with potential economic and environmental benefits that could be investigated further. Negative environmental impacts of photovoltaic systems are also associated with energy storage devices, their manufacturing and their relatively short life span. While recycling photovoltaics may be advantageous, it is evident that there is a need for more research on the end-of-life processes and their environmental impacts (Lamnatou & Chemisana, 2019). Recycling photovoltaic modules can be less energy-intensive than producing new products. Recycling thin-film photovoltaics can be economically advantageous, and chemical recycling may be preferable to mechanical and thermal processes in terms of environmental impact (Padoan, Altimari, & Pagnanelli, 2019). Lamnatou et al. (2020) also highlighted the environmental problems associated with storage elements of solar energy systems, with notes on embodied energy as well as the toxicity, fire hazard, and recycling issues of batteries in the context of BIPV and hybrid photovoltaic and thermal systems. End-of-life processes should be further improved with attention to the toxicity of the involved substances and the environmental impact of transportation (Lunardi et al., 2018), which was also noted by Seo, Kim & Chung (2021) and Celik et al. (2020).

Lisperguer et al. (2020) emphasised the importance of reducing the environmental impacts of current PV recycling methods relying on thermochemical processes, which suggests the need for more careful design from the onset of the life-cycle of photovoltaics. According to Deng et al. (2019), photovoltaic products should be easier to disassemble and recycle without involving harmful substances, and manufacturers could be responsible for the end-of-life stages. There need to be developments not just in the technologies for effective end-of-life processes but also in the socio-economic and policy aspects impacting them, which requires engaging the relevant stakeholders (Salim et al., 2019), techno-economic evaluations (Heath et al., 2020), and potentially, economic incentives for recycling practices (Sica et al., 2018). According to Lamnatou, Smyth, & Chemisana (2019), who examined the environmental and human toxicity of photovoltaics in particular, the system elements with the highest negative impact are the PV cells. Freier et al. (2018) noted that employing static non-imaging solar PV concentrators may lead to reducing the use of photovoltaic material as well as the environmental impact of photovoltaic systems. Ziemińska-Stolarska, Pietrzak & Zbiciński (2021) highlighted that those systems with concentrators achieve higher performance than those without and suggested an approach for assessing their life-cycle environmental impact. Freier Raine et al. (2021) compared the embodied energy and the cost of a static concentrating

photovoltaic module to that of a conventional flat module of equal electrical output, concluding that the concentrating photovoltaic solution involves lower embodied carbon but higher costs, thus requiring a trade-off to reach commercial viability. On the other hand, using solar concentrators may have a positive impact on the overall durability of photovoltaics, as breakage in the optical device can have a small detrimental effect on the system performance (Alzahrani et al., 2020). Thus, concentrating photovoltaics may potentially reduce the negative environmental impacts of photovoltaic technologies.

4 RESULTS

The previous sections showed that various photovoltaic technologies are available for building integration, and while some are commercially established, others continue to be developed to achieve better performance levels. It was found that different approaches for embedding photovoltaics into the building envelope have been proposed so far that suggest ways of visually integrating energy-generating components into façades. Those approaches are based predominantly on the use of crystalline silicon photovoltaics as well as some thin-film technologies. Common ways of adapting the appearance of photovoltaic installations for building integration involve colour alterations that can make solar modules resemble conventional building components or, instead, compose innovative designs. However, such solutions tend to reduce energy generation efficiency. As this depends on the extent of the active photovoltaic area, integrating solar cells into glazed elements to achieve semi-transparency involves reducing the photovoltaic cell coverage and, therefore, the generated energy output. Developing technologies such as concentrating photovoltaics may expand the possibilities for the visual integration of solar cells into façades with qualities such as reflectivity, refractivity and luminescence while increasing the energy generation efficiency with reduced amounts of photovoltaic materials. In façade renovation projects, photovoltaics may be integrated into the envelope invisibly or in a distinctive way. The latter option may be less suitable for heritage contexts, but in other cases, it can offer possibilities for exploring the visual communication potential of photovoltaics. With or without an innovative design that stands out, solar cells may be clearly distinguishable or not.

On the other hand, it was found that the environmental impact of photovoltaics throughout their whole life cycle is not negligible. Not only do the greenhouse gas emissions of production stages need more careful consideration, but also the durability of photovoltaic technologies needs to be improved to prevent breakages and degradation, for instance, due to moisture penetration. There are serious concerns about the end-of-life management of photovoltaic systems waste, which needs to be improved to reduce environmental and human health risks as well as the depletion of natural resources such as precious metals. More effective recycling processes need to be implemented with attention to minimising carbon emissions and pollution also due to transportation. Solutions must be found to problems such as the toxicity of certain materials used in photovoltaics and the possible contamination of drinking water. A greater effort is required to design photovoltaic installations for building façades that can be easily disassembled and recycled.

Given the environmental impact of solar cell materials, their continuing development and the relative uncertainty around the environmental impact of certain stages of their life-cycle, it can be suggested that a cautious approach to integrating photovoltaics into building façades would be appropriate. Reducing the amount of solar cell materials used and replacing them with materials with known, low environmental impact could improve the overall sustainability of solar façades. Adopting strategies for improving the performance of photovoltaics, such as solar concentration with low-concentration optical devices, spectral conversion or cooling, may increase the energy generation efficiency of photovoltaic installations with reduced solar cell coverage and improve their

environmental impact. However, more research is needed to develop such systems for façade integration, and the environmental impact of materials that would replace solar cells also needs to be investigated in depth.

5 CONCLUSIONS

In conclusion, this research has identified a range of possible strategies that may be pursued and further investigated towards enhancing the performance of photovoltaics integrated into façades in renovation projects, with attention to the façades' appearance and energy generation efficiency as well as the environmental impacts of solar technologies.

In architectural renovations, photovoltaic installations may be integrated into existing buildings to improve their energy performance as well as their appearance. They may visually blend with the rest of the building envelope and be in harmony with the surrounding context, or they may stand out with an unconventional design that can be composed through the arrangement of photovoltaic modules, with the solar cells being clearly distinguishable or not.

Reducing the solar cell coverage could lower the life cycle environmental impacts of photovoltaic façades but would also decrease the generated energy output. Developing solutions for increasing the efficiency of photovoltaics with smaller amounts of solar cell materials could improve the sustainability of solar façades. Strategies to be explored include the façade integration of low-concentration optical devices, spectral converters, and structures facilitating natural ventilation for the cooling of solar modules. These elements could visually enrich photovoltaic façade designs for building renovations with qualities such as colours, light reflections and refractions. However, more research is needed on their materials and associated environmental impacts.

Acknowledgements

This research was funded by the Faculty of Environment and Technology at the University of the West of England and builds on the author's PhD thesis Design of Effective Solar Architectural Skins for Visual Engagement, completed with the University of Brighton / University for the Creative Arts.

References

- Aldridge, D. (2005) Introduction to foamed concrete: what, why, how? University of Dundee
- Bauder, H.-J., Wolfrum, J., Caliskan, M., Gresser, G. (2015) Entwicklung gewebter Abstandsstrukturen für gekrümmte Bauteile, Melliand Newsletter 10/2015
- Gilka-Bötzow, A. (2015) Stabilität von ultraleichtem Schaumbeton - Betrachtung instationärer Zustände. TU Darmstadt
- Gries, T., Veit D., Wulfhorst, B. (2019) Textile Fertigungsverfahren: Eine Einführung, Hrsg. Carl Hanser Verlag, 3. Aufl., München
- Koch, A., Lüling A. (2017) BasFlair - Basaltfasern als ökologische Bewehrung für Textilbeton, Abschlussbericht des Projektpartners RWTH Aachen – ITA im Rahmen des Zentralen Innovationsprogramms Mittelstand (ZIM)
- Kulas, C.H. (2013) Zum Tragverhalten getränkter textiler Bewehrungselemente für Betonbauteile, Dissertation Fakultät Bauingenieurwesen, RWTH Aachen
- Lüling, C., Richter, I., (2018) Architecture Fully Fashioned - Exploration of foamed spacer fabrics for textile based building skins. Delft: Journal of Façade Design and Engineering, 1/2017, pp. 77-92, doi: <https://doi.org/10.7480/>
- Lüling, C., (2019) Architecture Fully Fashioned - Abstandstextilien in der Architektur Melliand Newsletter Online Ausgabe 9/2019
- Rybin, V., Utkin, A. & Baklanova, N. (2012) Alkali resistance, microstructural and mechanical performance of zirconia-coated basalt-fibers. Institute of Solid State Chemistry and Mechanochemistry, Novosibirsk
- Wolfrum, J., Bauder, H.-J., Caliskan, M., Gresser, G., Toma, B., Wendel, R., Rosenberg, P., Henning, F. (2017) Aus einem anderen Blickwinkel – ORW-Verfahren für RTM-Strukturbauteile, Kunststoff 2/2017

Suntex: Weaving Solar Energy Into the Building Skin



**Pauline van Dongen^{*1}, Ellen Britton¹, Anna Wetzel¹, Rogier Houtman²,
Ahmed Mohamed Ahmed³, Stephanie Ramos²**

* Corresponding author, pauline@paulinevandongen.nl

1 Pauline van Dongen, Netherlands

2 Tentech, Netherlands

3 Delft University of Technology, Netherlands

Abstract

The key objective of this research project is to "create a new architectural textile, Suntex, by interweaving thin film solar cells and electrically conductive yarn into a structural technical textile, so it can generate energy while it is providing shade, structure or an aesthetic update to a building."

Textile has strong potential as a sustainable building material because it can be lightweight, material efficient, and low carbon. Moreover, its flexibility provides great design freedom and its transparency makes it very suitable for façade applications, maintaining views to the outside while providing solar shading. Suntex is a solar textile, currently in development, intended for textile architecture applications like textile façades. By combining three qualities, namely providing the building with energy generation, solar shading, and a unique aesthetic appearance, which also promotes the acceptance of solar technology, it offers a positive climate impact.

Suntex can be considered as a new type of membrane material for Building Integrated Photovoltaics (BIPV). With this innovative, constructive fabric, enormous surfaces that are still unused can be outfitted with energy-generating potential.

This paper presents a design case to analyse the potential impact of Suntex as a textile façade. Based on insights into the development process and experiment results so far, it evaluates the feasibility and impact from a technical and design perspective.

Keywords

Textile architecture, solar textile, energy innovation, lightweight structures, BIPV

DOI 10.47982/jfde.2022.powerskin.28

The “Invisible-Solar-Panel” – Coloured Photovoltaic Panels with High Efficiency

Christof Erban*

- SUNOVATION Produktion GmbH, Glanzstoffstraße 21, 63820 Elsenfeld Germany, Tel: +49 6022 26573 32, christof.erban@sunovation.de

Abstract

We introduce a concept for coloured photovoltaic modules intended for the integration into buildings. The colour effect we utilise is based on transparent effect pigments that are screen printed onto the rear side of the cover glass of the photovoltaic modules. We compare this new approach with the current approach to either use coloured solar cells or absorption pigments also printed onto the cover glass. Using data taken from proof-of-concept modules, we have shown the extraordinary performance in terms of electrical output and optical appearance. Large-area sample modules have been manufactured to verify the laboratory results.

Keywords

Building integrated photovoltaics (BIPV), colour effect pigment, biomimetics, colour photovoltaic modules, optical losses

1 INTRODUCTION

The steadily increasing demand for electricity leads to an exponentially growing market not only for photovoltaics (PV) in general but also for building integrated photovoltaic modules. As shown by (Fischer, Woodhouse, Herritsch, Trube, 2022), the global shipments of PV modules reached 183 GWp in 2021, with a worldwide total capacity of 940 GWp installed. 20% of all the PV modules ever installed since 1954 have been put into operation in 2021. The growth rates for building integrated photovoltaics (BIPV) are predicted to reach about 40% (Ballif, Perret-Aebi, Lufkin, Rey, 2018), and thus the question arises of what the installed BIPV will look like. In a market study performed by (Erban, Ley, 2020) within the R&D project PrintPero – funded by the German Government under 03SF0557B –, the requirement of a flexible colour appearance has been ranked third important out of seven categories by architects, consultants, scientists and owners. First was freedom of size, and second was the combination with other building functions.

Since solar cells are optimised for the generation of electricity, practically all changes lead to a reduction in electrical performance and, thus, to price increases for the generated electricity. This is also true for the development of coloured solar modules, as the colour perceived by the observer cannot be transferred into electricity by the solar cell any longer. Therefore, the scope of the work described in this paper is to develop modules with a wide range of colours that, at the same time, provide high electrical efficiency.

2 COLOURED PHOTOVOLTAIC MODULES

As has been shown as an overview by (Eder et al., 2019) and discussed by (Kuhn, Erban, Heinrich, Eisenlohr, Ensslen, & Neuhaus, 2020), crystalline BIPV modules typically consist of a composition of principally three materials: glass, interlayer and solar cells. The colour appearance of the glass(es) and the interlayer(s) can be modified either by changing their bulk material or their surfaces by either single or multiple printings or coatings. The cells' colour can be altered by altering the thickness of their anti-reflex coating.

The colour itself can either be generated by absorption pigments or by coatings/pigments utilising the interference of incident light. A comparison of solar modules utilising three technologies has been shown by (Kutter, Bläsi, Wilson, Kroyer, Mittag, Höhn, Heinrich, 2018) and a development of a photonic concept by (Bläsi, Kroyer, Kuhn, Höhn, 2021). In contrast to (Basher, M., Nur-E-Alam, M., Rahman, M., Hinckley, S., and Alameh, K., 2022), a homogeneous colour appearance is intended in their and our works.

2.1 COLOURED PHOTOVOLTAIC MODULES USING COLOURED SOLAR CELLS

The colour of photovoltaic cells and modules has indirectly been developed ever since photovoltaic cells were developed as such. The reason is the continuous attempt to increase the cells' efficiency, e.g. by introducing coatings or surface structures on the cells' front surface. Uncoated /non-surface structured silicon, as shown in Figure 1 - left (Erban, 2000), has a shiny silverish appearance with high reflectance. Silicon-nitride coatings lead to darker colours, as shown in Figure 1 – middle, on a multi-crystalline wafer and on a surface-structured mono-crystalline wafer in Figure 1 - right. Colours – mostly blue and black – were the by-product of the attempt to reduce reflection, improve passivation and thus increase the efficiency of the solar cells.

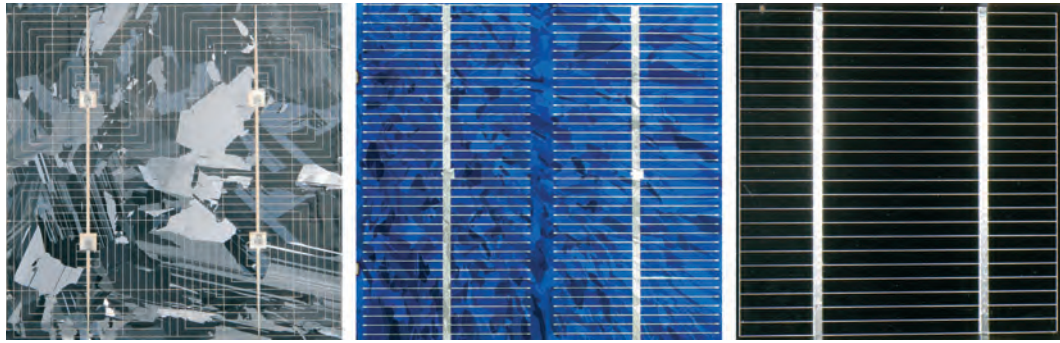


FIG. 1 Silicon solar cells as manufactured in the late 1990ies. Left: Kyocera 4-inch, multicrystalline uncoated, middle: AEG Telefunken 4-inch multicrystalline SiN coated, right: ASE, 4-inch monocrystalline SiN coated

Early suppliers of those cells in the 90ies were BP-Solar, Kyocera, Photowatt, AEG Telefunken (later ASE) and Solartec s.r.o.

The colour of the coated cells originates from the constructive interference of their SiN front coating, which not only changes with its thickness – as can be seen in Figure 2. (Raacke, 2022) -. In addition, it changes with the viewing angle, as can be seen in Figure 3 (Mod. from Raacke, 2022).

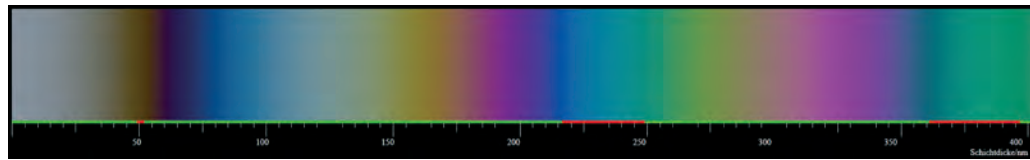


FIG. 2 Appearance of SiN-coated silicon crystal PV cell when varying the thickness of the coating on its front surface (Raacke, 2022).

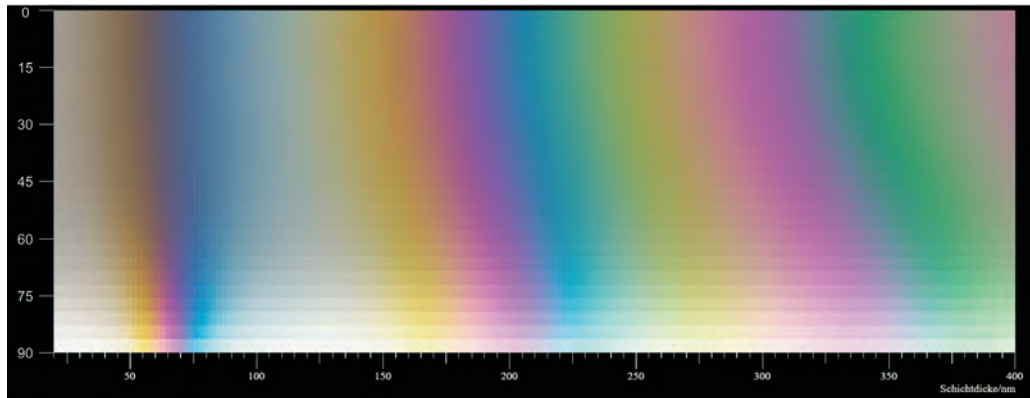


FIG. 3 Viewing angle dependency of SiN-coated silicon crystal PV cell when varying the thickness of the coating on its front (Mod. from Raacke, 2022).

The drawbacks of this early approach to utilise coloured solar cells are manifold. The price of coloured PV cells is significantly higher compared to conventional cells for the following reasons:

- The price for conventional cells is given in, for example, US\$/ Wp. As the intentional colourisation of the cells reduces their power output, the price per watt necessarily increases.
- The additional SiN coating required to achieve the desired colour is performed on the machines regularly used when manufacturing cells. As the duration to achieve the desired coating thickness is

three to six times as long as for conventional cells depending on the colour, the costs for coating not only rise proportionally, but the machines are not available for coating conventional cells.

- Solar cells are classified according to their power output into so-called BIN classes, and only cells of identical power output can be used within a solar module. Combining solar cells of different BIN classes results in excessive power loss due to cell mismatch. The coloured cells which cannot be used within a project still have to be paid for as they rarely can be sold elsewhere.
- The colour matching of the desired number of solar cells results in additional effort and costs.
- The colour stability significantly changes with the angle of perception, especially for multicrystalline solar cells, as the colour effect originating from the coating is superimposed by the local variation in the lattice structure of the bulk silicon material.
- The accuracy of colour matching of coloured PV cells is complicated since the colour of PV cells changes when it is embedded. The reason is the difference in the refractive index between air (when the colour is inspected during manufacturing) and the interlayer that serves as bonding between the cell in between the front glass. The change of colour by cell-interlayer-glass coupling is illustrated in Figure 4, where a monocrystalline photovoltaic cell is partly covered – thus optically coupled onto its surface glass – by a liquid interlayer.

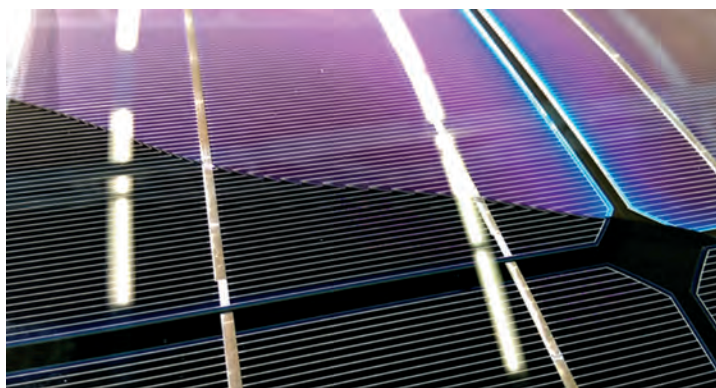


FIG. 4 Change of cell colour appearance due to cell-interlayer-glass coupling.

Cells that might look identical when not embedded might show significant colour differences when embedded and illuminated with natural daylight, as shown in Figure 5.



FIG. 5 Colour variation of cells that seemed to be of identical colour when not embedded.

First crystalline silicon cells with intentional modifications to achieve coloured solar cells were shown by (Tölle, Bruton 2000) and (Devenport, Roberts, Bruton, Heasman, Brown, Cole, Baistow, Webster, & Garrard, 2009). A systematic overview of how and at which location colours can be

introduced in PV modules is presented by (Kuhn, et. al., 2020) and a technology status by (Stamenic, Erban, 2021). Coloured crystalline silicon solar cells – with the exemption of blue and black, where the transformation from the non-coated silver solar cells to blue or black results in a performance improvement – always generate less electricity than non-coloured modules.

One of the first projects making use of coloured solar cells is the Photovoltaic façade of the Museu Nacional de la Ciència I la Tècnica de Catalunya in Terrassa, Figure 6 (MNACTEC).

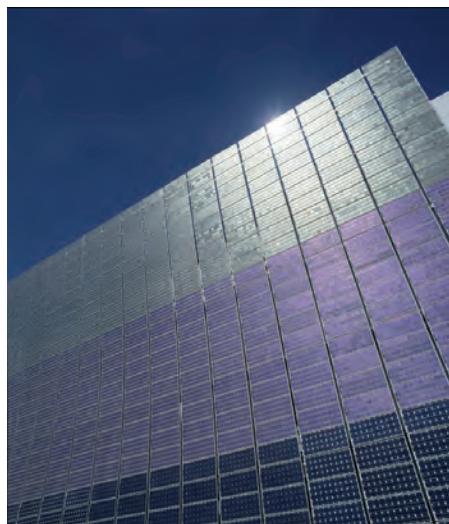


FIG. 6 One of the first projects using coloured solar cells is the Museu Nacional de la Ciència I la Tècnica de Catalunya in Terrassa (MNACTEC)

2.2 COLOURED PHOTOVOLTAIC MODULES USING ABSORPTION PIGMENTS

In order to achieve coloured solar panels using absorption pigments, the glass in front of the solar cells needs to provide the colour effect and hide the cells behind. Typically, the colour is either digitally or screen-printed. The colours being used are described and defined in so-called colour models or colour spaces such as CMYK (cyan, magenta, yellow and key), RGB (red, green, blue), HIS (hue, intensity, saturation) or CIE-L*a*b* (where L* represents the perceptual lightness, a* represents the red/green value and b* represents the blue/yellow value). The colours can – within limitations – mathematically be transformed into each other; for example, red is generated by adding magenta and yellow. The origin of the limitations of mathematical transformability is that the above colour spaces have different sizes. Since the CMYK colour space is smaller than the RGB colour space, CMYK colours can be transformed into RGB, whereas not all RGB colours can be transformed into CMYK. Likewise, printers based on CMYK colours cannot print certain RGB colours outside their CMYK colour range. The exact numbers on how to achieve a specific red are device-dependent. So-called ICC profiles provide the exact formulas on how to describe the transformation of an identical colour in different colour spaces for the specific printing method being used.

When combining colours and solar cells, it is obvious that the electrical performance of the cells depends on the transparency of the colour in front of them, which, in turn, depends on the colour itself and the density it is printed. Thus: coloured solar modules always generate less electricity than non-coloured modules.

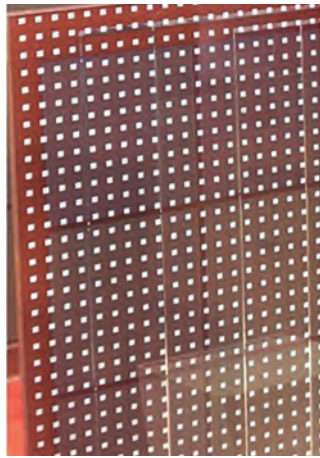


FIG. 7 PV module utilising a front glass featuring white screen printing.

Figure 7 shows a PV module utilising a front glass with white screen printing. The density of the printing is very high to achieve a bright white appearance; with the consequence that no light can pass through the printed areas. The power loss is directly proportional to the printed area and can reach values close to 100% if a homogeneous colour appearance is desired.

Higher power output can be achieved by using semi-transparent colours. Figure 8, left, exemplarily shows the spectral transparency of a 1mm thick soda-lime glass printed with cyan in saturations from 20 to 100%. As can be seen, cyan increasingly absorbs yellow and red with the consequence that, on the one side, the intensity of the colour cyan increases (as can be seen in Figure 8, left) and, on the other side, the red and yellow photons cannot be converted to electricity by the solar cell. On the right, Figure 8 shows a microscopic image (magnification 200x) of a 40% printed glass. It is important to note that the change of saturation necessarily changes the thickness of the colour since – as can be seen on the right – the printed dots begin to overlap with increasing saturation instead of being printed side by side.

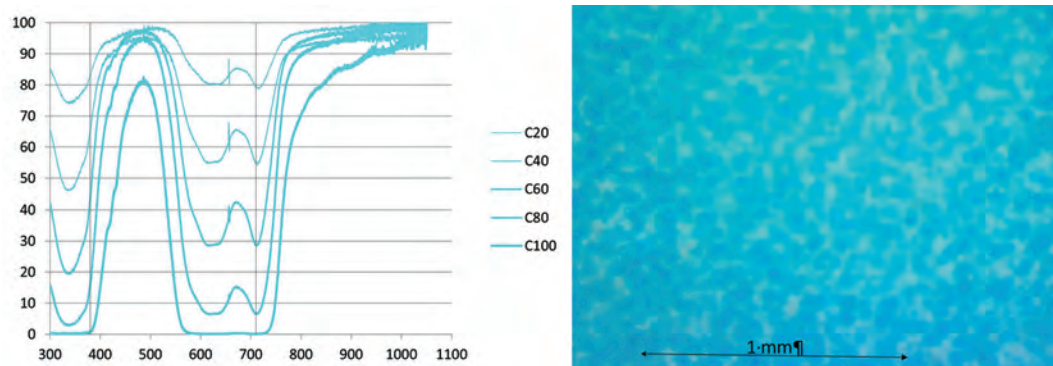


FIG. 8 Left: Spectral transparency of a 1mm soda-lime glass printed with cyan with 20%, 40%, 60%, 80% and 100% saturation. Right: Microscopy image (magnification 200x) of 1mm soda-lime glass printed with cyan with 40% saturation.

In conventional printing, it is always assumed that the media to be printed has a white colour. Thus, in areas not covered with ink, the underlying paper will appear in white. In areas that contain a low colour saturation, the underlying white medium will increasingly shine through.

This is illustrated in Figure 9 (no optical coupling has been applied between printed glass and the glossy white paper).



FIG. 9 4mm low iron glass printed in semi-transparent CMYK-White colours with increasing saturation from top to bottom as colour sample placed in front of a glossy white paper as reflecting surface.

In contrast, the glass area used in a solar panel that is not covered by paint will appear transparent, and the underlying solar cell will become visible. This is illustrated in Figure 10, where, again, no optical coupling has been applied between the printed glass and the glossy black paper serving as a dark background.



FIG. 10 4mm low iron glass printed semi-transparent CMYK-White colours with increasing saturation from top to bottom as colour sample placed in front of a glossy black paper as reflecting surface.

In order to make semi-transparent CMYK colours visible in front of solar cells, a second translucent printing in white is required, located between the colour and the solar cell. This white layer serves as a spectrally non-selective, thus broadband reflector, as shown in Figure 11.

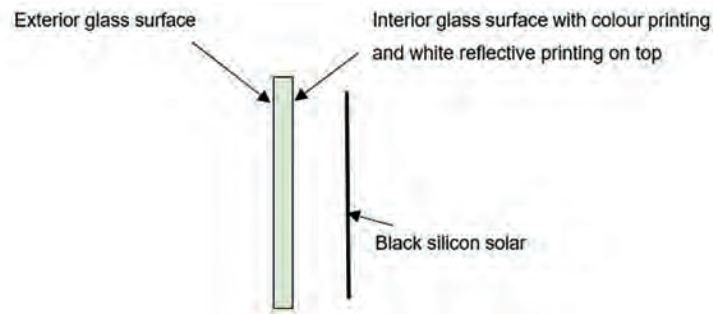


FIG. 11 Section illustrating the location of the colour printing and the white printing serving as a broadband reflector between colour printing and silicon solar cell.

Figure 12 shows the spectral transparency of a 1mm thick soda-lime glass printed with cyan, magenta, yellow and white, each in saturations 40%.

As can be seen, all colours – and especially white – significantly absorb light in the range the crystalline silicon solar cells are able to convert light into electricity (300 – 1100nm). Thus, the power loss of the solar cells increases with the amount of colour being printed.

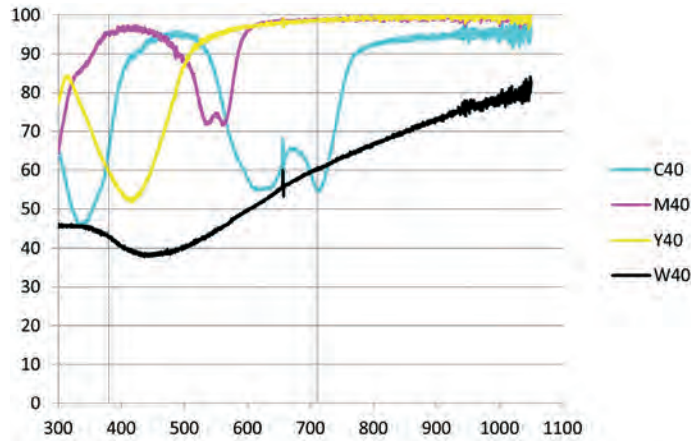


FIG. 12 Spectral transparency of a 1mm soda-lime glass printed with cyan, magenta, yellow and white each with 40% saturation.

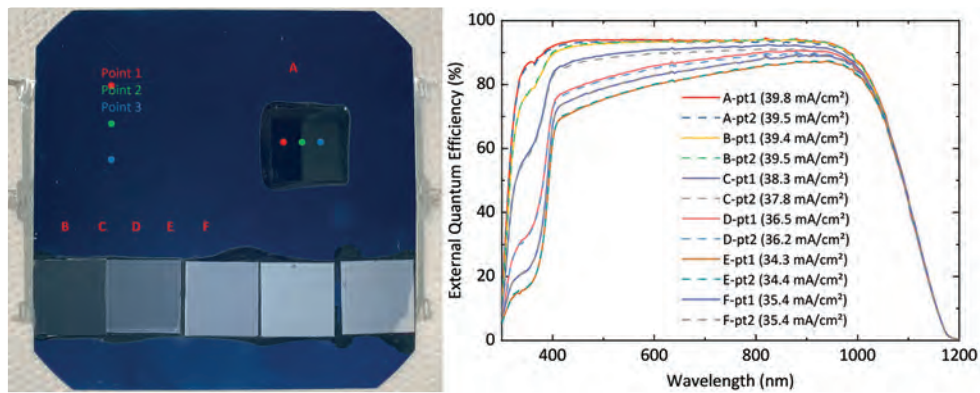


FIG. 13 Left: 0,16mm thick borosilicate glass square transparent (top) and digital printed glass squares with 20%, 40%, 60%, 80% 100% white saturation (bottom) embedded onto a 5" SUNPOWER cell. Right: 12 EQE curves of the indicated locations on the SUNPOWER cell to the left.

Figure 13 shows the effect of increasingly white printing upon the External Quantum Efficiency (EQE) of a monocrystalline SUNPOWER IBC solar cell.

This technology has successfully been developed and used during the development of coloured Perovskite Solar Cells. (Eggers, H., Gharibzadeh, S., Koch, S., Schackmar, F., Ritzer, D., Abzieher, T., Richards, B. S., Erban, C., & Paetzold U.W. 2022)

2.3 COLOURED PHOTOVOLTAIC MODULES USING TRANSPARENT EFFECT PIGMENTS

A different and innovative way to achieve coloured solar panels is using transparent effect pigments screen-printed onto the rear side of a low-iron glass in front of the solar cells. Transparent effect pigments are known from the mother of pearl that covers the inside surface of sea shells or from the silverish scales of fish. In contrast to the multilayer photonic concept called MorphoColor introduced by Fraunhofer ISE (Bläsi, Kroyer, Kuhn, Höhn, 2021), the colour effect using transparent effect pigments results in incident light reflecting on the top and bottom surfaces of single pigment particles that have a wavelength-dependent phase shift towards each other due to the thickness of the particle. All particles show a broadband reflection and transmission, as shown in Figure 14. The distinct reflection maximum depends on the thickness of the particle and leads to a distinct transmission maximum of the corresponding colour.

The pigment particles are embedded into a matrix of ground glass screen printed on the surface of the cover glass, as shown in Figure 14, and burned into the glass surface. The carrier glass and the molten glass particles containing the nanoparticles become one non-separable glass unit. Since the pigment particles are spatially distributed in the molten glass layer, each particle faces a reflection/transmission interaction with its surrounding particles. Given the strong interdependence of the interference on the phase shift, the optical responses for both reflection and transmission are wavelength-dependent and can be tuned to realise colourisation. It is important to note that the colour perception of a layer of these pigments is always a statistical response to many scattering events. As can be seen in Figure 15 right, the perceived colour of the reflected light corresponds to the wavelength of the peak reflection.

To enhance the colour angle stability, the colour pigments are then additionally coated with materials that generate a rough surface as the outer shell of the transparent effect pigments.

The key advantage of these transparent effect pigments over absorption pigments is their very low absorption loss. The pigments can be processed fully from low-absorptive materials. Consequently, the entire colourisation layer primarily transmits incident light, and a comparatively small amount of light is reflected and thus lost for the energy conversion of the underlying solar cell.

A mathematical description of interference with irradiance from one single side has, for example, been described by (Krauter, S., Grunow, P. 2006).

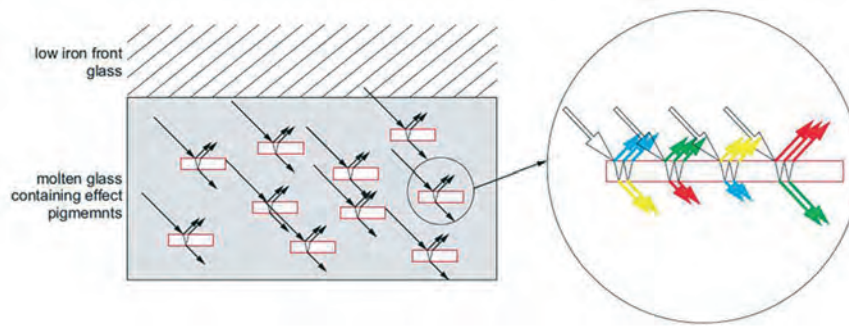


FIG. 14 Working principle of a transparent effect pigment, causing a broadband reflection with a peak in the red spectrum resulting in a transmission peak of its corresponding colour green.

Figure 15 shows the spectral transmission (left) and reflection (right) of the three exemplary investigated colours red, blue and green. As can be seen, all colours provide a high broadband transmission in the spectral range from 300 to 1100nm, which is desirable for their use in combination with crystalline solar cells. Therefore, the broadband reflection in the same spectrum is comparatively low. Due to this low reflection, a homogeneous black surface is required behind the pigment to prevent the outshining of the desired reflected colour by a rear-side irradiance. A rear-side irradiance would likewise traverse the same way through the transparent effect pigments with a resulting constructive interference; the initially reflected light would be superimposed by transmitted rear-side irradiance. This would lead to a mixing of complementary colours resulting in a non-coloured white light. Consequently, no colour impression can be observed. In coloured photovoltaic modules, this dark absorbing surface is provided by the broadband and highly light-absorbing solar cells.

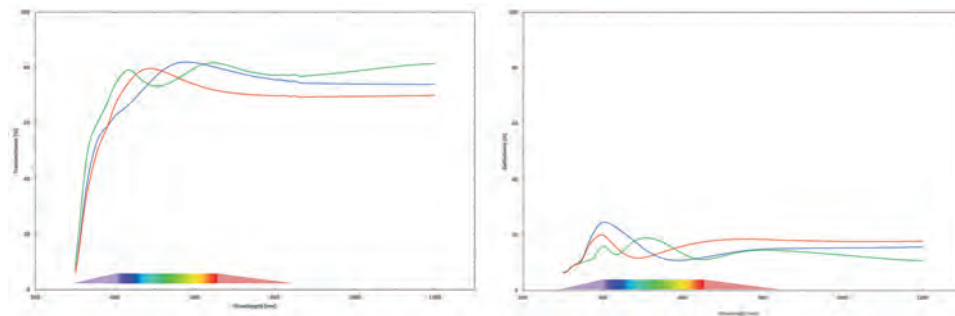


FIG. 15 Left: Spectral transmittance of a 4mm low-iron glass printed using red, green and blue effect pigments. Right: Spectral reflectance of a 4mm low-iron glass printed using red, green and blue effect pigments.

Figure 16 shows the three colour samples whose transmission and reflectance have been shown in Figure 15.



FIG. 16 The three colour samples investigated: red, blue and green.

Figure 17 shows the EQE of a SUNPOWER IBC cell, as shown in Figure 13, that is located behind a red, blue and green printed glass shown in Figure 16 in comparison to the solar panel with a transparent glass in front. The reduction in power induced by the screen-printed colour for red is -12,2%, for blue -10,2%, and for green -7,8%. Since the EQE of this specific solar cell shows a very small difference in the range of 400nm to 1000nm, the EQE curve is practically similar to the transmission curves of the screen-printed glass.

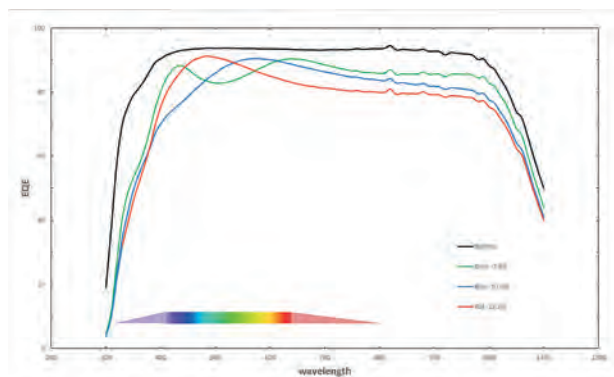


FIG. 17 External quantum efficiency (EQE) of green, blue and red SUNOVATION colour collection CQ compared to the non-covered solar cell (black).

Since interference colours generally are prone to colour variations – as the optical path length depends on the viewing angle – the following series of photographs (Figures 15 to 17) of the red, blue and green colour samples and two grey colour samples have been taken on the 17th and 18th of May 2022 at: 49° 55' 26,292 N at 9° 9' 0,198" E – resp. what3words: identical.shareholders.lewdly. Weather conditions on both days were natural daylight with approx. 20% cloud cover.

The images of Figure 15 were taken with a Canon 5D mark iv between 11h55 and 11h59, resulting in an airmass of AM 1,14. The images of Figures 16 and 17 were taken with a Canon 5D mark iv between 14h22 and 14h26 11h59, resulting in an airmass of AM 1,27. Colour calibration of the images was performed with SpyderCHECKR 24 colour reference target.

All five colour samples were made from a 1-mm thick soda-lime glass with a size of 50 x 75mm embedding a fit-to-size cut monocrystalline SUNPOWER IBC solar cell (see Figure 13 for its visual appearance) onto a rear polymer surface.

Figure 18 shows a series of photographs in natural daylight at 1055 W/m² global normal irradiation (GNI). The viewing angle alters from 0° (perpendicular to the solar panel surface) to 80° (left to right) while the angle of irradiance on the glass samples remains constant.



FIG. 18 Series of photographs of colour sample blue, red, green, dark grey, light grey taken from 9 different azimuth angles (0° left to 80° right) in natural daylight.

Figure 19 shows a series of photographs in direct sunlight at 810 W/m² direct irradiance. Since the direct irradiance was obtained by reflecting the direct incident light from the sun into a dark cabinet, the divergence angle Θ of the direct light used in this investigation equals 0,536°.

The viewing angle alters from 10° (close to perpendicular) to 80° (left to right) while, again, the angle of irradiance on the glass samples remains constant. In contrast to the image series under natural daylight, this image series does not show an image of 0° viewing angle since, in this case, the camera itself causes a distinct shadow on the solar module.



FIG. 19 Series of photographs of colour sample blue, red, green, dark grey, light grey taken from 8 different azimuth angles (10° left to 80° right) in direct sunlight

Figure 20 shows a series of photographs in direct sunlight at 840 W/m² direct irradiance. The viewing angle is kept constant at 0°(perpendicular) to the surface of the solar modules, and the angle of inclination of the direct irradiance alters from 10° (close to perpendicular) to 80° (left to right).



FIG. 20 Series of photographs of colour sample blue, red, green, dark grey, light grey taken with 8 different angles of direct irradiation (10° left to 80° right) while the angle of perception is kept constant perpendicular to the plane of the module.

Simultaneously to the images shown in Figures 18 to 20, CIE XYZ colour coordinates have been taken with a Samsung Galaxy S7 Edge using the ColourGrab (V 3.6.1 by Loomatix) software. The L*a*b* coordinates as well as chroma and hue have been calculated according to (Carter et al.).

Conversion from CIE XYZ to CIE L*a*b*:

$$L^* = 116 * f(Y/Y_n) - 16$$

$$a^* = 500 * [(f(X/X_n) - f(Y/Y_n))]$$

$$b^* = 200 * [(f(Y/Y_n) - f(Z/Z_n))]$$

with

$$X_n = 0.9505, Y_n = 1, Z_n = 1.0888 \text{ (values at the white point),}$$

and

$$f(X/X_n) = (X/X_n)^{1/3} \text{ if } X/X_n > (24/116)^3,$$

$$f(X/X_n) = 841/108 * (X/X_n) + 16/116 \text{ if } X/X_n \leq (24/116)^3$$

The CIELAB chroma, which represents the distance from the origin, and hue, which represents the angle in the CIELAB colour circle, are calculated by:

$$C^*_{ab} = (a^2 + b^2)^{1/2}$$

$$h_{ab} = \arctan (b^*/a^*)$$

Figure 21 shows the results of the measurements in the a^*b^* plane combined with the CIELAB colour circle. The numbers of each colour shown increase by a $\Delta\text{Hue} = 10$. Figure 22 shows the results of the measurements in the CIE chromaticity diagram. The mean hue and chromaticity of the colours are represented by the black dotted lines. The left graph shows the results under natural daylight irradiation. The graph to the right shows the results under direct – no diffuse – irradiation. Both graphs show excellent colour stability for all three colours. The colour stability is even better in natural daylight. These results correspond well to the MorphoColor called photonic layer concept by Fraunhofer ISE (Bläsi, Kroyer, Kuhn, Höhn, 2021).

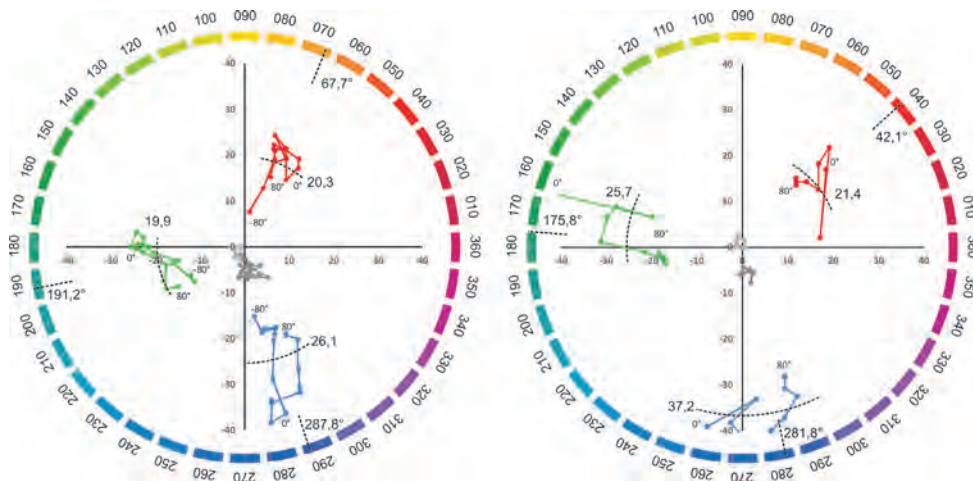


FIG. 21 Representation of the a^*b^* , mean chromaticity and mean hue data extracted from the angle-dependent measurements of the green, blue, and red modules in the a^*b^* plane. Left: Angle stability under clear sky illumination from -80° to $+80^\circ$ viewing angle. Right: Angle stability under direct illumination from 0° to $+80^\circ$ viewing angle.

A set of large sizes colour modules has been manufactured to verify the results taken from the 5×7 cm small samples (Figures 23 and 24). 20×30 cm samples were tested in the temperature cycle testing sequence (TC200) with 200 cycles between a low temperature of -40°C and a high temp of $+85^\circ\text{C}$ as defined in the MQT 11 (Module Quality Test) of DIN EN IEC 61215-1 and in a damp heat test sequence which requires 1000h at continuous 85°C and relative humidity of 85% (DH 1000) as defined in the MQT 13 of the DIN EN IEC 61215-1. Both tests are part of the type approval test protocol according to EN IEC 61215-1:2022, Terrestrial photovoltaic (PV) modules - Design qualification and type approval and the EN IEC 61730-1:2018 Photovoltaic (PV) module safety qualification. Both tests were passed. A cross-cut test according to EN ISO 2409:2013-06 could not be performed since the screen-printed surface could not be scratched at all, proving the resistance against scratching and, even more so, the adhesion of the print to the glass surface itself.

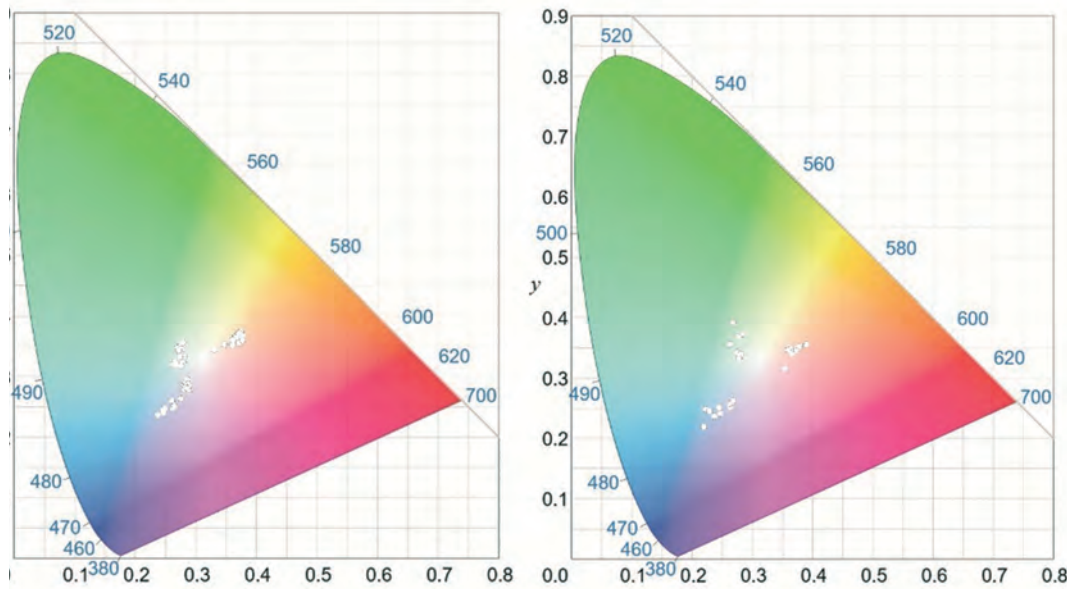


FIG. 22 Representation of the L* a* data determined for the red, blue and green colour samples in the CIE chromaticity diagram. Left: Natural daylight irradiation. Right: Natural direct irradiation.



FIG. 23 1 m² samples in the colours: golden, bronze and green.



FIG. 24 Colour sample using transparent effect pigments.

Since the screen printing is located on surface 2, which faces the interlayer of the photovoltaic module, it is not exposed to ambient conditions, such as dirt or rain. This not only permits standard cleaning for glass façades but also permits the combination with, for example, anti-reflective coatings on surface 1 to generate an even less visible surface as the typical reflection of glass is reduced. Due to the homogeneity of the colour, printing the solar cells pattern is no longer visible. The solar modules formerly perceived as too aesthetically dominant have become merely coloured surfaces and thus no longer perceivable as photovoltaic systems.

3 CONCLUSION

In this paper, we describe, discuss and compare three methods to generate coloured photovoltaic modules.

- 1 The use of coloured solar cells, which represents historic technology
- 2 The use of light-absorbing pigments, which represents a current technology
- 3 The use of transparent effect pigments, which represents an innovative technology.

We introduce innovative coloured photovoltaic modules based on the use of transparent effect pigments – for example, known from mother of pearl that covers the inside surface of sea shells – which are printed onto the rear side of the front glass of the investigated photovoltaic modules.

This technology is based on:

- The constructive spectral interference of incident sunlight on the surfaces of nanoparticles embedded by screen printing and molten into the surface of a carrier low iron front glass.
- Pigments that provide a high broadband transmission, resulting in a small reduction of module efficiency.
- The colour appearance of coloured PV modules using a layer of effect pigments is generated by the statistical interaction of multi-scattering effects of incident light at the pigments in the layers.
- The perceived colour results from the integral reflection of all particles and the multi-inter pigment reflection/ transmission amongst them. A pigment that provides a reflectance peak in the red spectrum will appear red.
- Preventing irradiance from the rear side of the PV module. Since the multi-scattering effects on effect pigments work identically from both sides, any irradiance from the rear will result in a reduction of the intended colourisation.
- The pigments can be processed fully from low-absorptive materials, and consequently, the entire colourisation layer primarily transmits or reflects incident light.

The nanoparticles show an outstanding colour angle stability for both the chroma C^*_{ab} and hue h_{ab} of the CIE $L^*a^*b^*$ colour system for the three investigated colours: red, blue and green for direct sunlight and even more so for natural daylight. The reduction of electrical power output compared to a technically identical non-coloured photovoltaic module is - 12,2% for red, -10,2% for blue and -7,8% for green. This is around two to three times lower than for equivalent coloured photovoltaic modules based on absorption colours, which have been developed and used previously. The two most crucial tests – were successfully passed: the TC 200 (MQT 11) and DH 1000 (MQT 13) as defined in DIN EN IEC 61215-1, the type approval test protocol for crystalline photovoltaic modules. A cross-cut test according to EN ISO 2409:2013-06 could not be performed since the screen-printed surface could not be scratched at all.

Due to the homogeneity of the screen-printed photovoltaic modules, the former square pattern of the photovoltaic cells is no longer perceivable. The photovoltaic modules, as such, become literally invisible.

References

- Fischer, M., Woodhouse, M., Herritsch, S., Trube, J. (2022). International Technology Roadmap for Photovoltaic (ITRPV) 2021 Results. VDMA e.V. Photovoltaic Equipment. itrPV.vdma.org
- Ballif, C., Perret-Aebi, L.E., Lufkin, S., Rey, E. (2018). Integrated thinking for photovoltaics in buildings. *Nature Energy* 3(6). DOI:10.1038/s41560-018-0176-2.

- Erban, C., Ley, H. (2020). Results from the worldwide performed questionnaire - BIPV market, technology and preferences. 37th PVSEC Lissabon. 10.4229/EUPVSEC20202020-7DV.1.7.
- Eder, G., Peharz, G., Trattig, R., Bonome, P., Frontini, F., Polo Lopez, C., Wilson, H-R., Eiselohr, J., Chivelet, N.M., Karlsson, S., Jaki-ca, N., (2019). COLOURED BIPV Market, Research and Development IEA PVPS Task 15, Subtask E Report T15-07.
- Kuhn, T., Erban, C., Heinrich, M., Eisenlohr, J., Ensslen, F., & Neuhaus, D.H. (2020). Review of Technological Design Options for Building. *Energy and Buildings* 231. <https://doi.org/10.1016/j.enbuild.2020.110381>
- Kutter, C. Bläsi, B., Wilson, H. R., Kroyer, T., Mittag, M., Höhn, O., Heinrich, M. (2018). Decorated building-integrated photovoltaic modules: Powerloss, colour appearance and cost analysis. 35th PVSEC Brussels
- Bläsi, B., Kroyer T., Kuhn, T. E., Höhn, O. (2021). The MorphoColour Concept for Coloured Photovoltaic Modules. *IEEE Journal of Photovoltaics* Volume: 11(5), 1305 – 1311. DOI: 10.1109/JPHOTOV.2021.3090158.
- Basher, M., Nur-E-Alam, M., Rahman, M., Hinckley, S., and Alameh, K. (2022). Design, Development, and Characterisation of Highly Efficient Coloured Photovoltaic Module for Sustainable Buildings Applications, *Sustainability* 2022, 14,4278. <https://doi.org/10.3390/su14074278>.
- Erban, C. (2000). Licht und Schatten - Photovoltaik zur Gebäudeintegration. VDI-GET Bautechnik Conference, Baden-Baden.
- Raacke, J. <http://www.raacke.de/index.html?airy.html>
- Tölle, R., Bruton T. M. (2000). Development of Bi-functional Photovoltaic Modules for Building Integration. "BIMODE". Report of the within JOULE III programme EU funded research, JOR3 - CT 97 – 0175.
- Devenport, S., Roberts, S., Bruton, T. M., Heasman, K., Brown, L., Cole, A., Baistow, I. Webster, K., & Garrard, B. (2009). A Summary of the HAVEMOR Project - Process Development of Shaped and Coloured Solar Cells for BIPB Applications. 24th PVSEC Hamburg. 10.4229/24thEUPVSEC2009-5BV.2.80.
- Stamenic, L. S., Erban, C. (2021). Building Integrated Photovoltaics - Technology Status. *Thermal Science* 25, 1523-1543. <https://doi.org/10.2298/TSCI200929342>.
- Eggers, H., Gharibzadeh, S., Koch, S., Schackmar, F., Ritzer, D., Abzieher, T., Richards, B. S., Erban, C., & Paetzold U.W. (2022). Perovskite Solar Cells with Vivid, Angle-Invariant and Customizable Inkjet Printed Colourization for Building-Integrated Photovoltaics. *Solar RRL* 6(4) <https://doi.org/10.1002/solr.202100897>.
- Krauter, S., Grunow, P. (2006). Optical modelling and simulation of PV module encapsulation to improve structure and material properties for maximum energy yield. Conference Record of the IEEE Photovoltaic Specialists Conference, DOI: 10.1109/WCPEC.2006.279926
- Carter, E. C. et al., Colourimetry, Technical report, 3rd ed. Vienna, Austria: CIE, Central Bureau, vol. 15, 2004.
- DIN EN IEC 61215-1: terrestrial photovoltaic (PV) modules – design qualification and type approval, Part 1: Test requirements.

PART 2 // ENVELOPE

Visions for a Paradigm Shift – Based on AM for Facade Application

Dr. Holger Strauß*

- * Innobuild GmbH, Saarbrücker Straße 24, 10405 Berlin, +49 30 2359648-74, holger.strauss@innobuild.de

Abstract

After more than 15 years of research and development, 3D printed façade nodes and components are finally ready for real-time application in recent building construction projects. Following his involvement in the early stages of developing these 3D printed parts, the author summarises the development of the last decade and gives an outlook from today's toward future applications. In combination with ever more urgent demands for environmentally positive performances of the building envelope, an even more complete picture of future building envelopes is described in combination with building technologies, building materials and planning parameters.

Next to evaluating emerging technologies, this contribution looks at building materials and the possibilities of traditional building construction principles to identify the potential for application. With the awareness of the building sector being part of the cause of climate change, ways to practical solutions are explored to achieve Germany's 2045 climate change mitigation goals.

To achieve this paradigm shift within the construction industry, the following research topics can be identified: Sustainability and the way to a circular economy, with a first step of introducing circularity in façade construction, the application and combination of new construction materials to achieve better recyclability of façade constructions, and the reformation of traditional planning processes to bring the life cycle of building envelopes toward contemporary realisation.

Keywords

Paradigm shift, circularity, climate change mitigation, façade engineering, building envelope, façade technology, 3D printing, Additive Manufacturing, sustainability, innovation

1 INTRODUCTION

This paper discusses the influences that new technologies have on the development of building envelopes toward carbon-positive buildings. It also describes possible changes within the building industry that can be witnessed and that lead toward new ways of design and production of our built environment.

Next to evaluating emerging technologies, this contribution looks at building materials and the possibilities of traditional building construction principles to identify the potential for application. With the awareness of the building sector being part of the cause of climate change, ways to practical solutions are explored to achieve the 2030 and 2050 climate change mitigation goals in Europe.[1]

2 METHODOLOGY

The underlying research work was conducted as a qualitative study based on the self-chosen hypothesis: "New technologies have an impact on the development of building envelopes toward carbon-positive buildings". A multi-method scenario was developed as a source for data and information requisition. With this scenario, all contributing single parts flow into an overall collection of source material.

The data from these sources, combined with personal experience and reliable (published) knowledge, form the basis for the approaches and results presented in this paper. As this paper is limited in length, further information can be obtained by carefully studying the sources in the list of references.

3 ADDITIVE MANUFACTURING – A LOOK BACK AT 15 YEARS OF DEVELOPMENT

In this paper, Additive Manufacturing (AM) processes exemplify how new technologies are changing construction engineering. The increasingly frequent use of AM in the construction sector shows a typical development of new technologies and can thus be used for evaluation and formulating a perspective for other currently pressing topics and techniques as well. After more than 15 years of research and development, 3D printed façade components are finally ready for use in actual building projects. To get to this point, considerable efforts have been made over the last 15 years, and many research and study papers have been written on this topic.

To provide a brief insight into the development of relevant components for façade application, the research project "AM Facades - Influence of additive processes on the development of facade constructions" [2] is summarised and evaluated below.

At the beginning of the research project, the system offerings of a façade system provider were screened, and components were identified that had a basic potential for optimisation with AM.

Due to the clear limitation of the AM build space for producing AM components in metal, restricting the selection to small to medium-sized components made sense. These included structural component connectors between mullions and transoms – so-called T-cleats. Not only were the advantages of direct digital production taken into account, but also the given performance characteristics within the façade system. The optimised component is thus an improved "digital connector" that, in combination with digital planning tools, allows for individual façade geometries and enables a structurally optimised system.

All necessary angles and drillings are digitally integrated into the AM design. This way, precisely fitting connections can be designed and manufactured for each connection point of the façade. The added value is achieved through material savings and force-path-optimised shaping (see Figure1). The assembly is analogous to orthogonal façade systems with the standard mullion-transom system components.



FIG. 1 From standard aluminium extrusion (left) to ABS prototype (middle) to 3D printed stainless steel connector (right)

The availability of additive processes thus added another link to the chain of a true “file-to-factory” production. It enables us to produce parts for a free-form façade with all angles and adjustments in the same quality as for an orthogonal façade with standard products.

In the research project, the next step was to advance these “digital connectors” into a neuralgic node that carries all the complexity of the free-form geometry and leaves the other façade components as much standard as possible. All of the advantages of the previously developed “digital connector” were further developed and combined into a customised, integral node. The resulting node was produced directly with AM. All required properties can be implemented digitally in the data set by specifying design parameters (parametric design). Due to the digital fusion of mullion and transom profiles, only right-angled saw cuts are necessary to assemble the façade. This reduces cutting scrap and facilitates assembly (see Figure 2 and 3).

With this approach, a combination of proven standards and digitally enhanced node solutions was realised for the existing façade technology in 2010. By integrating new “high-tech” parts into tested and verified systems, the advantages from both areas were combined into an even better solution.[3]



FIG. 2 3D façade node – rendering (left)



FIG. 3 Image of 3D façade node Nematox II – prototype (right)

To summarise the development of the last decade, it is necessary to differentiate the use and application of AM in various industries. Industries with small quantities and small component dimensions have been able to implement AM processes as an extension of traditional production technologies more quickly and easily than industries with large-scale components and large batch numbers.

Looking at the construction sector, the following developmental steps were crucial for the maturation of AM:

Materials

The AM industry has managed to further develop applications with metals from an initial idea to available technology. The variety of materials is almost unlimited and ranges from aluminium and tool steel to titanium and gold.

AM build space size

The AM build space size has changed only slightly over the last 15 years. As a rule, powder bed-based systems are still equipped with average AM build space dimensions of around width 300mm/depth 260mm/height 320mm.

For direct building-scale applications, for example, concrete structures are available that are printed directly on-site. Several suppliers have adapted the ContourCrafting technology [4] for house 3D printing. The component size is not determined by a limited AM build space but is aligned to the demand by using crane systems and gantry robot technology (cf. [5], [6]).

Printing speed

The acceleration of AM processes for metals has been accomplished with several light sources and, in some cases, several powder coaters. Nevertheless, there are still narrow limits to both the achievable AM build space and the printing speed (cf. [3], chapter 2.5.1)

Standards

In the meantime, the first binding standards have been established in addition to guidelines and manuals for Design for Additive Manufacturing. For example, by the US-American ASTM, the German VDI and also the German Institute for Standardisation (DIN).

Quality management

Today's service providers and AM users meet material quality standards; they are monitored and qualified with ISO certificates. Consistent component quality has, therefore, become the industry standard.

Printing cost

A calculation approach must be requested from the supplier based on concrete component geometries. The figures from the research project and current price quotations for an identical data set show that, today, costs have been approximately halved.

3.1 SUMMARY

As the described research process shows, it was possible to move from our initial project ideas for façade applications to resilient product development within ten years. It can be stated that AM is an available and proven building technology tool, but still a niche building technology tool. Only the combination of AM with other software applications leads to greater benefits for the building envelope – and ultimately for the user. The pure application of AM in the façade is certainly too short-sighted and would fall short of the development possibilities of digital tools.

The initial idea of complete design freedom by eliminating tools and moulds and creating shapes directly from a digital representation has only partially come to life. But 3D printing became an everyday business after starting out as crazy rocket science. Today we can buy fabbing machines in the electronics market just like any other tool (see Figure 4). (cf. [3], A1, pages 222 ff)



FIG. 4 Image of Conrad Electronics store, 3D department

Today, we already realise continuous 'file-to-factory' planning of entire façade projects, also based on digital planning and on a direct path with CAD-CAM production. In this respect, the fabricators of façade systems are now a big step further and ready to carry out production directly with digital planning data. This means that all the required information – literally every screw, every drilled hole and every accessory – is digitally mapped and automatically organised to virtual perfection via scripting. Automated planning algorithms translate the architectural form into the contractor's production planning.

With the use of increasingly powerful design support tools, improved functionalities can be integrated. These include, for example, solar radiation and shading of façades, wind and noise simulations and optimisation of surface orientation, e.g. to integrate BIPV.

4 NEW PERFORMANCE PROFILES FOR FUTURE BUILDING ENVELOPES

The combination of the purely technical possibilities in the façade and the necessary changes in the handling of resources and the environment also defines the requirements for the contemporary building envelope.

The performative properties of a sustainable building envelope must achieve significant improvements over conventional façade technology. Ideally, the requirements for a dynamic building envelope can be met: Climate regulation through breathable materials, material savings through topology-optimised load-bearing structures, comfort through active insulation and ventilation, integrated technology for the user, performance for lighting and shading with adaptive transparency, circularity-compatible construction and a design-compatible appearance.

4.1 FACADE DEVELOPMENT

For approximately 20,000 years, human beings have created housing for cultic as well as living purposes. In short, the built environment as we know it today has developed from those origins in small increments. Analogically, building technical details evolved from questions that arose and solutions that the relevant craft permitted, openings in structures as access routes for lighting and ventilation, and the desire of the user to create comfortable living quarters – via simple openings to covered frame constructions to the actual window and, at the beginning of the 20th century, to the façade as a clearly separated building component of the building envelope (see Figure 5).

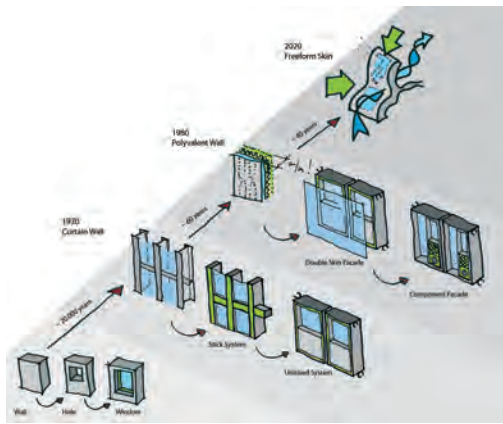


FIG. 5 Development of the Building Envelope toward Freeform Skin

Developments always involved specialisation/fine-tuning: simple drapes in front of wall openings evolved into operable windows; the curtain wall façade with single-glazing casement windows evolved into the post-beam system, later unitised façades; the mere building enclosure turned into the vision of a building skin with all of the necessary functions that allow for a comfortable and energy-efficient building, and as intermediate steps toward a true skin the double façade, then the decentralised HVAC units and, still unsolved, the 'Polyvalent Wall' by Mike Davies [7].

It is, therefore, essential to emphasise the importance of the building envelope as a neuralgic interface to the different requirements of the building itself:

- climate,
- load transfer,
- comfort,
- technology and assembly,
- performance,
- appearance.

[8], [9]

4.2 PERFORMANCE PROFILES

The performance profiles of a future building envelope can still be derived from these aspects, but they are supplemented by the pressing issues of our time.

The increasingly pressing demands on the **environmental performance of the building envelope** result in an even more comprehensive picture of the future building envelope, including a combination of building technologies, building materials and design parameters (see Figure 6).

Building envelopes must contribute to the further development of our buildings **toward carbon-positive buildings**. This has to be done in combination with the necessary changes and supported by the influence of new technologies.

One aspect that must be considered is **material consumption**. Here, the goal must be to only use what is really needed. Software-supported optimisations in structural design and material efficiency can save resources. One example of this is the topology-optimised AM façade node, which only uses material where it is needed. This principle can also be transferred from the supporting structure to other parts of the façade.

Another measure is to make adjustments and **changes to the design principles** for components and building materials and thus make the dimensions leaner. For example, valuable material can thus be saved in timber construction.

Even with one of the most defining building materials of modern architecture, reinforced concrete, the use of resources must be reconsidered. The production of cement accounts for approx. 10% of the greenhouse gas CO₂ emitted by humans.[10] Through optimisations, considerable CO₂ savings can be achieved in shell constructions by reducing concrete and thus cement. Examples of this are, for example, the long-established Cobiax floor constructions for material-reduced reinforced concrete construction. And also the results of research into mass-optimised building components, for example, the work of Prof. Werner Sobek on so-called gradient concrete.[10] This is not primarily about the building envelope but about a new understanding of building tasks in general.

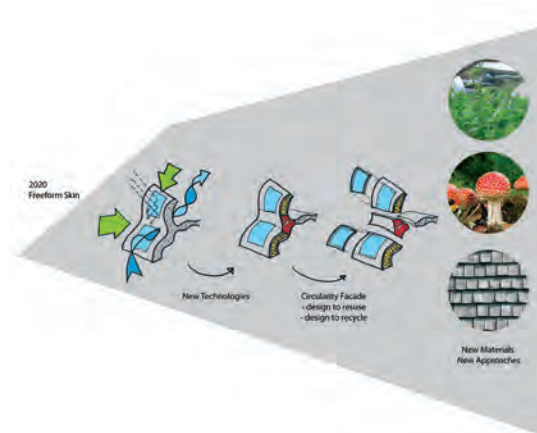


FIG. 6 Adopted development of the building envelope from the freeform skin

The new technologies will also lead to a reduction in carbon emissions in logistics when components are manufactured on-site rather than having to be prefabricated and transported to the construction site. Local materials can be used for this purpose. And this can also drastically reduce the grey energy involved during raw material production, transport and processing. Based on this development, façade components can also be produced and installed on-site in the future by applying new technologies. (see "3 Additive Manufacturing")

5 TRADITIONAL BUILDING – TRADITIONAL MATERIALS

The return to traditional, or rather regional, building materials, in combination with safer handling of robotics and automated manufacturing processes, leads to changed architecture and thus also to a change in façades. Modular timber construction is an example of this convergence. Through the use of gantry robots and consistent digital planning and production, the timber construction trade has become competitive again in recent years and, via the CO₂ discussion, is a sought-after trend. (see Figure 7)

New technologies and planning methods now also make it possible to erect high-rise buildings in timber construction. The sustainability of these approaches has yet to be proven because even the effects of building materials that appear "green" at first glance must be evaluated and questioned again and again.[11], [12] Nevertheless, the development leads to a multiplication of possibilities. The value of the processed timber is only meaningfully preserved through multiple use over several life cycles.[13] And CO₂-positive use of construction timber is only possible through consistent

reuse. This has been successfully implemented and was common practice over several centuries in traditional half-timbered construction, for example, with secondary timbering (Zweitverzimmerung) of structural timbers.



FIG. 7 Erne AG, gantry robot assembling a 3D roof truss

Traditional building materials and traditional building construction principles should be looked at to identify opportunities. Building with clay is another construction method that has been underestimated for a long time, offering the use of regional resources with reduced transport routes. These building techniques have been tried and tested for a long time and, with the introduction of DIN standards and rules for building with clay, are now accepted building techniques. The renaissance of local materials for the production of rammed earth walls or light-fired bricks minimises the need for transport. For the building envelope, this means, on the one hand, a return to solid walls as the basis for window and façade constructions and, on the other hand, a departure from the pure glass façades of past decades. As we need to combine modern digital tools with traditional crafting tools, we need to think about new, hybrid material combinations in the façade.

6 NEW APPROACHES – VISIONS FOR A PARADIGM SHIFT

A **holistic design approach** is needed for a Circular Built Environment (CBE, cf. [14]). The share of the façade in the performance of the entire building makes up a decisive proportion. In terms of construction costs, current façade constructions reach a share of up to 25%. The influence that improved façade technology can have on the resource efficiency of our buildings is similarly strong.

A **continuous digital building model** is needed in all service phases as the basis for real-time assessment of the cycle aspects of the building and its façades. We already realise 'file-to-factory'; it is, therefore, only a small step to make full use of the existing data in a digital twin for more than just the production dataset.

In the future, this will enable real-time assessment of the crucial aspects for all those involved in the construction:

- CO₂ footprint,
- recyclability/recycling potential of the materials used,
- secondary raw materials and materials already used,
- performance of energy generation and building services (solar, passive, technical, ...),
- standard BIM information: costs, masses, qualities.

One approach to this is **specialised LCA software**, with which the direct link between 3D planning and LCA data can be used to produce a detailed assessment. In the future, the 3D planning data will

be used to create a reliable building passport for new buildings and in a further step for existing buildings as well. This way, in the future, our buildings will be planned and implemented directly as assessable raw material storage facilities.^[13] A change in thinking is required on the part of all those involved to change the previous approach from "use and dispose" to the long-term use of valuable resources. This requires that long-term use is already considered in the design of the building, the façade, and the construction detail.

We have to **redefine the expectations** of the investor, the client, the owner in terms of the value of the "new". In the perception of the decision-makers, a new building is still more valuable than a renovated old building. The real values of reused raw materials and materials must be communicated and factored into the planning process and taken into account as added value.

One aspect that has been looked at before is material consumption, to only use what is really needed. And as a paradigm shift, we need to ensure that valuable resources can be used and reused for as long as possible to avoid waste and reduce resource consumption. To this end, **Design for Disassembly** should become common practice in our planning processes.

In a later step, the Design for Disassembly must be further developed into the Design for Circularity. Here, calculations must also take into account the higher planning and implementation costs for multiple use, as new material can be assembled much more freely. Multiple use requires more intensive processing, more rearrangement and more sorting. In turn, the calculation of construction costs must consider the potential for multiple use of all products and materials in the future. Building materials that can be used again with certainty will in future no longer be written off to zero in the first project but will retain a residual material value until their actual end of life in the building. Thus, the building becomes cheaper with the first use, and multiple use pays off, since the reduced price rather than the new price has to be paid. (cf. contribution by Nora Sophie Griefahn in ^[13])

7 CONCLUSION AND OUTLOOK

This paper discusses the possible changes and influences of new technologies and materials on the development of building envelopes towards carbon-positive buildings. To meet today's requirements for future building envelopes, we need to design visions for the paradigm shift today – various new approaches and options have been presented for this purpose. With the lessons learned from the past technology hype, through the trough of disillusionment and onto the plateau of productivity in AM, for example ^[15], it is possible to give an outlook from today's building technology toward future façade applications.

To achieve the necessary paradigm shift within the construction industry, the following research topics need to be addressed:

- Sustainability and the way to a circular economy, with a first step of introducing circularity in façade construction.
- Full-scale and climate-neutral use of solar regenerative energies in and on our buildings.
- The application and combination of new construction materials to achieve better re-usability and recyclability of façade constructions.
- Reformation of traditional planning processes to bring the lifecycle of building envelopes towards contemporary realisation with energy-, circular- and carbon-positive design.

With the initiatives of Fridays4Future, Architects4Future and finally, with the Pandemic, society has woken up to the fact that things have to change in order to meet the declared climate protection

goals – for our future, for the future of our children and for the sake of our way of life. With this change in awareness, a change in the building industry will become easier, and the discussion will shift towards a greater willingness of investors, builders and stakeholders in the building industry to explore new ways of realising projects. This will bring new solutions to the fore, even if they may initially involve higher costs. The façade industry is also slowly adapting to these new ways, and each individual can participate in this change by finding improved solutions to existing problems.

To achieve this, we need to educate stakeholders and collect and share even more data and information about existing solutions for a circular economy and for a sustainable built environment. In the façade industry, we need to use and apply the existing knowledge to realise a circular economy with real projects. This also requires getting all other stakeholders on board: builders, investors, project managers, architects and engineers. The “positive word” needs to be spread to raise awareness of the necessary change and the opportunities it brings. The new technologies lead to better or more plannable use of the building stock for the future conservation of the value of our scarce resources. In concrete terms, this means having an “as-built building passport” in your hand in the future when the building is completed!

Based on our experience in developing 3D printed façade parts and components, starting with early developments as mere prototypes and ending with accepted (building) technology, it must be stated that new technologies and innovations take ten to fifteen years to move from vision to application. So we have to start now to make changes for the future.

“In the end, it is a well thought-out combination of design and material that makes for sustainability.” [16]

References

- European Commission, et al., How to assess climate change mitigation potential at project-level? : an estimation based on life cycle assessment of project proposals submitted under the European green deal call. 2022.
- Strauss, H., AM Facades - Influence of additive processes on the development of facade constructions. 2010, Hochschule OWL - University of Applied Sciences: Detmold. p. 83.
- Strauss, H., AM Envelope - The potential of Additive Manufacturing for facade construction. A+BE ed. Architecture and the Built Environment. 2013: TU Delft. 270.
- Khoshnevis, D.B. Contour Crafting Corporation. 2017; Available from: <http://www.contourcrafting.com>.
- MENSE-KORTE_ingenieure+architekten. HOUS3DRUCK. 2020 [cited 2022; Available from: <https://www.housedruck.de/>.
- PERI_Vertrieb_Deutschland-GmbH&Co.KG. PERI druckt erstes Wohnhaus Deutschlands. 2020; Available from: <https://www.peri.de/informationsportal-news-medien/veroeffentlichungen-presse/peri-druckt-erstes-wohnhaus-deutschlands.html#q=3D%20Druck>.
- Davies, M., A Wall For All Seasons. RIBA Journal, 1981. 2(88).
- Knaack, K., Bilow, Auer, Facades - Principles of Construction. Principles of Construction. 2007, Basel: Birkhäuser Verlag AG.
- Martin Meijs, U.K., Components and Connections. Principles of Construction. 2009, Basel: Birkhäuser Verlag AG.
- Urban, K., Klimasünder Beton - Ein Baustoff sucht Nachfolger, in Wissenschaft im Brennpunkt. 2020, Deutschlandfunk: <https://www.deutschlandfunk.de/klimasuender-beton-ein-baustoff-sucht-nachfolger-100.html>.
- DGNB, Positionspapier Holzbau, DGNB-e.V., Editor. 2021, Deutsche Gesellschaft für Nachhaltiges Bauen.
- Lemaitre, C. Holz ja – aber nicht um jeden Preis! Forum Nachhaltig Wirtschaften “Der aktuelle Kommentar” 2022; Available from: <https://www.forum-csr.net/News/17344/Holzja%E2%80%93abernichtungumjedenPreis.html>.
- Scobel, G., scobel - Die große Rohstoffkrise, in Wissen, G. Scobel, Editor. 2022: ZDF 3sat Mediathek. p. min45 / 57min.
- TU-Delft, DelftX CESBE1x - Circular Economy for a Sustainable Built Environment, DelftX, Editor. 2022: [https://courses.edx.org. p. https://edx.org](https://courses.edx.org/p.https://edx.org).
- Peels, J. Where is 3D Printing in Gartner’s Hype Cycle? 2022; Available from: <https://3dprint.com/291020/is-3d-printing-in-gartners-trough-of-disillusionment-or-slope-of-enlightenment/>.
- Röder, D.A. Die Kombination aus Design und Material macht Nachhaltigkeit aus. UmweltDialog Wirtschaft-Verantwortung-Nachhaltigkeit, 2020.

CoolSkin



A Novel Façade Design for Sustainable Solar Cooling by Adsorption

Andreas Greiner ¹, Olaf Böckmann ², Simon Weber ³, Martin Ostermann ¹, Micha Schaefer ²

- * Corresponding author, andreas.greiner@ibk2.uni-stuttgart.de
- 1 Institute for Building Construction, University of Stuttgart, Germany
- 2 Institute for Building Energetics, University of Stuttgart, Germany
- 3 Institute for Acoustics and Building Physics, University of Stuttgart, Germany

Abstract

The article investigates the dependencies of façade design and construction in the integration of a sustainable solar-powered cooling system based on closed adsorption. The presented work focuses on the possible design variants of the envelope surface of the façade-integrated adsorber. The principle of adsorption cooling is presented and, based on this, architectural options for façade integration are investigated. This is done both constructively and visually. For each variant, the solar gains are summed up and compared with each other. A functionally designed adsorber, similar to a flat plate collector, serves as a reference and starting point for the modifications. It provides the comparative value for the energy evaluation. The modification is limited to the visible surface of the adsorber. The texture of the solar adsorbing sheet was changed and the glazing used was replaced by ETFE cushions and by a novel ETFE vacuum panel. Finally, the solar simulation results were integrated into the higher-level system simulation to evaluate the resulting gain in cooling capacity. The results show that the system could generate more than 100 W per installed square metre of adsorber façade. Furthermore, higher solar gains compared to the reference case can be obtained at particular times of the day due to geometry and material changes. However, the modifications always lead to a reduction of the total cooling power. In conclusion, the simulation results reveal that design flexibility is possible, but currently the studied design variants have a lower cooling capacity compared to the solely functionally designed adsorber.

Keywords

Solar cooling, adsorption, façade integrated cooling

DOI [10.47982/jfde.powerskin.3](https://doi.org/10.47982/jfde.powerskin.3)

Renovating Modern Heritage – The Upgraded Façade of Commerzbank Düsseldorf



Rouven S. Grom ^{*1}, Andreas W. Putz ¹

* Corresponding author, rouven.grom@tum.de

¹ Technical University of Munich, TUM School of Engineering and Design, Germany

Abstract

The post-war building stock is increasingly being transformed. Even objects that are protected as listed heritage, renovation usually results in a high degree of material change and replacement. This is especially the case in regard to historic curtain wall constructions. Based on the case study of the Commerzbank High-rise and original planning documents by Gartner, the paper focuses on the applied strategy of disassembling and reassembling the curtained aluminium sandwich elements, and the resulting upgrading of the original façade with a newly installed interlayer for insulation. The paper discusses the possible transfer of this strategy, which largely depended on the existing high quality of the aluminium components, their corrosion-resistant properties and low weight. The case study of the former Commerzbank High-rise indicates that a long-term preservation of post-war modern building stock can be achieved without wholesale replacement of original building components. The reuse of existing materials and components represents a promising approach.

Keywords

Façade renovation, reuse, retrofitting, aluminium curtain wall, Josef Gartner GmbH, modern building heritage conservation

DOI 10.47982/jfde.powerskin.4

Active, Passive and Cyber-Physical Adaptive Façade Strategies: a Comparative Analysis Through Case Studies



Jens Böke¹, Paul-Rouven Denz¹, Natchai Suwannapruk¹, Puttakhun Vongsingha¹

* Corresponding author, Jens.Boeke@priedemann.net

¹ Priedemann Fassadenberatung GmbH, Germany

Abstract

In view of the required energy savings in the building sector, there is an urgent need for innovative and sustainable solutions to increase the performance of building envelopes. Adaptive façades can make an important contribution, whereby passive low-tech strategies and active high-tech solutions are apparently incompatible. In current digitalization, new technologies and methods for the implementation of adaptive façades emerge in the framework of Cyber-Physical Systems. The investigation follows the research question: How can active and passive approaches of adaptive façades be mediated and what potential do Cyber-Physical Systems have for the implementation of hybrid solution approaches in the future? The article presents a comparative case study of the two research projects ADAPTEX and PRÄKLIMA as examples of passive and active adaptation strategies in the façade industry. In this context, the potential for further research of Cyber-Physical Systems in the application domain of adaptive façades as a catalyst for high-performance and multifunctional solutions, and as a mediator between both strategies, is highlighted. The main findings are the potential application of cyber-physical system technologies to the design and monitoring of passive adaptive façade solutions, as well as the possible integration of passively conceptualized components into active overall systems.

Keywords

Adaptive façade, smart material, intrinsic adaptation, extrinsic control, artificial intelligence, prototyping, monitoring, ADAPTEX, PRÄKLIMA

DOI 10.47982/jfde.powerskin.1

Scrolling Screen: A Responsive Building Envelope for Energetic Adaptations

Erik Hegre¹, Angie Müller-Puch¹, Randa Omar¹, David Horvarth¹, Ryan Maruyama¹, Avril Teo¹

¹ BEHNISCH Architekten, Weimar, Stuttgart and Boston research@behnisch.com

Abstract

Climate change, finite resources, and high demand for comfort are the main challenges facing the contemporary building industry. As a culture, the industry tends to design climate-defensive buildings, where we create a generic one-size-fits-all shell and then compensate for changes in temperature with energy-intensive building systems to support our needs. To break this convention, we should rather develop building skins that respond to and mitigate constantly-changing environmental conditions to enhance user comfort, optimize material use, and ultimately minimize energy demand. This paper proposes the development of a linearly-movable textile screen that can be used as a secondary building envelope to improve new façade systems or energetically-renovate existing structures. The approach attempts to respond to winter and summer conditions in one fabric that self-adjusts over time. Thus, it creates a material-based solution to reduce the need for energy-intensive systems to maintain user comfort.

Keywords

Responsive building envelope, seasonal adaptation, energetic renovation, reuse, material gradient, user comfort, low tech architecture.

1 INTRODUCTION

1.1 LIVING TOGETHER - WHY BUILDINGS SHOULD BECOME ADAPTIVE AGAIN

"Facades have always had moving elements. Doors, windows, awnings, shutters, louvers, blinds, lifting bridges, and other kinetic elements have been necessary to modulate the otherwise impenetrable and static building envelope." (Koolhaas, 2018)

For centuries, facades have been used as a flexible layer of protection between the inhabited space and its surroundings. Like donning a coat when leaving the house on a cold winter day, earlier generations would close windows and shutters to prevent the loss of heat and thus, intuitively manipulate the façade according to weather changes and seasons. From the light, translucent sliding shoji walls of the Katsura Villa in Kyoto, Japan, to the Swiss Zehnderhütte, a barn with a ring of buffer rooms that protect the living spaces from the harsh and cold weather, various traditional examples can be found that show how people and buildings have adapted to and lived with the climate.

Even in the height of modernism, at a time when the International Style dreamed of universal buildings, agnostic to geography, architects like Hassan Fathy, Jean Prouvé, Frei Otto, and others developed adaptive architectures that tried to transform the existing knowledge about climate-responsive buildings into new architectures. (Hönger, 2009) (Fathy, 1987)

Christine Kanstinger, the daughter and long-term colleague of Frei Otto, talks about their family life in Haus Otto Warmbronn, which, in 1967 Frei Otto and Rob Krier built as half Wintergarden — half house: "We lived in this house with the climate. We were used to closing and opening the sliding doors and the shading devices of the Wintergarden according to the movement of the sun and the outside temperatures to keep the Wintergarden cool in summer and to benefit from the solar heat in winter."



FIG. 1 Frei Otto und Rob Krier, Wohnhaus Otto, Warmbronn 1967 (Atelier Frei Otto Warmbronn)

In these examples the human had more control and participated in adapting the building to the outdoor climate, to receive good shelter in return. But why did this collaboration end? When did we accept to live or work in buildings without operable windows and without any human influence on the interior climate?

For the last decades, the predominant thinking around sustainable building has been driven by the ambition to make buildings more energy-efficient, in particular during the operational period of their lifecycle. In response, the construction market has focused on making highly efficient equipment, while designers strive to create buildings that require less energy to operate—a clever strategy because it simultaneously reduces energy consumption and minimizes the costs of operation. The result is highly mechanized building machines with static, massively insulated envelopes and mechanical ventilation systems that try to perfectly fulfill all demands in any condition without any human interaction.

These buildings, despite their use of carbon-intensive materials, are better than their recent predecessors, which used excessive energy due to poor construction detailing, inefficient mechanical systems, and inadequate insulation. However, as our renewable energy systems and energy use become more efficient over time, we would like to reiterate the following question enunciated in 2017 by Ryon Zizzo: Is now [not] the time to restart building lighter, simpler, and more flexible again to save more energy over the whole lifecycle of our buildings?

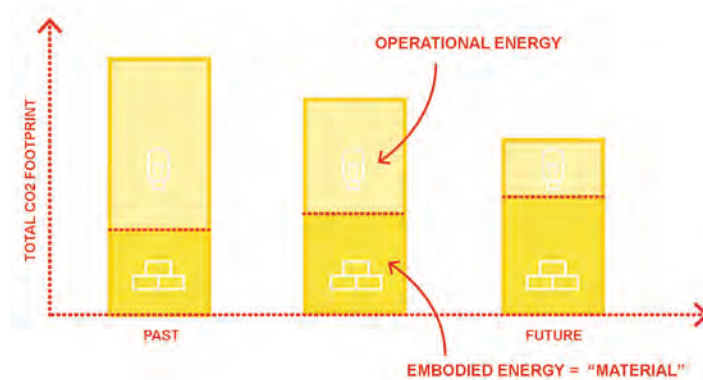


FIG. 2 Operational versus embodied energy

This doesn't mean that we want to go back to constructing buildings that waste the laboriously-gained renewable energies. On the contrary, the achievements of the last decades are the base of the development. But could we, by reintegrating nature and humans into an active team, create buildings that adapt to the climate and its users' needs over time and thus become flexible systems that help us address some of the challenges of climate change? This approach influences the whole building, its structure, its mechanical equipment, its inner organization, and its envelope. However, we would like to emphasize the importance of the role of the façade, because it is the interface between the indoor and outdoor environments. Similarly to how we dress differently in summer and winter, this research proposes that a "building's dress" changes, according to the climate—not only the seasons but also future climate changes—and with that, makes sustainable building understandable and human-centered again.

1.2 CLIMATE ADAPTIVE SCROLLING SCREEN

This paper proposes the development of a linearly-movable textile screen that can be used as a secondary building envelope to improve new façade systems or energetically-renovate existing structures. This approach attempts to respond to different climate conditions in one skin that self-adjusts over time. Thus, it creates a material-based solution that reduces the need for energy-intensive systems to maintain user comfort. Within one composite material, gradients in the form of a frit pattern (film-based screen) or a stitch density pattern (textile screen) are produced to service multiple functions using off-the-shelf textile products.

In nature, we see this use of patterns in a grove of trees during the winter months when layers of branches project a composite 2D image on the ground, an artifact of the structure of the tree as sunlight passes by and casts shadows on the ground. The intent is to use this layering to create “tuned” patterns.



FIG. 3 Tree shadows at Fredrick Law Olmstead designed Central Park in New York, NY. (Central Park Conservancy, 2022)



FIG. 4 Architectural and parametric designer, Yiran Zhou’s string art Rhino Grasshopper component (Yiran Zhou, 2022)

The functional principle of the scrolling screen is based on a linearly-guided screen that has different pattern densities across its surface and can be moved along the façade to adapt to changing environmental conditions over the course of a year. The textile surface has two main areas: a winter and summer zone, which differ in density and mitigate the thermal transmittance: in summer, the first part of the screen provides a porous sun-shading system that allows air to circulate and minimizes solar heat gain.

The basic mechanical system consists of two active rollers, which are installed at the height of the structural connection points at the top and bottom of each story. By moving the rollers, the position of the textile can be changed parallel to the facade. A third roller, located between the top and bottom rollers, gives the system depth, which primarily serves to improve the shading function of the screen during the summer months. This middle roller can move in and out on the x-axis to adjust the angle of the screen, and thus, the shading.

This, in turn, creates a thermal buffer zone between the existing façade and the proposed screen. During colder months this buffer zone thermally preconditions ambient air to allow a larger window of time for natural ventilation, which helps reduce energy consumption and connect users to fresh air and the outside environment.

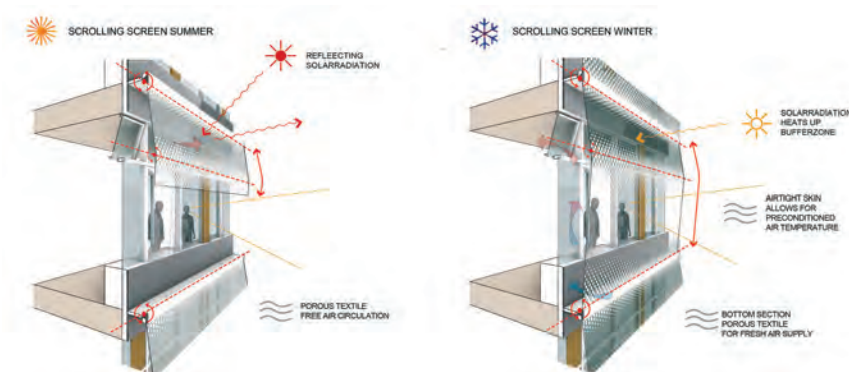


FIG. 5 Scrolling Screen Performance: Summer (l.), Winter (c.)

2 METHODOLOGY

2.1 ITERATIVE ANALYSIS

This research is approached as a design exercise. It engages in an iterative, often non-linear process with numerous competing interests and directions. Outcomes are led organically by evaluating qualitative and quantitative results. This means that the work happens in a feedback loop where performance and comfort considerations inform one another.

To work towards reducing the need for energy-intensive systems to maintain user comfort, with our proposed screen, we studied two parameters: solar radiation and daylight autonomy. All simulations were performed on a static façade panel facing south. The only changing element in our simulations was the scrolling screen. Rhinoceros 3D and Grasshopper were the main tools utilized for the screen's geometric explorations (ie. pattern composition). Working parametrically with inputs such as location, density, and size, the variations of the screen were then run through Climate Studio (Solemma) to measure radiation and daylight autonomy. Results from Climate Studio were then counter-checked with a control scenario (no screen) to evaluate the efficiency of the screen's geometry. Adjustments were then made to the Rhinoceros 3D and Grasshopper script to inform the next generation of screen geometry, and thus the iterative process continued.

Fundamental user requirements such as ensuring a clear view when standing or sitting, and regulating light intensity or avoiding glare from direct sunlight throughout the year, were also considered in the studies. The results of the computational analyses were tested in a physical model, in parallel, to evaluate their atmospheric qualities. By working in tandem between the empirical data and the physical qualities of the space, we began to find a balance between quantitative analysis and qualitative properties, informing the following iterations.

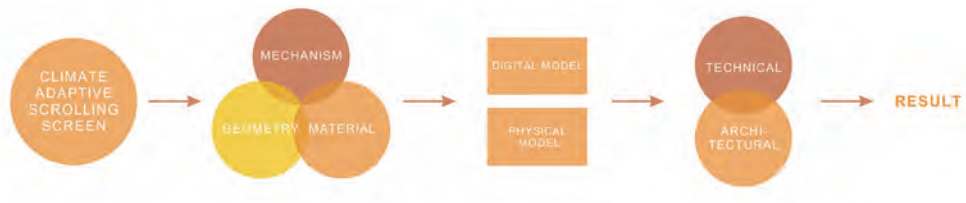


FIG. 6 Research process

2.2 GEOMETRIC PRINCIPLES

The positioning of the surfaces of the screen to the facade behind it depends on the global orientation and the alignment to the respective points of the compass. A southern orientation and weather data from Stuttgart, Germany were chosen for all subsequent tests to illustrate the principal function of the facade as well as limit additional complexity at this time. Further study of elevation and azimuth angles is necessary; however, the principal system can be assumed to function on any of the facades: the screen would simply host geometry and stitch density that is appropriate to its orientation.

Daylight and radiation analyses were done in tandem, to inform the design of the pattern and ensure that it provides adequate daylight, radiation reduction, etc. Following these analyses, the stitch or frit pattern densities and their sizes, and their positioning were designed to vary throughout the screen to accommodate and respond to different needs.

2.3 MATERIAL RESEARCH

Nylon, ETFE, PTFE, and PVC were chosen for their ubiquitous use in textile architecture and because they are readily available products. Cotton was added to the list for its natural properties and recyclability. These items were assessed for their Life Cycle Assessments (LCA), Global Warming Potentials (GWP), Recycling Rates, and ILFI Red List status.

This data was gathered through Environmental Product Declarations (EPD) which are documents developed voluntarily by manufacturers, providing data on their products including information regarding the environmental impacts associated with their manufacturing. These documents typically include LCAs which are assessments of the environmental impacts of a product, considering all relevant stages in its life cycle, from extraction of raw materials (the “cradle”) to the disposal at the end of the product’s useful life (the “grave”). The International Living Future Institute (ILFI) manages a list of chemicals known to cause human and environmental harm, which is referred to as the “Red List.”

TABLE 1 Properties of potential textile materials and global warming potential. (Authors note: EPDs and GWPs were not always available for recycled materials. While we have started gathering information on sources of waste, and the recycling rates of recycled versions of the above-mentioned materials, we could not always find EPDs and GWPs of recycled materials. Where a material product cited is recycled, the material information (first column) will indicate it.)

MATERIAL	PROPERTIES	GWP (KG CO ₂ /M ²)—PROD-UCT STAGE (A1-A3)	SOURCE OF WASTE (WHEN RECYCLED)	RECYCLING RATE
Recycled Nylon(Aquafil 2020)	Translucent	1.01	Fishing waste	100%
Cotton(Rosa and Grammatikos 2019)	Opaque	23.40	Clothing	Low + downcycling
ETFE (Taiyo Europe 2019)	Transparent Film	53.20	Building materials	100%
PTFE (woven fiberglass material with a PTFE coating) (Saint-Gobain Performance Plastics 2017)	Translucent and opaque	230.00	N/A	N/A
PVC-PES (Low & Bonar GmbH 2013)	Translucent and opaque	4.72	Architectural membranes and fabrics	100%

Nylon is a widely recycled material, often from discarded fishing gear– it is a good option for that reason as we would like to use recycled materials to limit the environmental impact of the screen. Of the sample materials group, it also has the smallest GWP. Cotton is an organic material typically used in textiles in the fashion industry, and has a very low GWP. However, it is not an adequate option for a building material without being treated with additional chemicals or materials, and can only be downcycled. This means that it would have to be woven with other materials to be recycled. PVC-PES is widely used in the building industry as it is accessible, affordable, and recyclable; however, recycling streams are not widely available and PVC is characterized by the International Living Future Institute as a Red List material (ILFI 2022). PTFE is not recyclable, and has the highest GWP— for those reasons, it is not the most appropriate choice.

3 EXPERIMENT/RESEARCH

3.1 MECHANISM AND GEOMETRY

The roller mechanism, as introduced in section 1.2, can be executed in different ways (figure 8).



FIG. 7 Roller configuration (l.) for intended material gradient (r.)

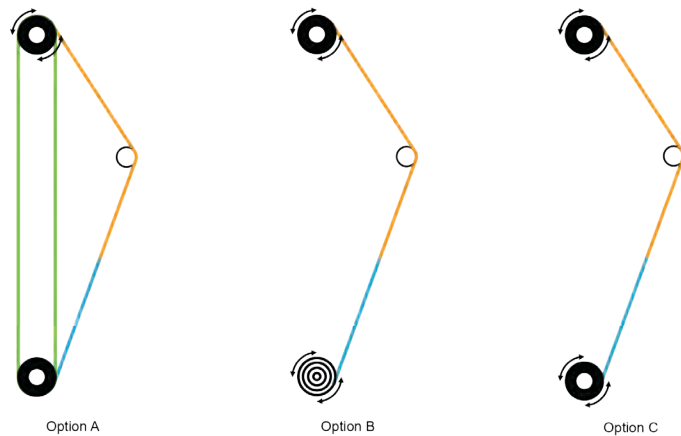


FIG. 8 Different iterations of the scrolling mechanism

The screen assembly on each floor is two times longer than the floor-to-floor height, which allows the bi-annual alternation between the summer and winter façade. In the summer, the unused part of the textile corresponding to the winter season is stored at the top roll, while the actively used part of the textile spans between the two rollers. Vice versa, in the winter, the inactive summer portion of the textile is stored at the bottom roll. This bi-annual change allows for basic performance adjustments of the textile façade over the warm and cold seasons. In the summer months the building skin is porous and shaded; in the winter months it transforms into an insulating skin. The latter is designed to use solar loads to thermally-activate the space between the screen and the existing façade. During the day, the position of the screen can be adjusted gradually to meet user-specific needs. This screen is designed on a story-by-story basis, but can also span several stories. However, this paper only analyzes systems that span one story.

Facade design often has to balance the extent of glazed and opaque wall assemblies to meet energy efficiency and user comfort targets. The screen aids in this effort by allowing adjustments across façade types to fit the ratio of glazed versus unglazed surface by varying the extent of the frit pattern. In buildings where facades are composed of a combination of brick/metal panels and glazing, the density of the frit pattern can be reduced to just the glazed area. In fully glazed facades, Fig 9, the density of the frit pattern can extend from floor to floor—possibly exceeding the extents of one floor in double-height areas.

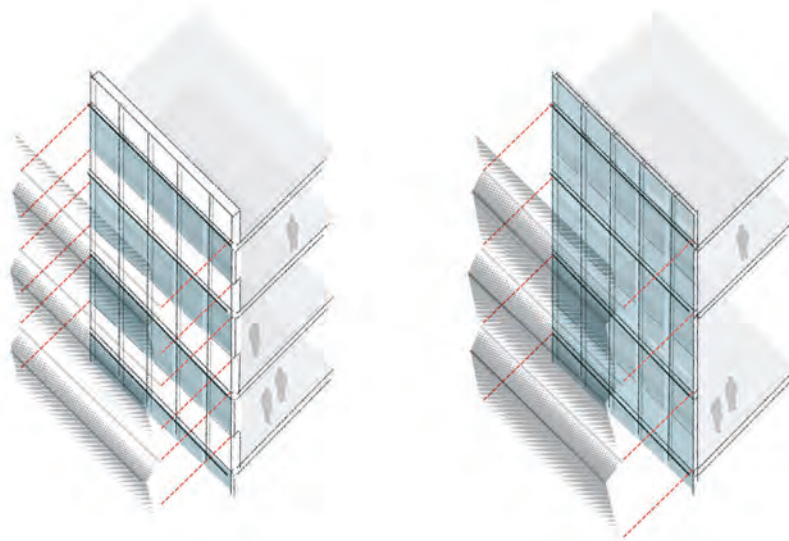


FIG. 9 Screen pattern matching glazed openings (left) and frit pattern optimized for fully glazed facades (right)

3.2 SKIN DESIGN

3.2.1 Fixed and Variable Design Parameters

In order to optimize the user comfort in the interior spaces with the proposed screen, hard and soft design parameters were defined. Hard parameters are user-based basic needs, such as an unrestricted view from the windows up to a minimum height of 1.80 meters; and a distance between the textile and the window pane of at least 50 centimeters. Strong light-shadow contrasts are avoided as they are irritating to the human eye—this is regulated by the gradual stitch (or frit) density of the textile and is difficult to quantify; therefore this parameter can only be evaluated qualitatively as a soft parameter.

3.2.2 Material Research

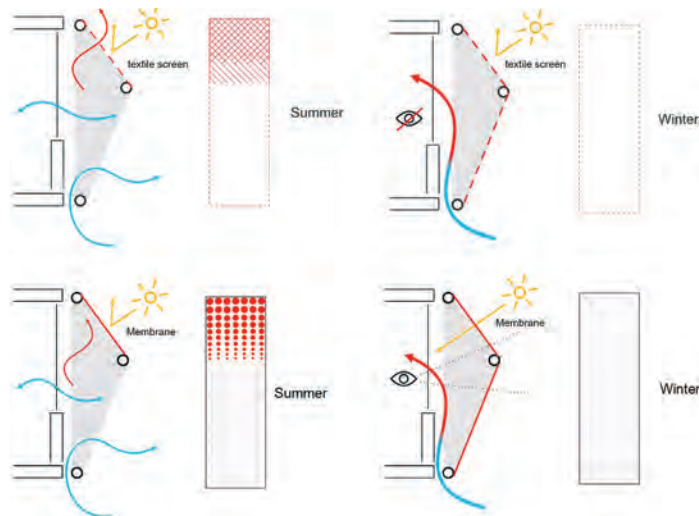


FIG. 10 Material properties: Textile screen summer (top left), winter (top right), Membrane summer (bottom left), winter (bottom right)

Based on the available materials and techniques on the market, an ETFE membrane skin in combination with a frit pattern would arguably be the most accessible solution for this scrolling screen. This option can provide sun shading by reducing the transparency of the membrane through a reflective frit pattern, as well as a second insulation layer by creating an insulating buffer zone between the actual façade and the scrolling screen. In conclusion, it can be said that the ETFE membrane exceeds the requirements because it provides an insulating, transparent solution in all conditions of use - even in summer when the screen is only a shading device. In consequence, it is a limited solution that does not fully exploit the possibilities of the screen.

Thus, a combination of different materials is proposed. In this case, the sun shading-fraction of the screen would be composed of a woven textile with different densities, which would allow the use of up-cycled or renewable materials. In addition, the possibility of using opaque materials in this part of the screen significantly enlarges the palette of potential textiles. The winter screen follows the above-mentioned ETFE-membrane solution. By interweaving the membrane and the textile, different densities and qualities can be obtained that offer diversity in use. Furthermore, weaving offers the possibility to deconstruct the combined materials at the end of their lifecycle and recycle them accordingly.

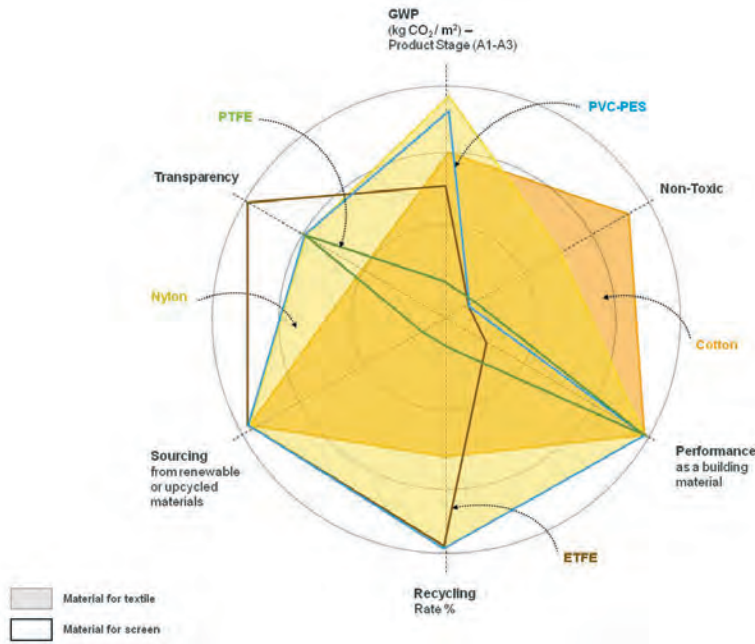


FIG. 11 Material analyses

3.2.3 Pattern

The study of frit patterns in our work, can also represent weave patterns. Studying frit patterns was more accessible to us, as they are relatively easy to quantify and modulate in modeling software—the density in the frit pattern represents the stitch density or increased layering in the textile screen (Fig 10). These densities, as well as the sizes of the dots and their positioning, vary throughout the screen to accommodate and respond to different needs. Daylight and radiation analyses were done in tandem, to inform the design of the pattern and ensure that it provides adequate daylight, radiation reduction etc.



FIG. 12 Serge Ferrari textile façade creating patterns (left), Dimension-Polyant's X-Ply® Reinforced Monofilm reinforcement layers (center), weaving frit patterns on a textile substrate (right)

3.2.4 Materialisation

A 1:5 physical scale model of a typical office space was constructed to simulate and visualize the effects of the screen and corresponding lighting levels and glare. Two screen prototypes were constructed, one for the summer season and one for the winter. Using a combination of tools and techniques such as a printer, laser cutter, stencils, and spray-paint, the designed frit pattern was printed or applied on acetate film. The various patterns were tested and photographed outdoors on a sunny day to observe and record daylight and shadow effects on the office space.

4 RESULTS

4.1 PERFORMANCE ANALYSES

4.1.1 Daylight Autonomy Analysis

Daylight autonomy analyses of an office located in Stuttgart, Germany (southern orientation) indicated that there is often excessive daylight, especially between 7:30 AM and 4:30 PM during summer months. When compared to the additional façade layer, the screen reduces this excessive daylight throughout the year, and increases autonomous daylight.

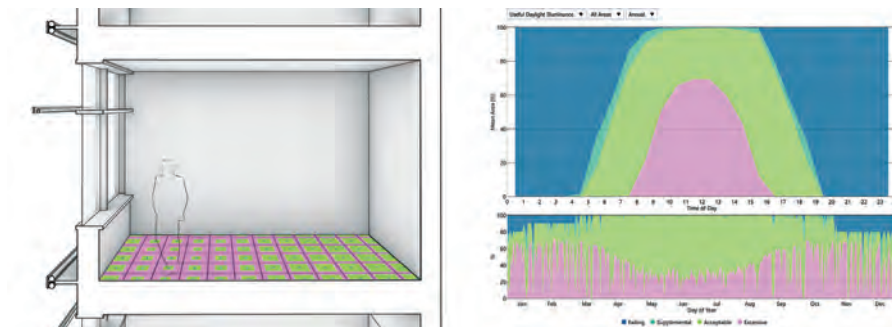


FIG. 13 Control daylighting analysis

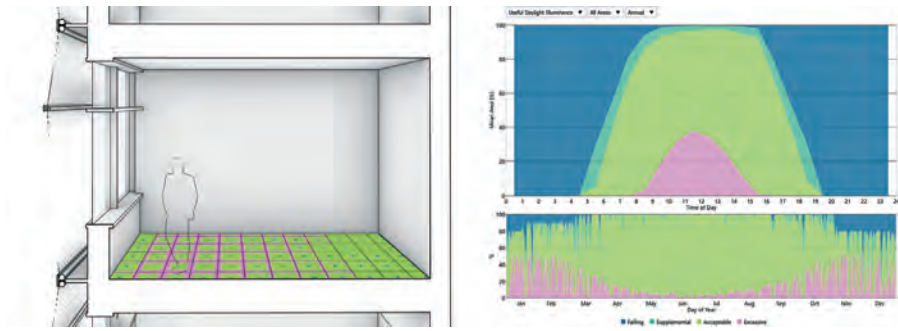


FIG. 14 Screen 5 Summer daylight analysis

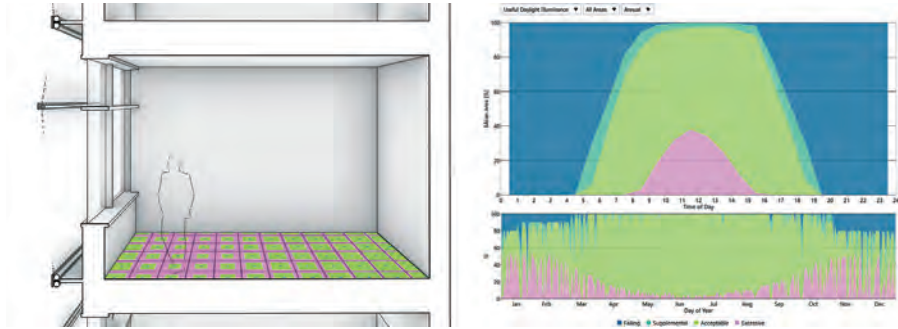


FIG. 15 Screen 5 Winter daylight analysis.

Radiation Analysis

Without our proposed screen the modeling study shows excess solar heat gain which creates a need for cooling during summer months, typically addressed with addition of A/C units or larger mechanical cooling systems designed for worst-case events. With the screen, solar heat gain is significantly reduced, which can eliminate the need for supplemental cooling.

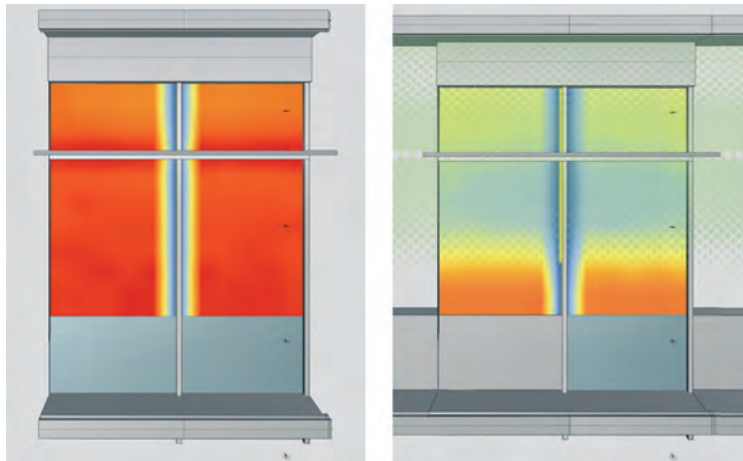


FIG. 16 Radiation levels on a regular façade (ie. without a scrolling screen) (right) - Summer Average Radiation: 81.9 kWh/m². Radiation levels with added scrolling screen (left) - Summer Average Radiation: 44.9 kWh/m²



FIG. 17 Section perspective illustrating a typical office environment relative to the screen façade.

In office areas, the designed pattern allows for views out of one's office while still providing shading from intense sunlight (Figure 15). The semi-transparent pattern, allows for light to be dappled and softened as it enters the space.

In the summer, the screen creates a mesh with a density gradient optimized for shading. The bottom is open, so air can freely circulate.

In the winter the screen creates an enclosed second skin— cold air gets heated up between the screen and the existing facade. The flow of air can be regulated between the floors. Hence, we can use preconditioned air, even on cold days, for the natural ventilation of the interior spaces.

The physical model and simulation allowed us to visualize and confirm the effects of the screen on the space, particularly how the light is diffused, dappled, and softened.



FIG. 18 Photograph of model taken outdoors with the winter screen (left) and the summer screen (right)

5 CONCLUSION

This research introduces both quantitative and qualitative parameters and results—the competing objectives being the performance of the skin and its ecological footprint, as well as the improvement of user comfort. The simulations allowed the team to test and demonstrate that the scrolling screen reduces heat gain in summer and increases daylight autonomy and natural ventilation in winter. The next steps will include further development of the pattern composition to maximize its performance, as well as implementing this pattern in textiles and experimenting with stitch densities. There are different possibilities in terms of the mechanical roller system, each of which has its advantages and disadvantages. Concluding which system is the most appropriate will depend on creating 1:1 prototypes, fabrication and manufacturing, and cost estimates. Similarly, while we have made initial deductions regarding the material choices for the screen, prototyping and manufacturing accessibility and cost estimates are necessary to move forward. It can be stated that the scrolling screen offers great possibilities in the creation of climate-adaptive building skins, especially concerning the adaptation of existing buildings.

We intend to continue expanding on this work through our upcoming residency at the Autodesk Technology Center in Boston, Massachusetts in the summer and fall of 2022.



FIG. 19 Section perspective illustrating a typical office environment relative to the screen façade. Combined textile and membrane screen (in progress)

References

- Aquafil Group Econyl® NTF Yarns. (2020). Environdec Environmental Product Declaration for Econyl®, Nylon Textile Filament Yards. Retrieved from <https://www.environdec.com>
- Fathy, Hassan. (1987). *Natürliche Energien und vernakuläre Architektur*. Arch+.
- Hönger, Christian. (2009). *Climate as a Design Factor*. Luzern: Quart Verlag.
- International Living Future Institute. (2022). About the LBC Red List. Retrieved from <https://living-future.org/lbc/red-list/>
- Koolhaas, Rem. (2018). *Elements of Architecture*. Köln: Taschen GmbH.
- Low & Bonar GmbH. (2013). Environmental Product Declaration VALMEX® FR 900. Retrieved from <https://epd-online.com>
- National Association for Olmsted Parks. (2022). Olmsted 200: Olmsted's Trees Tour. Retrieved from <https://olmsted200.org/events/olmsted-200-olmsteds-trees-tour/>
- Rosa, Angela, Grammatikos, Sotirios. (2019). Comparative Life Cycle Assessment of Cotton and Other Natural Fibers for Textile Applications. *Fibers* 2019, 7, 101; doi:10.3390/fib7120101
- Saint-Gobain Performance Plastics. (2017). Environmental Product Declaration SHEERFILL II ARCHITECTURAL MEMBRANE. Retrieved from <https://www.sheerfill.com/resources>
- Taiyo Europe GmbH, AGC Inc. (2019). Environmental Product Declaration TensoSky® - System with Fluon® ETFE-FILM. Retrieved from <https://epd-online.com>
- Zizzo, Ryon. (2017). Embodied Carbon of Buildings and Infrastructure. Retrieved from <https://www.naturallywood.com/resource/embodied-carbon-of-buildings-and-infrastructure/>
- Zhou, Yiran. (2022). String Art Generator is a self-developed grasshopper plug-in based on c#. Retrieved from <https://www.yiran-zhou.com/stringartgenerator>

Adobe Cavity Wall Envelopes with High Thermal Performance: the Middle-Eastern Scenario

Claudio Marini^{1*}, Alessandro D'Ambrosio¹, Erolcan Erdogan¹

* Corresponding author

¹ Buro Happold, Façade Engineering, UK, Claudio.Marini@BuroHappold.com

Abstract

Locally sourced earthen materials have been used for thousands of years and have shaped the built environment, creating a sense of cultural identity in many regions around the world. Due to the cultural and environmental pull to return to these materials and the modern performance requirements, new technical solutions must be discussed. The intention of this paper is to investigate the full potential of an adobe building envelope as a case study, to then derive a more generic understanding of earthen materials and provide insights useful for future research and practical applications. Furthermore, this work is meant to offer advice to the reader, based on research and extensive literature review, as to the potential standards and codes to be applied for testing adobe cavity wall envelopes for every design aspect that a modern and functional building envelope needs to fulfil. This study starts from a typical adobe solid wall build-up to then evaluate the effectiveness of using this earthen material in a fully engineered cavity wall; the focus is on the thermal performance comparison between the proposed build-up options. Then, a preliminary embodied carbon assessment is carried out to measure the impact that using locally-sourced materials – a big paradigm change – would have on the built environment.

Keywords

Earthen constructions, adobe blocks, cavity wall, façade design, holistic design, embodied energy, life cycle assessment, thermal performances

1 INTRODUCTION

Locally-sourced earthen materials have been used in the built environment for thousands of years; as a consequence, their presence in landscapes is tightly tied to cultural identity and heritage, as it is the case for the Najd architecture of Al-Diriyah (Alaidarous, 2014). In this example, buildings built with locally sourced adobe blocks stood the test of time and became crucial to the identity of the region (Alnaim, 2021). However, the systems in which these materials were used are not deemed on-par with the consistency expected from high-performing building envelopes, especially for occupant comfort and structural integrity, due to the variable nature of minimally-processed materials (Parra-Saldivar & Batty, 2005). For this reason, with the intent of giving new life to an old technique, low-tech earthen materials can be used as part of contemporary high-performing systems to increase their performance. In fact, the positive effect of coupling earthen materials with a modern solution is not potentially limited to matching the aesthetic value linked to a region's cultural identity with a renewed level of performance; with the exponential rise in climate change awareness that the building environment is facing, these materials might be one of the keys to a long-awaited, large-scale action.

The focus of this paper will be on the thermal performance of building envelopes made partly or entirely out of adobe mud blocks. To reach a required thermal performance standard, the adobe wall needs to be engineered into a cavity wall system; this implies increasing the complexity of the envelope build-up, which makes it harder to assess all the other performance requirements of a contemporary wall, including the structural behaviour. This research investigates what is required from a high-performance adobe cavity wall envelope, provides an overview of the main design criteria to be considered, and proposes a list of potentially applicable standards, based on literature review. The aim is to try and open a discussion about how earthen materials might be utilised more and more in the future for their beneficial influence on the built environment, given that the current performance data gaps are filled.

2 DEFINITIONS

The technical definitions used in this paper are presented in this section.

2.1 ADOBE BLOCKS

In contrast to in-situ monolithic earthen constructions, several types of earthen constructions are based on units, such as adobe blocks (Jaquin & Augarde, 2012). These sun-dried mud blocks are a type of traditional, locally sourced, earthen building material, which have been used for thousands of years in several parts of the world for bearing walls (Mortada, 2016), providing enough thermal mass to increase the occupant comfort. While the term "adobe" has different meanings in different cultures and geographical areas (Jaquin & Augarde, 2012), in the context of this work it will be used to describe an uncompacted unit formed by a mix of local soil and organic materials, such as natural fibres and straws. The block is manufactured in a reusable frame and then sun dried.

2.2 CAVITY WALL SYSTEMS

Cavity walls are double-leaf systems characterised by an air cavity between the internal and external leaf. Their widespread introduction as a building envelope system has helped with the thermal comfort and watertightness, thanks to offered lines of defence: water ingress is mostly impeded by the outer wall, while the water that reaches the cavity is drained (H. Hens, 2007).



FIG. 1 Traditional production of adobe blocks in Saudi Arabia. Adobe mixture is manually pressed into wooden frames. Source: Mortada (2016)

According to BS EN ISO 6946, air layers in cavity walls can be classified as unventilated, slightly ventilated, or well-ventilated depending on the air flow through ventilation and/or drainage openings. The type of air layer has an impact on the overall thermal performance of the cavity wall as it influences the heat exchange in the build-up, making this definition important.

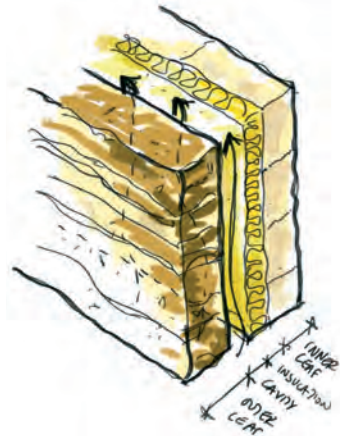


FIG. 2 Sketch showing the main components of an insulated cavity wall system: inner leaf, thermal insulation, air cavity, outer leaf. Source: Buro Happold

2.3 DEFINITION OF HIGH PERFORMANCE

81 In the context of this work, high performance building envelope is defined as above-standard level, capable of exceeding any requirement from current applicable codes, but also proving to be in line with what will be likely to be required in the foreseeable future. In order to assess the performance of a building envelope, test data is required in regard to different performance criteria, and this will be further discussed in the next sections of this paper. However, for this work, the focus will specifically be on high thermal performance. In fact, this is one of the main drivers for the design of building envelopes aimed at improving the occupant comfort, limiting the energy consumptions and limiting the operational carbon emissions. Building envelopes with high thermal performance, typically translating into low U-Values, are often a mandatory requirement according to local Building Codes in the majority of the Countries. Low U-Values are also a typical requirement needed to achieve reputable sustainability rating according to certification systems, such as LEED and Mostadam.

3 METHODOLOGY

3.1 SOURCES OF INFORMATION

This work is based on literature review, desktop studies and the Authors' professional experience from projects in the Middle Eastern region, including confidential test data from Clients and local Suppliers at both material and façade system level.

3.2 ASSUMPTIONS ON TARGET PERFORMANCES

For the scope of this paper, a generic typical two-storey building in the Commercial sector in the Middle Eastern region was considered. In terms of thermal performance, the target U-Value was assumed equal to 0.20 W/m²K, excluding thermal losses due to non-repetitive thermal bridging. This target was deemed as appropriate being in line with the target requirement of a confidential on-going project in the region.

3.3 ASSUMPTIONS ON EARTHEN MATERIALS

The following assumptions have been made for the earthen materials, taking into consideration the best practice in the region.

Adobe blocks are assumed being made from silty sandy clay mix design (gravel and sand composition: 55-75%, silt and clay composition: 25-45%), fermented with straw (50 Kg/m³, 80-100 mm long) and water for a minimum of 21 days. The fermented mix is assumed being used to manually manufacture the blocks in traditional open wood moulds, then naturally dried for a minimum of 7 days. Adobe blocks are assumed being unstabilised, therefore manufactured without the use of cement or stabilisers compromising the recyclability of the material at the end of the service life. The size of the adobe block is assumed being 100 mm x 200 mm x 400 mm.

The earthen mortar is assumed being composed of the same material to that of the adobe blocks, as recommended by Jaquin and Augarde (2012).

The earthen plaster is assumed being manufactured using the same mix design to that of the adobe blocks, with a longer fermentation period equal to 60 days. Plaster is applied through different coats, for a total thickness of approximately 50 mm.

3.4 DESIGN METHODOLOGY

The methodology adopted for the current research mainly consists of two separate phases: in the first phase (Section 4) the relevant design aspects that need to be taken into consideration through specific parameters and variables during the design process of a modern and functional building envelope, are presented. Furthermore, the standards and codes that the Authors recommend being used for testing of adobe cavity wall envelopes are listed. These are divided according to the design level: single material (e.g. adobe block and earthen mortar/plaster) and whole system level.

During the second phase (Section 5) four different design options are considered with the aim of moving from a non-engineered traditional adobe mass wall to a fully engineered adobe cavity wall. The build-ups have been designed taking into consideration buildability aspects, traditional construction techniques and material properties in the Middle East and the assumed target U-Value performance.

Finally, a comparison between the different build-ups is provided in terms of thermal performances (i.e. U-Value), sustainability-related aspects (e.g. recyclability of the materials and global warming potential) and buildability considerations.

3.5 U-VALUE CALCULATION METHODOLOGY

U-Values for the different build-ups considered have been calculated through 2D thermal finite element analysis using the software Physibel BISCO 11.0w. The thermal conductivity of materials is modelled in accordance with BS EN ISO 10456 and manufacturers' data, taking into consideration that earthen materials are subject to a change in their performance that is related to the variation in composition of the soil, fabrication process and water content (Augarde, Beckett, Smith, & Corbin, 2016).

For thermal transmittance, the temperatures and heat transfer coefficients have been assumed in accordance with BS EN ISO 6946 and BS EN ISO 10211. Thermal losses due to repetitive thermal bridging (e.g. cavity ties or mechanical fixings for the thermal insulation) have been calculated according to the methodology described by ISO 6946, where applicable. Thermal losses due to non-repetitive thermal bridging (e.g. interfaces with openings, slab edge, interface with roof etc.) have not been considered in this work.

The conducted study assumes unventilated air cavities for the cavity wall build-ups due to the weep hole surface area in the outer leaf of the masonry walls not exceeding the limiting amount for openings as recommended by BS EN ISO 6946

3.6 EMBODIED CARBON ASSESSMENT METHODOLOGY

Embodied carbon is a term used to define and quantify the greenhouse gas emissions and removals related to a certain material and the processes which that material goes through during its whole life cycle (A1-A5, B1-B5, C1-C4) (LETI, 2021). It is crucial for the construction industry to adopt calculating the embodied carbon of each component to define a clearer path to reduce resource consumption and to shift towards a circular economy (Gibbons, Orr, Archer-Jones, Arnold, & Green, 2022). As the embodied carbon calculation of a material's whole life cycle would require many project-specific data, this paper focuses on the raw material extraction, transport to manufacturing site and manufacturing emissions (A1-A3). The data for the embodied carbon factors for the modules A1-A3 have been taken from literature reviews, the ICE and ÖKOBAUDAT databases and certain supplier/manufacturer EPDs. The earthen materials considered in this study, namely the adobe blocks and plaster, have been assumed to be locally sourced, produced on-site with wheat straws transported to site, as per the projects Buro Happold have been involved in. Moreover, the high impact on the embodied energy of transportation of earthen constructions was highlighted in the study by Nanz, Rauch, Honermann & Auer (2019). The cradle-to-site global warming potential (kgCO₂-eq) for the adobe blocks and plaster (on-site production, locally sourced soil, transported wheat straw) have been taken as 1.76E-03 according to prior research (Christoforou, Kylili, Fokaidis, & Ioannou, 2015).

A quantity take-off for a 3.5-meter-high and 1.5-meter-wide facade panel for each analysed wall type has been taken into consideration. The build-up thicknesses vary depending on the wall type and, if set, the performance criteria for the analysed wall type. Each material quantity has been multiplied by its A1 to A3 global warming potential (kgCO₂-eq/FU) figure to calculate the total emissions and emissions per square meter of façade.

4 PERFORMANCES AND CODES

4.1 HOLISTIC DESIGN

Despite the main driver is thermal performance, this is only one of the many aspects that need to be considered during the design. The diagram in the image below shows the complexity of the design process of a generic modern and functional building envelope. Where blue and purple bubbles are the design aspects to be considered during the holistic design process. The yellow and green bubbles represent the deliverable outputs produced, based on design inputs (yellow) or on the decisions made during the design process (green). All the above result in the finalised design information, useful to procure and build.

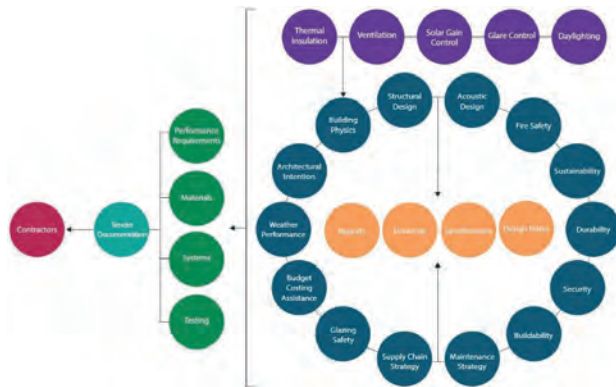


FIG. 3 Diagram showing the complex relationship between design aspects and deliverables required to procure a complex building, following a holistic design process. Source: Buro Happold

For an opaque adobe cavity wall, the majority of the design aspects are relevant and need to be taken into consideration through specific parameters and variables, which may interest the single material (e.g. adobe blocks, mortar, earthen plaster etc.) or the whole facade system.

The main design aspects that may need to be considered on a project-specific basis are listed below:

- Structural integrity:
 - Structural integrity under dead loads;
 - Resistance against live loads;
 - Resistance against environmental loads (e.g. wind, sand, seismic);
 - Resistance against impacts (soft body, hard body)
 - Structural integrity during construction
- Building physics:
 - Thermal transmittance;
 - Condensation risk analyses (superficial and interstitial);
- Fire safety:
 - Resistance against fire
- Water-tightness
- Air-tightness
- Security
- Acoustic:

- Sound insulation – Noise break-In
- Flanking
- Durability:
 - Resistance against superficial cracks due to thermal and moisture movements
 - Aggressivity Corrosion of cavity ties
 - Abrasion resistance
 - Frequency of maintenance regime
- Sustainability:
 - Embodied carbon
 - Recyclability of the material
- Aesthetics:
 - Colour, texture, pattern of finishes

4.2 PERFORMANCES AND APPLICABLE STANDARDS FOR TESTING

An obstacle to the performance assessment of earthen materials is the current lack of consistent test data, which results in building codes not yet being aligned in regards to these materials. The main issue is that the lack of general understanding of their performance in modern systems might prevent their utilisation on a larger scale (Alaidarous, 2014). Only a few countries developed standards or codes dealing with the topic of earthen constructions (e.g. Australian and German) and, amongst them, the New Zealand standard NZS 4298 is widely recognised as one of the most complete and suitable for earthen construction (Calatan, Hegyi, Dico, & Szilagyi, 2020).

Taking this into account, the intention of this Section is to offer advice to the reader, based on research and extensive literature review, highlighting remarkable standards and codes to be applied for testing of adobe cavity wall envelopes for each design aspect and parameter. Those standards and codes are listed in the table below, divided according to the design level: single material (e.g. adobe block and earthen mortar/plaster) and whole system level.

TABLE 1 List of performances and applicable standards for testing

Design aspect:	Design parameter:	Design level: single material		Design level: whole system
		Adobe block	Mortar/Plaster	
General	Density	NZS 4298:2020 Appendix M		X
	Moisture content	NZS 4298:2020 Section 2.6.1.2, Appendix H, I, M		X
Structural Integrity	Compressive strength	NZS 4298:2020 Appendix D, E	NZS 4298:2020 Appendix D, E	NZS 4298:2020 Appendix D, E
		EN 772-1	EN 1015-11:2019	ASTM C67 EN 1052-1:1998
	Flexural strength	NZS 4298:2020 Appendix D, G, N	NZS 4298:2020 Appendix D, G, N	NZS 4298:2020 Appendix D, G, N
			EN 1015-11:2019	EN 1052-2:2016
	Shear strength	X	X	NZS 4298:2020 Appendix D EN1052-3:2002
	Tensile strength	X	X	ASTM E519/E519M
	Cavity tie and reinforcing mesh pull-out resistance	X	X	ASTM D6637-11
			BRE Digest 401	
Soft body impact resistance	X	X	CWCT TN 76	
Hard body impact resistance	X	X	CWCT TN 76	

Building Physics	Thermal conductivity	ASTM E 1225-87		X
	Thermal mass	ASTM E 1225-87		X
Fire Safety*	Combustibility of the material / Reaction to fire	ASTM E136		X
	Full assembly fire test	X	X	NFPA 28
Water-tightness**	Water absorption assessment – Contact Sponge Method	UNI 11432		X
	Water absorption assessment by capillarity	EN 15801		X
	Water repellence assessment	EN 1015-18		X
	Water vapour permeability	EN 15802		X
Air-tightness	Air leakage rate	EN 15803		X
	Whole building air leakage rate calculated on-site	X	X	ASTM E7
Security	Burglar resistance**	X	X	**
	Bullet resistance	X	X	UL752
	Blast resistance**	X	X	**
Acoustic	Effective sound insulation	X	X	ISO 140
Durability	Thermal expansion and contraction	ASTM E831		X
	Moisture expansion and contraction	BS 5080 Part 1		X
	Chemical composition (pH value, Chloride and Sulphate concentrations, Resistivity)	NZS 4298:2020 Appendix H		X
	Abrasion resistance	X	DIN 18947	X
	Artificial aging test	NZS 4298:2020 Section 2, Appendix A, B		X
Sustainability***	Global warming potential	EPD	EPD	EPD
	Recyclability	EPD	EPD	EPD

Notes:

* It is noted that, in most countries, the fire requirements vary according to type and height of the building. Refer to the relative current Building Code for project-specific requirements.

** It is noted that several Standards providing guidance on testing for Water-tightness and Security aspects are designed for glazed systems. These may still be applicable to test junctions between adobe cavity walls and openings, where applicable.

*** EPD (Environmental Product Declaration) according to EN 15804 and ISO 14025 may be used to provide sustainability-related information.

It is noted that the application of standards and codes external to the interested Country should be agreed and approved by the relevant local Authorities: the previous codes are not calibrated for the traditional materials produced and used in the Middle Eastern region, where specific mix design and techniques are implemented. In fact, curing process and environmental conditions have an impact on the final mechanical properties of earthen materials. Because of this, while designing, available values coming from existing buildings located in the same area may also be taken into account.

This may help the designer to have an idea about ranges of realistic design parameters related to a specific construction technique and territory.

It is acknowledged that the tests suggested in the table above are time consuming and onerous from an economical perspective, at the same time they can represent a valuable source of information on local earthen constructions for future projects and applications in the Middle East.

5 PROPOSED DESIGN OPTION: MOVING FROM MASS WALL TO CAVITY WALL

Four different design options are here presented: a non-engineered traditional adobe mass wall (Case 1), a non-insulated all-adobe cavity wall (Case 2), an all-adobe cavity wall with thermal insulation (Case 3) and a hybrid adobe-concrete cavity wall with thermal insulation (Case 4). These Cases have been designed considering buildability aspects, traditional construction techniques and local material properties. Typical structural capabilities of each system have also been taken into account and Cases 3 and 4 achieve the assumed target U-Value performance.

5.1 CASE 1 – ADOBE MASS WALL

This Case represents a traditional, non-engineered adobe mass wall system and consists of the following layers:

- 50 mm earthen plaster
- ~450 mm adobe blocks
- 50 mm earthen plaster

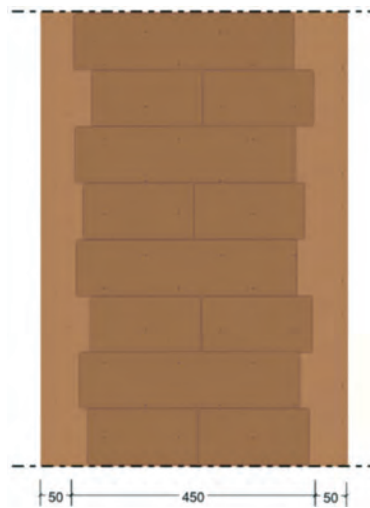


FIG. 4 Case 1, Traditional, non-engineered adobe mass wall, indicative vertical section

The variation in the dimension of the central layer takes into account the tolerance for the brick layout offset and plaster layer. As this build-up is widely found and used in modern designs all over the world, it will serve as a standard to compare the other options.

5.2 CASE 2 – ALL-ADOBE CAVITY WALL

Case 2 is an engineered adobe block cavity wall without insulation. Compared to Case 1, an air cavity has been introduced to increase the thermal performances and this required the introduction of stainless-steel cavity ties, in order to mechanically connect the inner and outer leaves of the wall for enhanced structural integrity. A stainless-steel reinforcing mesh was also integrated in the earthen plaster, to obtain higher resistance against impacts, thermal and structural movements and enhanced post-breakage resistance, in case of delamination of the plaster from the adobe blocks layer. Case 2 consists of the following layers:

- 50 mm external mesh-reinforced earthen plaster
- 200 mm adobe blocks front leaf tied to backing wall through wall ties on mesh patches
- 50 mm air cavity
- 200 mm adobe blocks backing wall
- 50 mm internal mesh-reinforced earthen plaster

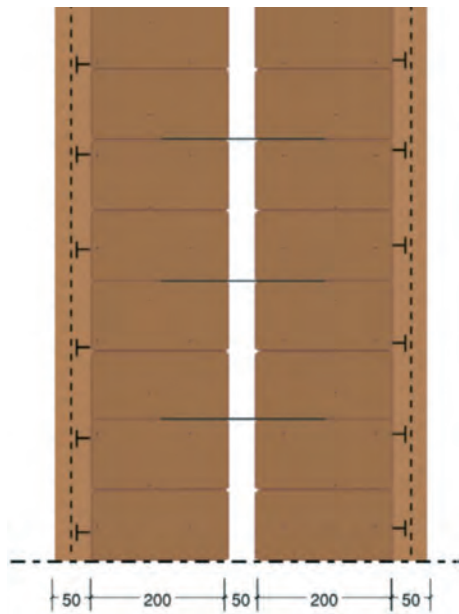


FIG. 5 Case 2, All-adobe cavity wall, indicative vertical section

5.3 CASE 3 – ALL-ADOBE CAVITY WALL WITH THERMAL INSULATION

Case 3 is an engineered adobe cavity wall with thermal insulation. The introduction of a layer of non-combustible thermal insulation allows to achieve lower U-Values compared to the previous Cases. Moreover, a Vapour Control Layer is introduced between the backing wall and the layer of thermal insulation. Case 3 consists of the following layers:

- 50 mm external mesh-reinforced earthen plaster
- 200 mm adobe blocks front leaf tied to backing wall through wall ties on mesh patches
- 50 mm air cavity
- 150 mm non-combustible insulation
- 200 mm adobe blocks backing wall
- 50 mm internal mesh-reinforced earthen plaster

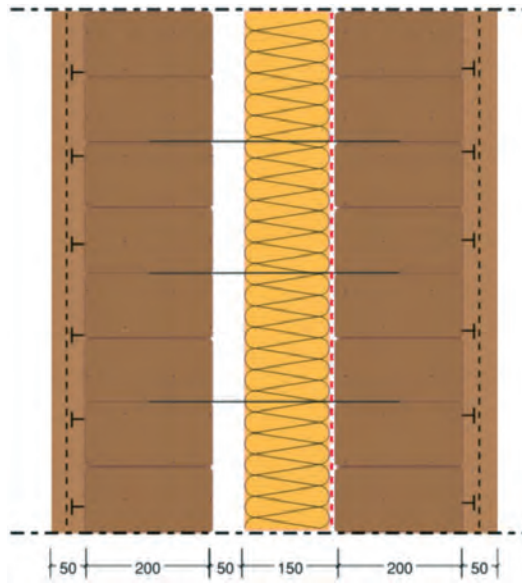


FIG. 6 Case 3, All-adobe cavity wall with thermal insulation, indicative vertical section

5.4 CASE 4 – HYBRID ADOBE-CONCRETE CAVITY WALL WITH THERMAL INSULATION

Case 4 is an engineered hybrid cavity wall with adobe front leaf and concrete blockwork backing wall, with non-combustible thermal insulation. Compared to Case 3, a concrete blockwork backing wall replaces the inner adobe block leaf in order to achieve more reliable structural performances due to the standardised mechanical characteristics of the material, compared to earthen materials. Case 4 consists of the following layers:

- 50 mm external mesh-reinforced earthen plaster
- 200 mm adobe blocks front leaf tied to backing wall through wall ties on mesh patches
- 50 mm air cavity
- 150 mm non-combustible insulation
- 150 mm concrete blockwork backing wall

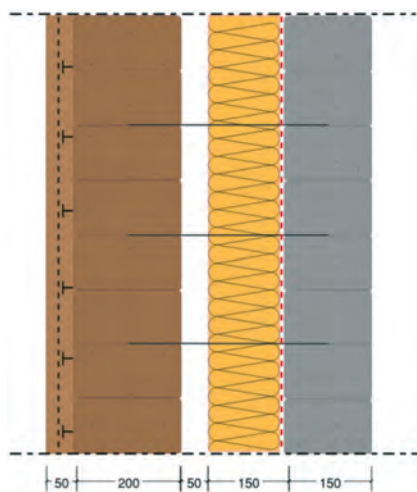


FIG. 7 Case 4, Hybrid adobe-concrete cavity wall with thermal insulation, indicative vertical section

6 RESULTS

6.1 THERMAL PERFORMANCES

As anticipated, U-Values for the different Cases have been calculated considering the thermal losses due to repetitive thermal bridging, namely the stainless-steel cavity ties (for Cases 2, 3 and 4) and the mechanical fixings for the thermal insulation (for Cases 3 and 4), while neglecting the thermal losses due to non-repetitive thermal bridging. The thermal conductivity (λ [W/mK]) of materials are modelled in accordance with BS EN ISO 10456 and manufacturers' data. For thermal transmittance, the temperatures and heat transfer coefficients have been assumed in accordance with BS EN ISO 6946 and BS EN ISO 10211. In the tables below, the thermal conductivities and assumed boundary conditions used in the assessment are available.

Material	Thermal Conductivity λ [W/mK]	Model Colour	Source
Earthen plaster	0.35		Project-specific test data
Adobe mud blocks	0.62		Project-specific test data
Concrete blockwork	2.00		BS EN ISO 10456:2007
Thermal insulation, mineral wool	0.035		BS EN ISO 10456:2007
Non-ventilated air cavity	N/A		BS EN ISO 6946:2017

TABLE 2 Material thermal conductivities

Material	Temperature [°C]	Heat transfer coefficient [W/m²K]	Model Colour
Internal boundary conditions	20	7.7	
External boundary conditions	0	25	

TABLE 3 Boundary conditions (thermal transmittance)

The isothermal lines for the different Cases are shown in the following Figures. For the sake of clarity, these represent the variation of temperature across the wall build-up considering a horizontal section.



FIG. 8 Build-up and isothermal lines for Case 1, horizontal section

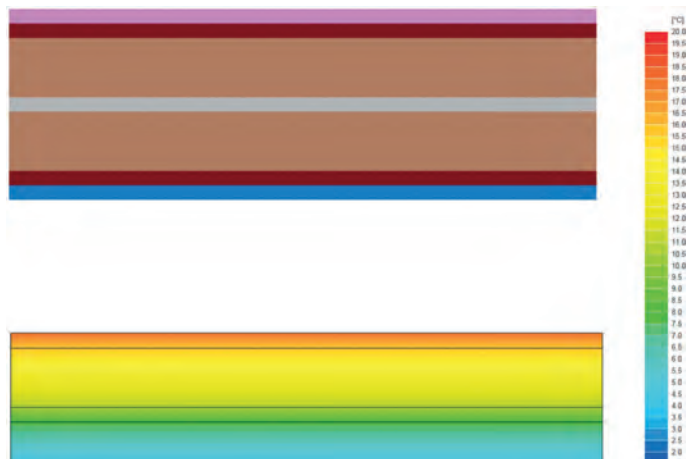


FIG. 9 Build-up and isothermal lines for Case 2, horizontal section

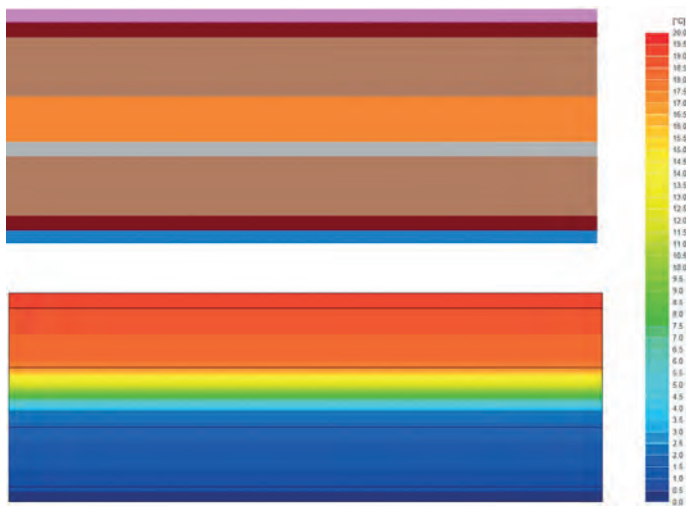


FIG. 10 Build-up and isothermal lines for Case 3, horizontal section

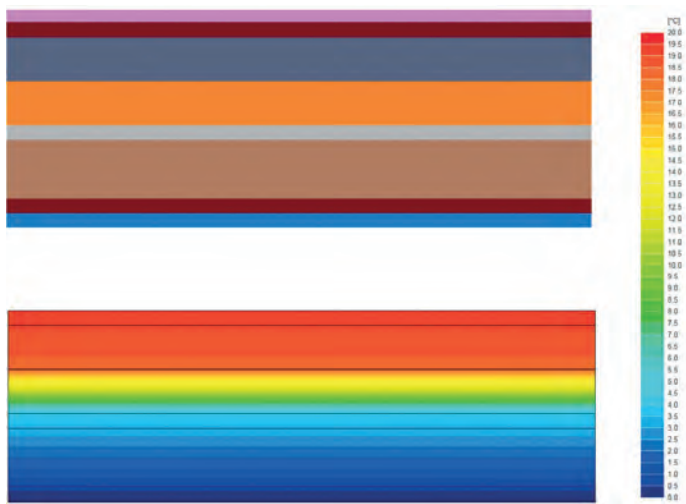


FIG. 11 Build-up and isothermal lines for Case 4, horizontal section

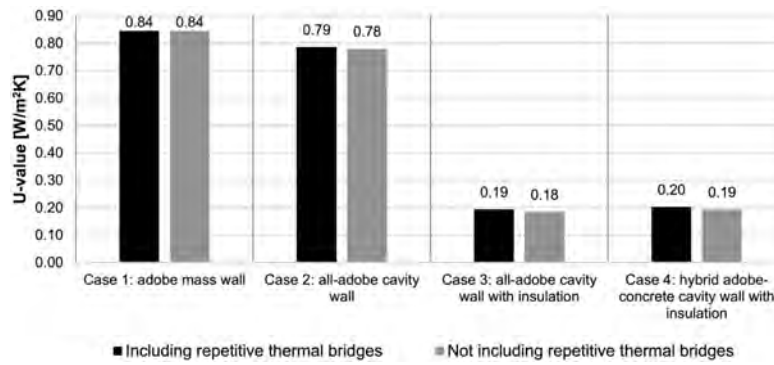


FIG. 12 U-Value comparison for the different Cases

The results shown above highlight the higher performance for Case 3 and Case 4, with values as low as 0.19 and 0.20 W/m²K respectively, compared to 0.84 W/m²K of Case 1 and 0.79 W/m²K of Case 2. The presence of the insulation layer in the cavity of the engineered walls greatly affects the thermal performance.

6.2 EMBODIED CARBON

Table 4 shows the information used to calculate the embodied carbon figures for the analysed adobe wall build-ups. The embodied carbon results for the four façade panels (3.5m x 1.5m) analysed for the study is provided in the Figure below. It illustrates the increment in embodied carbon as more energy-intensive material is added to the wall build-ups to increase performance, which is to be expected. Even though the cavity ties and reinforcing meshes are assumed to be of stainless steel, which is the material with the highest global warming potential within the build-ups, they do not have a large impact due to their material quantities. This relatively small jump can be observed from the change between Case 1 and Case 2. Whereas the increments between Case 2-3, and Case 3-4 show significant changes in the results. It can be said that the increase in embodied carbon has been largely driven by the implementation of mineral wool insulation and concrete blockwork.

Component	Source	GWP A1-A3 [kgCO ₂ eq/kg]	Density [kg/m³]
Adobe block	Academia	1.76E-03	2.5
Earthen plaster	Academia	1.76E-03	2.5
Stainless steel	ICE	4.407E+00	8000
Mineral wool insulation	Manufacturer	1.717E+00	45
Concrete block, medium density	ICE	9.3E-02	1300

TABLE 4 Information used to calculate embodied carbon figures

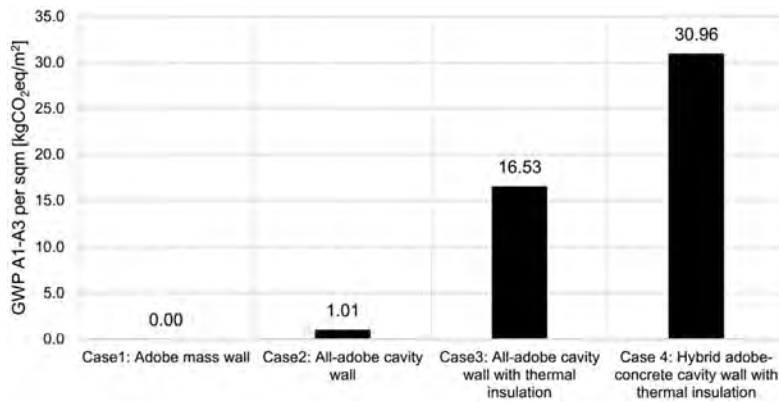


FIG. 13 Comparison of global warming potential for the different Cases

6.3 SUMMARY OF RESULTS

The table below provides a comparison of the four Cases, stressing the main results:

Case 1	Case 2	Case 3	Case 4
Adobe mass wall	All-adobe cavity wall	All-adobe cavity wall with thermal insulation	Hybrid adobe-concrete cavity wall with thermal insulation
Accessories:			
N/A	- Stainless-steel cavity ties; - Stainless-steel reinforcing mesh	- Stainless-steel cavity ties; - Stainless-steel reinforcing mesh	- Stainless-steel cavity ties; - Stainless-steel reinforcing mesh
U-Value without repetitive thermal bridging [W/m ² K] and variation [%]:			
0.84	0.78	0.18	0.19
Baseline	-7.1%	-78.6%	-77.4%
U-Value including repetitive thermal bridging [W/m ² K] and variation [%]:			
0.84	0.79	0.19	0.20
Baseline	-6.0%	-77.4%	-76.2%
Embodied Carbon - Global Warming Potential A1-A3 [kgCO ₂ eq/m ²]:			
2.42E-03	1.01E+00	1.65E+01	30.96E+01

TABLE 5 Comparison of the four Cases considered

As already stressed, from a thermal performance perspective Case 3 and Case 4 represent the best solutions amongst the considered Cases. This has a positive impact on the operational carbon emission of the building during its life. On the other hand, from an embodied carbon perspective, Case 3 and 4 are the worst-performing options. Additional sustainability-related considerations can be done. In fact, in theory, Case 1 can be entirely recycled at the end of its service life, being composed by earthen unstabilised materials only. However, the stainless-steel cavity ties and meshes integrated in Cases 2, 3 and 4 enhance the structural performances of the whole build-up.

7 CONCLUSIONS

This research work sets out the basis to investigate the use of earthen materials as part of modern building envelope systems on a large scale, considering the promising thermal performances that can be achieved and sustainability-related aspects. The preliminary analyses of the proposed Cases

show how the use of adobe blocks as part of a cavity wall system in the Middle Eastern scenario can greatly improve the envelope's performance, while keeping the traditional looks of this ancient, locally sourced earthen material. Additionally, it is important to highlight that the principles discussed in this research work can be transferred to other geographical areas worldwide being easily replicable using different local earthen materials. It is noted that, for a drastic change to happen in the built environment, more tests need to be carried out to better define and regulate the use of earthen materials. As a further development of this study and future work, other important aspects can be investigated, in order to push earthen materials to become a true sustainable alternative, such as: structural-related performances, maintenance requirements, buildability considerations and interfaces with openings and primary structure.

Acknowledgements

The authors would like to acknowledge support from Buro Happold and thank Panagiotis Papanastasis for his fundamental and influential contribution to this paper.

References

- Alaidarous, A. (2014). The documentation and analysis of the earthen architecture in Saudi Arabia. In F. V. C. Mileto, *Earthen Architecture: Past, Present and Future* (p. 17). CRC Press.
- Alnaim, M. (2021). Traditional Najdi Settlement Architectural Elements: Harmonizing Function, Aesthetics, and Shared Socio-Cultural Meaning.
- Augarde, C., Beckett, C., Smith, J., & Corbin, A. (2016). Challenges in treating earthen construction materials as unsaturated soils.
- Calatan, G., Hegyi, A., Dico, C., & Szilagyi, H. (2020). Opportunities Regarding the Use of Adobe-bricks within Contemporary Architecture. 13th International Conference Interdisciplinarity in Engineering (INTER-ENG 2019), (pp. 150–157).
- Christoforou, E., Kylili, A., Fokaides, P., & Ioannou, I. (2015). Cradle to site Life Cycle Assessment (LCA) of adobe bricks. *Journal of Cleaner Production*.
- Gibbons, Orr, Archer-Jones, Arnold, & Green. (2022). *How to Calculate Embodied Carbon* (2nd edition). London: The Institution of Structural Engineers.
- H. Hens, A. J. (2007). *Brick Cavity Walls: A Performance Analysis Based on Measurements and Simulations*.
- Jaquin, P., & Augarde, C. (2012). *Earth Building – History, science and conservation* (1st ed.). Bracknell, United Kingdom: HIS BRE Press.
- LETI, W. A. (2021, May). Improving Consistency in Whole Life Carbon Assessment and Reporting. Retrieved from <https://carbon.tips/consistency>
- Mortada, H. (2016). Sustainable Desert Traditional Architecture of the Central Region of Saudi Arabia. *Sustainable Development*.
- Nanz, L., Rauch, M., Honermann, T., & Auer, T. (2019). Impacts on the Embodied Energy of Rammed Earth Façades During Production and Construction Stages. *Journal of Facade Design & Engineering*, 7(1).
- Parra-Saldivar, M., & Batty, W. (2005). Thermal behaviour of adobe constructions.

6dTEX – Lightweight Building Components made of 3D Textiles in Combination with 3D Printing

**Claudia Lüling^{*1}, Sascha Biehl¹, Roxana Tennert¹, Gözdem Dittel²,
Marina Chernyshova², Thomas Gries²**

* Corresponding author

1 FRA-UAS, Frankfurt University of Applied Sciences, Faculty 1, Germany, clue@fb1.fra-uas.de

2 ITA, Institut für Textiltechnik of RWTH Aachen University, Aachen, Germany

Abstract

6dTEX explores the synergetic combination of two process technologies, previously considered separately, for new lightweight construction applications in the building industry: 3D textiles combined with 3D printing. The aim is to produce recyclable, material-reduced lightweight elements with maximum functionality. 6dTEX lays the procedural foundations for this. Printing and textile materials of the same material groups are identified to be processed with corresponding 3D printing techniques and 3D textile techniques. On this basis, the manufacturing techniques of 3D printing on flat textiles are combined in preliminary tests and key process parameters are identified. The processes have been established for textile as well as printable recycled polyester materials (PES textile and rPETG filament) and for non-combustible material (alkali-resistant (AR) glass textile and concrete). One key aspect is composite adhesion. Printing parameters as well as textile geometries had to be mutually modified and optimised. From the preliminary test series, key printing and textile parameters for both material groups are transferred to 3D printing on special 3D textiles. The 3D textiles used are so-called spacer warp-knitted non-crimp fabrics, which also serve to reinforce concrete. The improved bending tensile strength of the printing material with the aid of 3D textile reinforcements is verified using three- or four-point bending tensile tests. Geometrically, the printing on and also into the spatial textiles is considered, both for demonstrators in the field of solar protection and exterior walls. In parallel, the design potential of 6dTEX is explored in experimental design and build studios.

Keywords

Lightweight construction, 3D printing, 3D textile, additive manufacturing techniques, spacer textiles, pure composite materials.

1 INTRODUCTION

Lightweight construction is a driver for resource and energy efficiency, including in the construction industry. Material developments, manufacturing processes as well as constructive design are holistically considered using digital methods with the aim of developing recyclable, highly functional and material-reduced components. Disruptive approaches incorporating classic lightweight construction methods (tent and skeleton structures) and solid construction methods (clay, brick and concrete) are opening up new possibilities here.

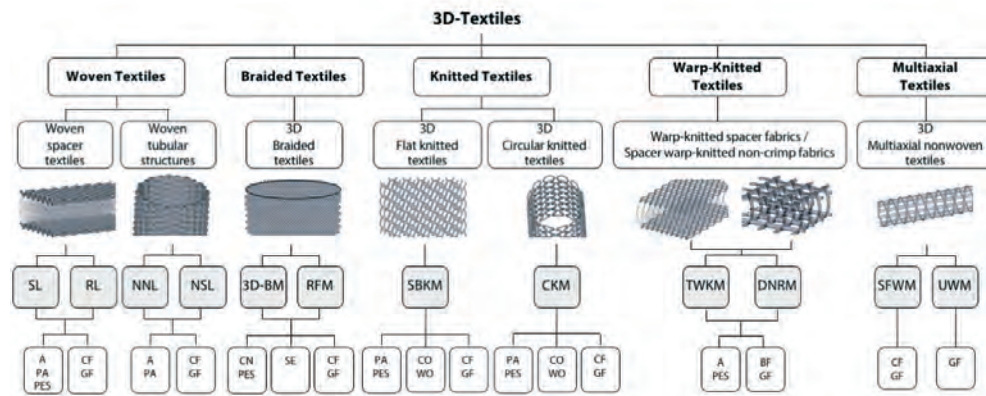


FIG. 1 3D Textile Techniques (© ITA):

- Lines 1 and 2 Textile typologies

- Line 3 Textile machinery: SL, Standard loom; RL, Rapier loom; NNL, Narrow needle loom; NSL, Narrow shuttle loom; 3D-BM, 3D-Braiding machine; RFM, Radial braiding machine; SBKM, Straight bar knitting machine; CKM, Circular knitting machine; DNRM, Double needle bar raschel machine; TWKM, Tricot warp-knitting machine; SFWM, Single filament winding machine; UWM, Ultrasonic welding machine

- Line 4 Material groups: S, synthetic; B, biological; M, mineral

- Line 5 Materials: A, aramid; BF, basalt fibres; CF, carbon fibres; CN, surgical sewing thread; CO, cotton; GF, glass fibres; PA, polyamide; PES, polyester; PP, polypropylene; K, ceramic; SE, silk; WO, wool

The combination of archaic textile processes such as braiding, weaving, knitting or warp-knitting using anisotropic materials, together with essentially isotropic solid construction materials such as concrete, opens up new sustainable, constructive and aesthetic possibilities. This is done especially in the context of cutting-edge, additive 3D manufacturing techniques. In solid construction, these involve 3D printers that are now being used to create 3D-printed houses from concrete but also from clay or sand. The state of the art here is essentially LDM processes for concrete printing (3DCP), with alternative research being conducted on "shotcrete printing" (Kloft, H. et al., 2019) and generally with mineral materials also on binder jetting techniques for sand printing or on glass printing from recycle (Ramsgaard et al., 2020), as well as in other material groups on metal printing and printing with biomaterials (Goidea et al., 2020, among others). However, additive 3D technologies also include processes for the production of technical 3D textiles, so-called spacer textiles (Figure 1). Their applications in the building industry have so far been limited to use as a filter medium; now and then, they become visible as fog traps or are used in interior finishing as mattress pads or upholstery. In research, own studies on the topic of ge3TEX ("Woven, Knitted, Foamed: 3D Textiles for the Building Envelope") have shown further potential (Lüling et al., 2021). The results were recognised in the DGNB Sustainability Challenge in the "Research" category. 6dTEX is investigating the extent to which, in addition to foaming as in ge3TEX, the combination of additive 3D printing and 3D textile manufacturing processes can be used to develop sustainable, prefabricated building envelope components that combine the advantages of skeletal and solid construction. Research is being conducted on textile-reinforced 3D-printed composite components in a mineral-based and synthetic-based variant. In the project, appropriate materials are identified, the respective textile

and print manufacturing processes are installed with a view to adhesion and composite effect, and components for the building sector are developed from the new composite material at scale from the meso to the macro level.

2 METHODOLOGY

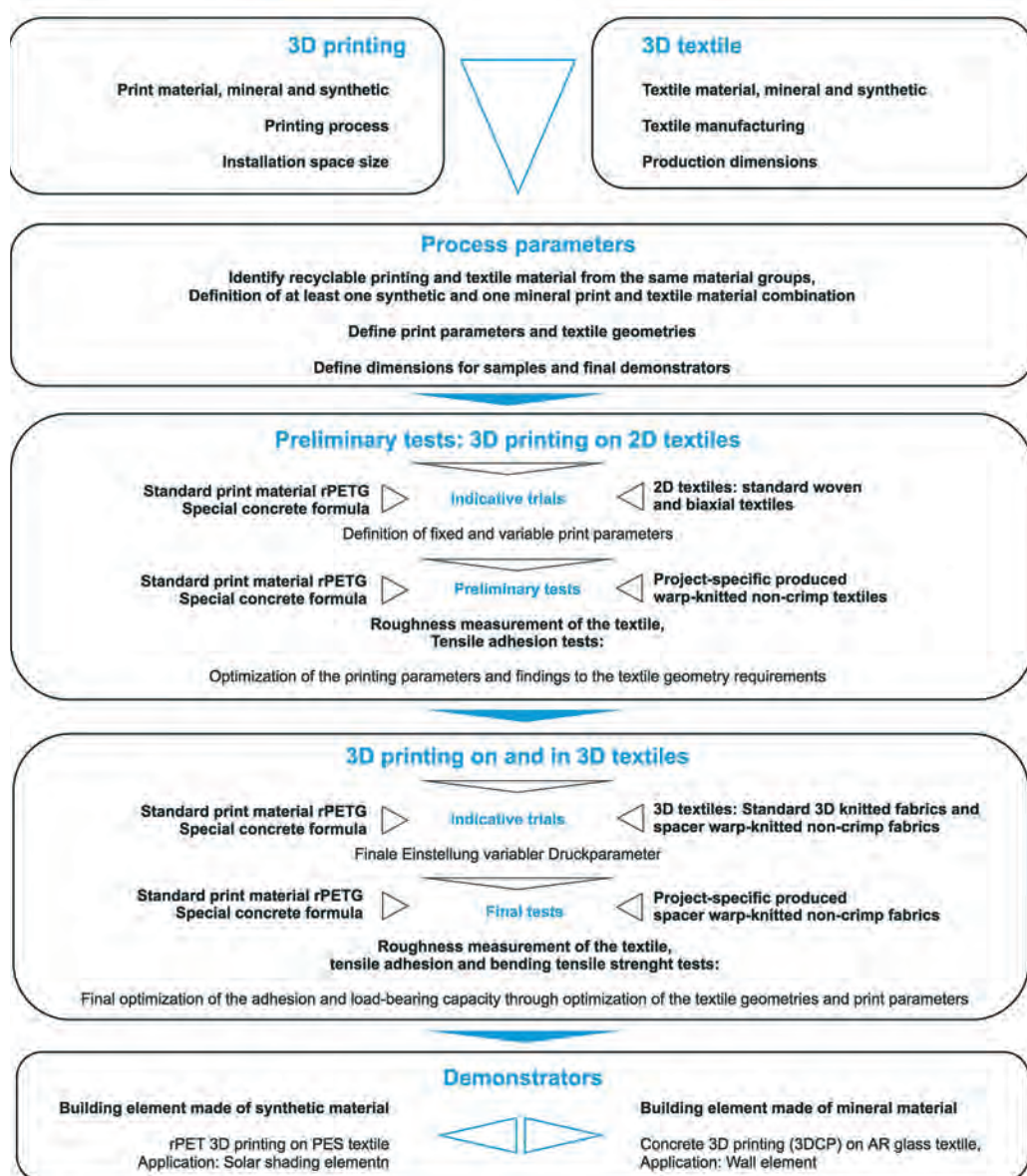


FIG. 2 Research design 6dTEX: experimental test series to determine the varietal purity of the textile-reinforced 3D-printed composite material, of the key process parameters, of the test series on and in the textile, and of the final development of two demonstrators in two material variants

The research design is based on an iterative experimental series. Figure 2 shows the general approach, starting from the synchronisation of the composite materials, i.e. the identification of a synthetic and a mineral composite variant, the optimisation of the process parameters for adhesion improvement via printing tests first on surfaces or 2D textiles and then on 3D textiles, and finally printing tests on and into the textiles for different demonstrators.

3 EXPERIMENT

3.1 3D PRINTING ON TEXTILE – PURE COMPOSITE MATERIAL, ADHESION

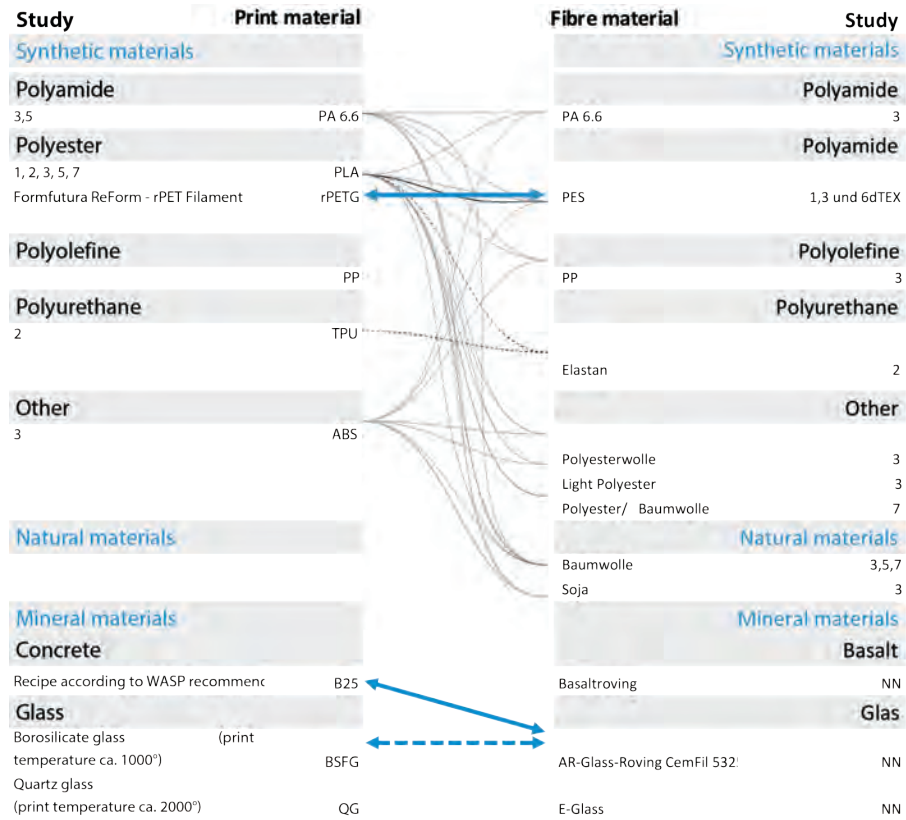


FIG. 3 Pure material composite of printing and textile material (grey lines: reference literature, 3D printing on 2D textile; blue line: target combination 6dTEX, 3D printing on 3D textile)

Due to a lack of references on 3D printing on 3D textiles, research on 3D printing on 2D textiles was evaluated (Narula et al., 2018; Pei et al., 2015; Gorchachova et al., 2021; Grothe et al., 2020; Ćuk et al., 2020; Malengier et al., 2018; Cuevas et al., 2020). Studies on 3D printing on elastic textile material with investigations through deformations via prestressing were excluded because the machine used in the project does not produce elastic 3D textiles. In particular, the topics of varietal purity of the print-textile compound and adhesion parameters were considered. The grey connection lines in Figure 3 show that varietal purity is not an issue in studies of 3D printing on 2D textiles. The fibre and printing materials ultimately selected for 6dTEX are marked with blue lines in Figure 3. The criteria were possible fire-protection classifications, UV resistance and process robustness when processing the print material. In the field of mineral materials, the alkali resistance of the fibre material to the alkaline concrete environment was another selection criterion. For the synthetic material, the deformation/melting temperatures were an important criterion. With regard to adhesion, the evaluation of the studies showed that essentially the roughness of the textile or its surface structure and, thus, the mechanical adhesion is decisive (roughness, porosity, hairiness, fibre waviness and undulation). For the printing, the Z-distance (the distance between the printhead and textile) is key or, depending on the material, heat (melting) and/or hydrophobicity.

3.2 3D TEXTILE

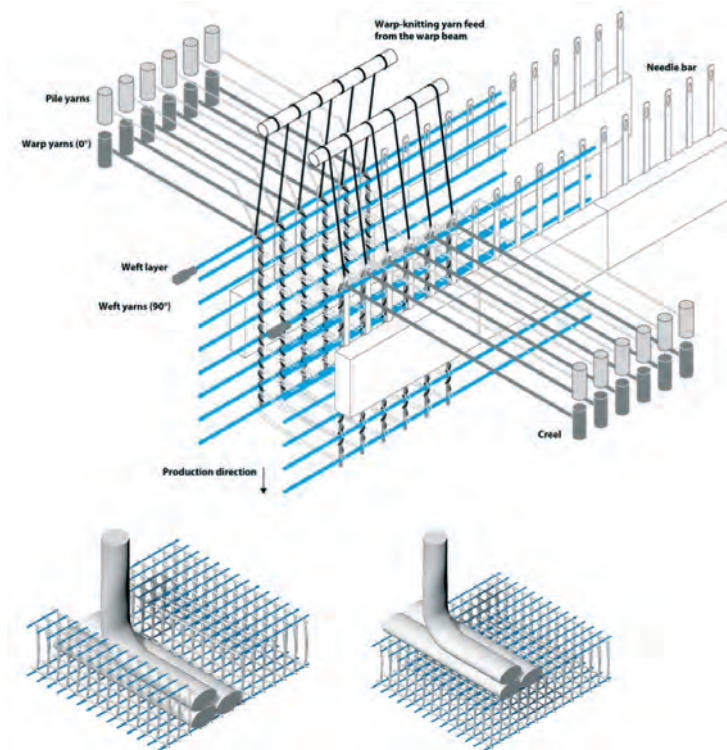


FIG. 4 Top: Principle of the production of spacer warp-knitted non-crimp fabric (blue weft yarns, grey warp yarns, black warp-knitting yarn, light grey pile yarns) © FRAUAS, bottom: Print on and in a 3D textile

Spacer warp-knitted non-crimp fabric parameters for the 6dTEX project								
□	Centre-distances□		Glass-rovings□		Basal-rovings□		PES-rovings□	
	minimal- (mm)□	maximal- (mm)□	minimal- (tex)□	maximal- (tex)□	minimal- (tex)□	maximal- (tex)□	minimal- (tex)□	maximal- (tex)□
Standing-threads□	4.23□	preferred-25.4□	600□	2,400□	600□	2,400□	1,100□	2,200□
Weft-threads□	0.5--5□	preferred-23□	600□	2,400□	600□	2,400□	1,100□	2,200□
Knitting-yarns□	Binding-type: -Open-pillar□		34□	34□	-□	-□	16.7□	16.7□
Pile-yarns□	Binding-type: -I, X, -, IXI□		approx. 100□	approx. 100□	approx. 100□	approx. 100□	ø 0.25 mm□	ø 0.25 mm□
□	Spacer warp-knitted non-crimp fabrics / Karl Mayer / Double needle bar raschel-machine□							
Max. product-width□	□		237 mm (knitting yarns are fed from the creels)□		237 mm (knitting yarns are fed from the creels)□		355 mm (knitting yarns are fed from the warp beam)□	
Production-height□	Trick-plate distance = 30 mm, Layer distance = ca. 20 mm□							

TABLE 1 Machine and material parameters for the textile machine used in the 6dTEX project and the selected mineral- and synthetic-based roving materials.

The manufacturing techniques, typologies and shapes of 3D textiles, from tubular to sandwich-like geometries, are shown in Figure 1. 6dTEX uses spacer warp-knitted non-crimp fabrics, which were developed especially for the reinforcement of concrete (el Kadi et al., 2019 and Haik et al. 2017). Figure 4 shows the complex machine technology and four different thread mechanisms of the textile structure. Similar to a woven fabric, the geometry of the two cover surfaces is defined by the warp and weft threads, which, however, are not woven together but warp-knitted. For optimal absorption of tensile loads, they thus lie straight and without undulation in the space. The warp-

knitted threads hold them in position mechanically. The interaction of the warp and weft threads decisively determines the geometry of the cover areas to be printed – in the case of the warp threads defined by the needle occupancy of the leads, and in the case of the weft by the minimum and maximum distances of the weft feeders. The spacing pile threads, in turn, define the height and resilience of the 3D textile. Table 1 shows the machine and material parameters for the textile machine used in the 6dTEX.

3.3 3D PRINTING ON TEXTILE – PROCESS PARAMETERS

3.3.1 3D printing, general process parameters

Due to the selected material combinations as shown in Figure 3, two different 3D printing processes were chosen, FDM and LDM printing. Figure 4 shows the making and general options of printing on and in a 3D textile. FDM printing was performed using a Prusa i3 MK3S+. For the FDM parameters, in addition to the print bed temperature (warping effects), air cooling of the nozzle unit via the fan, layer width, strand height and flow (influence on material thickness and penetration depth), the following print parameters were identified as key: infill (print direction in relation to textile orientation), print temperature (influence on material thickness and penetration depth) and Z-offset (influence on material width and penetration depth).

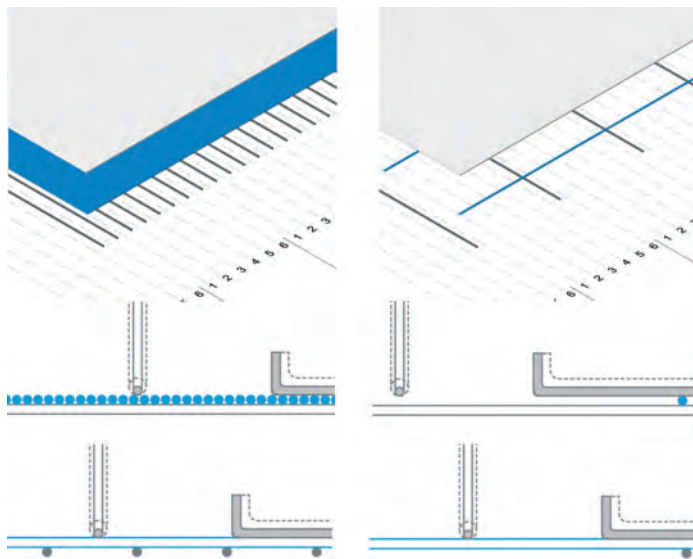


FIG. 5 3D printing and textile variants in PET/PES, left: densest textile structure, right: most open textile structure

The LDM tests were performed using the Delta WASP 40100 Clay Printer and a custom-designed hopper and motor-driven extruder screw from WASP for concrete printing. For concrete printing, the printer settings are less decisive. Unlike the melting material in FDM printing, the concrete mix hardens without external heat transfer, and the concrete recipe is the real challenge. The data provided by the manufacturer was insufficient. Decisive for a successful printing process and the implementation of desired geometry is the processability, in particular the extrusion capability, with simultaneous green strength. Accordingly, a total of 44 concrete mixes were investigated for formulation optimisation based on guideline values provided by the printer manufacturer. Figure 5 shows an example of the interaction of 3D printing with rPETG on PES textile, with a print nozzle diameter of 0.4 mm. The ratio for concrete print with a nozzle diameter of at least 6 mm looks correspondingly upscaled – as the roving diameter is not that much bigger

3.3.2 Textile attachment

For 3D printing on 2D as well as 3D textiles, a frame is developed that can be attached to the build platform of both the FDM and LDM printers (Figure 6). The frame is used to clamp the 2D textile or the top cover layer of the 3D textile between two battens so that the textile can be stretched wrinkle-free and evenly in all directions. The tension provides a surface that withstands the pressure of the extruder and allows the printing filament to penetrate deeper into the textile.

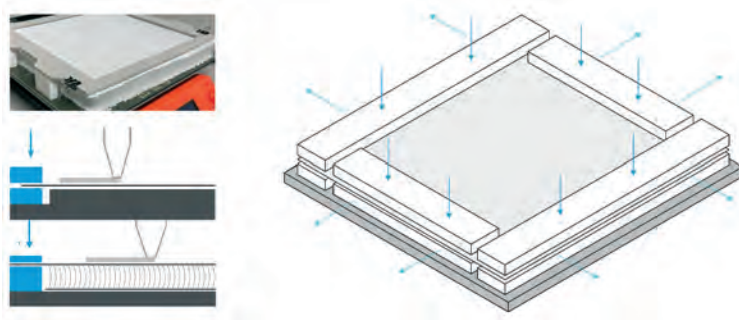


FIG. 6 Attachment of 2D and 3D textiles on the build platform of the FD and /LDM 3D printer, top left: Preliminary tests with clamps

3.3.3 Coatings

Especially when printing concrete on AR glass textiles and with the aim of activating the standing and/or weft filaments of the 3D textile for reinforcement purposes, the question arises as to how all the filaments of the rovings can be activated without equally affecting the adhesive bond. Studies by RWTH Aachen (Kimm et al., 2021) show that, depending on the component geometry and especially for planar systems, more than 20% unimpregnated AR rovings are used, with the remainder being AR rovings impregnated with epoxy resin or carbon. Styrene Butadiene Rubber (SBR) coatings are mainly used in renovation. It is decided to investigate both comparatively in the preliminary tests with 2D textiles with respect to the achieved bending tensile and adhesion results.

4 RESULTS

The tests are divided into preliminary tests on 2D textiles and tests on 3D textiles. Standard textiles available on the market or textiles from preliminary projects and project-specific manufactured spacer warp-knitted non-crimp fabrics made of PES and AR glass are used for the indicative preliminary tests. For the actual tests with 3D textiles, spacer warp-knitted non-crimp fabrics are used, as shown in Figure 4 and Table 1.

4.1 3D PRINTING WITH RPETG ON PES TEXTILE

4.1.1 Preliminary tests on 2D textiles

In the preliminary tests on 2D textiles, investigations were initially carried out with printed and textile materials from the following four material groups: PA, PETG flame-retardant, rPETG and PP. The respective print material was printed as squares on marketable 2D fabrics of the same materiality. The summary of the preliminary tests can be seen in Figure 7. It shows the qualifying tensile result of the tests in terms of peel and tensile adhesion in relation to the misprint rate or reproducibility, the material cost per kg, the level of printing requirements in terms of process

steps, and the recyclability of the filaments. The high misprint rate and difficult handling in the printing process, combined with the poor peel and tensile adhesion test results of PA, lead to its exclusion from further tests.

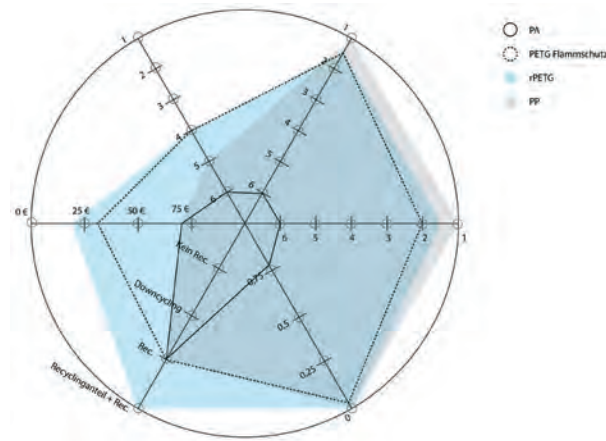


FIG. 7 Qualifying results of the indicative preliminary tests with four synthetic material combinations. In each case, printing and textile material of the same material group was used; Manufacture Process steps: 1. Cut textile; 2. Tape textile (only PP); 3. Apply spray adhesive; 4. Apply glue stick (PA only); 5. Apply anti-warping spray (PA only); 6. Clamp textile; 7. Prepare and start printing; Peel and tensile test: 1= Very good adhesion; 6= Very poor adhesion © FRAUAS

The material combinations of PETG flame retardant, rPETG and PP were then investigated further. The adhesion between 3D printing and the 2D fabrics was also determined via quantifying tests. Various compression die geometries were investigated and tested in the preliminary trials. As a result of the print form, a tensile adhesion stamp with a cylindrical base with a 50 mm diameter and a clamping surface for the testing machine was printed on the textile. An exemplary test series is shown in Figure 8. After evaluating the test results, it was decided to use a combination of rPETG as the printing material and PES textile.

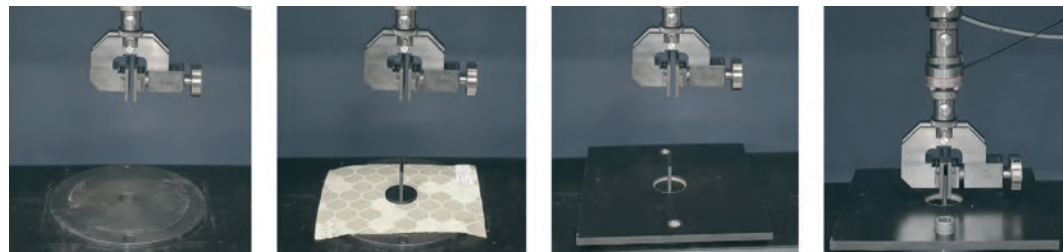


FIG. 8 Test series for an adhesion test, from left to right: Clamp – metal, smooth test piece, wooden frame, clamped sample © ITA

Printing tests with rPETG were continued on project-specific manufactured spacer warp-knitted non-crimp fabric with the aim of transferring the findings of the cover layer design to 3D warp-knitted spacer fabrics. For this purpose, and taking into account the findings from the reference studies as well as the test series on standard fabrics, an initial warp-knitted 2D fabric with PES weft threads was produced and printed. Figure 9 shows the planned textile geometry at the top left and the correspondingly manufactured textiles next to it. The process and material parameters of the investigated warp-knitted biaxial fabrics are as below:

Manufacture:

- Warp threads AR glass 2.400 tex, full feed (centre distance: 4.23 mm)
- Weft threads PES 220 tex, 10 threads to 1 cm (centre distance: 1 mm)

- Warp threads: PES 167 dtex

Dimensions - standing thread AR glass 2.400 tex:

- Theoretical roving diameter according to calculation tool: \varnothing approx. 1.1 mm
- Drawing - assumed deformation/width according to ITA: approx. 2 mm
- Reality - actual deformation/width according to FRAUAS measurement: approx. 2 mm

Weft thread PES 220 tex:

- Theoretical roving diameter according to calculation tool: \varnothing approx. 0.44 mm
- Drawing - assumed deformation/width acc. to ITA: approx. 0.5 mm
- Reality - actual deformation/width according to FRAUAS measurement: approx. 0.8-1 mm

Figure 9 shows below, from left to right, how the printing parameters of 3D printing with rPETG were further optimised. Above all, the Z-offset, the printing temperature and finally, the infill at 45° could be optimised until very good mechanical adhesion is achieved through material penetration, as shown on the far right. For the subsequent actual tensile adhesion test, tensile adhesion test pieces were again printed onto the textile in the same way as for the indicative preliminary tests. During the tests, the adhesion between the 3D print and the 2D fabric exceeded the maximum forces of the test device from the indicative preliminary tests. Overall, the tensile adhesion test confirmed the positive effect of mechanical adhesion due to the geometric interlocking of the printed and textile materials.



FIG. 9 Top left: Design of a biaxial warp-knitted fabric based on theoretically determined roving cross sections; top centre: Bottom view of the produced textile; top right: Top view; bottom left: 3D printing with rPETG on iaxial warp-knitted fabric; bottom centre: Print parameter optimisation – Z-offset and infill; bottom right: Close up, bottom view – textile with visible print material penetration © FRAUAS

4.1.2 Tests on 3D spacer fabric

Initial findings on 3D printing behaviour on three-dimensional textiles were collected in relation to commercially-available PES spacer fabrics, such as those used as mattress pads (Figure 10). Based on the preliminary tests on 2D textiles carried out in the project, tests with different PES spacer fabrics were also carried out. The textiles differ in the density of their surface structure. The initial findings, even before the start of printing, are: in order to be able to grip and clamp the top cover layer, the pile threads in the edge area must be cut open and off. Furthermore, 3D textiles

require more pre-tensioning than 2D textiles. Even though some of the knowledge gained from the preliminary tests could be applied to printing on 3D textiles, additional important experience was gained with printing on 3D textiles. Of the printed textiles, one has identical surfaces on both sides, the other a more open and a more closed surface; the latter surface was printed (Figure 10). In summary:

- Penetration of the top surface layer can be achieved with a correct Z-offset.
- An incorrect Z-value is very likely to result in more misprints and damage to the printer for 3D textiles than for 2D textiles.
- Too light or irregular pre-tensioning causes curvature of the textile surface, which increases the likelihood of misprints; clean and strong pre-tensioning of the textile is crucial for a successful printing process.

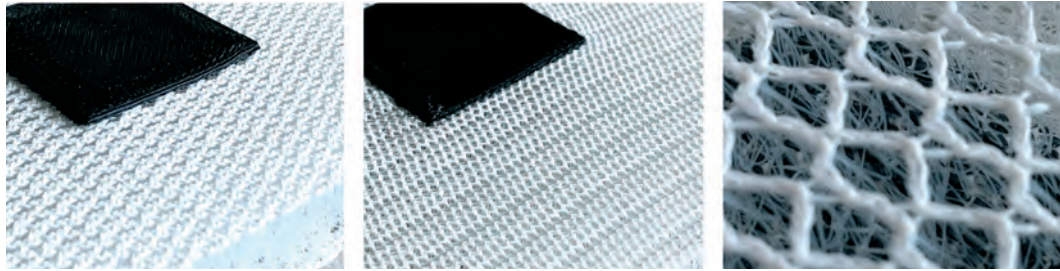


FIG. 10 Left: Print tests with rPETG on PES warp-knitted spacer fabric with two different surface structures, right – View from the back through the 3D textile shows the material penetration © FRAUAS

4.1.3 Planned demonstrators

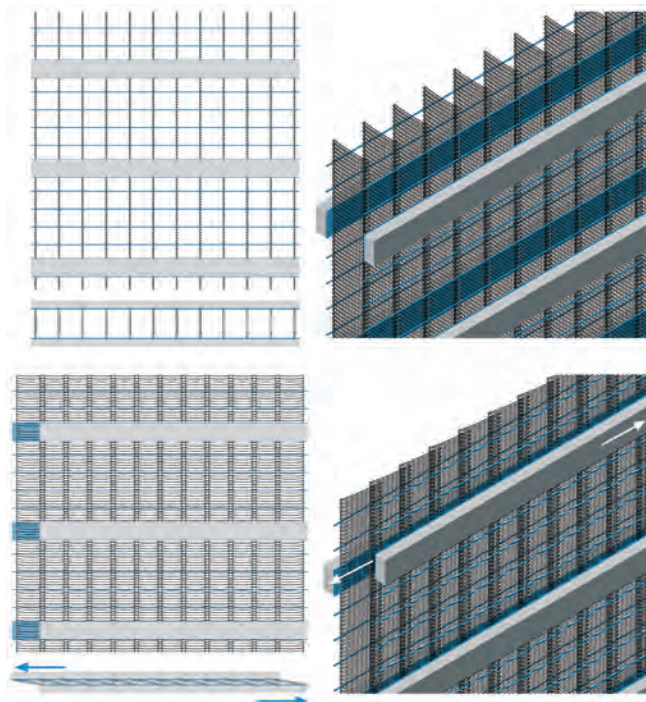


FIG. 11 Illustration of planned demonstrator solar shading element "SHIFT", above: Opened state, below: Closed state © FRAUAS

For possible application options as primary or secondary building components, it was decided in the next step and according to the investigated synthetic-polymer-based material composite to

develop concepts for solar-protection elements. The polyester (rPETG / PES) version studied could be classified in the flame retardant (B1) range in terms of fire protection. Preliminary investigations are also available here (Lüling & Beucher, 2019) from the “ReFaTex” project (“Reversibly foldable, energy-efficient 3D textiles”). Figure 11 shows the next step of the project, which was planned as a solar shading element under the name “SHIFT”.

The textile is woven very densely in strips on both opposite sides in the weft direction, and then 3D printed with rectangular profiles across the entire width in these areas. The warp threads lying free in between on both sides are evenly connected with pile threads. If the two cover layers are moved horizontally against each other over the print profiles of the three-dimensional textile, the pile threads fold over by almost 90° and compress the textile structure. The element changes its translucency, which can be preset to different densities via the textile structure. Figure 11 shows the two described stages of open and closed solar protection. The mechanism works without the use of hinges or joints but rather purely through the properties, the recovery behaviour of the spacer fabric and the displacement of the cover layers relative to each other.

4.2 6DTEX – 3D CONCRETE PRINTING ON 3D GLASS TEXTILE

4.2.1 Preliminary tests on 2D textile

Unlike the tests with synthetic polymers, there are fewer material options for textile production in the mineral area. The decision was made to use AR glass (see above). For the preliminary tests on two-dimensional warp-knitted biaxial fabrics, different dense surfaces were first drawn and produced, as in Figure 9. Here too, the deviations between the theoretical and real textile structure were analysed. The warp threads are always made of PES for production reasons, and, as later with the 3D textile, the pile threads are of PES, too. Figure 12 shows nine 2D textile surface structures, which ultimately differ in their surface density and in the proportion of the openings between the standing and weft threads. As part of indicative preliminary tests on the adhesion between the printing and textile materials, concrete was initially applied to the AR glass textiles solely in a formwork, with a concrete formulation based on the printer manufacturer’s recommendation.

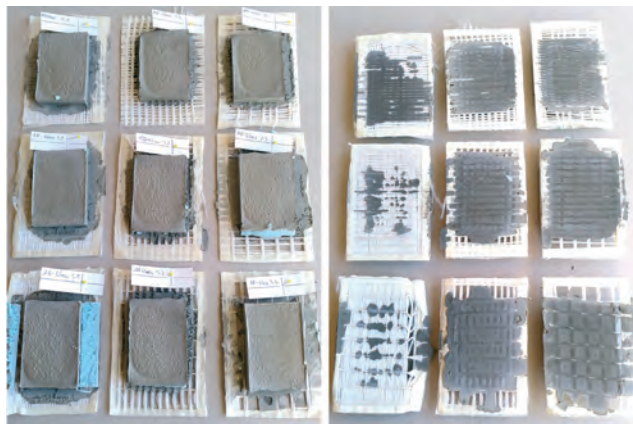


FIG. 12 Test series with nine warp-knitted biaxial fabrics made of AR glass, top and bottom view - in blue, the adhesion tests initially performed and evaluated by hand and with three different test subjects © FRAUAS

All nine textile surfaces were examined for their adhesion properties. The findings are as follows:

- Roughness: the adhesion is stronger in the areas where the warp-knitting yarns connect the weft threads with the underlying warp threads than in the areas where the concrete adheres only to the weft threads.

- Perforation: the adhesion is additionally mechanically improved by penetration between the weft and standing threads; results are correspondingly better with more open textile structures with lower weft density; if the structure is too open, the concrete runs through it.
- The combination of the “roughness” and “perforation” parameters leads to the best adhesion with the textiles.

For the first 3D printing tests with a small-format WASP 43100 concrete printer, those textiles are selected which have shown the best adhesion in the previous indicative test. They are marked in blue in Figure 12. Now the textile is also freely stretched in the mounting frame to simulate the spatial situation of the top layer of a three-dimensional textile. Figure 13 shows a printed concrete cylinder on a warp-knit spacer fabric on the left and the bottom view of the print on the right. The concrete of the first printing layer presses through the openings in the textile surface and interlocks with the textile. The penetration of the textile means good adhesion between the concrete and the textile.

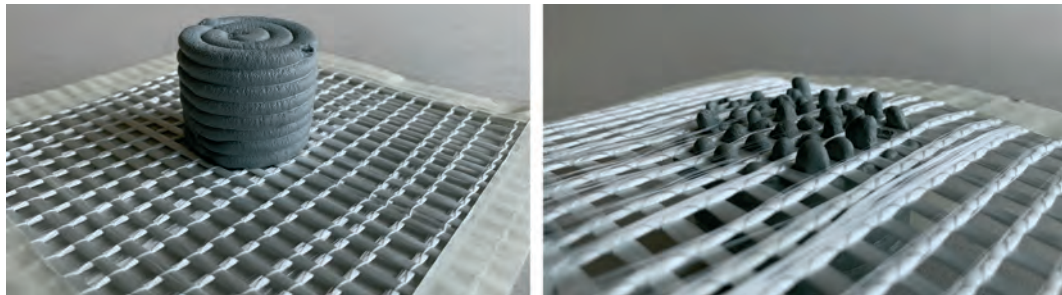


FIG. 13 3D concrete printing on warp-knitted biaxial fabrics made of AR glass © FRAUAS

4.2.2 Tests on 3D textile

For initial indicative trials with spacer warp-knitted non-crimp fabrics made of glass fibres, textiles from previous projects of the project partner ITA were initially selected for technical production reasons. Here, too, the concrete was initially poured rather than printed, as in the indicative preliminary tests with 2D textiles. The criterion with regard to the 3D textiles were surfaces as similar as possible to the structures found to be good in previous adhesion tests with 2D textiles. Figure 14 shows the three selected surface structures – dense, medium-dense and open. Below are the manual tests carried out on them with concrete formulations according to the specifications of the printer manufacturer WASP.

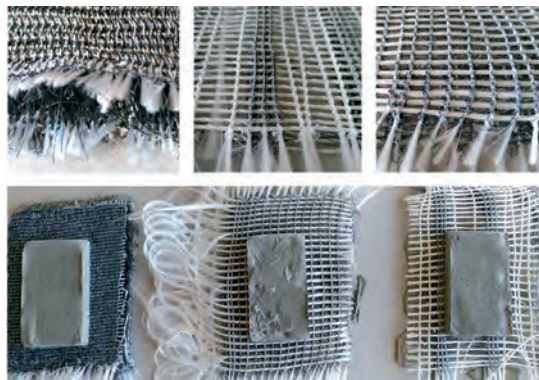


FIG. 14 above: Spacer warp-knitted non-crimp fabrics made of AR glass, three selected surfaces, below: first indicative tests with a concrete formulation based on the planned 3D concrete printing formula and using a manual spreading or casting process with formwork © FRAUAS

Summary:

- The more open the textile structures, the better the concrete is able to penetrate them and the better the distribution compared with closed surfaces.
- With open structures, the concrete penetrates down to the bottom cover layer.
- Depending on their density, the pile threads limit the spread of the concrete in the 3D textile (Figure 15)



FIG. 15 Side view of spacer warp-knitted non-crimp textile with the distribution of the concrete © FRAUAS

Figure 16 shows the subsequent tests on a 3D textile and the 3D printing process performed with a small-format 3D concrete printer. The textile is cut and clamped into the attachment for printing as described. Currently, the concrete formulations are being further adapted to the printer, the textile and the planned printing geometry. The concrete is mixed, the spreading dimensions are determined, and the concrete is then filled into the hopper with the extruder screw of the 3D printer. The textile is placed in the installation space of the printer, and printing is started. Figure 17 shows the final 3D concrete print. The printing geometry in cylindrical form is subsequently required for tensile adhesion tests.



FIG. 16 3D printing process from top left to bottom right: Textile attachment, concrete mix, breakout test, 3D printer preparation, printer hopper filling, 3D printing on spacer textile made of AR glass © FRAUAS



FIG. 17 3D printing with concrete on a chain-knitted biaxial spacer fabric made of AR glass with knitted and pile threads from PES © FRAUAS

4.2.3 Planned demonstrators

For possible application options, it was decided in the next step to develop concepts for wall or ceiling elements based on the mineral material composite. Unlike the polyester-based components, see Section 4.1.3, fire protection classifications in the “non-combustible” range (A2) are to be expected here. On the one hand, 3D textiles with uniformly dense, printable surfaces on both sides are envisaged. Each surface is printed diagonally and in opposite directions with rectangular profiles. The result is a supporting structure comparable to the constructional principle of a yurt. Unlike a yurt, however, which is insulated additively and seasonally with different layers of felt layers, the 3D textile serves integratively for thermal decoupling and, in the future, insulation (Lüling et al., 2022). The orthogonally placed warp and weft threads, which are connected to the concrete via 3D print, also provide reinforcement of the element. In addition, initial evaluations from ITA show that the printed AR glass rovings, together with the concrete, increase the flexural strength of the printed profiles.

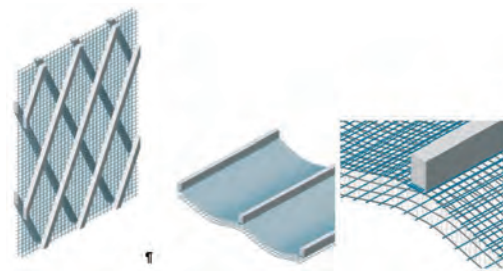


FIG. 18 Left: Planned demonstrator for a wall element: The 3D textile is printed on both sides diagonally and in opposite directions (similar to the supporting structure of a yurt) and serves to provide thermal separation as well as reinforcement for the printed concrete support profiles. Right: Planned demonstrator for a textile semi-finished part for ceiling elements: The 3D textile serves as lost formwork on the top side and has an acoustic sound-absorbing effect on the underside; the printed load-bearing profiles are also reinforced here by the textile upper cover layer © FRAUAS

On the left, Figure 18 shows the planned demonstrator for a wall element. At the same time, it is also being examined (see Figure 18 on the right) what semi-finished textile parts in the ceiling area could look like. The planned ceiling element offers the possibility, as a semi-finished part after unrolling on-site and similar to filigree ceilings, to serve on the one hand with its upper cover layer as lost formwork and as lower reinforcement of the imprinted load-bearing profiles. On the other hand, the remaining textile, i.e. the area of the downwardly open structure consisting of pile threads and the lower cover layer, can be used for sound absorption.

5 CONCLUSION

This paper explores how well-known additive manufacturing processes from 3D printing can be usefully combined with fairly unknown additive 3D textile manufacturing processes for new lightweight applications. The goal is to use printed 3D structures for stabilisation, while the 3D textiles contribute equally as lost formwork to reinforcement and to further functionalisation. Results from the ongoing 6dTEX research project to develop appropriate textile-based composite components are discussed. The results show two different processes, each with different complexities depending on the material and process.

Firstly, following a selection process on commercially available, sustainable, recyclable and synthetically produced polymers, a decision was made in favour of polyester-based materials with recycled content (rPETG printing filaments and PES textile). The 3D printing process used is FDM printing, printed with commercially-available filaments. The printing parameters were optimised, particularly with regard to the Z-distance and the infill. Indicative preliminary tests on commercially available fabrics followed by project-specific warp-knitted biaxial fabrics made of PES material demonstrated how the mechanical adhesion could be specifically increased by the type of printing material application and in interaction with specially designed textile surfaces (porosity, roughness, undulation). The results are currently being transferred to commercially-available spacer fabrics and then to project-specific manufactured spacer warp-knitted non-crimp fabrics. Initial trials show promising results. The mechanical adhesion of the printed material to the PES weft threads of the 3D fabric is also expected to increase the flexural strength of the printed structures.

Three-dimensional AR glass textiles and 3D concrete printing are also combined by using an LDM printing process. The original plan was to purchase 3D-printed concrete mixes, but this is currently unfeasible despite market availability, as they are only supplied in conjunction with non-disclosure agreements. In addition, the grain sizes are rather too coarse for the planned rather filigree printing. Accordingly, in contrast to PET filaments, concrete printing formulations had to be further developed based on references from the manufacturer of the concrete printer used. LDM printing itself is easier to handle than temperature-dependent FDM printing. Here, too, the results show the essential interaction of an actively designed textile surface structure with a balanced porosity and roughness. The first manual adhesion results are very good. It is expected that the flexural tensile strength will also increase. So far, the AR glass textiles used to activate the rovings as reinforcement have not been coated. It is planned to carry out the tests with coated surface textiles as well.

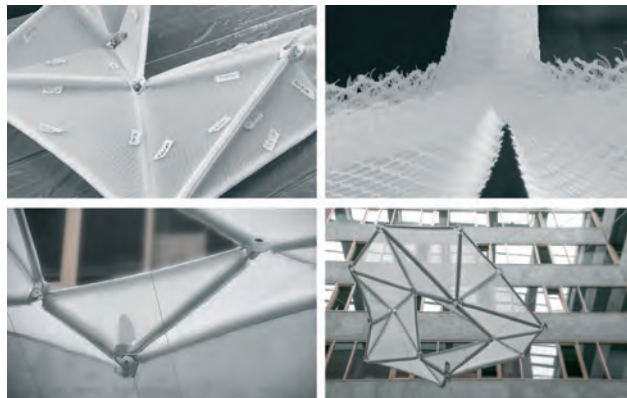


FIG. 19 Student design-build project (seminars - Prof. Timo Carl and Prof. Claudia Lüling) on the topic: "FoldedFabric": A textile folding structure from individual modules

Special textile geometries of different fire protection classifications – flame retardant, rPETg/PES, and non-combustible concrete/AR glass – are the basis for 1:1-scale demonstrators. In the next work package, the realisation of linearly-applied print structures made of rPETG for solar protection elements with adjustable translucency on PES textiles is planned. Also planned are self-supporting wall elements made of glass-based 3D textiles with a 3D-printed concrete load-bearing structure on both sides. The joining of textile solar protection elements in the roof area via half-imprinted beams per textile element was also addressed as part of a design-build seminar and in parallel with 6dTEX. Figure 19 shows how individual 3D printing and 3D textile elements joined on-site can be assembled into larger structures in the medium term. The research is currently in further development to upscale the process for both material combinations. In conclusion, the planned solar shading element made from PET print and PET textile material as well as a wall and/or ceiling element made from glass fibre reinforced 3D concrete print will demonstrate new findings for sustainable, lightweight building elements.

References

- Čuk, Marjeta; Bizjak, Matejka; Muck, Deja; Kočevar, Tanja Nuša, 2020: 3D PRINTING AND FUNCTIONALISATION OF TEXTILES. University of Novi Sad, Faculty of Technical Sciences, Department of Graphic Engineering and Design. Access: doi: 10.24867/GRID-2020-p56
- El Kadi, M.; Tysmans, M., Verbruggen, S., Vervloet, J., De Munck, M., Wastiels, J., Van Hemelrijck, D.: Experimental study and benchmarking of 3D textile reinforced cement composites (2019) Access from > journals.elsevier.com/cement-and-concrete-composites
- FraunhoferUMSICHT, 2022: FungiFactoring. Access: <https://fungifactoring.de/fungi-factoring/projekt-steckbrief/> [retrieved on 13.04.2022].
- Garcia Cuevas, Diego; Pugliese, Gianluca, 2020: Advanced 3D Printing with Grasshopper®: Clay and FDM
- Goidea, Ana; Andreen, David; Floudas, Dimitrio: Pulp Faction: 3D printed material assemblies through microbial biotransformation; in Fabricate. London (2020)
- Gorlachova, Maryna; Mahltig, Boris, 2021: 3D-printing on textiles – an investigation on adhesion properties of the produced composite materials. *Journal of Polymer Research*, 2021, 28:207. Access: doi: 10.1007/s10965-021-02567-1
- Grothe, Timo; Brockhagen, Bennet; Storck, Jan Lukas, 2020: Three-dimensional printing resin on different textile substrates using stereolithography: A proof of concept. *Journal of Engineered Fibers and Fabrics*, 2020, 15, p. 1-7. Access: doi: 10.1177/1558925020933440
- Haik, R., Adiel Sasi, E., Peled, A: Influence of three-dimensional (3D) fabric orientation on flexural properties of cement-based composites, *Cement and Concrete Composites*, Volume 80, 2017, Pages 1-9, ISSN 0958-9465 (2017) <https://doi.org/10.1016/j.cemconcomp.2017.02.007>.
- Kimm, M., Gries, T: Vom Stahlbeton zum Textilbeton – nur wie? (From reinforced concrete to textile concrete - but how?); in BFT International 08/2021 (2021) Access: https://www.bft-international.com/de/artikel/bft_Vom_Stahlbeton_zum_Textilbeton_nur_wie__3670472.html
- Kloft, H., Hack, N.; Mainka, J., Brohmann, L., Herrmann, E., Ledderose, L., Lowke, D.: Additive Fertigung im Bauwesen: Erste 3-D-gedruckte und bewehrte Betonbauteile im Shotcrete-3-D- Printing-Verfahren in Bautechnik. (Additive manufacturing in construction: First 3-D printed and reinforced concrete components using the shotcrete 3D printing process in construction technology.) *96(12)*, p. 929-938 (2019)
- Lüling, C., Rucker-Gramm, P., Weilandt, A. et al.: Advanced 3D Textile Applications for the Building Envelope, in: *Applied Composites Materials* 29, 343–356 (2022). <https://doi.org/10.1007/s10443-021-09941-8>
- Lüling, C.; Rucker-Gramm, P.; Weilandt, A.; Schneider, J.; Bauder, H-J.: G3TEX – Multifunctional monomaterials made from foamed glass-, basalt- or PET- based 3D textiles, *04/21 Proceedings Powerskin*, S.37 - S.50 (2021)
- Lüling C., Beuscher, J.: 4dTEX – Exploration of Movement Mechanisms for 3D Textiles Used as Solar Shading Devices. *Powerskin Conference Proceedings* p. 159–172 (2019)
- Malengier, Benny; Hertleer, Carla; Cardon, Ludwig; Van Langenhove, Lieva, 2018: 3D Printing on Textiles: Testing of Adhesion. *J Fashion Technol Textile*, 2018, p. 4. Access: doi:10.4172/2329-9568.S4-013
- Narula, A.; Pastore, C. M.; Schmelzeisen, D.; El Basri, S.; Schenk, J.; Shajoo, S., 2018: Effect of knit and print parameters on peel strength of hybrid 3-D printed textiles. *Journal of Textiles and Fibrous Materials*, 1:1-10. Access: doi:10.1177/2515221117749251
- Pei, Eujin; Shen, Jinsong; Watling, Jennifer, 2015: Direct 3D printing of polymers onto textiles: Experimental studies and applications. *Rapid Prototyping Journal*, 2015, 21/5, p. 556–571. Access: doi: 10.1108/RPJ-09-2014-0126
- Ramsgaard Thomsen, Mette; Tamke, Martin; Sparre-Petersen, Maria; Buchwald, Emil Fabritius; Hnídková, Simona 2020: Silica – A circular material paradigm by 3D printing recycled glass. Werner, L and Koering, D (eds.), *Anthropologic: Architecture and Fabrication in the cognitive age - Proceedings of the 38th eCAADe Conference - Volume 2*, TU Berlin, Berlin, Germany, 16-18 September 2020, pp. 613-622

Interactive Façade Impact Tool for Evolutional Trade-off Analysis

**Xiaofei Shen^{1*}, Aman Singhvi², Nick Novelli, PHD³, Maria Aiolova⁴,
Kieran Rice⁵, Jason Vollen, PHD^{6*}**

* Corresponding author

- 1 AECOM iLAB, xiaofei.shen@aecom.com, China
- 2 AECOM iLAB, aman.singhvi@aecom.com, USA
- 3 AECOM High Performance Design, nick.novelli@aecom.com, USA
- 4 AECOM iLAB, maria.aiolova@aecom.com, USA
- 5 AECOM Façade Design, kieran.rice@aecom.com, Australia
- 6 AECOM iLAB, jason.vollen@aecom.com, USA

Abstract

Progress in high-performance, low-carbon building design is throttled by the myriad of intercoupled options that must be analysed in early project stages. The design of enclosures exemplifies this issue, with multiple disciplines required and objectives pursued, and the significant impacts of decisions on metrics of constructability, cost, comfort, performance, and sustainability. Automation of analyses, optimisation, and data exchange can be leveraged to navigate this complex design space, but available methods lack the full complement of capabilities that track a complete enclosures design workflow. To support this workflow, AECOM's Innovation Laboratory (iLAB) is developing an interactive digital optimisation dashboard to assess façade performance in the early design stages. The dashboard reveals the environmental impacts of façade shapes, materials, and construction simultaneously and synthesises impacts into informative indicators which can be compared across options and optimised against objectives. The dashboard environment, termed the Façade Impact Tool (FIT), informs design for daylight, energy, and embodied carbon, supporting confidence in realistic, high-resolution targets for façade design performance in support of carbon-neutral capable buildings.

Keywords

Façade, optimisation, carbon

1 INTRODUCTION

A comprehensive façade design is critical when targeting minimal environmental and carbon impact for a building project, as a great deal of a project's operational and up-front carbon profile – as well as visual and thermal comfort performance – is driven by the façade. Exploring design ideas within a short time to achieve balanced performance targets, especially when dealing with conflicting objectives, is challenging. It is not feasible to continue the conventional method of testing the performance improvement of a single aspect – an individual design bundle – one by one and selecting the “best” bundle after a minimal number of options are tested.

An iterative process is helpful for exploring the sensitivity of building performance (across categories of metrics) to façade design options. But modelling, conducting, and analysing many design iterations is time-consuming, which limits such comprehensiveness to a small fraction of design and construction projects.

Automated evolutionary trade-off analysis can enable the vetting of façade design options by highlighting their performance against overall goals (in real-time or otherwise). Its crucial value is the generation and assembly of pertinent, reliable data early in design development when critical decisions are made and the design is largely stabilised. Despite these benefits, the evolutionary trade-off is not standard practice. This rarity persists because the process requires the configuration and integration of many components:

- Evolutionary (or related) solver engines
- Multiple building simulation engines (energy, daylight, embodied carbon, etc.)
- Parameterised project data, building models, and façade models
- Structured results data
- Analytics, visualisation, and interpretation
- Export and reporting

Suppose we integrate this custom assembly of the iterative process into a cohesive workflow early in design – and lower the bar for employing automated evolutionary trade-off analysis with an interactive digital optimisation dashboard. In that case, we will reduce the effort in exploring the solutions and improve the reliability of the “best” option, which will broaden the implementation of High-Performance Façade Design.

2 DEFINITIONS

High-Performance Building Design (HPB) Design: The process of designing low energy and carbon footprint buildings with high indoor air quality and thermal comfort in comparison to conventional building designs.

High-Performance Façade (HPF) Design: The process involves collaboration between multiple disciplines towards developing the dynamic relationship between building occupants and the indoor and outdoor environments. Trade-offs are developed between performance, well-being, cost and architectural vision, so informed decisions can be made around how a passively optimised façade influences metrics such as MEP systems cost (Figure 1).

Multi-Objective Optimisation: The use of mathematical techniques to simultaneously optimise more than one objective subject to pre-determined constraints.

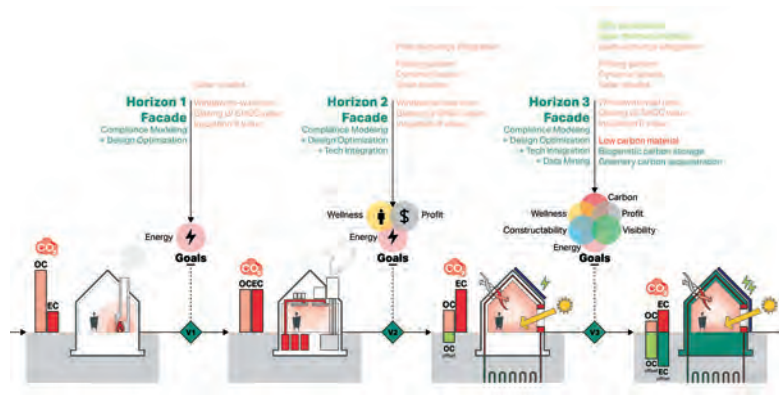


FIG. 1 High-Performance Façade Design considerations at three levels of scheme development.

Pareto Optimal: A solution whose performance in response to a given problem is equal to all other available solutions, i.e. is non-dominated and non-inferior.

Genetic Algorithm: A type of evolutionary algorithm which uses natural selection principles on a population and its subsequent generations to identify multi-objective solutions with the most optimal characteristics.

Grasshopper Plugin: Grasshopper is an algorithmic modelling plugin for the 3D modelling application Rhinoceros (Rhino) that uses a visual programming language (developed by David Rutten) as an official Rhino plugin. It is a parametric design tool.

3 BACKGROUND RESEARCH

A wide range of tools is available that can be applied to façade design and optimisation. Many of these tools are developed towards broad adoption by professional consultants who are not necessarily subject matter experts. This potential for the breadth of use is developed by simulating judgement – including optioning, optioneering and optimisation – in the backend of the software platform. For example, the tools FenestraPro, Cove.tool, Sefaira, Autodesk Generative Design, and SkinDesigner represent a selection of platforms that address the performance of façades, each supporting early-stage simulation for design decision-making. Each is a flavour of varying complexity where the magic is produced by a wizard at best far removed from the individual project, its goals, and the multiple stakeholders, design, and maker groups that govern the advancement of any building project.

Most of these platforms present as black-box simulations with little transparency around their data sources. The interfaces are designed as a relatively standard package with few controls or customisation to fit different projects in different regions. This leaves little flexibility to adapt to the various needs of clients and design teams. While customisation and geolocation will almost certainly improve, high resolution in and of itself does not necessarily translate to better decision-making. However, suppose we view the software not as a surrogate for subject matter experience but rather as an interface for augmenting that experience and judgement. In that case, we shift intent away from simulation as a form of virtual reality (where results are governed by the quality of the inputs and assumptions that calculations in the black box are correct) and towards augmented reality. Here the judgment of subject matter experts is supercharged by holding comparable critical frameworks at a task-appropriate resolution. The development of a bespoke workflow/tool is rooted in the desire for this augmentation of subject matter expertise (rather than in improving the broader design practice).

4 METHODOLOGY

To this end of consolidating the multiple analyses useful in early-stage envelope design, an interactive digital optimisation environment (a dashboard) has been developed that templates and facilitates the design and optioneering process. By surfacing the environmental impacts of façade geometry, materials, and construction, the process holistically informs the design impacts on daylight, energy, and embodied carbon, creating realistic high-resolution targets for façade design performance in support of carbon-neutral capable buildings.

The envelope design workflow is aligned with the hypothesis that a project's baseline energy and carbon can be effectively modelled by combining code-minimum energy modelling settings with regional carbon benchmarks based on location and building program. The dashboard extracts embodied carbon factors from an actively managed carbon database, which is updated and reviewed frequently, incorporating industry standards and publicly available carbon databases.

The dashboard intends to codify and template this design workflow with a series of modules that can be selectively employed and configured to proceed through all necessary steps of definition, simulation, analysis, and reporting. The environment developed around the design workflow examined in this study is termed the Façade Impact Tool, or FIT.

4.1 WORKFLOW

A typical HPB design workflow starts with defining program and project targets in the Feasibility Study and Programming stages, then conceptualising ideas in the Schematic Design stage, synthesising solutions in Design Development, verifying performance, and materialising design beyond Construction Documentation.

The proposed cohesive HPF design workflow aligned to the HPB design workflow is defined as follows (Figure 2):

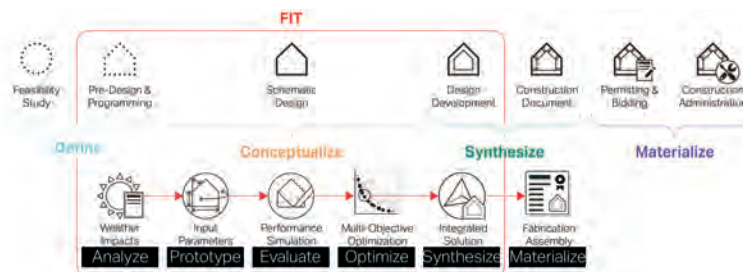


FIG. 2 High-Performance Building/ Façade Design Workflow templated by the dashboard tool.

During the Programming stage, weather conditions are analysed to support defining the whole building's performance targets, including solar and wind resources, to understand the challenges and opportunities they present.

In the Schematic Design stage, a parametric sketch module is employed to prototype conceptual massing and façade ideas – including design options such as external fins or pre-cast modules. A set of metrics is evaluated – including energy consumption, carbon emission, daylight distribution, glare potential, structural stability, and cost – as parameters of the design option are manipulated. The simulation results then feed into the optioneering process to optimise the design iterations based on the determined objectives. The trade-off analysis supports the final

determination of the optimal individual solutions, which will be synthesised into the recommended façade design bundles.

The complexity inherent in a building project (and spread across disciplines and knowledge centres) is usually prohibitive, especially during the early stage, to integrating all the above evaluations and optimisations with a design focusing on aesthetics. It is essential, however, to link cost and carbon, as well as all other criteria mentioned above, in early design optioneering, to ensure the performance potential of a façade design is achieved. Therefore, the workflow dashboard's utility is maximised through its application in the earlier stages of Pre-design, Schematic Design, and Design Development.

4.2 USER INTERFACE

A graphical user interface has been designed to facilitate user interaction. The interface (Figure 3) is designed to: structure the workflow, be easy to use, be easy to interpret, and encourage design exploration.

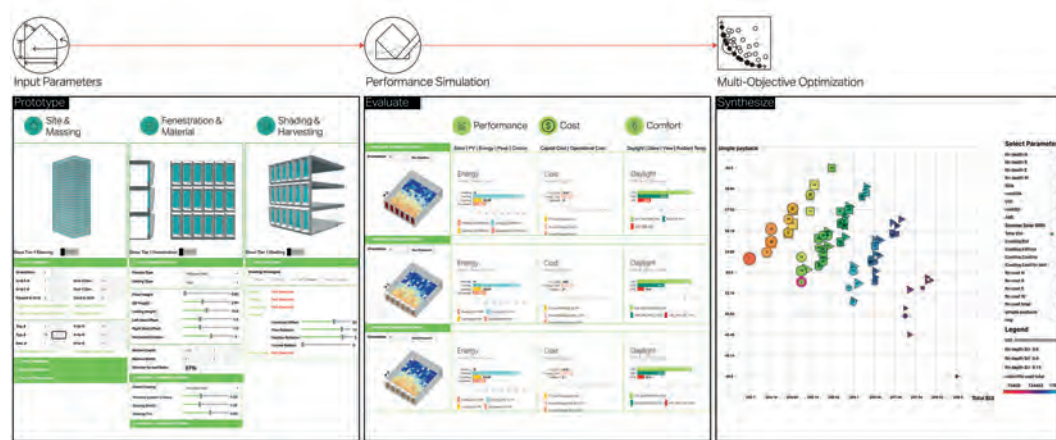


FIG. 3 Dashboard interface simultaneously displaying selected input parameters, selected simulation summaries, and multi-objective optimisation.

From left to right, the interface structure follows the typical façade design workflow defined in the previous section in three panels: Prototyping, Evaluating, and Synthesizing.

In the Prototyping panel, the process starts by initialising building massing with a specific project location and building program setup, followed by manipulating façade fenestration (window-to-wall ratio), identifying building enclosure materials, and customising conservation (shading) and generation (renewables) strategies. The interface displays a 3D building massing, an elevation, a section, and a 3D façade bay section adjacent to the parameter controls manipulated to generate the geometries.

In the Evaluating panel, a side-by-side comparison is employed to highlight the differences between two selected façade schemes. The interface displays daylight, solar, energy, carbon, and cost performance (as bar charts) and visualises solar and daylight area distributions as heat maps overlaid on 3D bay sections.

The Synthesizing panel can be toggled on and off as needed. This panel can also be used as a separate Multi-Objective Optimisation Dashboard (or MOO DASH). To enable this function, a user selects automated generation and recording of solutions in the Evaluating panel. Recorded

simulation runs are imported into MOO DASH for better visualisation and ease of the optioneering process and synthesising solutions.

In designing the interface, multiple tabs or separate windows corresponding to different workflow stages are avoided. All components are simplified, so they fit into one window. This provides users with a holistic image of an overall façade optimisation process, obviating the need to go back and forth to check inputs and outputs. The dashboard provides feedback (performance impacts) with every change that is made to inputs on the same page. The specific functions in the dash are described in detail in the following sections.

4.3 PROTOTYPING PANEL

FIT functions through a generative methodology, gamifying definition of the façade geometry, window-to-wall ratio, building enclosure typologies, and proposed shading solutions (FIG 4). In the Prototyping panel, levels of detail are specified, and design decisions are made that propagate further through the workflow.

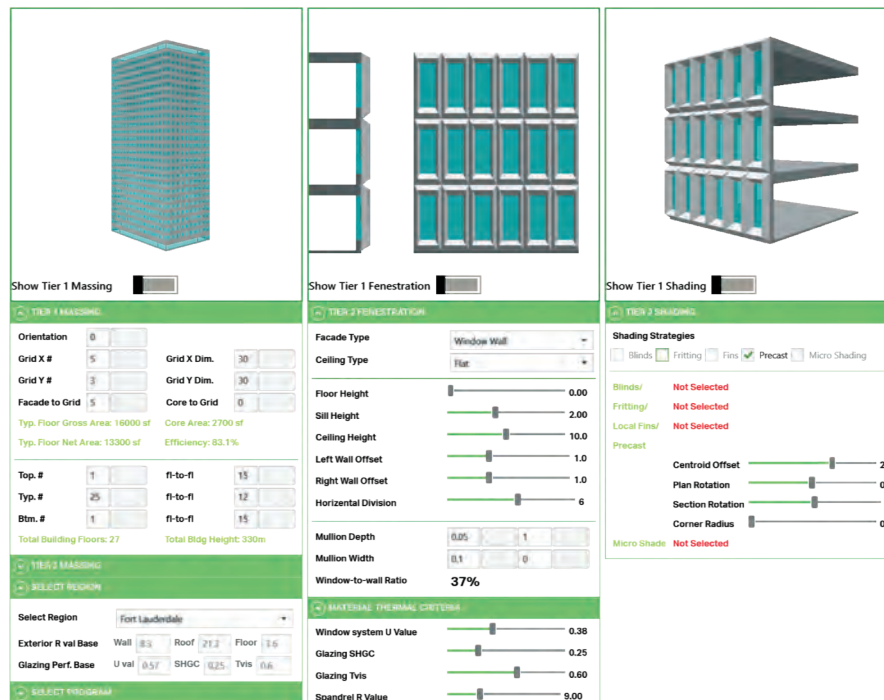


FIG. 4 Dashboard: Prototyping panel.

Base geometry can either be imported (from Rhino or Autodesk Revit) and modified as necessary or generated directly via simplified selections and parameters.

4.3.1 Site, Climate, Code Requirements and Massing

Project Location: The dashboard requires users to first select the project location to import hourly local weather data for energy and daylight simulation. Users verify the location’s climate zone and the current energy code baseline, and code minimum requirements for building envelopes, including the minimum R values of exterior walls, roofs, and exposed floors, as well as the maximum fenestration assembly U factors, SHGC values, and visible transmittance (Tvis) values. These performance parameters will be set for the mandatory façade scheme as the baseline for calculating the performance improvement of the proposed strategies. The proposed building envelope performance is created in the Material Thermal Criteria panel.

Building Operation: Users can select one or two building program types and assign them to the spatial geometry. The tool automatically generates all code-specified building operation conditions of the selected program. Users verify auto-generated internal loads and, when needed, override them with project-specific values. Parameters include Lighting Power Density (LPD), Equipment Power Density (EPD), occupant density, ventilation/ infiltration rate, peak occupancy hours, off-peak reduction factors, heating/ cooling set points, and setback temperatures. These parameter inputs are generally considered static in the workflow and remain unchanged for all façade schemes to maintain comparability.

Building Massing: The dashboard can set the general building massing from two approaches: White Box (“Tier 1”) Massing and Conceptual (“Tier 2”) Massing. Tier 1 Massing requires users to set the Structural Grid Dimension and Floor-to-Floor Height to generate a simple box building with approximately similar total floor area as the target building for the solar analysis. Tier 2 Massing requires users to pick the Core & Shell Massing from the Rhino/ Revit model that will be studied, as well as the Context Massing that will affect the solar analysis.

4.3.2 Fenestration and Material

Typically, the most cost-efficient façade design strategies for energy savings and low embodied carbon emissions are: Balancing Glazing Area, Solar Control Glazing, and Low Carbon Alternative products.

Balance Glazing Area: The Window-to-Wall Ratio (WWR) can be specified through one of two different approaches, and apertures are created given the ratio provided. The Tier 1 approach allows direct entry of the WWR, and the positions of the apertures are generated. The Tier 2 approach provides a series of input parameters, including: Floor Height, Ceiling Height, Sill Height, Module Width, Left/ Right Wall Offset (if the Window Wall System is selected), and Mullion/ Transom Width. The WWR is calculated accordingly. Users select a façade system to initialise the applicable input variables (FIG 5).

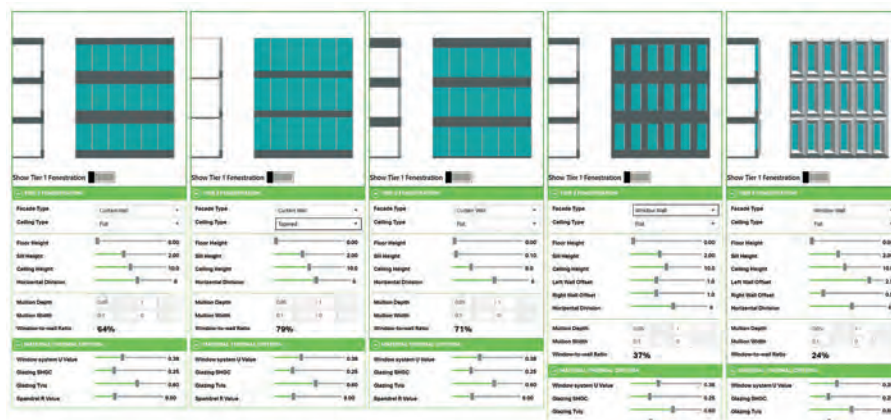


FIG. 5 Dashboard view of Tier 2 method for defining 5 fenestration schemes via Input Parameters.

Solar Control Glazing and Low Carbon Material Alternatives: Window thermal properties can be determined through one of two approaches in the workflow. One approach is to select a pre-specified window system (with known thermal properties) from a database. The other approach is direct input (via slider controls) of thermal conductance values (U-Value), Solar Heat Gain Coefficient (SHGC), and Visible Light Transmittance (Tvis). The thermal resistance (R-Value) of opaque elements can also be specified in this way. Input values will be highlighted in red if they are not in compliance with the local code requirements. Under development is additional functionality where users can replace

regular façade materials with low-carbon alternatives. Glass, mullion, insulation, and spandrel panel systems/materials will be specifiable.

4.3.3 Shading and Harvesting

Solar shades, natural ventilation, and integrated BIPV are the most commonly used façade design strategies to add additional values to the building, including human comfort, project visibility, and reduced carbon profile. The dashboard supports designers' investigation of optimal shading and climatic resource harvesting options.

Fritting: Glass with well-designed fritted patterns can combat excess solar loads and avoid both space overheating and glare. In the dashboard, designers can define Pattern Sizes, Frit Ratio, and Frit Color to modify the SHGC and T_{vis} values of the original glass.

External Fins: Multiple regular external fin types can be identified with a series of input parameters provided, including whether the fins are Horizontal or Vertical, the number of fins, the Interval Spacing, the Offset of the fins from the glazing, the Depth to extrude the fins, and the Angle to rotate the fins (FIG 6).

Precast Module: More customised external solar shades geometry can be identified based on discussions with design teams. One example provided here is proposing precast concrete modules, the configuration of which is determined by controlling the seed geometry's Centroid Offset, Plan Rotation, and Section Rotation (FIG 6).

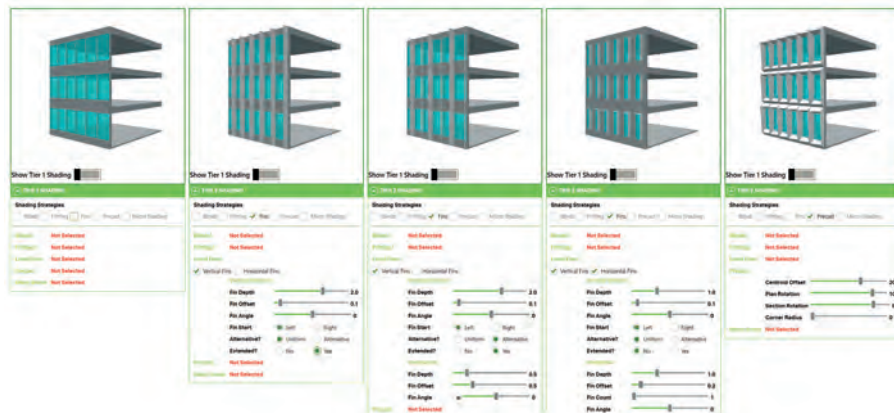


FIG. 6 External Fins and Precast Module Input Parameters – 5 examples displayed in the dashboard tool.

Other Shading Types: Designers can specify the input parameters for additional shading types like Micro Shading, Dynamic Glazing, and Internal Blinds. These modules are under development.

Natural Ventilation: Designers can select surfaces for natural ventilation or input the Opening Area (m^2) and specify the input parameters, such as Airflow Volume (m^3/h), Outdoor Wind Speed (m/h), and Coefficient of Effectiveness, to measure the impacts of Natural Ventilation. This module is under development.

Energy Harvesting: Designers can select surfaces to install BIPV modules or input the System Projected Area (m^2) and specify the input parameters, such as PV Module Type and PV Module Support Structure, to measure the system size and the amount of energy generated. This module is under development.

4.4 EVALUATING PANEL

FIT performs real-time simulation through a collection of Grasshopper scripts, including Ladybug, Honeybee, and OneClick (which support climate analysis, energy modelling, and embodied carbon analysis, respectively). Impacts of design decisions on thermal and visual comfort are determined and balanced against energy and carbon performance, as well as capital and operational cost metrics, to inform design decisions (FIG 7).



FIG. 7 Dashboard interface view: Evaluating panel.

4.4.1 Solar Simulation

This evaluation contributes a preliminary check on the viability of proposing shading strategies and building integrated photovoltaics (BIPV). The dashboard module quantifies total solar radiation gain falling on the building's façade, accounting for orientation and proposed shading strategies. The tool employs Ladybug scripts to perform solar irradiation simulation, and a custom Grasshopper script to generate a radiation map and apply it to the façade of the model.

4.4.2 Energy Simulation

This evaluation contributes to the space heating and cooling energy reduction impacts of the fenestration design, façade thermal properties, and proposed shading strategies. The tool calculates the annual heating and cooling Energy Use Intensity (EUI) of a typical bay adjacent to the façade. The tool employs Honeybee scripts to conduct annual energy simulations, leveraging the OpenStudio interface to Energy Plus.

4.4.3 Carbon Modelling

The carbon modelling evaluation is part of the study to estimate the embodied and operational carbon emissions over the user-defined lifetime of the building. The dashboard module accesses scope A1-A3 material embodied carbon information from EC3 (an open-source database platform) and material quantity information extracted in real-time from the designed geometry of the façade to produce a high-level estimate of the embodied carbon of the façade. Users can visually assess the before-and-after impact of façade elements such as added fins and window-to-wall ratio. In addition, using the project location and electricity grid emission factors from the U.S. EPA's eGrid program,

the estimated annual energy consumption is converted to lifetime operational carbon. The trade-off between increasing embodied carbon by the added material and reducing operational carbon is one of the key metrics provided to the users as visual feedback.

4.4.4 Daylight Simulation

Daylighting performance of the envelope system is evaluated via the fenestration design, glazing visible light transmission values, and proposed shading strategies. The dashboard module simulates daylighting environments, parses hourly output, and reports daylight metrics, including those required for LEED credit: Spatial Daylight Autonomy (sDA), Annual Sun Exposure (ASE), Useful Daylight Illuminance (UDI). The tool employs Honeybee scripts to manage and visualise daylight simulation, which is performed with the Radiance engine. A separate script is developed to generate a daylight distribution map and apply it to the horizontal surface of the typical bay adjacent to the analysed façade.

4.4.5 PV Harvesting Simulation

The dashboard contains a module for assessing the viability of building integrated photovoltaics (BIPV), where reasonable resources are noted (the ASE metric). The module reports both the total size of the system for a given PV surface in kW and the amount of annual electrical energy produced from the given surface. The module employs the NREL PVWatts v1 algorithm via Ladybug scripts to perform the PV harvesting simulation.

4.4.6 Cost Modelling

The cost modelling evaluation forecasts costs for developed design schemes to support budgetary and feasibility determinations, both for Cap-Ex considerations and whole-life cycle cost analysis. The module evaluates the probable cost premium of implementing strategies compared to the relevant baseline, focusing on hard construction costs. The module also calculates Return on Investment (ROI) with Rough Order of Magnitude (ROM) estimates if the energy simulation is completed and utility rates have been supplied. The module connects to a centralised unit cost database. It determines quantities of materials, either automatically from the parametric 3D model or manually from text box inputs for quantity take-offs.

4.4.7 KPI Scorecard

A multi-dimensional spider diagram is used in the dashboard module reporting interface as a uniform scoring system to compare each design scheme's Key Performance Indicators (KPI). The scorecard reflects a design's impacts on Carbon, Energy, Cost, Wellness, Constructability, Operational Impact, and Visibility. The methodology to measure each KPI is developed in the back end of the dashboard but can be viewed and edited if desired. For instance, Wellness is measured based on the alignment with WELL and Living Building Challenge certifications in daylight, indoor air quality, and connection to nature. Constructability is measured based on the lead time difference between the proposed scheme and the baseline scheme, product availability, and technology readiness. Operational Impact is measured based on the negative or positive impacts on operations, maintenance requirements, and lifespan, assuming the baseline has no or few impacts on the above categories. Visibility is evaluated based on whether the design strategy is exposed to being outstandingly visible and accessible. The intention is for project stakeholders to discuss and agree on selected KPIs (and their generation) prior to any optimisation efforts.

4.5 SYNTHESISING PANEL

The final step in the workflow is data interpretation and down-selection of synthesised solutions that attain identified objectives and meet the constraints that ensure realistically achievable performance.

4.5.1 Optioning

Optioning is understood as a quick exploration of the performance impacts of potential candidate façade schemes (typically from 2 to 5). The process is useful when the design team does not yet know which input parameter(s) primarily drive differences in performance. After Optioning, a design team can determine the key metrics to optimise in the Optioneering process. Optioning requires users to manually change variables in the input panels and check the performance results illustrated in side-by-side columns in the interface (two or more, as determined by the user). This layout maximises the visibility of learning the performance difference between the schemes.

4.5.2 Optioneering

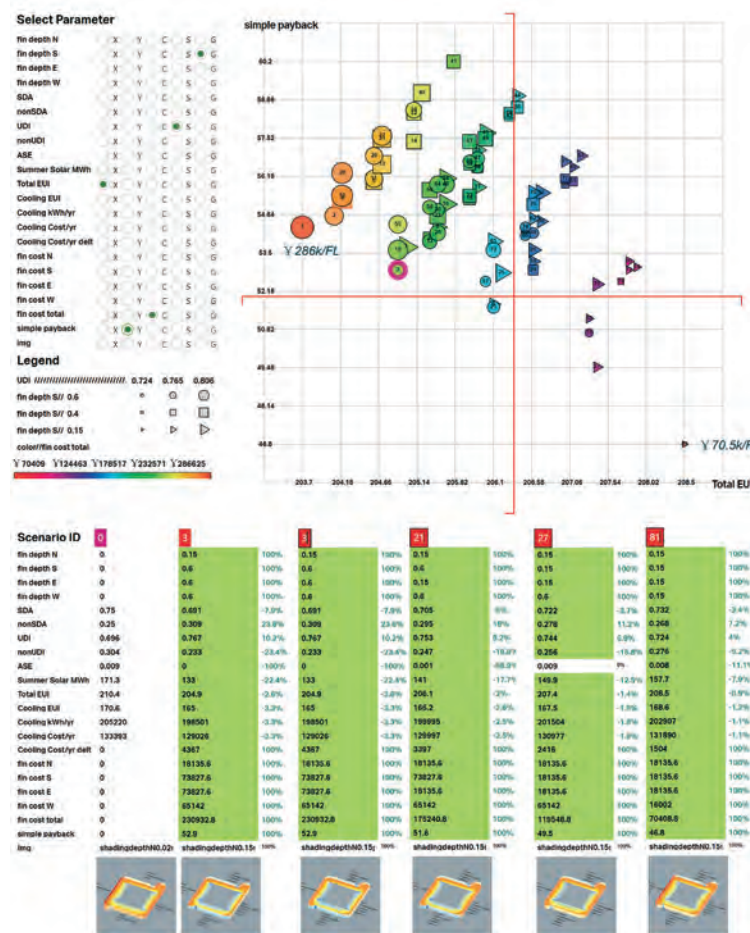


FIG. 8 Dashboard Optioneering panel (M00 DASH).

Optioneering is understood as searching for better façade design solutions by maximising or minimising selected objectives. The solutions to be explored could be either individual input parameters, such as the optimal WWR of a particular façade, or design schemes that involve multiple input parameters, such as the most desired external solar shades design. The objectives,

considered the optimising goals, could be the quantifiable KPIs, such as EUI or cost premium, or other quantifiable outputs, such as total solar irradiation. A minimum of two interrelated objectives are required for Optioneering, such as minimising energy and maximising daylight. The maximum number of objectives in the current version of the dashboard is five. The biggest challenge during Optioneering is settling on reasonable trade-offs between two or more competing objectives. This process is known as Multi-Objective Optimisation (MOO). A set of potential solutions, rather than one universally optimal solution, will be determined in a typical MOO process.

The dashboard Optioneering panel provides excellent detail of synthetic information (MOO DASH, Figure 8). When optimisation is toggled on, every generated design solution is recorded and populated onto a scatter plot which compares two variables from a set of options. Critical criteria can be compared between multiple design strategies by assigning either inputs/variables or outputs/objectives that have been identified in Optioning. The interface enables users to select the values to be displayed on the abscissa and ordinate, as well as make visual adjustments (to the colouring and size of displayed data points) to improve interpretability over the chart defaults.

4.5.3 Validation

Validation is a crucial step for any new tool or methodology. Although as an early-stage design aid, the various outputs of the dashboard tool are not optimised for extreme accuracy, it is still crucial to validate these outputs to ensure that the primary objectives of the tool are fulfilled. Validation is approached in two parts:

- **Outputs generated using a combination of industry-validated software:** FIT comprises open-source and industry-validated software and carbon databases as its various components (Table 1). These components are developed by various 3rd parties over multiple years, resulting in stable and reliable builds. Hence, the tool does not program any of the core physics or material science properties. The core functionality comes from analysing, combining, and displaying the inputs and outputs that connect across all these industry-validated components. Since the calculations and outputs from one software are independent of the calculations and outputs of the other, this validates the sum of the individual parts.
- **Outputs replicated outside of the dashboard:** When simulating the same geometry with the same inputs directly in the individual software packages, the output results are the same. This equivalence suggests the dashboard tool can be used and compared across the industry.

The table below outlines the software components employed for the various functions in FIT.

TABLE 1 Industry-validated software engines and databases used in FIT.

FUNCTION	CORE SOFTWARE
Energy Simulation	Energy Plus ¹ and Open Studio ²
Solar Irradiation	Ladybug Tools ³
Daylight Simulation	Radiance ⁴
Solar PV Simulation	NREL PVWatts v1 ⁵
Embodied Carbon Database	EC3 ⁶
Operational Carbon	U.S. EPA eGrid ⁷

1 <https://energyplus.net/>

2 <https://openstudio.net/>

3 www.ladybugtools.com

4 <https://www.radiance-online.org/>

5 <https://pvwatts.nrel.gov/>

6 <https://buildingtransparency.org/ec3>

7 <https://www.epa.gov/egrid>

5 EXPERIMENT

Two studies were conducted by exercising the dashboard environment (the FIT) to exercise the methodology discussed above. An optimisation of a possible external fin design was investigated, as was a possible pre-cast modular design.

5.1 OPTIMISING EXTERNAL FINS

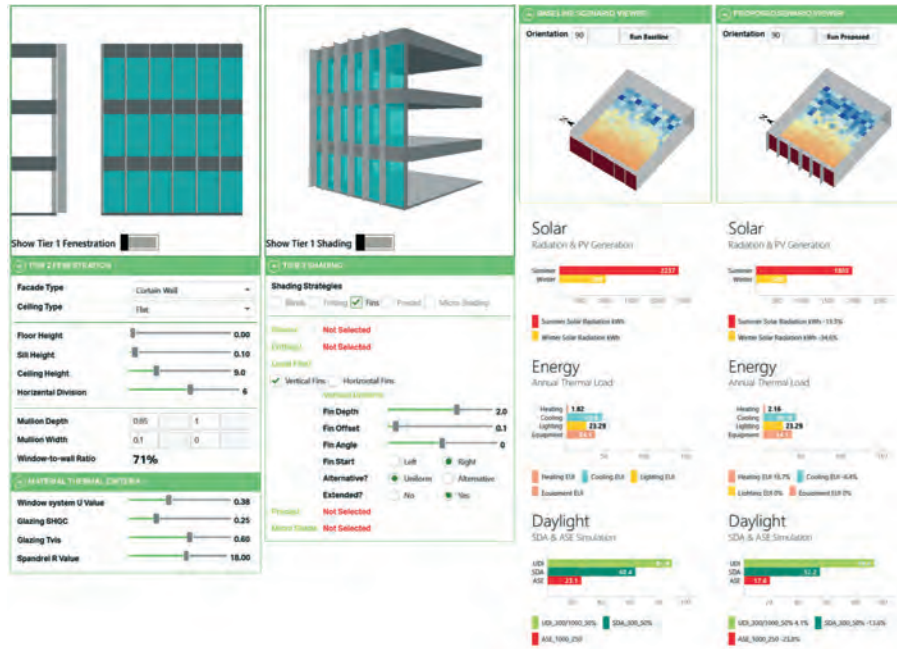


FIG. 9 Interface display of definition and results of optimised external fins scheme performance relative to baseline.

Optimal external vertical fins dimensions were explored for each façade of a building located in Wenzhou, China. Building geometry was imported through the Prototyping panel, and three viable external Vertical Fin Depths were defined for each façade (150mm, 400mm, and 600mm). With all design permutations, the tool generated 81 façade schemes for analysis.

Two key objectives were defined: minimising space Energy Use Intensity (EUI) and minimising Simple Payback (the time period, in years, at which energy cost savings of a proposed measure are equivalent to the construction cost premium of the proposal). The objectives are displayed on the orthogonal axes of a scatter plot in the module interface. Cost premium (displayed as data point colours) and Useful Daylight Index (UDI) (displayed as data point sizes) were considered as additional objectives while exploring façade solutions (Figure 8, Figure 9, Figure 10).

Plotting all façade schemes indicated that 150mm fins for the southern and northern façades and the 600mm fins for the eastern and western façades were optimal dimensions for minimising energy consumption and maximising daylight performance. The tool also reported preliminary embodied carbon and cost premiums for the vertical fin strategies.



FIG. 10 View of the interface of the summary report module of the External Fins Optioneering case.

5.2 OPTIMISING PRE-CAST CONCRETE MODULE

A pre-cast concrete modular façade design was explored for a building in Florida, USA. Driving variables were selected for the early-stage trade-off study, including Window-to-Wall Ratio (WWR), concrete typology, and pre-cast façade module dimensions (Figure 11).

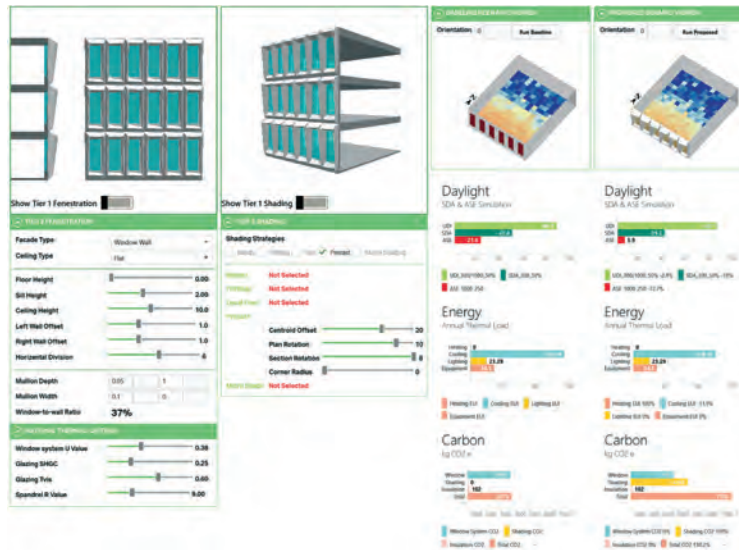


FIG. 11 Input parameters and results of proposed and baseline schemes displayed adjacently in the dashboard.

The design team requested a multi-criteria analysis to ensure that optimal parameters were picked for each façade strategy. Key objectives were down-selected from available KPIs, which included: minimising the façade solar exposure and solar heat gain, maximising the percentage of the floor areas within the Useful Daylight Illuminance (UDI) range of 300 lux to 1000 lux, minimising annual cooling Energy Use Intensity (EUI), optimising the material usage (reducing up-front carbon impact), and lowering both capital costs and operational costs. Additional KPIs, such as supply chain impacts, constructability, and supply chain impacts, were requested to be considered when making selections. Input parameters were defined in the dashboard environment's Prototyping panel, and the key objectives and additional KPIs were configured in the Evaluating panel (Figure 12).

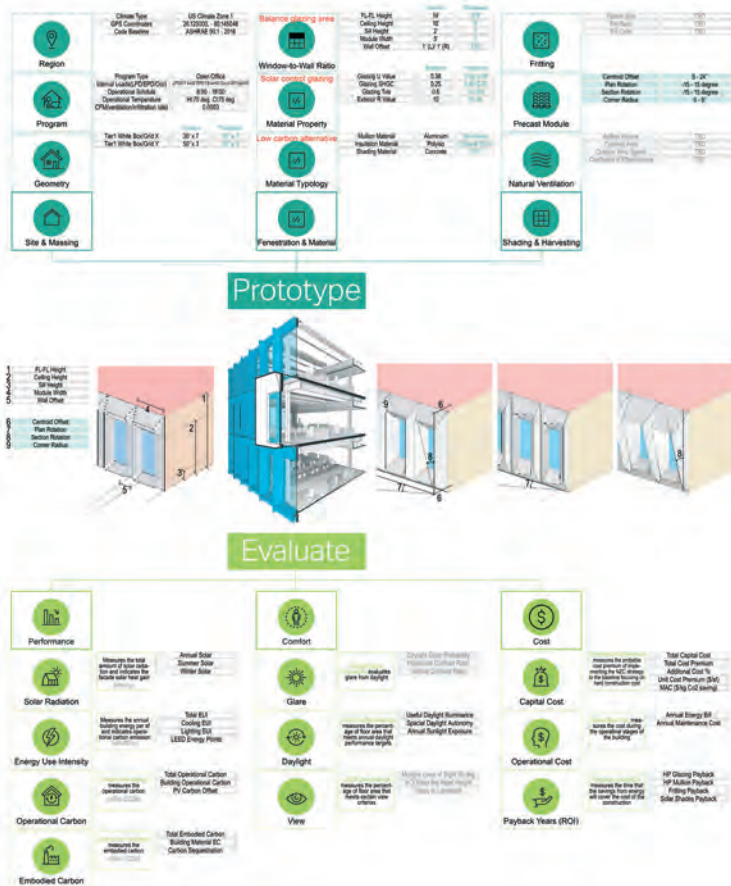


FIG. 12 Input/Output summary graphics of Pre-cast Concrete Module Optioneering in the dashboard environment.

6 RESULTS AND ANALYSIS

Decision-making on high-performance façade design and decarbonisation strategies was found to be augmented by employing FIT, which provided visibility of the building performance quantification. The workflow improvements generally fell into two categories: definition flexibility and analysis efficiency.

6.1 INCREASING FLEXIBILITY

The workflow templated by FIT remained stable across both experimental trials, but the customizability provided by the scripting environment made it straightforward to tune the definition and analysis to different types of buildings and façade design measures. We notice that this combination of a stable workflow with modular configurability suggests the broad applicability of the tool to different types of buildings (in different climatic regions) since all components in each FIT module can be selected and de-selected. Compared to other current tools in the industry, where only a stable workflow is provided, and the new functionalities will have to wait until the next version is released, the FIT workflow shortens the response time between the tool development team and project stakeholders. The flexibility ensures that the process is scalable to different types of projects in different regions. The tool keeps the specific functionalities turned on based on time constraints and design comprehensiveness to make the design process more concentrated and the targeted performance objectives more achievable.

Therefore, it was found that a working session at the project outset (between the tool development team and project stakeholders) was valuable for verifying consensus on input parameters and key objectives. This decision point allowed the configuration of the tool to be largely completed prior to the execution of analyses, which ensured consistency between results determined for different strategies and minimised time and effort for re-configuration required if parameters and objectives were revised.

6.2 INCREASING EFFICIENCY

FIT streamlines the early-stage façade design workflow, which requires rapid decision-making due to time constraints when conceptualising ideas and delivering projects. We notice in the experiments that the cohesive FIT process supported by the interactive dashboard, compared to the conventional process without FIT, not only facilitates multi-disciplinary collaborations with fewer conversations required between the project stakeholders but also provides higher possibilities of exploring more iterations within a shorter time.

An efficient approach to prototype design iterations and evaluating the environmental performance is the key to saving design hours and costs. Firstly, the consistent format in configuring the iterations and visualising the data reduces the educational efforts so the team can input the models and read the values with minimum instructions. On the other hand, because of the automation of simulation, reporting, and optimisation provided by the tool, even if revisions are required to initially agreed-upon input parameters and key objectives (and re-configuration of modules within the tool are required). Once the parametric model was prototyped and the multiple KPIs were agreed upon during the project stakeholders' engagement, the later phases of analysis would not require significant additional effort, still allowing the approach's insights to be available to early-stage design.

7 LIMITATIONS AND FUTURE WORKS

Given its current state as a Minimum Viable Prototype (MVP), FIT exhibits scalability, usability, and computation speed limitations. These limitations form the basis for the roadmap for the next development phases of the tool. As FIT is as much a workflow as it is a tool to make better decisions faster within a whole project framework, there are complex variables that limit developing a baseline where individual variables can be evaluated for increased efficacy. The development of a comparable baseline within a project framework is being explored for future work.

7.1 DEVELOPMENT ENVIRONMENT

FIT is a script-based tool that currently utilises Rhino and Grasshopper as the primary development environment. This presents challenges to scaling, user-friendliness, and computation speed which are constrained by the Rhino platform. Hence, FIT is not currently accessible to users outside the development team. In addition, separate installation and configuration of a stack of other components are required to enable all functions of the tool, including Ladybug Tools as well as OpenStudio and Radiance.

An alternative web-based development environment is under consideration which could alleviate some of the above-mentioned limitations. This environment would utilise HTML and JavaScript, with open-source libraries such as three.js and Pollination. The aim of this re-platforming would be to make FIT accessible to a broader array of subject matter experts for project analysis in any location.

7.2 DECENTRALISED COMPUTATION/CLOUD COMPUTATION

FIT is currently constrained by the computation resource availability of a single PC (whether physical or virtual). Hence, the response time becomes exceedingly long when proceeding with heavy simulations such as energy and daylight modelling and when manipulating complex façade models. Utilising either recently developed parallel computing functionality provided by Rhino and Grasshopper or cloud-based computation management methods could speed response times multi-fold.

7.3 DYNAMIC INPUTS AND DATABASES

Currently, input files and databases are locally hosted on the same PC on which FIT is operating. It is possible to deploy a centralised cloud-based database from where all inputs and databases can be dynamically managed. In addition to streamlining the undertaking of multiple projects and analyses in parallel (by multiple users), this centralisation would allow two-way read/write functionality and version control. Based on the current MVP, multiple tool instances have been developed and employed for different project types, including logistics centres, commercial towers, and transportation terminal buildings, to suit a range of performance targets for multiple clients. Dynamic centralisation would expand this flexibility and reduce the time and effort overhead required for configuration in advance of analysis for a given project.

7.4 INTEROPERABILITY

Currently, FIT has limited interoperability in terms of connected software outside of the Rhino and Grasshopper development environment. The current build does allow for two-way translation with Autodesk Revit, albeit with numerous constraints. The development team is exploring ways to streamline the connection with Revit, as well as interoperability with other web-based platforms.

8 CONCLUSION

A dashboard environment of FIT lowers the bar for early-design-stages exploration of façade design solutions by automating analysis phases and providing simultaneous visibility of inputs and outputs. Further, the MOO DASH can be deployed using resulting data sets from FIT to find the trade-offs between conflicting or aligning criteria such as human comfort, energy consumption, capital cost, EUI, life cycle costs etc.

Evidence-led design is one methodology for architecture – and façade design – to directly engage and affect the ecological and sustainability footprint of the building design and construction industry. Tools that provide near-real-time analysis can help to generate insight into the deliberations around organic low-carbon materials vs inorganic but reusable materials by providing structured and comprehensive comparisons of their impacts. FIT and MOO DASH, developed as customisable expert augmentation, support generation and comparison of meaningful datasets, enabling evidence-based early-stage decision-making for a broader range of building projects than would otherwise be possible.

Acknowledgements

The study is funded by AECOM Innovation Laboratory (iLAB). Special thanks are due to the co-developers.

References

- Berquist, J., Tessier, A., O'Brien, W., Attar, R. and Khan, A. (2017). An Investigation of Generative Design for Heating, Ventilation, and Air-Conditioning. SimAUD 2017 Conference.
- De Weck, O.L. (2004). Multi-objective Optimisation: History and Promise. Available from http://strategic.mit.edu/docs/3_46_CJK-OSM3-Keynote.pdf (published 2004).
- Gerber, D. J., Lin, S.H., Pan, B. and Solmaz, A.S. (2012). Design optioneering: multi-disciplinary design optimisation through parameterisation, domain integration and automation of a genetic algorithm. Proc. Symposium on Simulation for Architecture and Urban Design, Society for Computer Simulation International. pp. 32-39
- Gunantara, N. (2018). A review of multi-objective optimisation: Methods and its applications. Cogent Engineering, 5:1, DOI: 10.1080/23311916.2018.1502242
- Howes, B. (2016). Design Explorer – Natural History. Available from <http://core.thorntontomasetti.com/blog/> (accessed September 2016).
- Negendahl, K. (2015). Building Performance Simulation in Early Design Stage: An Introduction to Integrated Dynamic Models. Automation in Construction 54:39–53
- Roudsari, M.S. (2016). "Seeing the Process: Ladybug + Honeybee, Dynamic Building Simulation Solutions for Integrated Iterative Design" Energy Accounts: Architectural Representations of Energy, Climate, and the Future. Ed. Willis, Dan; Braham, William W.; Muramoto, Katsuhiko; Barber, Daniel A. Routledge, pp 112-11
- Roudsari, M.S., Pak, M. and Smith, A. (2013). Ladybug: A Parametric Environmental Plugin for Grasshopper to Help Designers Create an Environmentally-Conscious Design. Proceedings of the 13th International conference of Building Performance Simulation Association. Chambéry, France, Aug 25-28 2013. pp. 3128-3135
- Shen, X., Singhvi, A., Mengual, A., Spastri, M., and Watson, V. (2018). Assessing the Multi-Objective Optimisation Methodology for Performance-Based Building Design in Professional Practice. 2018 Building Performance Analysis Conference and SimBuild, 646-653
- Shen, X. (2018). Environmental parametric multi-objective optimisation for high performance façade design. Proceedings of the 23rd CAADRIA Conference - Volume 2, Tsinghua University, Beijing, China, 17-19 May 2018, pp. 103-112
- Vilcekova, S. and Burdova, E.K. (2014). Multi-criteria analysis of building assessment regarding energy performance using a life-cycle approach. International Journal of Energy and Environmental Engineering 5, Article number: 83 (2014)

Generative Design as a Technique for Creating Energy-Efficient Building Envelopes

Venus Kashyap^{1*}, Bhavya Jain²

* Corresponding author

1 Indira Gandhi Delhi Technical University for Women, Department of Architecture and Planning, India, venuskashyap@igdtuw.ac.in

2 Indira Gandhi Delhi Technical University for Women, Department of Architecture and Planning, bhavyaj10@gmail.com

Abstract

As the importance of energy-efficient design grows in today's world, architects are finding it increasingly difficult to balance a variety of user-imposed criteria and objectives with cost and space constraints, aesthetics, and energy efficiency. Several tools and methodologies have been developed, largely based on Multi-Objective Optimisation Algorithms. This study aims to evaluate the applicability of deep learning and generative design techniques for creating energy-efficient building envelopes by generating comparable simulations for different façade alternatives in an early stage of building design. Following a thorough examination of both previously published works and case studies of buildings where the generative design technique was applied, a new design workflow technique is offered in which diverse factors are addressed concurrently. The technique explores various iterations that can be made, such as geometrical forms, solar and shadow analysis for optimum size and location of openings, etc., to provide an optimised solution for façade design alternatives. A residential building envelope is investigated as a base model research. The angle and size of openings on the building's façade are optimised through analysis and energy simulations in different scenarios. The simulation results are compared before and after, which show significant energy savings. Thus, the investigation yields a conclusion.

Keywords

Generative design, building energy-saving, building envelopes, deep learning, energy optimisation

1 INTRODUCTION

Today's most pressing problems are the earth's limited energy resources and the rising cost of energy. As we become more concerned with energy conservation and the environment, the significance of energy-efficient design increases. But the task of balancing a variety of user-imposed criteria and needs with cost and space constraints, aesthetics, and energy efficiency is becoming ever more difficult for architects. (Mukkavaara & Sandberg, 2022)

Generative design is a technique that generates a large number of design alternatives based on a set of design characteristics. Several ways in which generative design contributes to sustainability include the development of energy-efficient buildings, which helps in using fewer construction materials as additive manufacturing consumes less energy. It further accelerates the construction of the structure. Users can input a variety of design criteria, such as the amount of material to be used, specifications for performance, geographical requirements, conditions of operation, size and weight restrictions, methods of production, economic limits, etc., using generative design technology (Stainer, 2021). It can reduce the usage of construction materials by up to 40%. Generative design can increase sustainability through additive manufacturing, commonly known as 3D printing, in addition to material reduction. (Gigante, 2020). It integrates parametric design (PD) with artificial intelligence (AI), along with the limitations and data provided by the architect.

Generative design is a strategy for increasing human resources by automating design logic with algorithms. The architect still defines the parameters, but instead of modelling one thing at a time, generative design software assists in the creation of many solutions concurrently and, in some cases, in the discovery of 'happy accidents' or unique and unforeseen solutions that would be difficult to discover using traditional methods. Rather than simulating a single operation at a time, generative design software aids in the creation of multiple alternatives at the same time and can even uncover unique and unexpected ideas that would be a challenge to find using conventional methods. (Souza, 2020).

1.1 DESIGN OF ENERGY-EFFICIENT BUILDINGS

Energy consumption is one of the world's most pressing issues today. Humanity is facing the exhaustibility of the fossil fuels on which it has become reliant, while their use significantly pollutes the environment. The built environment is a significant contributor to this problem: buildings are everywhere, and the majority of them require energy to heat, cool, and light themselves. These energy needs might be reduced if the envelope materials are chosen wisely. Energy-efficient architecture is becoming increasingly important as we become more concerned about energy conservation and the environment. In order to address the need for a sustainable and low-carbon society, energy conservation measures have been introduced in the building design and construction industry. Consequently, environmental design has evolved into a major research area.

According to IEA, buildings and the construction of buildings account for about one-third of the overall energy consumption and approximately 40% of overall direct and indirect carbon dioxide emissions. Building and construction energy requirements continue to rise, owing to increasing energy availability in developing nations, increased occupancy and use of energy-consuming appliances, and significant development in global building floor space. Building-related pollutants have increased in recent years. Several reasons have contributed to this rise, including increasing energy usage for heating and cooling, greater air-conditioning adoption, and extreme weather events. Due to the continuous use of fossil fuel-based resources, inadequacy of energy-efficiency policies,

and inadequate financing in sustainable building design, tremendous emissions reduction capability remains elusive. (IEA, 2021)

The current methods for designing nearly zero-energy buildings (nZEBs) rely on architects applying standardised bioclimatic design measures based on their professional expertise and intuition. The simulation of these measures' impact on the building's energy performance and the thermal/optical comfort of its occupants is a complex procedure that normally necessitates a significant amount of effort, time, and special skills. For these reasons, it is usually carried out after a decision has been made on major building elements or in tow to three alternative solutions.

The evaluation of energy performance in the initial design stage through analysis is a vital yet difficult and complex approach in order to successfully construct nearly zero-energy buildings. Various statistical tools and methodologies have been created over the last few decades to tackle performance-related design challenges, the majority of which use Multi-Objective Optimisation Algorithms.

Advancements in technology have changed the way architects build and think, automating difficult operations and enabling simultaneous evaluation of various alternatives. (Eleftheria Touloupaki, 2017). Technological advances have revolutionised the way architects design and think, allowing them to partially automate the design process and incorporate massive amounts of data into it. Computational Generative Design, also known as Parametric/Algorithmic Modelling, has emerged as a valuable tool for exploring design potential and enriching the architectural synthesis process in recent decades. This method provides dynamic control over geometry and components when designing forms or systems, allowing the designer to seek appropriate solutions to complex problems while evaluating multiple variants at the same time. Visual/graphical design coding tools, such as Dynamo Studio for Autodesk Revit or Grasshopper for Rhinoceros 3D, enable the implementation of parametric design concepts using visual logic, thereby automating complex tasks.

Envelope design is one of the most important architectural decisions in modern energy-efficient construction. There is no one-size-fits-all solution for sustainable buildings, and the best techniques must consider the building's location and function. The purpose of this paper is to investigate the capabilities and limitations of generative design for envelope design using current applications.

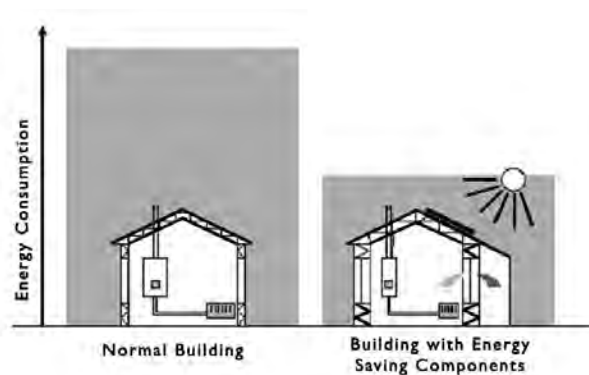


FIG. 1 Energy-saving building components. Source: Pieter de Wilde, 2004

Building computational approaches appear to be an appropriate tool to support decision-making related to the selection and incorporation of energy-saving building façades. Generative design tools provide extensive information on the thermal efficiency of yet-to-be-built buildings, enabling objective comparison among design options under similar circumstances. (Pieter de Wilde, 2004).

The process includes the following steps:

- 1 Generation
- 2 Analysis
- 3 Evaluation
- 4 Evolution
- 5 Exploration
- 6 Adoption

It utilises the Darwinian concept of survival of the fittest to maintain a set of solutions, with the weakest being eliminated at the end of each cycle. Mutation (random modification inclusion) and crossovers are two common “operators” used to develop unique solutions (switching elements from different solutions). Depending on the application, one can provide the tool with a 3D model or a collection of variables that describe the same framework for running an energy analysis simulation. Once the model is created, the tool will evaluate it. Its structure is based on three main components:

- 1 A 3D model that defines a ‘design space’ of viable system solutions.
- 2 A collection of variables that characterise the objectives or aims of the design.
- 3 An evolutionary computing approach, such as a genetic algorithm, that searches the design space for several efficient design choices based on the provided design parameters

1.2 GENERATIVE DESIGN FOR ARCHITECTURE

1.2.1 1.2.1 Introduction

Generative design is the combination of parametric design (PD) with artificial intelligence (AI) and a set of design parameters supplied by the architect. By rapidly repeating the algorithm, Metaheuristic Search Algorithms are used to develop a large number of original, innovative, and efficient design options simultaneously. (Souza, 2020).

1.2.2 History

The idea of generative design is not novel. Its origins are unknown, but since the 1970s it has been used as a strategy for tackling complex design challenges. Due to the need for innovative solutions to design challenges, its popularity in architecture and construction has risen. Computer simulation tools are increasingly being used to assess a building’s energy performance as well as the thermal/optical comfort of its occupants. They are a powerful tool for studying building environmental performance because they provide useful feedback for the ongoing design process. W. N. Hien et al. (2000) concluded that the main reasons architectural firms would not use simulation tools in the design process were a lack of client pressure/appreciation, the high cost of software acquisition, and insufficient staff training/skills due to steep learning curves and non-user friendly interfaces, which would extend the, already limited, design time. Since then, much has changed in the field, with simulation software becoming more widely available and specialised, influencing how buildings are designed, analysed, and built. As technology has become more accessible, this design method has gained popularity because it lets people quickly and easily experiment with a wide range of concepts and theories.

1.2.3 How generative design works

Typically, computer-aided design (CAD) software is used in generative design to generate a stream of (possibly uncommon) options based on a fundamental concept. Design needs and parameters can then be entered into an application to increase the variety of possible results and produce new designs that are more in accordance with feasible techniques. These outcomes are then analysed so that the designer can eliminate ineffective ideas and arrive at the optimal option. (W. Wang, 2005)

In 2013, W. Jabi defined Parametric Design as “a process based on algorithmic thinking that allows the expression of parameters and rules that define, encode, and clarify the relationship between design intent and design response”. Parametric, generative, or algorithmic design is principally an efficient method of flexibly describing – and creating – geometry via scripting, in which decision variables are linked to geometry. P. Janssen identified four types of parametric modelling techniques: object modelling, associative modelling, data flow modelling, and procedural modelling, which differ primarily in their ability to support iteration.

Visual Programming (VP) systems were created to assist designers in the process of writing scripts in order to generate parametric models. In 1990, B. A. Myers defined a VP system as “any system that allows the user to specify a program in two-(or more) dimensions.” D. C. Halbert had already identified VP systems as a valuable tool for nonprogrammers to use in order to create fairly complex programs with little training. Since then, it is clear that VP systems have evolved dramatically, with software like Grasshopper, Dynamo, and Generative Components making parametric modelling increasingly accessible to the design practice.

1.3 FRAMEWORK FOR DIGITAL ARCHITECTURAL DESIGN

A design framework can be generally characterised as a process that is composed of different individual operations (Brown, Jusiega, Mueller, 2020). The three frameworks depicted in Figure 3 constitute an adaptation of the work of Oxman (2006) and Wortmann (2018), respectively.

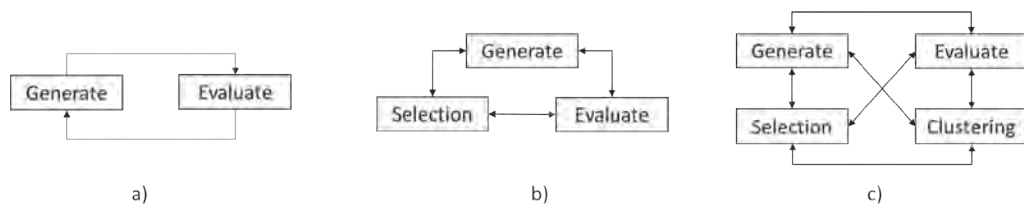


FIG. 2 Three architectural design frameworks, with actions and relationships. Source: Bertagna, Federico & D'Acunto, Pierluigi & Ohlbrock, Patrick Ole & Moosavi, Vahid, 2021

Generating design possibilities and then evaluating them in accordance with a set of criteria constitutes a typical design strategy. Repeating this procedure enables designers to create novel possibilities based on the results of the examination using a trial-and-error methodology (Figure 3a). Digital parametric tools have made it possible for designers to automatically generate a huge number of alternate options with little computational effort. Such a problem-oriented approach is frequently ineffective and time-consuming when dealing with multi-dimensional design spaces that involve a large number of design factors. One strategy to deal with this issue could be to use optimisation techniques like multi-objective optimisation (MOO). (Bertagna et al., 2021) These methods make it possible to streamline the evaluation phase of looking for the best-performing options. In the case of multi-objective optimisation, they support guided explorations of the design space by offering sub-optimal options from which the designer must choose (Brown & Mueller, 2017; Turrin, Von Buelow, & Stouffs, 2011; Yang Ren, Turrin, Sariyildiz, & Sun, 2018). (Figure 3b). The flexibility and

responsiveness required in the early, vague stages of design are not always provided by optimisation approaches, despite their extreme effectiveness in solving well-defined problems. The main issue in this situation is that all design objectives must be stated explicitly before they are even known (Harding & Olsen, 2018), which makes it challenging to incorporate qualitative factors. The addition of an intermediate clustering step makes it possible to systematically include such attributes (Figure 3c). Machine learning-based clustering techniques, for instance, can offer additional assistance by automatically classifying enormous collections of various design possibilities in accordance with similarities pertaining to particular criteria (Wortmann & Schroepfer, 2019).

When combined with filtering functions, these algorithms enable designers to manage vast, multi-dimensional design options and eventually negotiate quantitative and qualitative aspects based on their own preferences (Harding & Olsen, 2018; Fuhrmann, Moosavi, Ohlbrock, & D'Acunto, 2018; Saldana Ochoa, Ohlbrock, D'Acunto, & Moosavi, 2020). By taking this approach, the designer avoids being overwhelmed by examining each option individually and is not forced to focus solely on quantitative aspects (Brown & Mueller, 2017). The current study, like the one by Saldana Ochoa et al. (2020), employs a design process that includes generation, evaluation, clustering, and selection steps, with the goal of taking into account both quantitative performance criteria and qualitative designer preferences while maintaining the simplicity and adaptability required in the early design stage.

1.4 OBJECTIVES AND CONTENT OF THE PAPER

This study aims to evaluate the applicability of deep learning and generative design techniques for creating energy-efficient building envelopes by generating comparable simulations for different façade alternatives in an early stage of building design. This study looks at how to ensure the flexibility and interactive response that designers require in the early stage of façade design. The technique explores various iterations that can be made, such as geometrical forms, solar and shadow analysis for optimum size and location of openings, etc., to provide an optimised solution for façade design alternatives.

The paper is structured as follows. Section 2 outlines the methods that form the basis of the research, introducing the applied geometry-based approach, the digital tools involved, and the metrics considered. Section 3 illustrates an experiment to demonstrate the proposed energy-efficient building generative design workflow and the benefits of the proposed framework, as well as to investigate the proposed design approach for the façade design to achieve energy efficiency, followed by a discussion hereof. Finally, section 4 outlines the conclusion and presents an outlook on future work.

2 METHODOLOGY

An extensive review of previously published works on generative design techniques and deep learning is conducted to acquire a deeper grasp of the topic. Additional case studies of buildings where generative design technique was applied were also studied. After careful examination of both, a new design workflow technique is offered using generative architecture and deep learning technology, in which diverse factors are addressed concurrently. The proposed workflow methodology combines parametric modelling and MOEAs to integrate energy simulation in the early design stages of a building to minimise its lifecycle energy requirements and meet nZEB standards. The software tools proposed for seamless operation are Grasshopper for Rhinoceros3d with Galapagos Evolutionary Solver, Ladybug and Honeybee. As a result, a decision support tool is introduced to overcome the limitations of current practises in energy-efficient building design (bioclimatic design), which are based on the architect's intuitive application of fragmentary measures rather than the objective of optimising the building as a whole system of

interconnected parameters. The proposed design method is created utilising daylight and heat modelling. A residential building envelope is investigated as a base model research. The angle and size of openings on a building's façade are optimised through analysis and energy simulations in different scenarios. The simulation results are compared before and after, which show significant energy savings. Finally, the investigation yields a conclusion.

2.1 GEOMETRY-BASED DESIGN APPROACH

The development of architectural space is heavily dependent on geometry. This dependence on geometry is the same in other disciplines, making geometry a common ground where parts of other disciplines converge. In structural design, for instance, geometry plays a crucial role in determining the overall behaviour of a structure. Equilibrium-based methods such as graphic statics (Culmann, 1866; Maxwell, 1864; Cremona, 1872) and their modern digital implementations have proven to be effective tools for the generation of structures (Van Mele, Rippmann, Lachauer, & Block, 2012; Rippmann, Lachauer, & Block, 2012; Beghini et al., 2014; D'Acunto et al., 2019; Konstantatou. In contrast to analytical methods, which are typically implemented through quantitative numerical approaches, geometry-based methods provide significant support during the conceptual stages of design when a visual understanding of forces is necessary to generate creative design options (Schwartz, 2012; Kotnik & D'Acunto, 2013). Geometry also plays an important role in the evaluation phase of given design possibilities. Digital technologies for structural and energy analysis can now do extremely precise calculations on models with a high resolution. However, this is frequently accompanied by a lengthy calculation time and a consistent effort for the building of the models. As such precision is typically not required in the early stages of design, material-independent geometry-based techniques are a suitable simplification for conceptual design tasks and serve as the foundation for this study. Later, detailed models that account for material attributes might be incorporated into the design process.

2.2 DIGITAL TOOLS INVOLVED IN GENERATIVE DESIGN

2.2.1 Rhinoceros:

Rhino or Rhino3D is a commercial computer-aided design (CAD) and 3D computer graphics product designed by Robert McNeel & Associates. In contrast to polygon mesh-based applications, Rhinoceros geometry is based on the NURBS mathematical model, which enables mathematically accurate representations of curves and freeform surfaces in computer graphics. (Rhinoceros 3D, 2021)

2.2.2 Grasshopper

Grasshopper is a visual programming language and environment for the Rhinoceros 3D computer-aided design (CAD) software. Components are dragged onto a canvas to construct programs. These components' outputs are subsequently linked to the following components' inputs. (Grasshopper3d, 2021)

2.2.3 Ladybug Tools

Ladybug tool consists of Ladybug, Honeybee, Butterfly, and Dragonfly that support environmental building design. It links Grasshopper to daylighting and energy simulation engines like Radiance, Dayism, Energy Plus, and Open Studio. It includes weather data, solar radiation research, climate visualisation, sunshine hour analysis, thermal comfort, and computational fluid dynamics components.

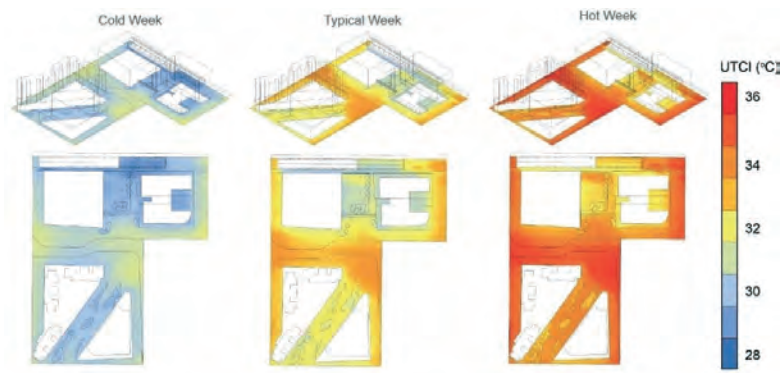


FIG. 3 Radiation simulation in Ladybug, Source: Butterfly

2.2.4 Galapagos

Galapagos is a Grasshopper component capable of optimising a form to best serve a user-defined purpose. Galapagos requires a set of options or genes to test as well as a stated objective or fitness value in order to function.

2.3 METRIC CONSIDERATIONS

Various design tools proposed for the conceptual design of building envelopes are summarised in Figure 4. The proposed framework is based on the methodology described by Saldana Ochoa et al. (2020) and consists of four basic steps: generation, evaluation, clustering, and selection. The entire framework is created utilising the CAD software Rhinoceros (www.rhino3d.com) and the Grasshopper visual scripting environment (www.rhino3d.com). The evaluation of environmental criteria, such as solar radiation and daylight availability, is performed using Ladybug Tools (Roudsari, Pak, & Smith, 2013).

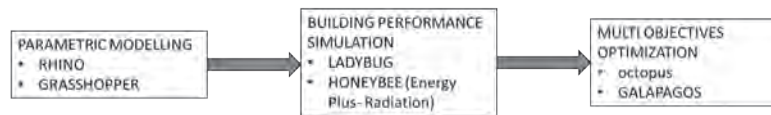


FIG. 4 Different tools integrated into the proposed framework for the conceptual design of building envelopes.

Table 1 shows the parameters and metrics used to describe each design option (form related).

TABLE 1 List of parameters and metrics used to characterise each design option.

SOURCE	PARAMETER/METRIC	LABEL	DESCRIPTION	UNITS
Ladybug	solar radiation reduction	SRR	reduction in percentage of the total amount of solar radiation on a test point without shading elements (SRi) and with shading elements (SRf)	(%)
	daylight factor	DF	ratio between the illuminance at an indoor test point (E) and the illuminance at an outdoor test point (E0)[%]	(%)

2.4 PROPOSED ENERGY-EFFICIENT BUILDING WORKFLOW METHODOLOGY

A proposed design approach is developed by using daylight and thermal simulation in the early stage of design by combining parametric modelling with MOEAs (Multi-Objective Evolutionary Algorithms). It helps reduce the lifetime energy consumption of the building. (Eleftheria Touloupaki, 2017) Ladybug and Honeybee are taken as the primarily driven tool for conceptual design. It enhances the potential of using parametric tools in the architecture design process to achieve specific daylight and thermal quality. If existing nZEB design procedures are followed, the resulting solutions can be further optimised by employing the proposed workflow methodology. (S. Attia, 2011)

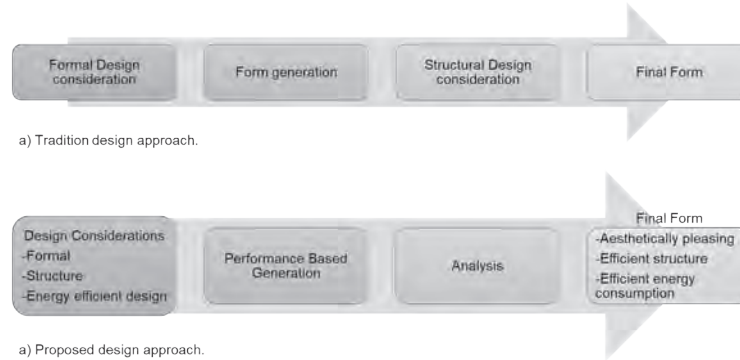


FIG. 5 Conceptual design approach

2.4.1 Stage 1: Parametrisation

The architect may make decisions about the building's features, which may have an impact on the thermal properties of the building, such as:

- Form and general layout, and orientation of built
- The thermal properties and material thickness (walls, roof, floor, windows, etc.)
- The location and size of openings
- Shading elements
- The rate of air ventilation
- Internal partition characteristics
- Electronic and mechanical systems (heating, cooling, etc.)

The architect can define rules relating the chosen parameters and other standard building constraints (surface area, number of levels, etc.) to geometry inside the Grasshopper interface, which is hosted in Rhinoceros 3D, to create an initial population of design options that will initiate to the "breeding" process. (T. Ostergard, 2016)

2.4.2 Building performance simulation

Building optimisation techniques, according to Ostergard et al., generally consist of six different phases that can be performed iteratively:

- Determine the genomes and limitations.
- Choosing a simulation software and developing a base 3D model
- Objective function(s) selection.
- Algorithm selection for optimisation

- Carry out simulations till the optimisation convergence is reached.
- Data interpretation and presentation

Ladybug and Honeybee for Grasshopper are two software tools that can be used for linking parametric models to energy and other variables.

2.4.3 Multi-objective optimisation

Using genetic algorithm processors like the Galapagos Evolutionary Solver (Grasshopper plugin) and the Darwinian theory of evolution creates design options.

Energy performance analysis is performed on parametric models complementing structural analysis, resulting in substantially faster performance-based research. According to the proposed technique, the architect will be able to select from a number of design possibilities based on their objectives. When implementing this approach to mimic environmental and structural performance, the results are shown using colour coding, allowing all members of the project team to understand the results.

The parameters are defined to fulfil the needs of the users while also obtaining unique and significant project data. This is later defined and comprehended by the relevant specialists before being input into the 3D model. The criteria presented are the product of considerable study and expertise from the collaborating teams, which include the design, research, and planning teams. A large number of designs are generated, and a collection of high-performing designs are given as output. Once the option has been selected, to a few designs, refining will be performed utilising Project Refinery and the R&D team’s knowledge to further improve the design and ensure limitations and criteria are satisfied while keeping engineering thumb rules in mind. The best design solution produced combines human ingenuity with artificial intelligence. Generative Design is the future of architecture because it enables architects to design more efficiently and quickly while also reducing energy consumption.

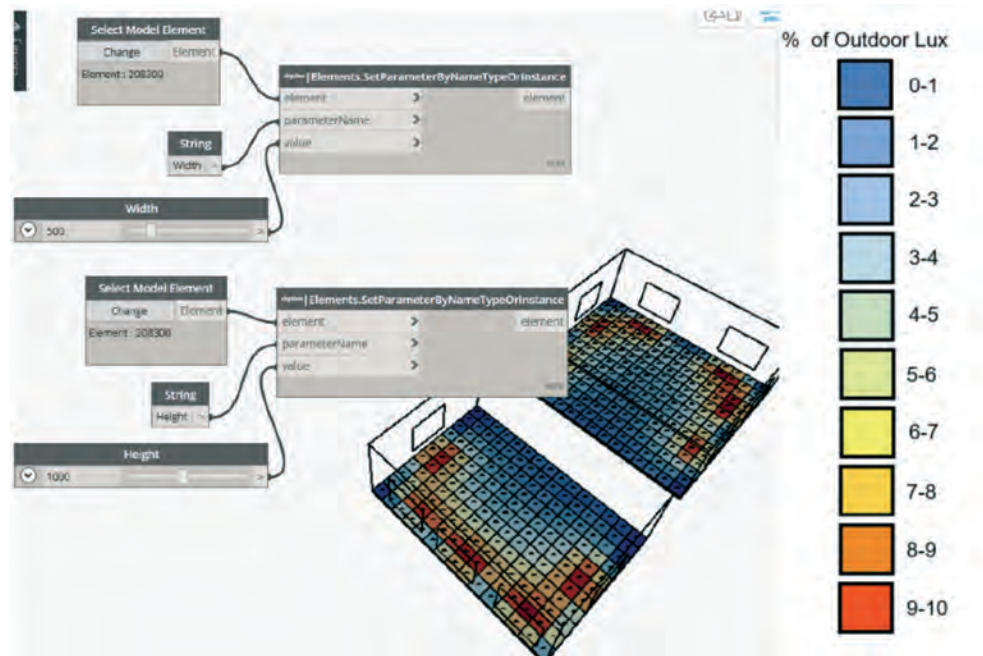


FIG. 6 Multi-objective optimisation application for Lux level

3 EXPERIMENT/RESEARCH

3.1 INTRODUCTION TO THE CASE STUDY

“The Street” building is selected for the experiment and analysis of the generative design process. The selected structure is an 800-room student residence constructed on a 24,000-square-meter lot in Mathura, Uttar Pradesh, India. The architect who designed the structure is Sanjay Puri. The structure is situated in India’s mixed climate zone.

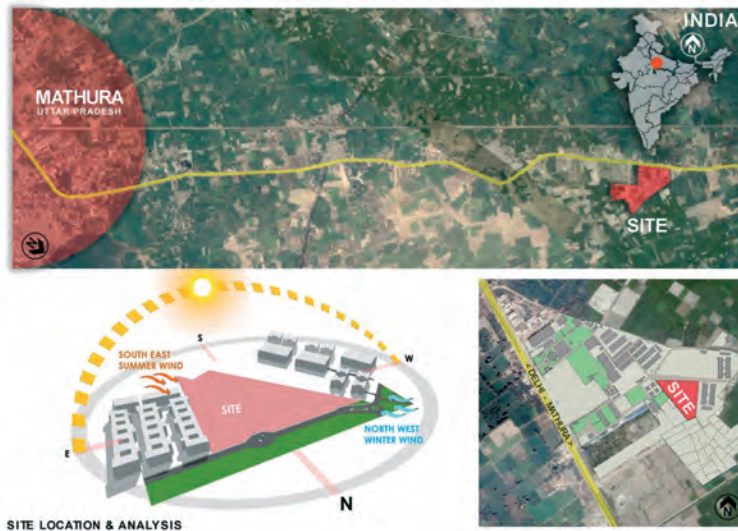


FIG. 7 Site location and analysis, The Street. Source: Sanjay Puri Architects



FIG. 8 Wedge-shaped bay window in the building. North-oriented windows overlooking gardens. Source: Sanjay Puri Architects

This 800-room student hostel draws inspiration from the city streets of Mathura, India, where this project is located, to create organic spaces. Designed as four-story, five-block linear structures, the created spaces serpentine across a wedge-shaped site, twisting and turning along their length. These new dormitories on a big university campus, close to similar hostel blocks on the east and west, generate distinctive places with a unique identity in each portion of the pattern. In addition, each room in the hostel features a wedge-shaped bay window facing north and the playground.

3.2 UNDERSTANDING LAYOUTS AND FENESTRATION OF THE BUILDING

On a wedge-shaped site comprised of five linear blocks, the building rooms twist and curve along their length. These new forms on a large university campus, situated beside repeating hostel buildings on each side, give individual identities for various places. (2021, The Street, Mathura) The buildings are angled to provide expansive gardens facing north that overlook a vast playground to the north. Each room in the hostel has a wedge-shaped, north-looking bay window and ventilators facing the internal hallway, providing cross ventilation and light throughout the year. At each bend, these structures create small openings that allow natural light to enter the inner circulation spaces.

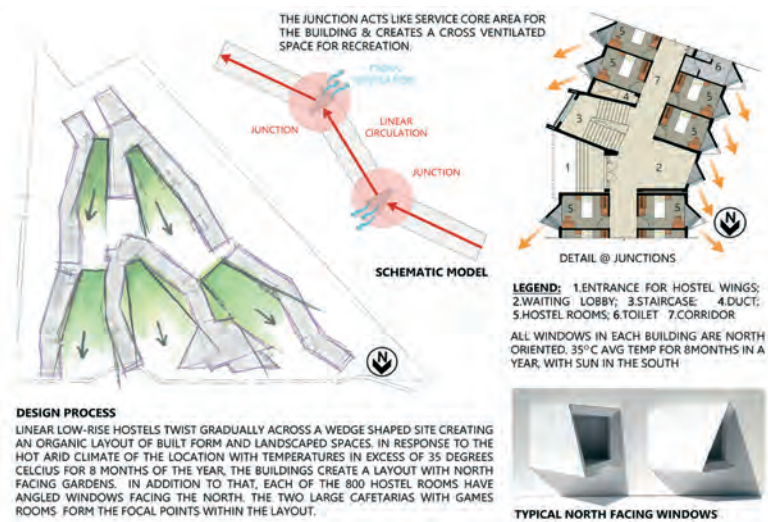


FIG. 9 The Street – Design process. Source: Sanjay Puri Architects

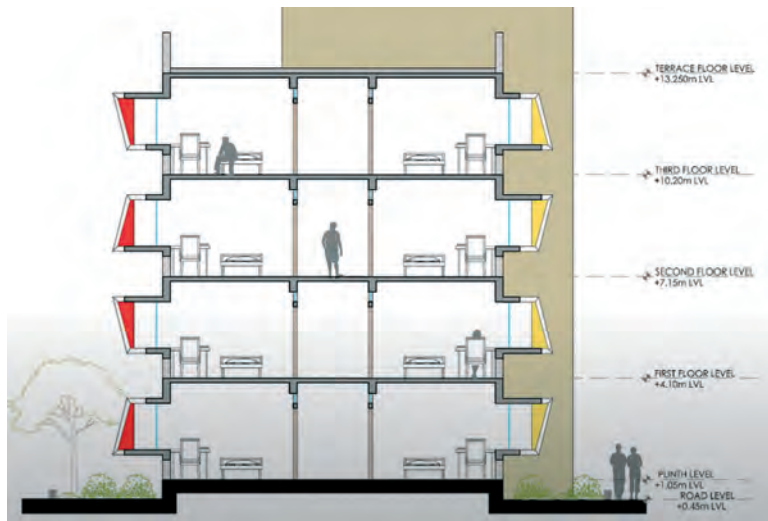


FIG. 10 Typical section through the hostel block, The Street. Source: Sanjay Puri Architect

These variables contribute to an energy-efficient structure that minimises heat absorption in response to the environment, which averages 30 degrees Celsius for eight months of the year when the sun is in the Southern Hemisphere. Cafeterias, game rooms, and gymnasiums are located in two primary spaces built at the buildings' extremities, which open onto gardens and terraces facing north. Each public space has a 20-foot-high ceiling and a substantial capacity. Each block is coloured differently, as are the interior faces of the bay windows, to create a sense of identity.



FIG. 11 The Street - Design process. Source: Sanjay Puri Architects

The site's numerous locations are distinguished by its organic layout, and individual blocks are highlighted by colour. Directing and encouraging natural ventilation, rainwater collection, water recycling, and the installation of solar panels all cut energy consumption. The Street is contextual to the temperature and direction of the site, resulting in diverse experiences and altering ideas of space across the 6-acre site. The architecture of these student dorms incorporates the organic curving pathways of ancient Indian cities, giving each area a personality while orienting all 800 rooms toward north-facing gardens and a playground.



FIG. 12 North-oriented bay windows, The Street - Design process. Source: Sanjay Puri Architects

3.3 EVALUATING THE BUILDING FAÇADE

The building façade model is scripted in Grasshopper software. Firstly, the façade modelled in Grasshopper incorporated window openings of the same size. Then, these windows were randomly sized.

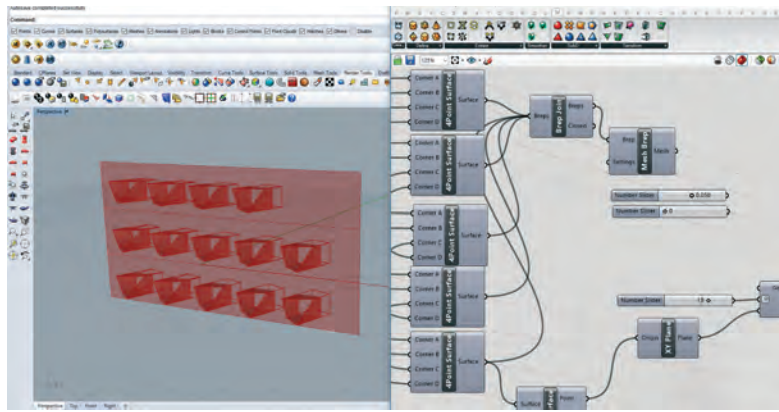


FIG. 13 Scripting of basic façade model in Grasshopper software

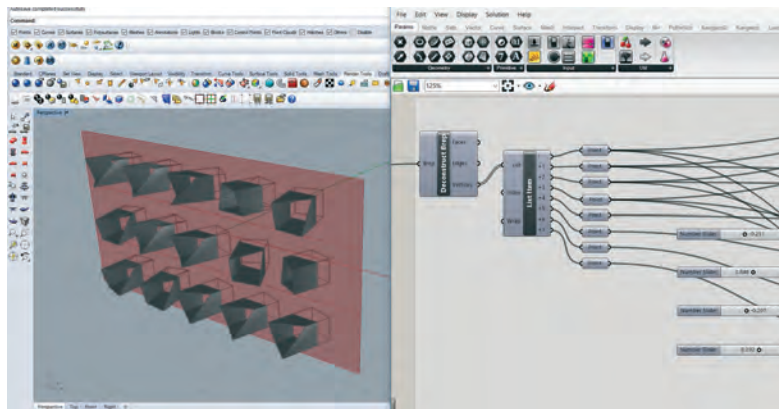


FIG. 14 Randomly sizing the window boxes.

In order to analyse daylight simulation within the fenestrations, a daylight simulation script was modelled using Honeybee software.

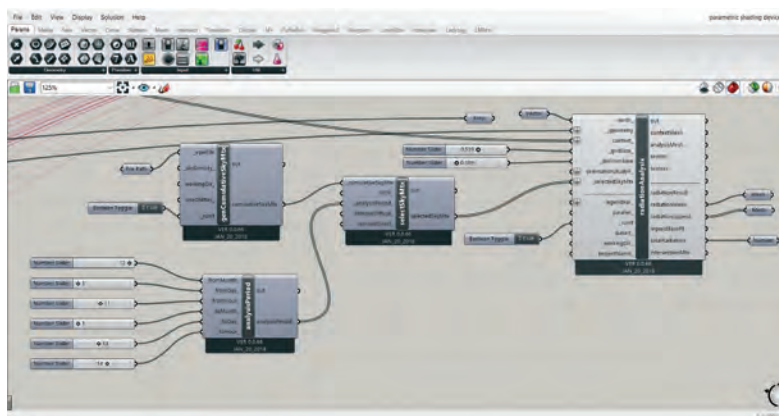


FIG. 15 Rolling daylight simulation on the model using the Ladybug plugin, Honeybee software

Various inputs were set for Radiation Analysis, like Sky Matrix for Mathura (.epw file), North Direction. Analysis Period was specified separately for the summer and winter seasons to avoid overlapping results. May 1 to July 15 was specified for summer. December 1 to January 15 for winter.

3.4 IDENTIFICATION OF VARIABLE (GENOME) TO OPTIMISE THE FAÇADE

The Galapagos Evolutionary Solver for optimisation of form is used.

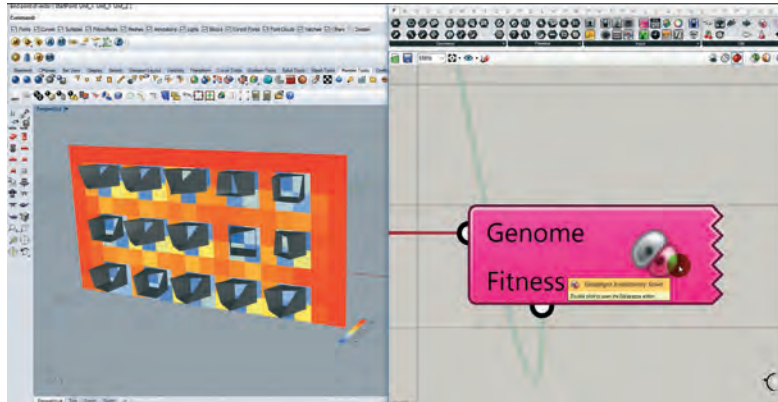


FIG. 16 Using Galapagos Evolutionary Solver for optimisation of form

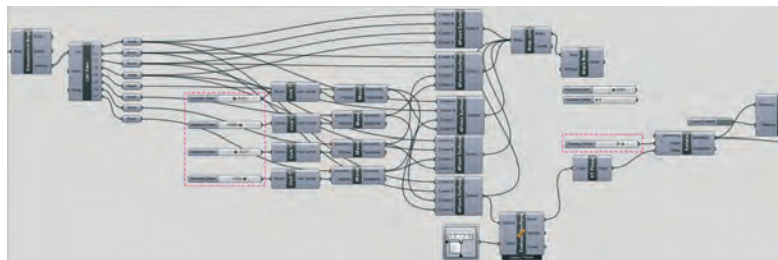


FIG. 17 Genomes are the inputs, where are setting variable that the designer is willing to adjust, to achieve fitness. The fitness is set to minimise solar radiation.

3.5 GENERATION AND EVALUATION OF DESIGN OPTIONS

Various design iterations are made by Galpagos.

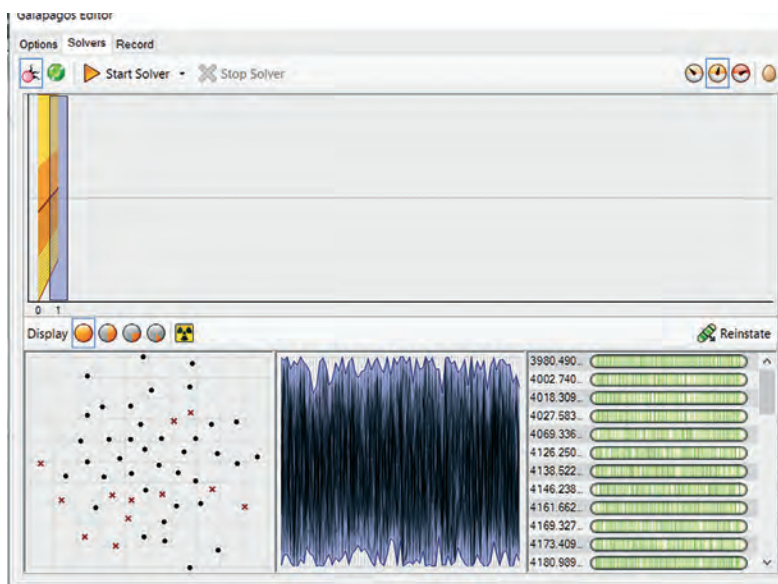


FIG. 18 Various design iterations made by Galpagos.

3.6 RESULTS

Before Energy Simulation, the total radiation on the façade was 4383 kWh/ sqm. Post simulation, the result came out to be 3980 kWh/sqm. There is a 10 % difference in the radiation values.

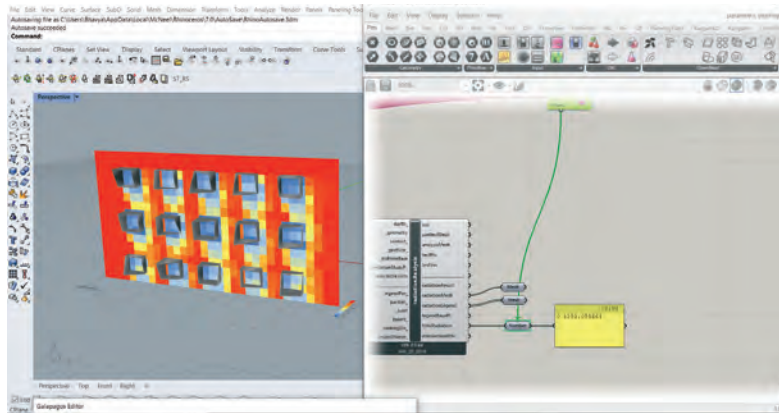


FIG. 19 Pre-simulation radiation -4383 kWh/sqm.

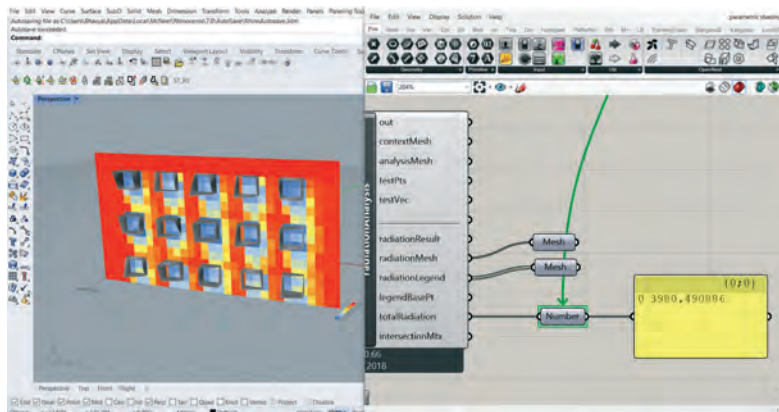


FIG. 20 Post-simulation radiation results -3980 kWh/sqm.

4 CONCLUSION AND FUTURE DIRECTIONS

Manual design explorations frequently exhibit severe constraints due to the limited evaluation capabilities of the designer when dealing with enormous, multi-dimensional design spaces, despite the fact that they provide complete control over the design process. In an effort to combine the advantages of traditional interactive manual explorations with the power of modern computational approaches, this paper examined how generative design techniques could be used in the context of architectural design to aid in creating an energy-efficient building envelope.

It is anticipated that the proposed design method will assist architects and designers in quantifying the energy savings of various façade systems during the early stages of design decisions.

References

- "The Street / Sanjay Puri Architects" 16 Nov 2017. ArchDaily. ISSN 0719-8884 <https://www.archdaily.com/883770/the-street-sanjay-puri-architects>, (2021, 10 18). Retrieved from Rhinoceros 3D: <https://www.rhino3d.com/>
- Attia, S. (2011). State of the Art of Existing Early Design Simulation Tools for Net Zero Energy Buildings: A Comparison of Ten Tools. Université catholique de Louvain, Louvain La Neuve.
- Bertagna, F., D'Acunto, P., Ohlbrock, P. O., & Moosavi, V. (2021). Holistic Design Explorations of Building Envelopes Supported by Machine Learning. *Journal of Facade Design and Engineering*, 9(1), 31–46. <https://doi.org/10.7480/jfde.2021.1.5423>
- Brown, N., Jusiega, V., & Mueller, C. (2020). Implementing data-driven parametric building design with a flexible toolbox. *Automation in Construction*, 118: pp.1-16., <https://doi.org/10.1016/j.autcon.2020.103252>
- Brown, N., & Mueller, C. (2017). Designing with data: Moving beyond the design space catalog. In T. Nagakura, C. Mueller, S. Tibbits, & M. Ibanez (Eds.), *Disciplines and Disruption - Proceedings Catalog of the 37th Annual Conference of the Association for Computer Aided Design in Architecture, ACADIA 2017* (pp. 154-163).
- Catarina Rocha, A. M. (n.d.). Using Generative Design for Evaluating and Improving. Universidade de Lisboa. Retrieved from http://web.ist.utl.pt/antonio.menezes.leitao/ADA/documents/publications_docs/2017_UsingGenerativeDesignForEvaluatingAndImprovingEnergyEfficiencyInArchitecture.pdf
- Eleftheria Touloupaki, T. T. (2017). Energy Performance Optimization as a Generative Design Tool for Nearly Zero Energy Buildings. doi:10.1016/j.proeng.2017.04.278
- Generative_design. (2021, June 22). Retrieved from designingbuildings.: https://www.designingbuildings.co.uk/wiki/Generative_design
- Gigante, M. (2020, January 27). How Generative Design Supports Sustainability. Retrieved from G2: <https://www.g2.com/articles/how-generative-design-supports-sustainability>
- Gigante, M. (2020, January 27). How Generative Design Supports Sustainability. Retrieved May 29, 2022, from <https://www.g2.com/website:https://www.g2.com/articles/how-generative-design-supports-sustainability>
- Grasshopper3d. (2021, 10 18). Retrieved from Grasshopper3d: <http://www.grasshopper3d.com/>
- Harding, J., & Brandt-Olsen, C. (2018). Biomorpher: Interactive evolution for parametric design. *International Journal of Architectural Computing*, 16(2), pp.144–163, <https://doi.org/10.1177%2F1478077118778579>
- IEA. (2021). Buildings A source of enormous untapped efficiency potential. Retrieved from IEA: <https://www.iea.org/topics/buildings>
- Mukkavaara, J. S. M. (2020). Architectural Design Exploration Using Generative Design: Framework Development and Case Study of a Residential Block. Luleå, Sweden. doi:<https://doi.org/10.3390/buildings10110201>
- Pieter de Wilde, M. v. (2004). Providing computational support for the selection of energy saving building components. Netherlands.
- S. Attia, A. D. (2011). Early design simulation tools for net zero energy buildings: a comparison of ten tools design process & tools of NZEBProceedings of Building Simulation.
- Souza, E. (2020, April 23). How Will Generative Design Impact Architecture? | ArchDaily. Retrieved May 29, 2022, from [How Will Generative Design Impact Architecture? website:https://www.archdaily.com/937772/how-will-generative-design-impact-architecture](https://www.archdaily.com/937772/how-will-generative-design-impact-architecture)
- Stainer, J. (2021, June 29). 8 Big Benefits of Generative Design. Retrieved from Insights For Professionals: <https://www.insights-forprofessionals.com/marketing/leadership/8-big-benefits-of-generative-design>
- T. Ostergard, R. J. (2016). Building simulations supporting decision making in early design - A review. *Renew. Sustain Energy Rev.* 61.
- Tian, W. (2013). A review of sensitivity analysis methods in building energy analysis.
- Turrin, M., Von Buelow, P., & Stouffs, R. (2011). Design explorations of performance driven geometry in architectural design using parametric modeling and genetic algorithms. *Advanced Engineering Informatics*. 25(4), 656-675. <https://doi.org/10.1016/j.aei.2011.07.009>
- W. Wang, H. R. (2005). An object-oriented framework for simulation-based green building design optimization with genetic algorithm.
- Wortmann, T., & Schroepfer, T. (2019, April). From optimization to performance-informed design. In *Proceedings of the Symposium on Simulation for Architecture and Urban Design* (pp. 1-8). <https://dl.acm.org/doi/pdf/10.5555/3390098.3390104>
- Yang, D., Ren, S., Turrin, M., Sariyildiz, S., & Sun, Y. (2018). Multi-disciplinary and multi-objective optimization problem re-formulation in computational design exploration: A case of conceptual sports building design. *Automation in Construction*, 92, 242–269. <https://doi.org/10.1016/j.autcon.2018.03.023>

Adaptive Building Skins Inspired by Lizards in the Hot Desert Climate of Egypt

Mina Ishac¹

1 German University in Cairo, New Cairo, +20227589990, mina.ishac@guc.edu.eg

Abstract

The reptile skin has long been a source of ingenuity for architects. The Animalia Kingdom of lizards is famous for its remarkable behavioural mechanisms in adaptation. Not only does the lizard excel in its behavioural adaptation to physical habitat, but its micro-architectural skin also reveals genius intricate capacities with adaptive capabilities evolved by natural selection to live in severe hot desert places. The diverse variations of microornamentations in the dorsal skin of lizards appear to enrich their adaptability in the hot desert climate. Numerous adaptation mechanisms are documented in literature, some exerted by lizards. These are on behavioural and microstructure levels, from how skin scales and profiles work together to perform their functions to how light is redirected and scattered on convex scales affecting shine and camouflage, to how pits react to dirt adhesion, to how scales minimise their contact surface temperature and area for thermoregulation. This paper aims to provide architects with insights into the extent to which building envelopes can be inspired by the skin morphological and typological mechanisms of Mesalina Lacertid lizards which live in the hot desert of Egypt. This paper will contribute to understanding the mechanics behind the skin rather than mimicking the shape, which arguably can inform us about ingenious unprecedented solutions of skins that are adaptive to local habitats. It can give us answers for improving daylighting and thermoregulation conditions in desert areas, which will arguably mitigate the energy consumption of buildings in Egypt and consequently lessen the impact of climate change. The paper, firstly, reviews the adaptation mechanisms and strategies performed by Mesalina lizards, followed by reviewing various dorsal scale microornamentations from literature. Secondly, skins relevant to the desert habitats will be modelled in Rhino and MATLAB. Then, energy model, thermal comfort and shading simulations are conducted to experiment and evaluate the performance of the resulting skin mechanism in terms of daylighting and shading performance. Thermally insulated walls were found to have the highest capacity in thermal insulation, leading to a significant reduction of energy loads. Further wall variations and shading systems will be studied to comprehensively test the effect of densely packed, woven lattice walls and extruded skin patches on the heat. This furthermore aims to establish a comprehensive performance map to connect all the parameters and their sensitivities affecting thermal comfort, energy, daylighting and shading.

Keywords

Mesalina lizard, bioinspired surface, scale microornamentation, dorsal skin, daylight, shading, adaptation behaviour mechanism, thermoregulation.

1 INTRODUCTION

Reptile skins have long been a source of ingenuity for architects. The Animalia Kingdom of lizards is famous for its remarkable behavioural mechanisms in adaptation. The behavioural and functional capacities lizards developed have emergent properties (Irschick & Higham, 2015), inspiring naturalists, biologists and architects.

The climate has an impact on the architecture and materials of buildings. Buildings in hot climates are designed to sustain very high desert temperatures, which is different from designing buildings for colder climates. Thus, the adaptation of architecture to various climates is of significant importance when designing long-living buildings. Natural selection forms the boundary conditions based on which of our design conditions parameters will vary to adapt from one place to another. This has affected the kingdom of Animalia for billions of years, making them excellent survivors to study outstanding behavioural changes in their movements and the composition of their skins.

Decades ago, buildings in hot zones had begun to promote the use of glass in the entire building envelope as an expression of modernism. This approach goes against the norms of building with local materials in the Egyptian architectural context and defies climatic adaptation to the hot desert regions, producing architecture without identity to the context and climate. Thus, the paper unfolds the questions of the locality of architecture in the Egyptian context and climatic adaptability to desert environments. The fundamental question is whether we can design and reach a performative building envelope which closely adapts to the aridity of hot environments of Egyptian deserts as the lizard does. Furthermore, the paper provides architects with insights into the extent to which building envelopes can be inspired by the skin morphological and typological mechanisms of *Mesalina Lacertid* lizards which live in the hot desert of Egypt. This paper will contribute to understanding the mechanics behind the skin rather than mimicking the shape, which arguably can inform us about ingenious unprecedented solutions for skins that are adaptive to local habitats. This, furthermore, can give us answers for improving daylighting and thermoregulation conditions in desert areas, which will arguably mitigate the energy consumption of buildings in Egypt and consequently lessen the impact of climate change.

1.1 EGYPTIAN DESERT AND HERPETOFAUNA

In the Köppen climatic zones, Egypt is classified as a hot arid desert climate zone (Peel, Finalyson, & McMahon, 2007), featuring at least 118 species of herpetofauna which enriches the biological diversity of the country. Reptiles live and adapt in the arid desert environment in large parts of Egypt's western desert, which accounts for up to 90% of the Egyptian territory (Baha El Din, 2006).

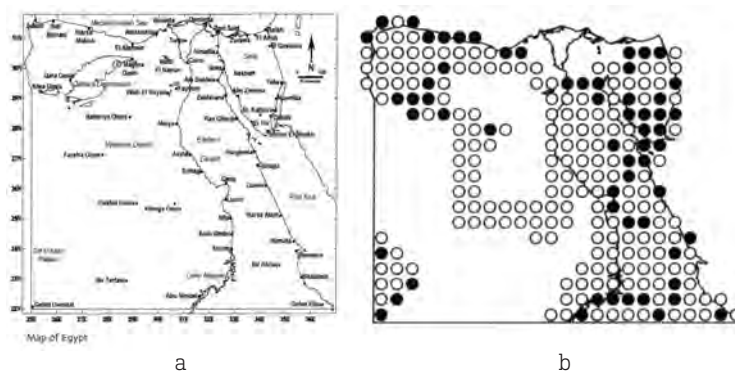


FIG. 1 a) Map of the western desert in Egypt, b) *M. Guttulata* current and predicted existence throughout Egypt, (Baha El Din, 2006)

The western desert region is characterised by infrequent annual precipitation of less than 3 mm and mean temperatures of 9.5°C-41.8°C (Goodman & Meininger, 1989). The paper will study lizards living in the western desert since it occupies two thirds of the country's area, and thus represents a wide spectrum of the city's desertic nature (Figure 1).

1.2 DESERT ARCHITECTURE

The architecture of desert buildings follows specific requirements, as documented in the literature and climate consultant strategies. In the hot season, buildings should minimise internal heat gains and control solar radiation in the daytime. This can be achieved by shading systems and at night by maximising heat loss by expelling heat to the outside, which makes ventilation necessary. Whereas in the cold season, buildings should maximise heat gains in the daytime and minimise heat loss at night by thermal storage. According to the Egyptian code, window-to-wall ratios of up to 30% or larger are normalised in all directions, except for east and west, where a maximum window area of 30% is allowed (ECP 306-2 2005). A south opening is preferred as it can be easily shaded using projections, overhang, or recessed parts of the building.

Thermal insulation on the outside with large thermal mass in the inside layers of the wall is advisable (Gut & Ackerknecht, 1993). Buildings are formed in a way to induce air movement in summer and retain heat in winter. Thick walls are used for large thermal mass to shift the high temperature in the daytime and for the movement of air to the outside at night by ventilation (Kamel & Ibrahim, 2004).

Compact building types in close proximity, with small surface-to-volume areas and narrow urban fabric and structure, resist the desert climate. This proximity minimises exposure to harsh outdoor conditions, and the ratio of the surface area to volume is correlated with the magnitude of heat transfer in the building (Nayak & Prajapati, 2006) (Eltrapolsi, 2016). During summer, east and west-facing façades receive the most radiation; thus, openings to east and west should be minimised as much as possible. Buildings with courtyards benefit from being shaded on all sides by the building itself. The glazing percentage and orientation influence the energy requirements of cooling by up to 30%. External shading reduces the cooling demand by 20%, reducing the g-value of glass from 0.3 to 0.20 reduces the cooling demand by 10%, and 5 cm insulation layer and reduced glazing reduces the cooling demand by 10% (Hausladen, Liedl, & Saldanha, 2012).

1.3 ARCHITECTURAL WORKS INSPIRED BY THE LIZARD

The literature contained few architectural works inspired by the lizard. Some works attempted to translate lessons learnt from side-blotched lizards into architecture by designing a pavilion with an envelope which uses a smart solar tracking system and is actuated by a hydraulic system in SCALES prototype (Mazzoleni, 2013).

1.4 LACERTIDAE – ANIMALIA KINGDOM

Lizards are ectotherms that rely on a suit of behavioural strategies to maintain an optimal body temperature (Bels & Russell, 2019) and thus depend on external heat sources to maintain their body temperature rather than on metabolically generated heat. The external sources of heat could be solar radiation, and conductive heat transfer from the substrate. As a result, lizards thermoregulate primarily through behaviours such as basking, postural changes, and shuttling, which alter heat transfer from or to the environment.

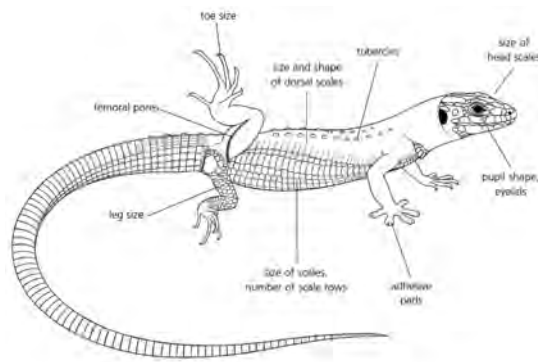


FIG. 2 Lizard parts (adapted from Speybroeck, Beukema, Bok, Van Der Voort, & Velikov, 2016)

1.4.1 *Mesalina Guttulata* Lacertid – class and type of lizard

In the Squamata of Lacertidae, from the genus class of *Mesalina*, which widely inhabits the North Africa Sahara region, the *Mesalina Guttulata* (Lichtenstein 1823) lizard endemics throughout the whole Egypt region, and especially in the El Kharga Desert (Figure 1). *Mesalina Guttulata* is a small, slender lizard with a long, narrow and light brown-grey body, with body and tail lengths of 78.3 and 31.8 mm, respectively. The dorsal part has light and dark spots, and is thus called spotted, the spots forming a pattern, while the ventral part is whitish (AbuKashawa & Mahmoud, 2015) and wider than the dorsal (Baha El Din, 2006). The dorsals contain very small granular or subimbricate (slightly overlapping) scales, which may be the reason for reducing heat loss (Hellmich, 1951). Under a scanning electron microscope, the scales appear to have minute pits on the outer surface of the scale (Abdel-Hady, El-Amir, Al-Muttri, & El-Hariri, 2021). Figure 3 (a and b) shows photographs taken of the dorsa of *Mesalina Guttulata*.



FIG. 3 Desert *Lacerta Mesalina Guttulata*. Left photo taken by Boerekamps (2021), right photo taken by Moser (2017)

On the other hand, keeled scales on the dorsum of other species go along with lizards living in more humid environments; they reduce shininess and improve camouflage (Keeled scales, n.d.) and are highly associated with off-ground locomotion capacity. It is outstanding how the lizard develops different scale types and patterns in different areas of its body independently from each other (Arnold, 2002). This paper aims to study the dorsum part of *M. Guttulata* as it is the part that is exposed to the sun and weather in the hot desert.

M. Guttulata is diurnal (Baha El Din, 2006) and can survive the extreme desert and semi-desert regions with various terrains; it prefers hard substrates and scattered rocks (Volynchik, 2014). A link has been proven which affects the spatial variation of species and links the morphology of species to the unique environments they inhabit, which emphasises the significance of the precipitation factor in deserts and the temperature factor in Mediterranean regions. Thus, precipitation is of more impact on the morphological development of lizards in desert habitats. According to the study of Volynchik

(2014), precipitation mostly contributes to hot dry habitats and better correlates with body size than temperature. Thus, the behavioural component of thermoregulation on lizard phenotype is of higher importance than temperature. Aubret et al. (2004) stated that the morphology of animals was well matched to their habitats' conditions; thus, a hypothesis merged that the micromorphology of the lizard surface appears to mimic the topography of the habitat where they live (Allam, Abo-Eleneen, & Othman, 2017). Similarly, other studies revealed the same conclusion that the dorsum design of the lizard (patterning and colouration) is the product which closely matches the spectral properties of the substrate to blend in the environment (Bels & Russell, 2019), and the skin is correlated with the aridity of the habitat (Dmi'el, 2001).

Numerous adaptation mechanisms are exerted by lizards, irrespective of a specific lizard type, on two adaptational levels: behavioural and microstructural. To the best of the author's knowledge, it needs to be noted that the body of literature still lacks a comprehensive understanding of the minute details of these behaviours. Also, the existing literature is full of differences between several classes of lizards. These were summarised to best match the common characteristics of the desert lizard in the North Africa region to extract architectural analogy lessons.

1.5 BEHAVIOURAL ADAPTATION MECHANISMS (ON BODY'S SCALE)

M. Guttulata living at higher altitudes in the South of Egypt survive higher temperatures than those in lower regions. They have darker and more patterned, striate skins than those living in lower desert areas (Baha El Din, 2006). It can therefore be concluded that dark skin colour is a mechanism to absorb more heat than light-coloured skin (Pianka & Vitt, 2003).

The evolution and adaptation of lizards in the environment are influenced by abiotic and biotic constraints imposed on the animal. The abiotic factors are temperature and humidity. Both of these represent the homeostatic system of the lizard with conflicting requirements that suggest a trade-off adapted by different species depending on the environment. While the biotic is the presence of predators and prey (Bels & Russell, 2019). In arid desert environments, natural selection might favour smaller-sized individuals, which readjust their body temperature, have better thermoregulatory capacity, and develop skin surfaces which limit water loss, exerting higher levels of activity. Thus, thermoregulation is achieved behaviourally by the lizard. Unlike in the Arboreal environment, evolved skins have the capability to exhibit increased adhesive forces. Table 1 outlines how the skin is developed in dry and moist habitats.

TABLE 1 Skin development of lizards in dry and moist habitats

DRY HABITAT	MOIST HABITAT
High friction, matte, rough surface	Low friction, smooth surface for locomotion and dirt shedding
Reduced shine, low reflection for camouflage	Increased shine, high reflection
Develops skin which limits water loss (adhesion is not a problem, no adhesion needed)	Develop skin with adhesive forces, (adhesion is a problem and requirement in that habitat)
Exhibit adaptation mechanics to shade and shelter from the sun to regulate their internal body temperature	Shade and shelter by vegetation in temperate climates
Adhesion is not a problem, pitted surfaces can hold dirt, pits are not associated with large scales	Less or no pitting

1.5.1 Variation of body size vs latitude – Bergmann's Rule

As a behavioural adaptation mechanism, small and large animals developed strategies to protect their bodies from the heat or cold conditions governed by Bergmann and Allen's rules, coming into play where they expressed the bodily dimensions and variation in external morphology of animals with response to the latitude. They expressed the relationship between body size/shape and environmental temperature. The rules state that the heat-producing volume of an animal is proportional to the length of the body cube, the (heat exchanging) skin only squared, which explains why desert animals develop forms with more heat-exchanging surface area in proportion to volume, unlike arctic animals, which are large and develop thicker insulating fur layers (Pohl & Nachtigall, 2015). As we go north or south of the equator, the body size changes as a response to the temperature gradients. Reduced surface area-to-volume ratio provides better heat retention. In cooler climates, large and heavier endothermic bodies with a low body surface area to volume ratio have greater thermal inertia and retain body heat better than smaller bodies. Animals in cold climates tend to have shorter, protruding body parts and darker colours to minimise heat loss, while larger limbs appear in hot countries (needs parah. (Volynchik, 2014). Animals in hot climates have smaller bodies, larger limbs, and less thermal inertia that would facilitate the easy exchange and loss of heat. Therefore, they move more and faster, unlike lizards dwelling in cooler and moister climates (Hellmich, 1951). Behavioural thermoregulation with physiological adaptations enhances thermoregulation and the preferred body temperature of lizards (Bels & Russell, 2019).

Lizards perform one of two strategies (in a suite of behavioural attributes) to attain and maintain body temperature within a preferred range: 1) seek external heat sources or 2) shelter from heat sources. Lizards move, orient themselves and readjust their bodies perpendicular to the sun when heat is needed in the cold season and face towards the sun or away from the sun when they begin overheating to minimise body surface area exposed to solar radiation. They capture the morning sun rays. When it gets excessively hot in the afternoon, they bury themselves in deep and cool burrows. Sometimes, they lift their four legs to keep them away from the ground to reduce contact with the hot earth. Based on the literature, adaptation mechanisms and strategies performed by lizards are outlined in Table 2.

TABLE 2 Adaptation mechanism and strategies of lizards on behavioural level from literature

ADAPTATIVE BEHAVIORAL / PHYSIOLOGICAL MECHANISM	LITERATURE REFERENCE
Microhabitat selection, shuttling between sun and shade, basking in the sun, orientation and posture, gaping, digging in burrows, ventilatory behaviour, cardiovascular adjustments, cutaneous reflectance adjustment, hydration, cryptic dorsal colouration, hydroregulation, skin resistance	Bels and Russell, 2019; Bereiter-Hahn, Matoltsy, Richards, 1986
Change to darker colour in the cold, lighter shade colour and more reflective in the heat known as Thermal Melanism Hypothesis (TMH)	Carey 1978; Cole 1943; Cowles 1958; King, Hauff, and Phillips 1994; Smith et al. 2016a, b
Lizards curl their toes up to cool them off	Pianka and Vitt, 2003
Blotched colouring advantages the camouflage	Mazzoleni, 2013
Bergmann's Rule, variation of body size and parts vs latitude	Pohl and Nachtigall 2015
Skin is darker in higher altitude, dark skin absorbs more heat	Pianka and Vitt, 2003
Episodic shedding in patches	Chang et al. 2009
Sheds the tail when danger threatens	
Blood spitting from edges of eyeballs to deter predators (only the horned lizard Phrynosoma, thorny devil, Arabian toad-headed agama Phrynocephalus arabicus)	Michael Pawlyn 2016
Thermoregulation, capture heat	

ADAPTATIVE BEHAVIORAL / PHYSIOLOGICAL MECHANISM	LITERATURE REFERENCE
Eye-closing behaviour, inactive state, can save water	Lanham et al., 2004; Mathews et al., 2000
Inactive state in burrows	Bulova, 2002
Obtain water moisture from the food	Mark O'Shea 2021
Lizard enters into lethargy, isolating itself from the environment	

1.6 MICROSTRUCTURE ADAPTATION MECHANISMS (ON SKIN MICROARCHITECTURE'S SCALE)

The functions of lizards' scales are numerous. Many of the scales function in a complex way that we know remarkably little about. Especially when it comes to understanding how the intraspecific variations appear on the skin surface translates into functional variation, how the minute microornamentation on the scale functions and varies in shape across the whole surface (S. Baeckens et al. 2019).

Many studies sought to explain how the skin of reptiles was developed to respond to adaptational challenges (Chang, et al., 2009). Scales protect the body of a squamate from mechanical abrasion, acting as a tenacious shield in rough terrestrial habitats. They also protect against UV solar radiation and water loss (Wegener, Gartner, & Losos, 2014), provide signalling, camouflage (Arnold, 2002) and thermoregulation, and they absorb moisture from the air to produce water (El-Ghawaby, 2010). They also prevent the loss of water to the external environment (Chang, et al., 2009), aid locomotion (Allam, Abo-Eleneen, & Othman, 2017), prevent UV radiation damage (Chang, 2003; Ringvold, 2003; Chang et al., 2009), develop adaptive structures and sensors (Von Düring and Miller, 1979; Cooper and Greenberg, 1992; Pianka and Vitt, 2003; Landmann, 1986), and are responsible for self-cleaning (O'Shea, 2021). The shapes of dorsal scales range from granular, flat, keeled, smooth, circular, quadrangular, tuberculate to overlapping (Wegener, Gartner, & Losos, 2014), and they are granular in the *M. Guttulata*.

1.6.1 Skin microornamentation

The skin of the lizard is composed of two groups of layers, the epidermis and the dermis. The epidermis is the outer group of layers, which contains the stratum corneum as the outermost layer of the epidermis. The scales of squamates are horny and tough extensions made of keratin in the stratum corneum. The structure of the epidermis consists of Oberhäutchen, β -layer (β -keratin), the meso, α -keratin and the germinal layer, under which the dermis layers are formed. The keratin has been suggested to help reduce evaporative water loss (Bentley and Schmidt-Nielsen, 1966; MacLean, 1985; Eynan and Dmi'el, 1993; Dmi'el et al. 1997; (Baeckens, Wainwright, Weaver, Irschick, & Losos, 2019). Figures 4-5 show the lizard skin layers in the skin renewal process, known as sloughing, and an analogy between human skin and building skin layers, respectively.

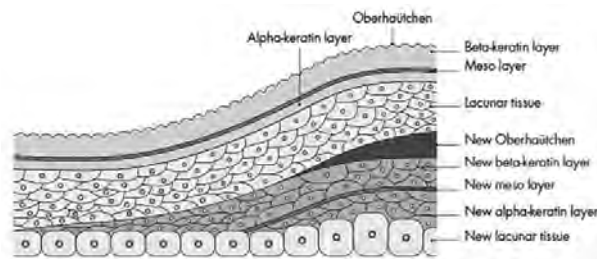


FIG. 4 Sloughing of squamate skin (adapted from O'Shea, 2021)

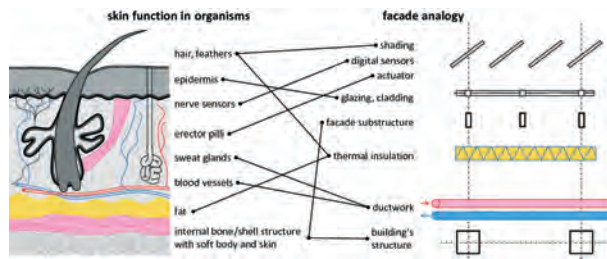


FIG. 5 Human vs building skin analogy (adapted from Sandak, Sandak, Brzezicki, & Kutnar, 2019)

The outermost structure of the squamate scales is known as Oberhäutchen; it covers the β -layer (Irish et al., 1988) and exhibits a complex, microscopical, three-dimensional structure with sensory organs (Leydig, 1873; O'Shea, 2021). The Oberhäutchen and underlying layers may be rucked to produce ridges on the scale's surface (Harvey and Gutberlet, 1995). The structure of the Oberhäutchen and epidermal folding is usually referred to as microornamentation (Ruibal, 1968; Arnold, 2002) or microstructure (Perret and Wuest, 1983; Allam and Abo-Eleneen, 2012; Allam et al., 2017; Allam, E. Abo-Eleneen, and Othman 2017). The β -keratin layer with its proteins is extremely tough and lightweight, increases the mechanical resistance of the epidermis and protects the underlying softer α -keratin layer (Bragulla and Homberger 2009; Lingham-Soliar et al. 2010; Lingham-Soliar and Murugan 2013). Locomotion of the lizard depends on the movement of the body, and thus the skin was developed to allow a certain degree of mechanical flexibility. This is achieved when the harder outer β -keratin layer with the softer inner layer of α -keratin allows the flexibility and stretching of the skin and develops the joints or hinges between the scales. The meso-layer of mucus and α -layer act as a barrier to prevent water loss (Bentley et al., 1966; Davis et al., 1980; Dunson and Mazzotti, 1988; Landmann, 1979, 1986; Landmann et al., 1981; Lillywhite and Maderson, 1982; 2006; Menon et al., 1986, 1996; Lillywhite, 2006). As soon as the epidermal layers of the lizard die and when the body size changes, the old layers are shed, and new epidermal layers are developed in patches in a process known as 'ecdysis'. In dermis layers, 'osteoderms' structures are overlaid to strengthen the scale known as the 'bone-skin', and the cells responsible for colour pigmentation are known as 'Melanophores'. Figure 6 shows the microornamentation of the dorsal scale of the Iguana lizard.

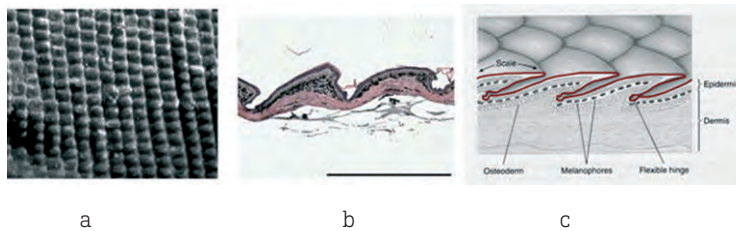


FIG. 6 a, b) Microornamentations and section of dorsal scales of the Iguana lizard (adapted from Chang et al. 2009), c) skin section (adapted from Biocyclopedia 2022)

The microarchitecture of the Oberhäutchen cell showed to be a smooth surface, and when magnified, it showed that it contains an array of pits (0.5 μm in diameter) (Figure 7a). The pits are sensory organs, follicle-like structures which vary in depth, located on the inner surface or hinge area of some scales. In *M. Guttulata*, they are scattered; unlike in other species, they are irregular and densely packed. According to Arnold (2002), the literature's interpretations and hypotheses for the microornamentation functions do not yet explain the structural variation occurring at the microarchitecture levels of the scale. This lack of knowledge has to be investigated, entailing a closer correlation of how the skin microstructure evolves with the environment and the performance advantage of the different patterns. The microarchitecture of the scales performs important functions

in three aspects, which are explained below: properties of light transmission, water preservation, and thermoregulation.

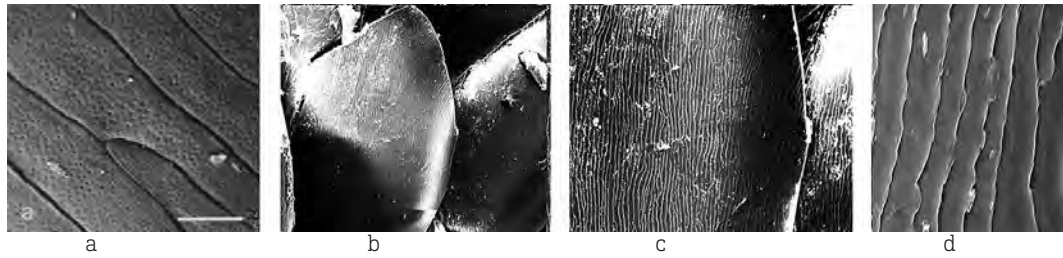


FIG. 7 Microornamentation on dorsal scales of lacertid lizards. a) *Nucras boulengeri* (Arnold, 2002), b-d) *Mesalina Guttulata* (Abdel-Hady, El-Amir, Al-Muttri, & El-Hariri, 2021)

1.6.2 Reflection of light and heat

The skin plays an important role in absorbing and reflecting electromagnetic radiation. The study by Porter (1967) suggested that the Oberhäutchen's projections reduce the visible and ultraviolet radiation, which, if it penetrates the skin, may damage the viscera. The refractions within projections are hypothesised to increase the path of radiation passing through the body's skin. The epidermis is highly transparent to the incident light, which permits transmission to the upper dermis. A flat smooth surface, such as in Figure 8, reflects the light coherently off a large continuous area which enlarges the shining area. In contrast, the convex and dished scales scatter light in many directions. Shine will be visible from a very small area of the convex scale which reflects light to the observer or predator at steeper angles of incidence and observation (Arnold 2002). This will cause a discontinuity of bright reflections and reduced shining spots on the skin, and thus improves camouflage. The same study indicated that microornamentation also affects the amount and intensity of shine. It was also noted that the diameter of the very small pits is less than the wavelength of the visible light; thus, pits are not connected to reducing shine (Arnold 2002).

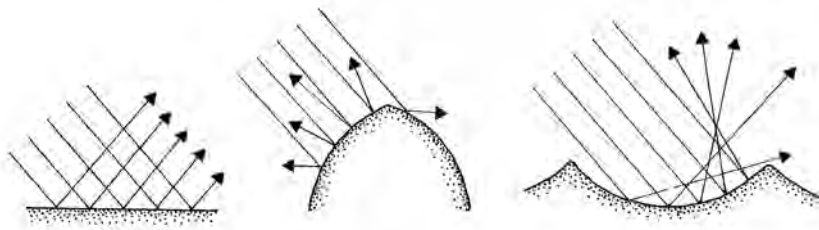


FIG. 8 Effect of microornamentation surface on light diffusion and reflection (Arnold, 2002)

1.6.3 Transport water by capillary action

Some other lizard species than *M. Guttulata*, based on the study of Comanns et al. (2011), were found to have a honeycomb hexagonal structure (Figure 9) in their microornamentation outer surface. This facilitates capillary action and forms a complex capillary system which holds a water film, soaks and transports droplets of water from between the scale to the mouth. It also enhances the condensation of moisture from air compared to non-structured surfaces. Gans et al. (1982) noted similar conclusions for the interscale movement of water. The skin also has the intrinsic property to resist water loss by the epidermal lipids being the main barrier (Dmi'el, 2001; Lillywhite, 2006).

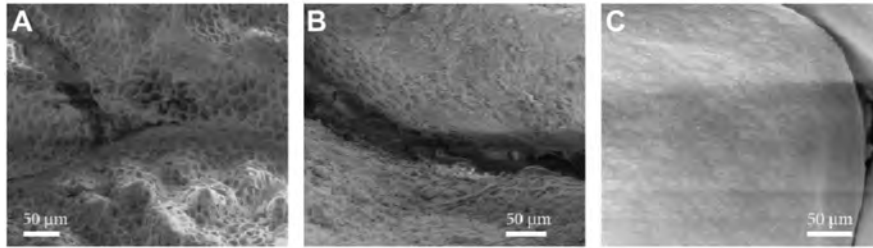


FIG. 9 The hexagonal honeycomb structure evident in the microornamentation of some species (Comanns et al., 2011)

1.6.4 Thermoregulation capacity

All organisms seek a balance in their internal temperature to perform optimal functions (Angilletta, 2009), a process known as thermoregulation. The first step in how lizards regulate their body temperature is choosing a suitable, thermally-preferred habitat. After that, other behavioural control mechanisms exerted by lizards take over, such as gaping or panting, orientation and postural adjustments, and regulation of activities.

Gaping allows the bearded dragon lizard to dissipate body heat. Since lizards do not sweat, this is how they effectively regulate their body temperature. The gaping effort allows evaporative cooling at high temperatures. Also, shuttling mode between moving to shaded or sunny areas happens when they move into either a warm place to heat up or a cooler place to cool off (Health 1970). Posture allows lizards to alter the absorbed heat from the sun or the substrate. Darker skins absorb more heat than light-coloured skins. By rotating towards a preferred orientation, lizards make slight adjustments to body temperature leading to improved comfort (Bartholomew 1966). By facing the sun during morning basking or by lifting parts of their bodies off extremely hot surfaces, lizards minimise the amount of surface area exposed to direct solar radiation and thus reduce overheating (Brain 1962). In the cool periods, they flatten their bodies to increase the surface area exposed to sunlight to absorb more heat (Bartholomew 1966; Cowles and Bogert 1944; Heath 1965). They also exhibit cardiovascular adaptations in maintaining thermal inertia, which was observed in basking to retain the heat at cold times.

1.6.5 Transferred capacities and components: from lizard skin to building envelope

Transferring the adaptations performed by lizards to a building skin would result in a complex façade system, where all capacities should work together and complete each other. Front layers of the façade act as an epidermis controlling light, heat and energy transmitted. And these are backed by the dermis group of layers which act as the backbone of the building skin, holding the façade modules mechanically and structurally and containing thermoregulation capacities. Granular scales in lizards can be transferred to skin modules that can admit natural day-light and self-shade to reduce heat gains without obstructing views. Minute pittings can be integrated into the micro design of these building layers to filter light transmission and reduce glare. Table 3 outlines the attributes extracted from lizards in literature and how each attribute can be interpreted and functionally transferred to the building skin.

TABLE 3 Extracted attributes from lizards and their transfer to building skin capacity

EXTRACTED ATTRIBUTE FROM LIZARDS	TRANSFER TO BUILDING SKIN
Pitting	Can be used to filter and purify direct sunlight to convert direct into indirect light
Granular convex scale	Rigid façade structural wall, brise soleil, self-generating granules, self-adapting

EXTRACTED ATTRIBUTE FROM LIZARDS	TRANSFER TO BUILDING SKIN
Scales subimbricate (minimum overlapping)	Cast shadow on itself, extrusions, to reduce heat gain
Honeycomb hexagonal microstructure	Moves the water by capillarity action
Bones	Structural façade system
Dermis	Support the façade with the building bones/structure, colour pigmentation
Epidermis	Allows flexibility and plasticity, gives mechanical strength, necessary shading and contains evaporative cooling, capillarity capabilities to retain water, contains openings in the façade

2 METHODOLOGY

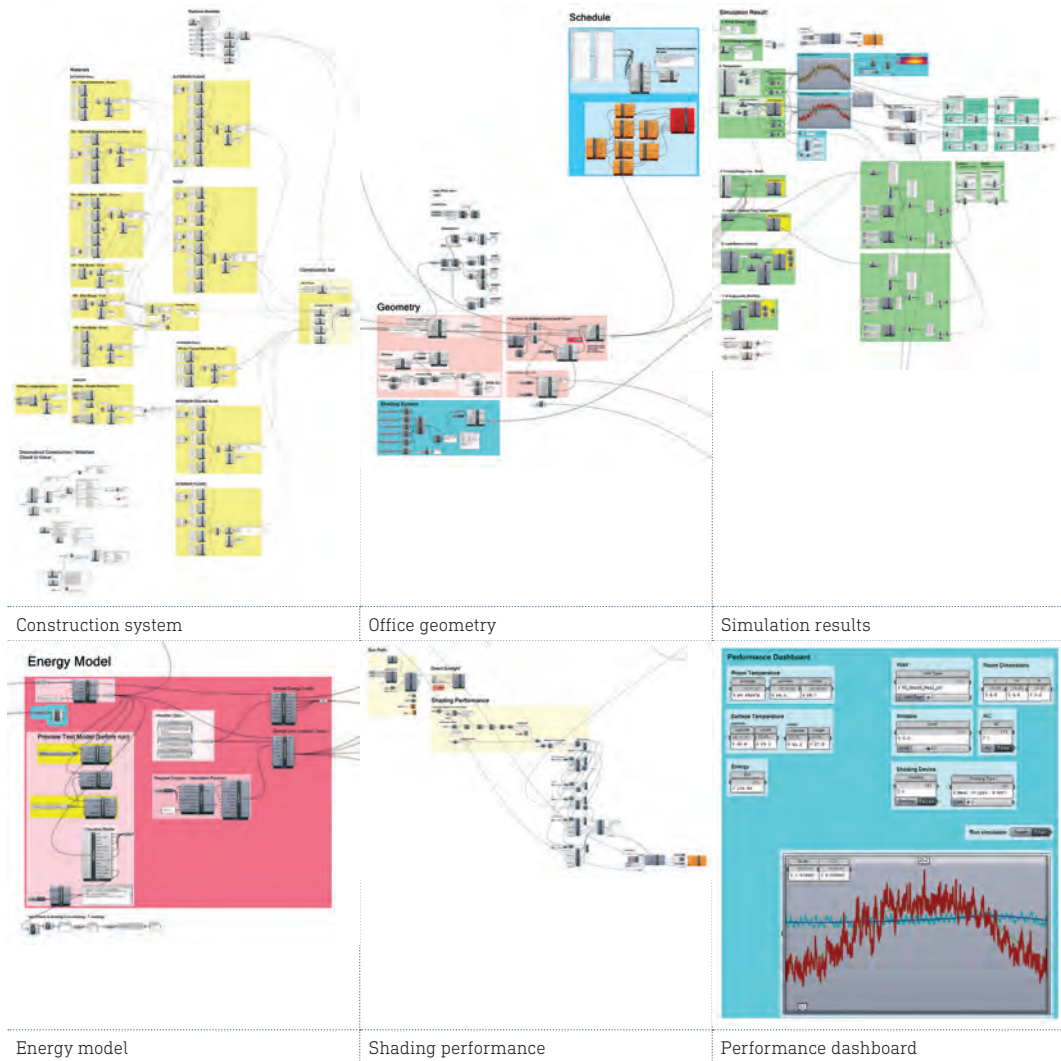


FIG. 10 Parametric model and performance dashboard

The aim of this paper is to reach an optimised building skin that reflects the adaptation to the aridity of the hot Egyptian desert. For this purpose, experimental and quantitative methods will be used to reach the most suitable passive measures that are effective in creating an adaptive envelope. Given the fact that most buildings newly constructed in Egypt are office buildings, promoting the use of excessive amounts of glass in their façades to provide as much light as possible to workers with little awareness of protection from direct sunlight and overheating, the author decided to select an office

activity for the study. The passive measures taken are: 1) changing wall thickness, 2) adding thermal insulation, and 3) adding a shading system.

A dashboard is developed in Grasshopper to parametrically control variables and produce simulation results (Figure 10). A basic office room is modelled parametrically and simulated for thermal comfort, energy, and shading performance. The energy model is simulated in Energy Plus and Open Studio, interfaced on Honeybee and Ladybug in Grasshopper. Firstly, in measuring the comfort, dry bulb and operative temperatures are simulated for each wall. Secondly, the energy model outputs energy loads and use intensity. Finally, the shading areas on the south façade are computed as an average percentage of the year. The data is processed and plotted in MATLAB.

2.1 BASE OFFICE

A typical office room for two workers is employed in the study with dimensions of 6.50 x 4.50 x 3.3 m and a south-facing window with a window-to-wall ratio of 30-50%. According to the Egyptian code, a maximum opening area of 30% is used in the south façade in the southern part of Upper Egypt regions. Workers use the space for eight hours a day, five days per week, starting from Sunday to Thursday. A typical wall construction system is composed of plastered brickwork. Construction layers and simulation cases are elaborated, as shown in Figures 14-15 and Figure 19. The construction of the south façade is the only changing parameter that varies in all simulation cases, while all other building elements are fixed to monitor only the effect of the south window on the performance. Table 4 shows the simulation parameters.

2.2 FAÇADE DEVELOPMENT

The paper aims to develop a conceptual façade system inspired by the lizard's scales (Figure 11).

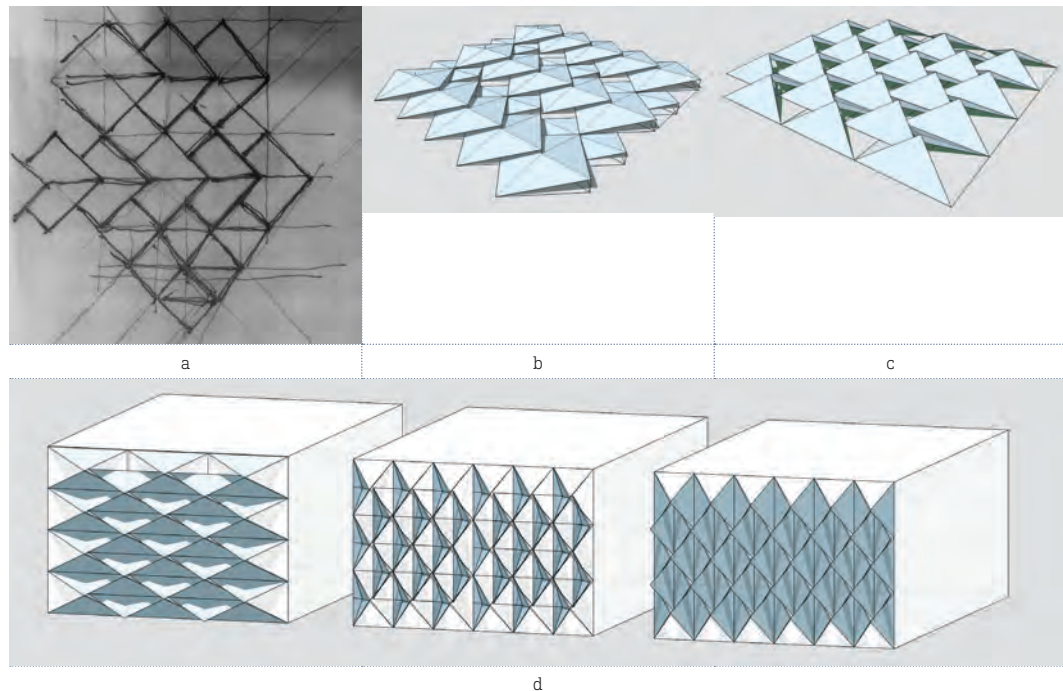


FIG. 11 Facade development (a sketch by author, b and c modelling of overlapping skin, d testing skin of office room)

Scales are a composition of repetitive granulated modules. The relationship between overlapping and sizes of scales is sketched and analysed (Figure 12a), and based hereupon, many skin variations were developed (Figure 19b-d), leading to the design of three prototypes of base unit modules (Figure 12) which were designed following a system of rules. These rules are 1) repetition of the base unit modules, which, when assembled, act as a complex system that protects the building's envelope in an attempt to mimic the repetitive granular scales in lizards, and 2) each base unit module is designed to admit only natural daylight, with an integrated shading brise-soleil system that cuts off critical sunlight angles in summer and winter, maintaining a view which is an important quality in a healthy working environment and opens the outside to the inside. The shading system is a typical horizontal and vertical brise-soleil, with inclinations to wash out the light to the inside to minimise glare. Prototype a has a wider vertical shade element than other prototypes to increase blockage of low sunlight angles, in addition to a continuous horizontal shading element to avoid any admission of direct sunlight (Figure 12). 3) The base module's thickness is around 30 cm which acts as a protective shield increasing thermal mass and delaying the heat transmission to the inside in summer while maintaining a comfortable temperature in winter. 4) Conceptually, within the thickness of each module, a thermoregulation system can also be activated, which can absorb air moisture, and circulate water in thin tubes to cool off the façade. Minute parts inside each module can also be opened to allow for natural ventilation and evaporative cooling.

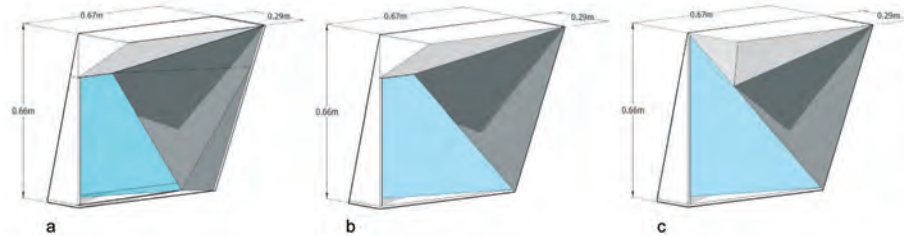


FIG. 12 Development of adaptive base unit module (prototypes a-c, a is the chosen prototype)

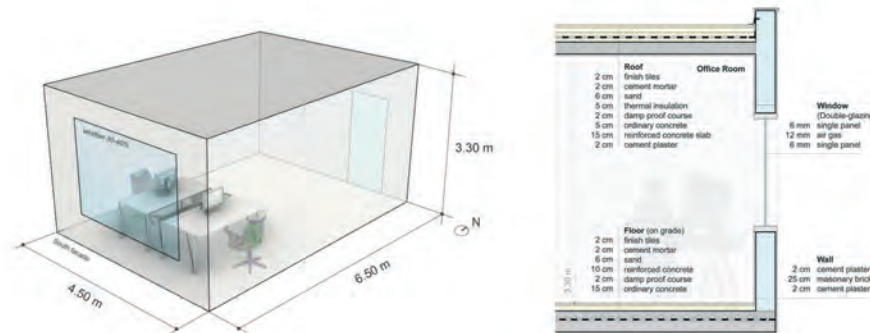


FIG. 13 Base office dimensions and envelope profile section showing construction layers

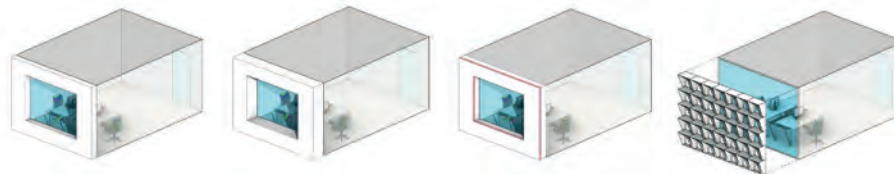


FIG. 14 Simulation cases

TABLE 4 Simulation parameters and boundary conditions

VARIABLE	VALUE
Room Dimensions	6.50 × 4.50 × 3.3 m
Window-to-Wall Ratio	Variable, 30-40%
Window orientation	Fixed, South
Occupancy Schedule	5 days/week, 9 hours (From 8 am-4 pm)
Weather File	El Kharga Desert, Egypt (Lat. 25°)
Typical summer days	21-22 July, 9 hours (8 am-5 pm)
Typical winter days	21-22 January, 9 hours (8 am-5 pm)
Hot month	July
Cold month	January
Boundary conditions	No surfaces were treated as adiabatic – floor is treated as ground.

3 RESULTS

El Kharga desert lies in the western desert of Egypt, which receives higher temperatures than Cairo and lower temperatures than Aswan. Based on the ASHRAE standard 55 model in climate consultant 6.0 (Figure 15), the most effective design strategies used in the El Kharga desert are evaporative cooling at 60% of the year and in Cairo internal heat gains at 33% of the year. Thermal mass and shading impact the design solutions more in El Kharga than in Cairo, with 20% and 12% in thermal mass and 24% and 20% in shading, respectively. Very high temperatures (above 38°C) are observed in Kharga compared to Cairo in summer, and temperatures fluctuate between 27-38°C during the night in summer. The dry bulb temperatures of Cairo, Kharga desert and Aswan are shown in Figure 16. According to the typical weather data, the thermal profile in the Egyptian context shows that the hottest months are July and August, with temperatures of around 33°C, while the cooler months are January and February. Temperature profiles of the base room are shown in Figure 18. The resulting surface temperatures show that the wall with 10 cm insulation (W3) improved thermal comfort in summer, despite the highest difference between the inside and outside temperatures, whereby a significant difference (15° C) between all four walls was noticed.

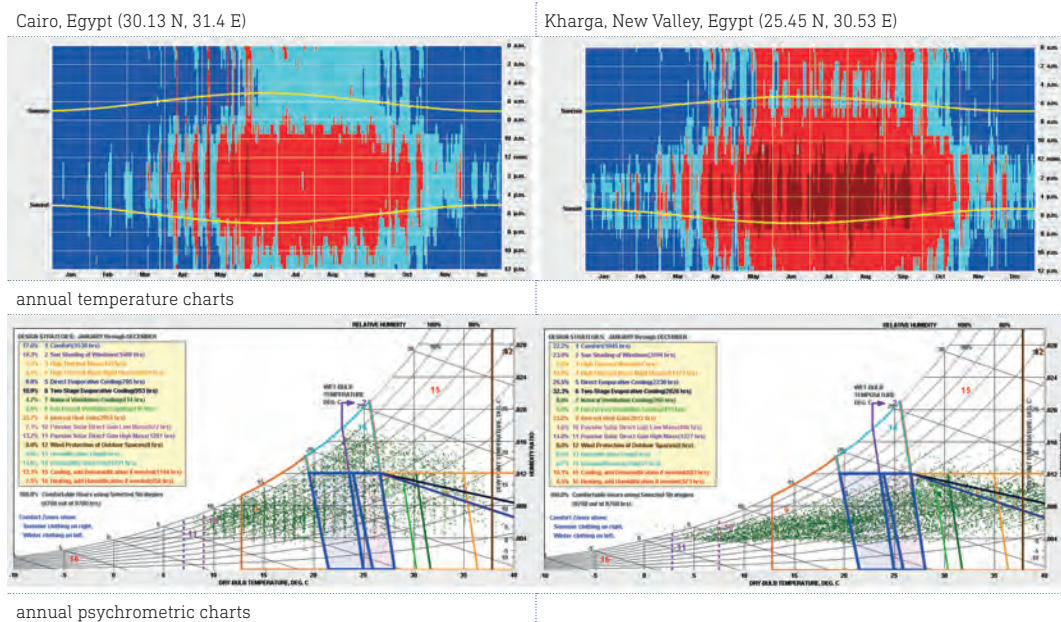


FIG. 15 Annual temperature and psychrometric charts of Cairo and Kharga (Climate Consultant 6.0, Milne & Ligett)

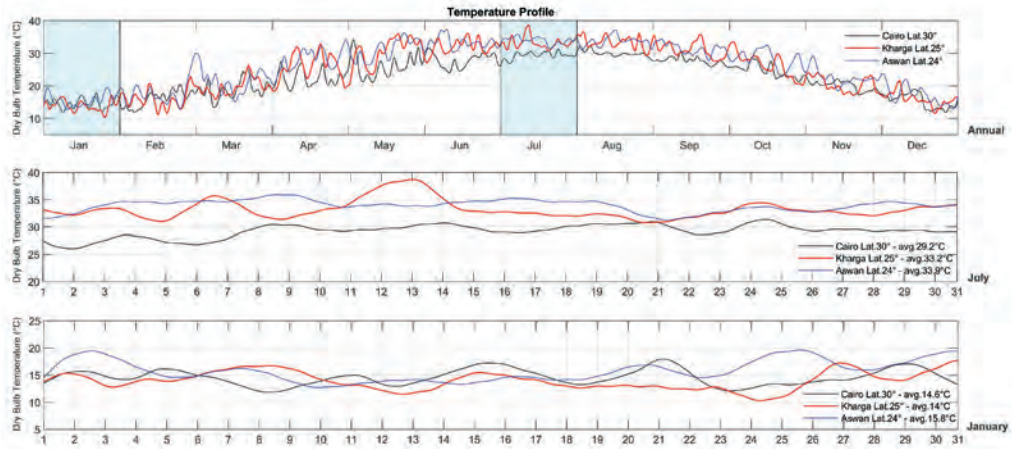


FIG. 16 Dry bulb temperature in Cairo, Kharga and Aswan cities annually and in July, highlighting summer and winter

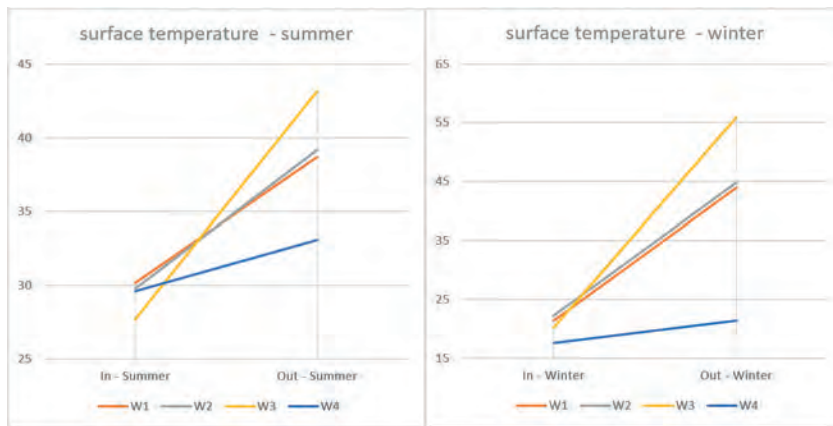


FIG. 17 Surface temperature performance

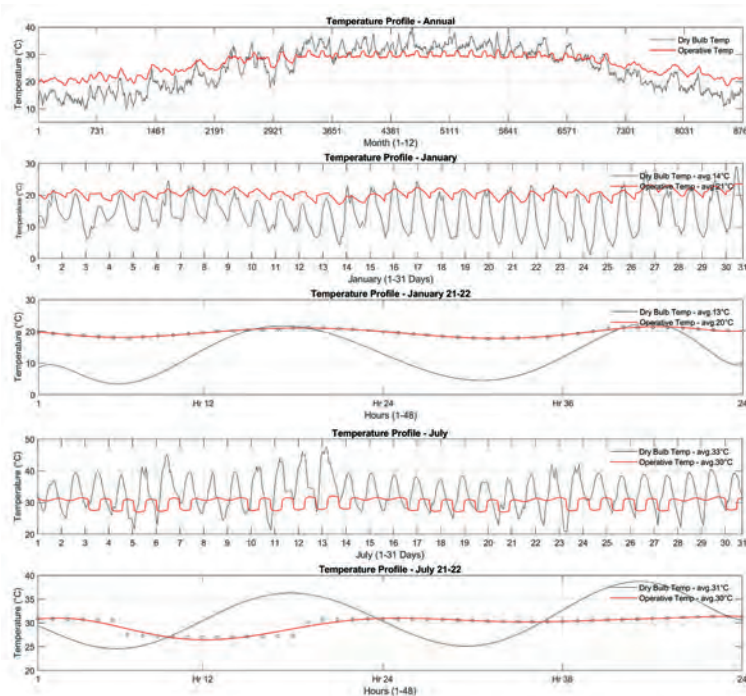


FIG. 18 Temperature profile of base office

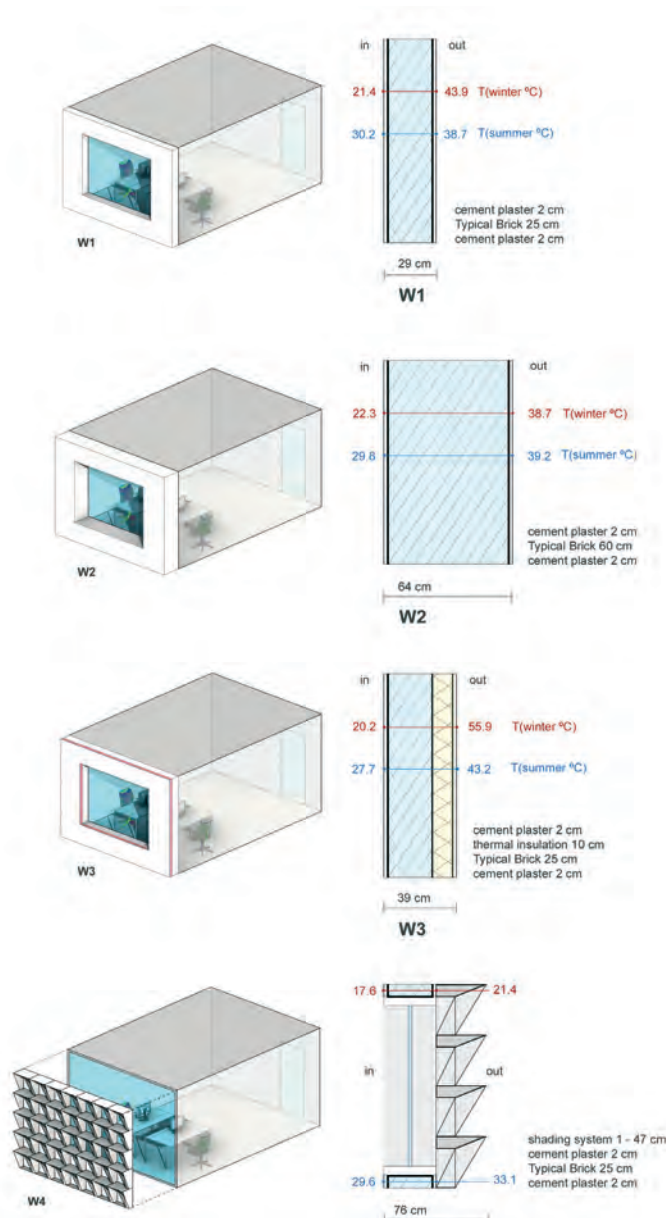


FIG. 19 Wall construction and surface temperature

In winter, Wall 3 also acted as a good thermal barrier insulator against the solar radiation outside. The 60 cm-thick brick of Wall 2 allowed slightly higher containment of heat. Wall 4 proved to have the lowest capacity to insulate the heat. The annual temperature profile and overall envelope performance for all walls are shown in Figures 21-22, respectively. The temperature profiles show that Wall 3 with insulation is an effective strategy that demonstrates the capacity to reduce high temperatures in summer and maintain comfortable conditions in winter. This is followed by Wall 2, the 60 cm-thick brick wall. Wall 3 also reduced the energy use intensity to a minimum of 174 kWh/m², whereas W1, the standard 25 cm brick wall, had the highest energy use. This shows that a little bit of shading fixed on the wall would have an impact on reducing energy use even if the reductions are small. The thicker the walls used in this climate, the more resistant they will be to heat transmission and will, thus, lower energy consumption. Wall 4 outperformed other walls in shading capability achieving 100% shading in summer and 90% in winter (Figure 20).

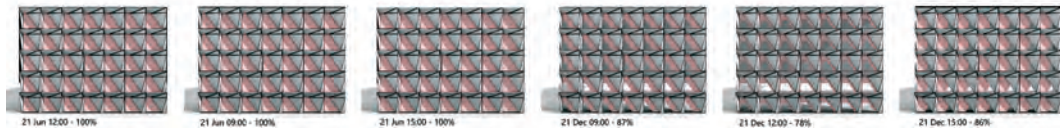


FIG. 20 Parametric shading performance of the developed envelope in summer and winter (pink indicates shaded part)

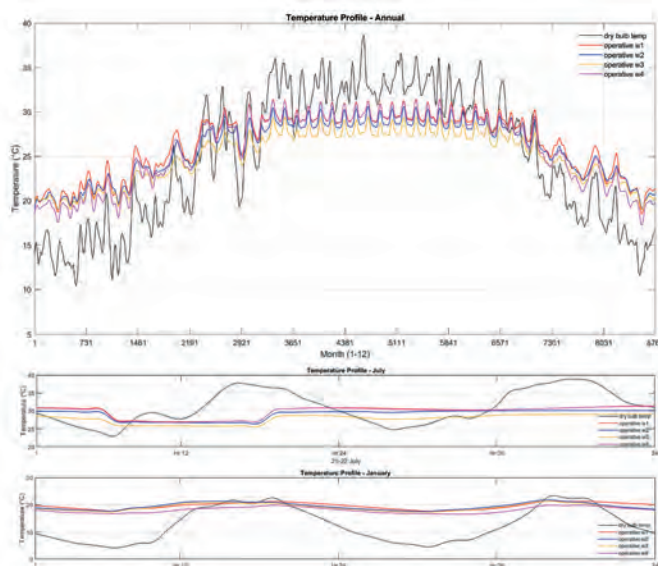


FIG. 21 Dry bulb temperature and operative temperature of all walls

Wall	Window Ratio	Construction South Wall	Shading system	AC	Energy Performance					Shading Performance		Temperature Profile		Summer Day 21st July (8am-5pm)		Winter Day 21st Jan (8am-5pm)	
					Energy Cooling Loads (kWh/m ²)	Energy Heating Loads (kWh/m ²)	Energy Cooling Use (kWh/m ²)	Energy Heating Use (kWh/m ²)	EUI (kWh/m ²)	Summer Shading	Winter Shading	Summer Operative (avg. °T)	Winter Operative (avg. °T)	Inside Temp	Outside Temp	Inside Temp	Outside Temp
Base Room	30%	Typical thick: 29 cm u-value 2.04 w/m ² .k	N/A	Yes	228	3.80	224.51	4.18	290	N/A	N/A	30°C	21°C	30.2	38.7	21.4	43.9
W2	30%	60 brick wall, thick 64 cm. u: 1.13	N/A	Yes	174	3.36	172.25	3.62	238	N/A	N/A	29°C	20°C	29.8	39.2	22.3	44.8
W3	30%	Insulation 10 cm, thick: 39 cm. u: 0.32	N/A	Yes	108	4.3	107.75	4.46	174	N/A	N/A	28°C	20°C	27.7	43.2	20.2	55.9
W4 - Self-shading	43%	Typical thick: 29 cm u-value 2.04 w/m ² .k	Yes	Yes	233	4.15	205.29	8.54	275.6	100% shaded	Avg. of 3 hours (9, 12, 15 on 21st Jan); 90.3%	30°C	19°C	29.6	33.1	17.6	21.4*

FIG. 22 Envelope performance of simulated walls

4 CONCLUSIONS

Reptile skins have a long history of inspiring architects and biologists. The Animalia Kingdom of lizards is remarkably famous for its behavioural and microstructural adaptation mechanisms. This paper outlines the understanding of knowledge in literature to date of the mechanisms and strategies performed by the *Mesalina Guttulata*, which inhabits the El Kharga Desert in Egypt. Various scale microornamentations of lizards' dorsals are reviewed, which arguably can exhibit many functions. However, since many of these functions are not yet proven to correlate with their

adaptation to the habitat, they remain the subject of broad investigation and research. Following the literature, this study conducted parametric simulations for the envelope of four passive measures in a typical office room. This is to evaluate the comfort, energy and shading performance to conclude the most suitable strategy for the hot arid climate of Egypt.

Thermal mass and insulated walls were found to outperform all other strategies in having the highest thermal capacity, leading to reduced energy loads and significantly enhanced indoor comfort. In the desert climate of Egypt, thermal mass was found suitable as a way that impedes heat transmission and overheating during daytime in summer and causes a shift in the heat transfer throughout the day. It shifts the heat to nighttime when it can be expelled by natural ventilation systems.

Further studies are needed to cover other shading systems, for example, woven lattice walls and extruded skin patches, to monitor their impacts on heat transmission. This will also help establish a comprehensive performance network, connecting all parameters with their sensitivities that affect thermal comfort, energy, daylighting and shading. Also, the effect of heat containment by Wall 3 and the lag of heat transmission during nighttime needs to be further investigated.

References

- Abdel-Hady, A. E., El-Amir, S. M., Al-Muttri, N. S., & El-Hariri, H. M. (2021). Scale Microornamentation in Some Lizard Species. *Pakistan Journal of Zoology*, 1-7.
- AbuKashawa, S., & Mahmoud, M. (2015). New Record of the Small-Spotted Lizard, *Mesalina Guttulata* (Lichtenstein, 1823) from Dongonab Bay, Red Sea. *Russian Journal of Herpetology*.
- Allam, A., Abo-Eleneen, R., & Othman, S. (2017). Microstructure of scales in selected lizard species. *Saudi Journal of Biological Sciences*.
- Angilletta, J. M. (2009). *Thermal Adaptation A Theoretical and Empirical Synthesis*. New York: Oxford University Press.
- Arnold, E. N. (2002). History and Function of Scale Microornamentation in Lacertid Lizards. *Journal of Morphology*, 252, 145-169.
- Aubret, F., Shine, R., & Bonnet, X. (2004). Evolutionary biology: adaptive developmental plasticity in snakes. *Nature*.
- Baeckens, S., Wainwright, D. K., Weaver, J. C., Irschick, D. J., & Losos, J. B. (2019). Ontogenetic scaling patterns of lizard skin surface structure as revealed by gel-based stereo-profilometry. *Journal of Anatomy*, 346-356.
- Baha El Din, S. (2006). *A Guide to the Reptiles and Amphibians of Egypt*.
- Bels, V., & Russell, A. (2019). *Behavior of Lizards Evolutionary and Mechanistic Perspectives*. CRC Press.
- Bereiter-Hahn, J., Matoltsy, G., & Richards, S. (1984). *Biology of the Integument: Vertebrates*.
- Boerekamps, J. (2021). iNaturalist.org. Von <https://www.inaturalist.org/photos/168228651> abgerufen
- Bulova, S. (2002). How temperature, humidity, and burrow selection affect evaporative water loss in desert tortoises. *Journal of Thermal Biology*.
- Chang, C., Wu, P., Baker, R. E., Maini, P. K., Alibardi, L., & Chuong, C. (2009). Reptile scale paradigm: Evo-Devo, pattern formation and regeneration. *The International Journal of Developmental Biology*, 813-826.
- Comanns, P., Effertz, C., Hischen, F., Staudt, K., Böhme, W., & Baumgartner, W. (2011). Moisture harvesting and water transport through specialised micro-structures on the integument of lizards. *Beilstein Journal of Nanotechnology*, 204-214.
- Dmi'el, R. (2001). Skin resistance to evaporative water loss in reptiles: a physiological adaptive mechanism to environmental stress or a phylogenetically dictated trait? *Israel Journal of Zoology*.
- ECP-306-2. (2005). *Egyptian Standard Code for Efficient Energy Use in Commercial Buildings*. Housing and Building Research Council HBRC.
- El-Ghawaby, M. (2010). *Biomimicry: A New Approach to Enhance the Efficiency of Natural Ventilation Systems in Hot Climate*. International Seminar Architectonics Network, Architecture and Research. Barcelona.
- Eltrapolsi, A. (2016). *The Efficient Strategy of Passive Cooling Design in Desert Housing: A Case Study in Ghadames, Libya* (PhD Thesis). Von White Rose eTheses Online: <https://etheses.whiterose.ac.uk/12001/> abgerufen
- Fathy, H. (1986). *Natural Energy and Vernacular Architecture: Principles and Examples with Reference to Hot Arid Climates*. United Nations University Press.
- Goodman, S. M., & Meininger, P. L. (1989). *The birds of Egypt*. England: Oxford University Press.
- Gut, P., & Ackerknecht, D. (1993). *Climate Responsive Building: Appropriate Building Construction in Tropical and Subtropical Regions*. Berkeley: SKAT.
- Hausladen, G., Liedl, P., & Saldanha, M. (2012). *Building to Suit the Climate A Handbook*. Birkhauser Architecture.
- Hellmich, W. (1951). On Ecotypic and Autotypic Characters, A Contribution to the Knowledge of the Evolution of the Genus *Iguana* (Iguanidae).
- Hildebrand, M. (1995). *Analysis of Vertebrate Structure* (4th Ausg.). New York: Wiley.
- Irschick, D., & Higham, T. (2015). *Animal Athletes: An Ecological and Evolutionary Approach*.

- Kamel, S., & Ibrahim, M. A. (2004). The Architectural Expression of Local Climate Responsive Building. Von <https://www.cpas-egypt.com/pdf/Dr-Mohamed-Abdel-Baki/Researches/005-THE%20ARCHITECTURAL%20EXPRESSION.pdf> abgerufen
- Keeled scales. (kein Datum). Von https://en.wikipedia.org/wiki/Keeled_scales abgerufen
- Mazzoleni, I. (2013). *Architecture Follows Nature Biomimetic Principles For Innovative Design*. CRC Press.
- Milne, M., & Ligett, R. (kein Datum). *Climate Consultant 6*. Von <https://climate-consultant.informer.com/6.0/> abgerufen
- Moser, V. (2017). iNaturalist.org. Von <https://www.inaturalist.org/observations/8837109> abgerufen
- Nayak, J. K., & Prajapati, J. A. (2006). *Handbook on Energy Conscious Buildings*. Prepared under the interactive R&D Project between IIT, Mumbai and Solar Energy Centre, Ministre of Non-Conventional Energy Sources.
- O'Shea, M. (2021). *Lizards of the World A Guide to Every Family*. Princeton and Oxford: James Evans.
- Pawlyn, M. (2016). *Biomimicry in Architecture*.
- Peel, M. C., Finalyson, B. L., & McMahon, T. A. (2007). Updated World map of the Köppen-Geiger Climate Classification. *Hydrology and Earth System Sciences*, 11, 1633-1644.
- Pianka, E. R., & Vitt, L. J. (2003). *Lizards: Windows to the Evolution of Diversity*. Berkeley Los Angeles London: University of California Press.
- Pohl, G., & Nachtigall, W. (2015). *Biomimetics for architecture & design : nature--analogies--technology*.
- Porter, W. P. (1967). *orgSolar radiation through the Living Body Walls of Vertebrates with Emphasis on Desert Rep-tiles*. *Ecological Monographs*, 273-296.
- Sandak, A., Sandak, J., Brzezicki, M., & Kutnar, A. (2019). *Bio-based Building Skin*. Singapore: Springer.
- Sherbrooke, W. C., Scardino, A. J., Nys, R., & Schwarzkopf, L. (2007). Functional morphology of scale hinges used to transport water: convergent drinking adaptations in desert lizards (*Moloch horridus* and *Phrynosoma cornutum*). *Zoomorphology*, 89-102.
- Speybroeck, J., Beukema, W., Bok, B., Van Der Voort, J., & Velikov, I. (2016). *Field Guide to the Amphibians and Reptiles of Britain and Europe*. Bloomsbury Natural History.
- Volynchik, S. (2014). Climate-Related Variation in Body Dimensions within Four Lacertid Species. *International Journal of Zoology*.
- Wegener, J., Gartner, G., & Losos, J. (2014). Lizard scales in an adaptive radiation: variation in scale number follows climatic and structural habitat diversity in *Anolis* lizards. *Biological Journal of the Linnean Society*.
- Werner, Y. L., & Ashkenazi, S. (2010). Notes on some Egyptian Lacertidae, including a new subspecies of *Mesalina*, involving the Seligmann effect. *Turkish Journal of Zoology*, 123-133.

Influence of Automated Façades on Occupants: A Review

Pedro de la Barra ^{*1}, Alessandra Luna-Navarro ¹, Ulrick Knaack ¹,
Claudio Vásquez ², Alejandro Prieto ²

- * Corresponding author, P.delabarra@tudelft.nl
1 Delft University of Technology, Netherlands
2 Pontificia Universidad Católica de Chile, Chile



Abstract

Several studies performing building simulations showed that the automated control of façades can provide higher levels of indoor environmental quality and lower energy demand in buildings, in comparison to manually controlled scenarios. However, in several case studies with human volunteers, automated controls were found to be disruptive or unsatisfactory for occupants. For instance, automated façades became a source of dissatisfaction for occupants when they did not fulfil individual environmental requirements, did not provide personal control options, or did not correctly integrate occupant preferences with façade operation in energy-efficient controls. This article reviews current evidence from empirical studies with human volunteers to identify the key factors that affect occupant response to automated façades. Only twenty-six studies were found to empirically investigate occupant response to automated façades from 1998 onwards. Among the reviewed studies, five groups of factors were found to influence occupant interaction with automated façades and namely: (1) personal factors, (2) indoor environmental conditions, (3) type of control logic, (4) façade technology, and (5) contextual factors. Overall, occupant response to automated façades is often poorly considered in research studies reviewed because of the following three reasons: (i) the lack of established methods or procedures for assessing occupant response to automated façade controls, (ii) poor understanding of occupant multi-domain comfort preferences in terms of façade operation, (iii) fragmented research landscape, on one hand results are mainly related to similar contextual or climatic conditions, which undermines their applicability to other climates, while on the other hand the lack of replication within the same conditions, which also undermines replicability within the same condition. Lastly, this paper suggests future research directions to achieve a holistic and more comprehensive understanding of occupant response to automated façades, aiming to achieve more user-centric automated façade solutions and advanced control algorithms. In particular, research on the impact of personal factors on occupant satisfaction with automated controls is deemed paramount.

Keywords

Automated control, automated façades, occupant-façade interaction, occupant acceptance, occupant comfort, dynamic façades

DOI 10.47982/jfde.powerskin.2

PART 3 // ENVIRONMENT

Digital Imperfection

Christian Schmitt¹, Federico Garrido², Rodrigo Brum³

- 1 Associate Professor, German University in Cairo, Architecture and Urban Design Program, Department Building Technology and Integrated Design, El Tagamoa El Khames, New Cairo City, Egypt, +20 101 5797127, +41 78 815 94 20, christian.schmitt@guc.edu.eg, christian.schmitt@alltag.org
- 2 Postdoc Researcher at Bau- und Architekturgeschichte, KIT (Karlsruher Institut für Technologie) Kaiserstrasse 215, Karlsruhe, Germany, +49 160 98 40 10 91, federico.garrido@kit.edu, federgarrido@gmail.com
- 3 Lecturer in Film & Media Installation, German University in Cairo, Faculty of Applied Sciences and Art, Media Design Department, El Tagamoa El Khames, New Cairo City, Egypt, +20 102 2780087, +1 312 678 8969, rodrigogratacosbrum@gmail.com

Abstract

Although Europe has seen a recent trend in using and studying earthen building methods, it is in the Global South that these techniques have developed most and achieved widespread use. As a vernacular solution, earthen building methods have evolved over thousands of years. Although these techniques gradually gave way to other construction methods, there are cases where earthen structures were highlighted by modern architectural movements, as is the case of Egypt.

This project aims to reconnect students (and people) with the handmade craft of using earth bricks through digital tools. The bricks made by the students were stacked on a wall with the help of a HoloLens that laid a digital 4-dimensional model over the physical world. Despite the mediation of a digital apparatus, the idea is to engage students or, later, the community in a comprehensive workflow involving handmade production and interactive assembly rather than promoting a mere robotic process and get answers to these questions:

- What does handmade mean?

- How can we incorporate digital technology without losing human interaction?

- How can the 'imperfections' of handmade bricks be part of a calculative digital scheme?

- How can we bring elements of vernacular architecture to new generations through a technology-mediated exercise?

The brick structure was developed with parametric design software that generated a real-time procedure directly streamed to the HoloLens, overlaying a digital 4-dimensional model over the physical world. This parametric procedure told the worker on a field of mixed reality where to pick up the brick and precisely where to place it.

During the assembly process, the height of the bricks was constantly adjusted to account for the thickness of the mortar. This back-and-forth movement was a crucial point of this collaborative project, as the cycle evolved from the inherently unique interference of each participant. Ultimately, the goal of Digital Imperfection was to place humans in the focus of the digital assembly.

Keywords

Earthen, global south, circular, digital imperfection, mixed reality integration, handmade, collective experience

1 INTRODUCTION

Digital Imperfection is a temporary installation made at the German University Cairo, combining mixed-reality tools and handmade earth bricks. The project involved two separate processes that came together during the final assembly procedure; on the one hand, the design of handmade bricks and, on the other hand, the design of a parametric wall and the coding of the assembly procedure on a mixed-reality platform. The objective of the installation was twofold: first, to explore the possible relationships between handmade crafts and digital tools, and second, to design a comprehensive workflow involving design and assembly while taking into account discrepancies and errors in the construction elements, which was expected in compressed earth bricks. Another objective was to showcase the non-traditional digitally generated designs using low-tech materials with a minimum carbon footprint and to encourage the students to experiment with earthen materials.

The wall was designed with parametric design software and, at the same time, generated a real-time procedure that was streamed to the HoloLens device (a mixed reality headset) in the field. The parametric procedure told the user/worker where to pick up the bricks (there were two different brick types) and then where to precisely position them.

The research questions are related to the relationship between high-tech and low-tech tools: how to measure and account for the imperfections in manufacturing the pieces? How to minimize these imperfections within the design and assembly? What are the benefits and opportunities in the combination of low- and high-tech techniques?

The process accounted for the different imperfections and heights (like the mortar thickness and manufacturing differences), sustaining a constant loop with real-time feedback: the physical model was updated with new bricks, while the digital model was updated with the actual heights.

Digital Imperfection places humans in the focus of the digital assembly, not by replacing them with robots or algorithms but by collaboration for mutual benefit. Humans (students in our case) brought their bodies and dexterities, while computers contributed with the organization and precision of the building procedure.

The benefits of the research are multiple: firstly, by introducing students (and a broader academic public) to the use of sustainable materials in combination with parametric design. Secondly, by producing a digitally-designed installation (of relative complexity) without the need for printed documentation and finally, by saving resources because no framework is needed, as the building procedure and instructions are entirely virtual and self-supporting. During the workshop process, many aspects have been considered, such as ecological, economic, social, participative and even material aesthetics. These aspects were key factors in developing a sustainable activity through a new holistic approach.

As a collaborative work between two courses at the GUC (on the topics of sustainable construction and robotic construction), the research intended to combine both core interests in every stage. Regardless of the fact that in the contemporary architectural discourse it is almost impossible to avoid digital technologies, the collaboration also proposed to augment not only the capacities of each sub-discipline but also the perception (and auto-perception) of them by associating low-tech building techniques with high-tech design procedures.

As one of the involved courses was entitled "Introduction to Robotics in Architecture", the intention was to expose students to the most complex tools available for design and construction. Hereby, an interesting aspect is that Mixed Reality (MR) technologies such as Augmented Reality (AR) and

Virtual Reality (VR) are becoming ubiquitous in everyday life (in the form of real-time image and video filters on social media platforms such as Snapchat and Instagram) but that they are somehow not that present in the everyday work of an architecture studio or the building site.

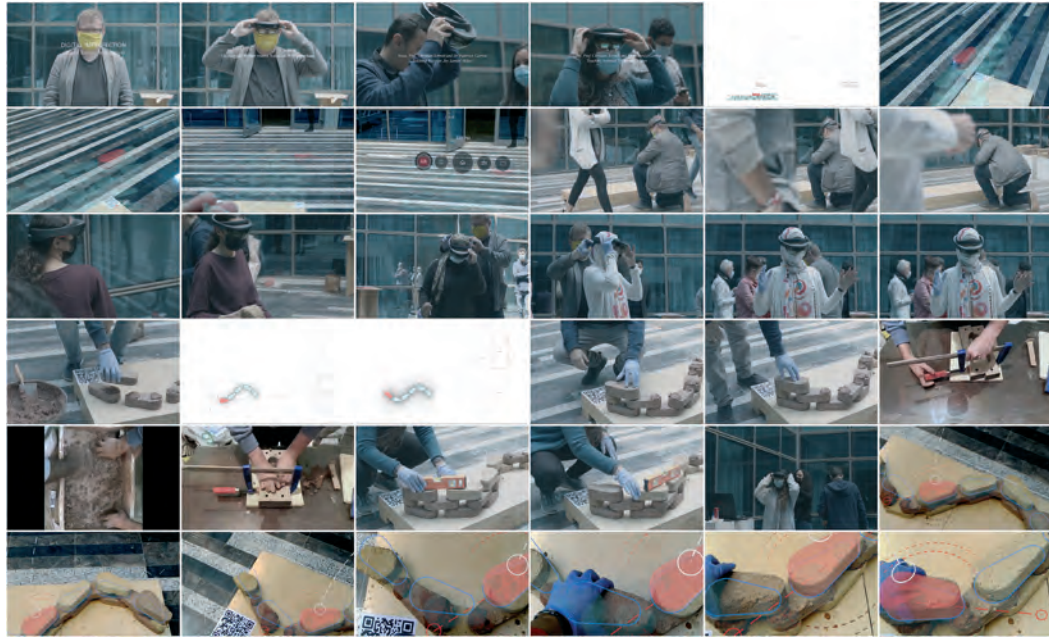


FIG. 1 Assembly Process

This particular research used the HoloLens, a device developed by Microsoft consisting of a smart glass projection system and a complex array of sensors and cameras to ‘sense’ its environment. The device can interpret its position in a given environment and project information seamlessly into a transparent glass, which gives the impression of a holographic projection, that is, the superposition of digital imagery over reality.

The HoloLens is Microsoft’s take on Mixed Reality (Speicher, 2019, pp. 1-15), a combination of technologies that fosters interactions between real and virtual environments by using instinctual interfaces such as precise motion detection and environmental sensing. Mixed Reality is designed as a blend between physical and digital worlds by seamlessly locating and positioning both in physical as well as in virtual spaces.

According to the HoloLens developer, Microsoft (Qian, 2022), Mixed Reality is actually a spectrum that has the physical world on one end and the digital world on the other. Inside this spectrum, Augmented Reality (AR) is often understood as closer to the ‘physical world’ end and Virtual Reality (VR) closer to the ‘digital world’ node.

Within the scope of this research, we will not be dealing with the complex functions of Mixed Reality technologies such as motion sensing or cloud computing; instead, we will use the HoloLens as a location and projection device closer to the Augmented Reality spectrum for tracking the user in three-dimensional space, overlaying graphics and providing precise visual feedback.

2 METHODOLOGY

The main objective of this research project is to explore possible relationships between manual crafting techniques and digital tools. The research installation was designed as a collaboration between two courses, one dealing with earth construction and the other with robotics and parametric design. For this reason, the intention was to find common topics and concepts to cross-fertilize each field of expertise with the other one.

The possible fields for collaboration were defined by the different stages of a design, either analogue or digital. These stages were defined as follows:

- Material workshop
- Conceptual design
- Constructive / detail design
- Design procedure
- Design of construction procedure
- Construction process

The elective Unplugged Matter started with a workshop with engineer Adel Fahmy in the Oasis of Fayoum, where the students got familiar with different raw earth techniques and several tests to analyze the specific percentages of the local earthen materials: clay, silt and sand. Furthermore, the students learned how the components get separated and which components need to be added for the different earthen techniques like mud bricks, rammed earth or CEB (compressed earth bricks).

CEB and earth have been the key focus of this semester's work. The intention was to use the technique to produce the necessary number of bricks. A very regular brick that could be used perfectly and pressed in form. During the semester, the teaching was influenced by Covid-19. Changing teaching directives also changed our idea of how to produce these bricks and with which technique. As the production of the bricks fell into the time of lockdown, we switched from pressed bricks to handmade bricks made with a wooden form that could be exchanged among the students. Students rammed the earthen bricks by hand at home and let them dry until assembly day. The imperfections caused by the manual procedure forced or even inspired us to deal – digitally – with the resulting challenge of different heights that had to be implemented into the digital design and build setup.

The concept behind the collaboration was to hybridize these stages as much as possible, blending both analogue and digital techniques. As previously stated, understanding that most contemporary design procedures more or less include a digital component, we intended to maximize this feature by using parametric design or remote sensing instead of just using three-dimensional modelling or CAD drawing. For example, when designing the final pieces or 'bricks', the student did not only model them in 3D but also parametrized their design, exploring different format and size variations of the same design.

In the conceptual design stage, once we decided to work with earth bricks, we evaluated the possibilities of building two distinct types of objects: either a sculpture or bench or a wall. The possibilities of digitalization allowed us to parametrize a shape, for example a bench, and then the formwork that would limit the rammed earth.

The parametric wall was designed by considering two parametric variables: the brick and the wall itself. Design research could explore both, testing different dimensions and geometries of forms and

their interactions. At this point, before any material input, this conceptual design stage was only limited to the decision to build either a wall or a sculpture.

The constructive design phase was carried out by the students of the "Unplugged Matter" course. They explored several brick types with different earth construction techniques, such as mud (adobe), unstabilized CEB or rammed earth. The shapes of the bricks were diverse, as each student group tested and developed their own ideas, ranging from 'tileable' shapes like hexagons or traditional bricks to other more complex forms with interlocked shapes and Tetris-like geometries. This stage was entirely designed with analogue tools such as sketches and models, trying to take into account the material qualities and characteristics such as resistance, rigidity, overall load-bearing capacity and other visual features such as textures or colours.

During this semester the teaching was influenced by Covid 19. During a lockdown we changed the idea from CEB bricks to handmade bricks by a wooden form that could be exchanged among the students. Students rammed the bricks by hand out of earth at home let them dry until the assembly day. This increased and unusual imperfection caused by the distributed handmade procedure forced or even inspired us to deal – digitally – with this new challenge of different heights that has to be implemented into the digital design and build setup. The design of the construction procedure was carried out in parallel by the students from "Introduction to Architectural Robotics", consisting of a wall composed of single bricks. The wall could have any shape, both in section and floorplan, with the possibility of a slope, inclination or curvature in any plane.

The solution for the wall definition was quite simple; a surface is defined by two curves or polygons (top and bottom). If both curves have the same dimensions and are displaced vertically, the wall will be perfectly vertical. If they are misaligned or offset, rotated or scaled in any direction, then the wall or parts of it will be sloped.

Finally, the wall is 'sectioned' or 'sliced' in horizontal lines that will be the guiding lines for the bricks. Each brick will be located along these horizontal lines, either aligned to them or re-oriented according to other geometric criteria.

Lastly, the construction procedure (Figure 2) was designed by both teams while negotiating the particularities of the material and construction technologies and translating them to the digital project. The assembly procedure should also be embedded with the final design of the wall, the brick size and their unique positions in the wall. Since the procedure would be performed with the HoloLens device, certain differentiation between the different bricks had to be defined, for example, the bricks on the wall, the bricks in the pick-up area and the 'current' brick, the one that the user carries.



FIG. 2 Assembly procedure, from parametric design to bricklaying

The intention was to create a seamless workflow that would allow the user to visualize any change in the wall design (either its overall shape or the position or type of bricks) in real-time, on a one-to-one scale and superimposed to the actual site.

It was also intended to account for different imprecisions such as geometric inaccuracies due to the manufacturing process, assembly mistakes or discrepancies in the material thicknesses, for example, in the 'mortar'. Since these types of errors are embedded in the material and the construction procedure itself, one purpose of this research was to create a design process that could effectively account for them.

2.1 BRICK DESIGN

The design of the earth bricks was an integral part of the "Unplugged Matter" course. The students were divided into teams, and each group designed and manufactured several brick types, first in a digital medium, later as a model and finally with earth in real scale.

Each brick should comply with a series of characteristics such as overall dimension and geometry; that is, one worker should be able to handle each brick without any mechanical assistance. Also, the bricks should have some flat sides to be stacked or combined horizontally and vertically or other possible combinations. Similarly, each brick should have geometrical characteristics to 'lock' it to its vertical or horizontal neighbours.

Adding to these geometric constraints, the students experimented with the materials and rammed earth techniques, informing their designs with this particular material knowledge. Several bricks were tested to design different types of walls, starting with straight, vertical walls and then trying combinations like zig-zag and curved walls.

With these particular parameters, the teaching team and the students selected the final design of the brick (Figure 3), an isosceles trapezoid with curved edges. The edges allow to 'articulate' the bricks and rotate them incrementally without exposing edges, which would be a material weakness.

Once this brick design was established, several wall designs were tested, taking into account the number of rows, overall weight, number of bricks and structural resistance. Keeping in mind that the wall would be built without any physical reference or measurement, the final design of the wall was limited only by its material characteristics.



FIG. 3 Different brick types designed by the students (left) and selected brick (right)

2.2 DESIGN PROCEDURE

The wall was designed with parametric design software (Rhinoceros Grasshopper). At the same time, it generated a real-time procedure that was streamed to the HoloLens device in the field. The parametric definition takes two curves (one on the bottom and the other one at the top) and creates a surface between them. If both curves are straight parallel lines, the resulting surface will

be a straight surface; if they are not parallel, the result will be a ruled surface. Finally, if one or both curves are curved, Rhinoceros will interpolate a surface connecting them, resulting in any number of complex surfaces like hyperboloid or paraboloid patches, among other irregular surfaces.

In the next step, this surface is 'divided' into rows according to the height of each brick row (calculated as the thickness of the brick and the mortar combined), resulting in a series of stacked curves that run parallel to the ground. A line of bricks is laid on each of these curves, separated by a user-defined parameter.

Because of the design of the brick, the relevant characteristic is that the centre of the curved parts is aligned so that the relative rotation angle between each brick can vary without compromising its structural capacity. This way, the separation between bricks remains constant, but the relative rotation might change while adapting to the wall geometry. Following this principle, the position of each brick is precisely defined in a three-dimensional space as well as its angle in the XY plane (parallel to the ground).

3 EXPERIMENT / RESEARCH

3.1 ASSEMBLY PROCEDURE

Each brick's position and rotation angle are pin-pointed in space, making it possible to precisely stream it to the HoloLens user (Figure 4). Due to fabrication issues, there were two different brick types with two different thicknesses. This means that each brick row must maintain the same brick height, and the user must be able to identify them easily.

Since the height difference could be felt but not easily seen, two different piles of bricks were defined, one with each brick type (A and B). The parametric procedure indicated to the user where to pick up the bricks (either pile A or B) and then where to position them.

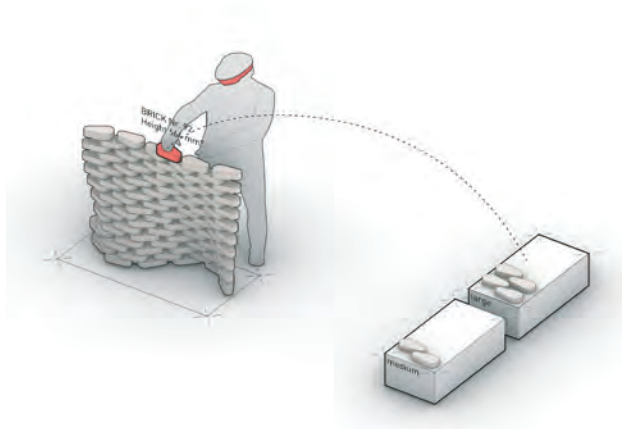


FIG. 4 Brick type location and assembly procedure

The assembly process required two persons: a user or bricklayer using the HoloLens device and an operator at the computer. The operator should control the overall procedure and select the 'active brick', that is, the brick that is highlighted in the wall composition and streamed to the HoloLens device (Figure 5).

The bricklayer receives the 'active brick' location (either pile A or B) as well as the final position in the wall. Once the brick is positioned in its final position, the operator should switch to the next brick, defining a new 'active brick' and starting the process over again (Figure 5 - 7). A video of the installation assembly process can be seen here: <https://vimeo.com/714403348>.



FIG. 5 HoloLens process. Active brick is highlighted in red



FIG. 6 Bricklaying with HoloLens and hands



FIG. 7 Bricklaying with earth mortar

3.2 HEIGHT COMPENSATION

One of the key difficulties of this research was the precisional difference between the three main components of the procedure. The parametric model was obviously the most precise of all, as it is mathematically perfect, the HoloLens device has a small error due to its positioning sensors and, most importantly, the bricks have manufacturing ‘imperfections’ that produce differences in their geometries. Finally, the application of mortar adds yet another source of discrepancies (Figure 6).

To compensate for these errors, the parametric definition allows the operator to readjust every brick row to match the actual position of the physical bricks. This error compensation is performed after each row, with the feedback provided by the HoloLens user via visual aids projected by the parametric definition. Once the operator makes the corresponding adjustments, the bricklayer should see the next row of virtual bricks positioned exactly on top of the last real brick row.

This feedback procedure proved to be fundamental and was used every two or three rows, thus adjusting the virtual brick wall to the dimensions of the real one. Therefore, both walls were built simultaneously, each continuously informing the other.

The brick structure was developed with parametric design software that generated a real-time procedure directly streamed to the HoloLens. This parametric procedure told the worker in a field of Mixed Reality (integration) where to pick up the brick and place it. In addition, during the assembly process, the height of the bricks were constantly readjusted to account for the thickness of the mortar. This back-and-forth movement was a crucial point of this collaborative project, as the cycle evolved from the inherently unique interference of each participant.

4 RESULTS

The benefits of Mixed Reality devices in the field of construction are mostly related to the display of spatial and geometrical data to provide the user with contextual information, for example, for assembly or maintenance operations. In this case, MR technologies were combined with low-tech construction materials (earth bricks), speeding up the design process and avoiding the use of traditional construction documentation (plans or sections).

The research work questions the relationship between high-tech and low-tech tools, measuring and accounting for variations in manufacturing, assembly and design. It is also intended to compensate and/or minimize discrepancies between design and assembly by establishing extra parameters and a feedback loop between the operator and the bricklayer.

The process accounted for the different imperfections and heights (like the mortar thickness and manufacturing differences), sustaining a constant loop with real-time feedback: the physical model is updated with new bricks, while the digital model is updated with the corrected heights.

The imperfection of earth bricks is often understood as a synonym for low-tech construction and deprived communities. However, earth bricks remain to be a simple, cheap and often perfect construction material in many parts of the world. And by involving digital tools, we can augment their use in a contemporary, elegant way.

It is not only possible but exciting to use digital technologies to enhance and promote locally sourced materials. Particularly in countries of the global south, a “technical” or even a “digital” augmentation

may help communities reconnect with their own material traditions and projects and participate in the planning and construction processes.

5 CONCLUSIONS

The imperfection of earth bricks is often understood as a synonym for low-tech construction in deprived communities. However, it is a simple and, per nature, circular material to build with. With Digital Imperfection, we wanted to underline that earth is more than a vernacular material. The project links state-of-the-art approaches with local traditions by highlighting earth as a contemporary building material.

We emphasize the collective experience of building with sustainable materials, using technology to create a shared understanding of building with the community's hands and finding a post-vernacular narrative for material that is available nearly everywhere.

References

- Brum, R., Digital Imperfection, Cairo, (2022), video of the installation assembly process: <https://vimeo.com/714403348>
- Dethier, J., The art of earth architecture: past, present, future, Thames & Hudson
- Fahmy, A., Appropriate Building Technology: Tradition and Innovation in Atkinson, A., Graetz, M., Karsch D. (2008), Techniques and Technologies for Sustainability, ISR-Sonderpublication Universitätsverlag der Technischen Universität Berlin
- Heringer, A., Howe, L. B., Rauch, M., (2019), Upscaling Earth. Material Process Catalyst, gta Verlag ETH Zurich
- Houben, H., Guillaud H., (1994), Earth Construction. A comprehensive Guide. Intermediate Technology Publications, London, UK
- Jahn, G., Newnham, C., van den Berg, N., Iraheta, M., & Wells, J., (2019), Holographic construction. In Design Modelling Symposium Berlin (pp. 314-324). Springer, Cham.
- Loporcaro G, Bellamy L, McKenzie P, Riley H (2019). Evaluation of Microsoft HoloLens Augmented Reality Technology as a construction checking tool. Bangkok, Thailand: 19th International Conference on Construction Applications of Virtual Reality. 13/09/2020-15/09/2020.
- Mitterberger, D., Dörfler, K., Sandy, T., Salveridou, F., Hutter, M., Gramazio, F., & Kohler, M. 2020. Augmented bricklaying. Construction Robotics, 4(3), 151-161.
- Qian Wen, "What is mixed reality?", Microsoft, May 25, 2022 <https://docs.microsoft.com/en-us/windows/mixed-reality/discover/mixed-reality>
- Speicher, M., Hall, B. D., & Nebeling, M. 2019. What is mixed reality?. 2019. In Proceedings of the 2019 CHI Conference on Human Factors in Computing Systems (pp. 1-15)

Establishing Benchmarks for Low-carbon, Circular Façade Design on Refurbishment Projects

Laura Craft¹, Christina Koukelli², Melissa Tanuharja^{3*}

- 1 Arup, Building Envelope Design, Germany
- 2 Arup, Building Envelope Design, Germany
- 3 Arup, Building Envelope Design, Germany, melissa.tanuharja@arup.com

Abstract

The built environment has a significant impact on our natural environment, depleting non-renewable resources, overwhelming landfills, and contributing to GHG emissions. The European Commission estimates that the construction industry is responsible for ~50% of all extracted raw materials and 35% of total waste generation. Buildings' operational energy consumption accounts for ~36% of total GHG emissions, and 10% is attributed to material manufacturing embodied carbon.

The adoption of lifecycle assessments demonstrates the environmental benefits of material re-use, refurbishment, recycling, and recovery, specifically on carbon emission, waste generation and resource consumption.

The paper's objective is to establish benchmarks for low-carbon and circular façade design on refurbishment projects by establishing a baseline through an academic and industry review of existing and projected benchmarks and targets.

A circular design framework for façade design is presented. A curtain wall system is used as a test case to quantify the current business-as-usual environmental impact. Alternative 'circular' options are proposed for comparison to demonstrate the environmental benefits of adopting circular design principles, including re-use, refurbishment, component replacement with low-carbon inorganic and organic alternatives.

The paper concludes with targets, barriers and opportunities, including next steps for the façade industry and how it can support the shift towards holistic sustainability.

Keywords

Façade, refurbishment, retrofit, circular design, lifecycle performance, embodied carbon, recycling, non-renewable resources

1 INTRODUCTION

Currently, the European Union (EU) built environment industry is responsible for approximately 50% of all extracted raw materials, over 35% of total waste generation and up to 12% of greenhouse gas emissions (GHG) from material extraction, product manufacturing and construction activities. In addition, the operational energy consumption for EU27 building stock accounts for 36% of total greenhouse gas emissions.

In pursuit of the Paris Agreement objective to keep the global temperature increase below 1.5°C, the EU has set out to reach net-zero greenhouse gas emissions by 2050 and decouple economic growth from resource consumption ("Paris Agreement", 2015). This requires an interim 2030 carbon emissions target reduction of at least 55% from 1990 levels and the transition to a circular economy. As a key contributor to greenhouse gas emissions, extracted raw minerals and waste generation, the construction industry must fundamentally re-evaluate the existing linear take-make-use-dispose model.

The building envelope, specifically the façade, is a key contributor to building operational energy performance. The heat transmission of a façade system – both glazed systems and opaque cladding systems – directly impacts the heating and cooling demands of a building in operation. While the industry has excelled in thermal and solar performance optimisation of façade components and systems, it has overlooked the environmental burdens of the façade beyond its operational life.

Existing buildings present a great opportunity to reduce greenhouse gas emissions and have a high ecological value. Extending the use and life of existing buildings through re-use, refurbishment, and/or conversion contributes significantly to minimising carbon emissions, saving resources, and reducing waste; therefore, playing an important role in the circular industry.

Circular economy models and waste hierarchies provide a framework for the transition to a circular economy in the built environment. The models and hierarchies are extensively discussed in academic literature and increasingly implemented on built environment projects. Various EU policies, strategies and targets related to circularity are increasing the need for industry best-practice benchmarks; however, environmental assessments of circular design present a gap in literature.

Life Cycle Assessment (LCA) is identified as an effective tool to evaluate the environmental impacts of a building over its whole life, from material mining, production, and manufacturing to end-of-life (EoL) waste management and recovery (BS EN 15978:2011). Academic literature and current industry best practices reveal a focus on life cycle carbon assessments, ignoring resource, waste and other environmental indicators. While the approach is holistic across a project's life cycle, it highlights the current industry's carbon tunnel vision.

The aim of this paper is to establish benchmarks for low-carbon and circular façade design, specifically on refurbishment projects. The paper proposes an LCA methodology for circular assessment and nominates lifecycle indicators to calculate resource consumption, waste generation and carbon emissions. The proposed methodology is tested on a façade refurbishment case study, which features both a stick and a unitised curtain wall system. Additionally, a circular façade design framework is proposed and used as a basis to formulate the case study scenarios.

The findings of this paper will demonstrate the value of the above methodology to quantify the environmental benefits of various circular façade system options. The findings will also demonstrate the increasing savings – across all indicators – as the case study scenarios move up the circular façade design framework.

2 LITERATURE REVIEW

2.1 INTRODUCTION

2.1.1 Circular Economy Model

The concept of circular economy has gained recent momentum both among academics and practitioners. The circular economy is a regenerative economic model synthesised from several major schools of thought, including Cradle to Cradle, Performance Economy and Biomimicry. Economic growth, sustainability and societal benefits are facilitated through restorative biological and technical resource cycles. It is a radical shift from the current take-make-use-dispose linear economy model – decoupling economic growth from finite resource consumption. The circular economy is based on three main objectives; design out waste, pollution, and greenhouse gas emissions, sustain materials and products in use and regenerate natural systems.

The circular economy model defines two resources cycles; biological and technical, as illustrated in Figure 1 (“The Butterfly Diagram: Visualising the Circular Economy,” 2017.). The biological cycle, on the left, reflects the regenerative process of agriculture products, such as food. Bio-based materials are designed to feed back into the system through processes such as composting, anaerobic digestion or biochemical. The technical cycle, on the right, reflects the recovery of manufactured products, components, and materials feed back into the system through processes such as maintenance, re-use, restoration, or recycling. It must be noted here that recycling materials – breaking down to base materials and feeding back into the manufacturing process – is the least desirable cycle as it requires the most primary energy.

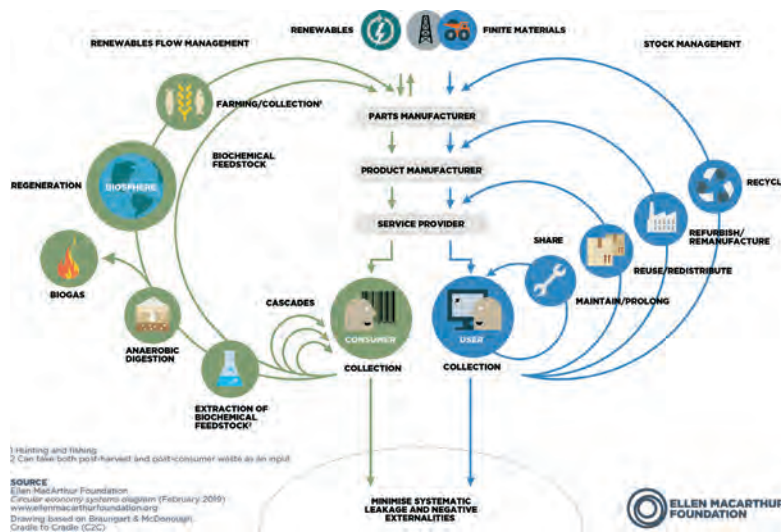


FIG. 1 The Butterfly Diagram: Visualising the Circular Economy. Source: Ellen MacArthur Foundation, 2017.

The circular economy model provides a framework for designers and engineers to facilitate the built environment industry transition to net-zero impact buildings: energy, waste, and resources. The technical cycle is most critical for the transition to a circular built environment and the primary focus of this paper.

2.1.2 Life Cycle Design

Life cycle design or life cycle engineering is a holistic approach to sustainable material or product design. Life cycle design considers the technical, environmental, and economic impacts of a material or product across its life cycle; resource mining, processing of raw materials, material or product manufacturing, transportation, installation, operational use and EoL use. While the built environment has increasingly optimised building operational sustainability, it has largely overlooked the significant environmental burdens associated with manufacturing and disposing of construction materials and products. A shift to holistic sustainability is broadly recognised within the industry, and building life cycle assessments are increasingly referenced in academic literature and adopted on projects.

This shift in sustainability can be observed at a façade level. The façade is a key contributor to building operational energy performance. The heat transmission of a façade system – both glazed and opaque cladding systems – directly impacts the heating and cooling demands of a building in operation. While the industry has excelled in thermal and solar performance optimisation of façade components and systems, it has overlooked the environmental burdens of the façade beyond its operational life. Aluminium, steel, glass, and insulation are key façade materials with significant manufacturing and installation environmental burdens. Life cycle design is a key mechanism to facilitate the transition to a circular built environment industry.

2.2 CIRCULAR ECONOMY FRAMEWORK

2.2.1 Waste and re-use hierarchies

The EU Waste Framework Directive (WFD) outlines the basic concepts for waste management within the economic region, including definitions of waste, recycling and recovery (“Waste Framework Directive,” n.d.). The basis of EU WFD is the five-step “waste hierarchy”, which establishes an order of preference for waste management. The EU waste hierarchy, as illustrated in Figure 2, mimics the circular economy model technical cycles. Both frameworks aim to divert waste from landfill and propose the same order of preference; in the first instance, maintaining products for as long as possible, preparing products for re-use or refurbishment, recycling products, and finally, recovering products for energy production.



FIG. 2 Waste hierarchy diagram as described in the EU Waste Framework Directive. Source: EU Waste Framework Directive

The EU waste hierarchy builds on the 3R's of waste management – ‘reduce, re-use & recycle’ – a term which dates back to the 1970s. It also provides a basis for the 9 R's of product management chains, a circular framework proposed by the Dutch Council for the Environment and Infrastructure (Potting,

Hekkert, Worrell, & Hanemaaijer, 2017). As illustrated in Figure 3, the 9R framework provides a more comprehensive hierarchy for adopting circular economy principles into product manufacturing.

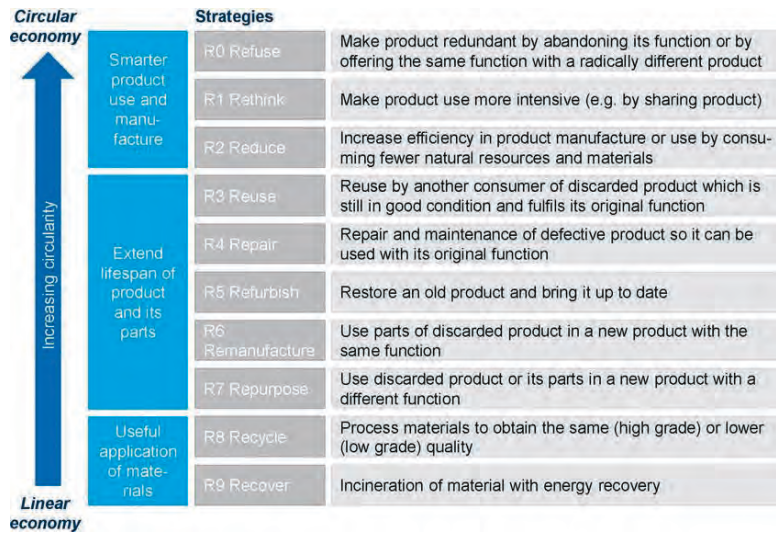


FIG. 3 The 9R framework. Source: Adapted from Potting, Hekkert, Worrell, & Hanemaaijer, 2017, p. 5.

2.2.2 Policies, strategies, guidelines and targets

Table 1 summarises the findings of a circular design requirements scan relating to the built environment within the European Economic region.

TABLE 1 Summary of circular design requirements relating to the built environment within the European Economic region.

REFERENCE	REQUIREMENT(S)	DRIVER	TIMELINE	NOTES
EU Circular Economy Action Plan ("Circular Economy Action Plan," 2022)	<ul style="list-style-type: none"> - possible introduction of recycle content minimum requirements for certain construction products - revision of material recovery targets for construction and demolition waste - promotion of circular economy design principles 	Policy	Current	
EU Strategy for a Sustainable Built Environment ("EU Sustainable Development Strategy - Environment - European Commission," n.d.)	<ul style="list-style-type: none"> - visibility of the construction value chain as a whole and a clear commitment by the EU to develop a coherent legislative framework - establishment of circular economy practices and links between existing legislative proposals to tackle the impacts of buildings and the construction sector 	Policy	2022	Strategy draft set for release 2022
EU Taxonomy ("EU Taxonomy for Sustainable Activities," n.d.)	<ul style="list-style-type: none"> - ≥90% (by weight) of non-hazardous construction and demolition waste is prepared for re-use or recycling. - ≥30% (by weight) of construction products contain recycled content, re-used or remanufactured components - Construction that demonstrates resource efficiency, longevity, adaptability, flexibility, disassembly, re-use and recycling 	Market	2022	Requirements for building assets or renovations which demonstrate a significant contribution to the transition to the circular economy
EU Waste Framework Directive ("Waste Framework Directive," n.d.)	<ul style="list-style-type: none"> - ≥70% (by weight) of non-hazardous construction and demolition waste is prepared for re-use, recycling or other material recovery 	Policy	Current	2020 Target is currently under revision

REFERENCE	REQUIREMENT(S)	DRIVER	TIMELINE	NOTES
EU Level(s) Framework (European Commission, 2020)	<ul style="list-style-type: none"> - ≥95% (by weight) of non-hazardous construction and demolition waste is prepared for re-use, recycling or other material recovery - ≥40% (by weight) of non-hazardous construction and demolition waste is prepared for re-use or recycling - Construction that demonstrates resource efficiency, longevity, adaptability, flexibility, disassembly, re-use and recycling 	Policy	Current	Mandatory for public procurement projects from 2022
DGNB Certification ("DGNB e.V. – Deutsche Gesellschaft Für Nachhaltiges Bauen," 2022)	Circular Economy Bonuses per circular economy solution or component. Among others: <ul style="list-style-type: none"> - re-used components and recycled materials - elimination of the need to use raw or secondary materials - for at least 50% of the building's usable area, area usage concepts that allow a higher intensity of use - use and integration of building technology, providing significant storage capacity and/or using renewable energy generated in the district - waste prevention on the construction site 	Market	Current	Indicator for evaluation as part of the "Building life cycle assessment" criterium. Circular Economy Bonuses within the DGNB Evaluation system
BREEAM Certification ("BREEAM - BRE Group," 2022)	Credit points according to minimum standards and benchmarks. Among others: <ul style="list-style-type: none"> - Up to 7 credits for reducing buildings' environmental life cycle impacts through conducting LCA and integrating its outcomes in the design decision-making process - 1 credit by rewarding the specification of products with environmental products declarations - 3 credits for responsible sourcing of construction products - 1 credit for designing for durability and resilience - 1 credit for material efficiency through optimising the use of materials through all stages of the project 	Market	Current	For each of BREEAM's nine categories, the percentage of credits achieved in each section is multiplied by the corresponding weighting for each section to give the overall environmental category score. The section scores are added together to give the overall BREEAM score.
London Energy Transformation Initiative (LETI) Best Practice Guidelines ("LETI," n.d.)	<ul style="list-style-type: none"> - 80% (by weight) of non-hazardous construction and demolition waste is prepared for re-use or recycling - 50% (by weight) of construction products contain recycled content, re-used or remanufactured components 	Market	Current	Best Practice recommendations for 2030. Current best practice recommendations 50% and 30% respectively.

2.3 DESIGN STRATEGIES, ASSESSMENT METHODOLOGIES AND TOOLS

2.3.1 Circular Building Toolkit – 2022

Circular Building Toolkit (CBT) is a web-based toolkit developed by Arup in partnership with the Ellen MacArthur Foundation to support designers, developers, construction firms, as well as asset owners and operators in making the transition to circular design ("Circular Buildings Toolkit," n.d.). It is a practical circular design framework that brings together the four key principles of build nothing, build for long-term use, build efficiently, and build with the right materials. The framework adopted several KPIs developed by external guidelines such as the EU Level(s), the German certification system DGNB and the Dutch MPG (Milieuprestatie Gebouwen) methodology ("Milieuprestatie Gebouwen (MPG) - Hoe Maak Je Een Milieuprestatieberekening?", 2021).

Rather than pursuing an approach that would differentiate from other existing frameworks, the toolkit has aligned with existing international frameworks and policies such as the EU Level(s) and the EU Taxonomy.

2.3.2 EU Level(s) – 2020

EU Level(s) is an open-source tool and a European framework for sustainable buildings to speed up the transition towards a more circular economic model in Europe (European Commission, 2020).

Level(s) assesses, monitors, and improves the sustainability performance of buildings by measuring carbon, material, water, health, comfort, and climate change impacts throughout a building's full life cycle.

It is a voluntary reporting tool that aligns with existing recognised European certification or rating schemes and standards. It is not intended as a rating scheme or to set a benchmark but rather to provide prompt circularity and lifecycle thinking in preliminary project design with consistent assessment methods and data comparison between projects and countries.

2.3.3 DGNB Certification System – 2009

DGNB certification system is a certification system developed by the German Sustainable Building Council (DGNB, Deutsche Gesellschaft für Nachhaltiges Bauen) to make sustainable construction measurable and comparable ("DGNB e.V. – Deutsche Gesellschaft Für Nachhaltiges Bauen," 2022). The system is based on three key paradigms: life cycle assessment, holistic and performance orientation. The certification system directly promotes a circular design approach by introducing performance indicators related to adaptability potential and ease of recovery, re-use and recycling.

2.3.4 Life Cycle Assessment (LCA)

A life cycle assessment (LCA) is an internationally standardised methodology (ISO 14040, 2006) (ISO 14044, 2006) to quantify the environmental impacts of products across the whole life cycle. The following provides a summary of LCA parameters:

- LCA is carried out for a chosen 'reference study period,' typically the required service life of the building or project.
- The 'system boundary' of an LCA determines the project or building stages taken into consideration for the assessment. For a new building, the system boundary shall include the project or building life cycle, as illustrated in Figure 4.

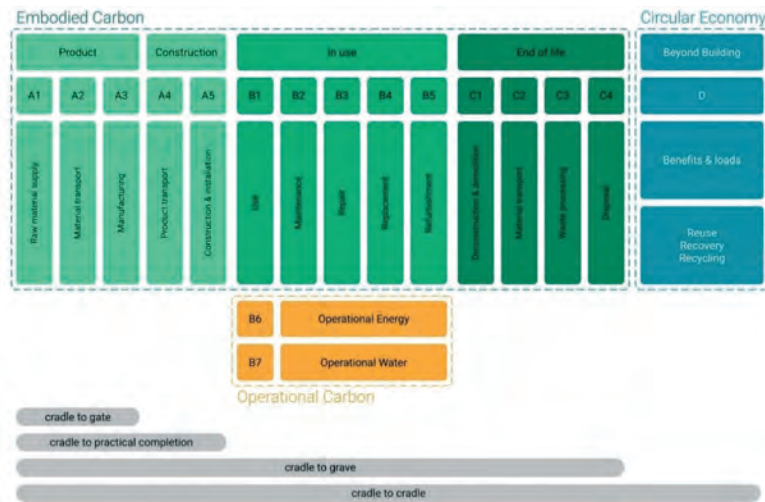


FIG. 4 Lifecycle modules defined in BS EN 15978. Adapted from BS EN 15978, 2011.

2.3.5 Design for longevity, maintenance, testing, replacement, and disassembly

These strategies are set up to reach the main purpose of building for long-term use. Long-term use property is essentially a great foundation for the circular economy principles. It aims at maximising the value of the building and its components over time, optimising value retention and value recovery potential. A long-life cycle of components is directly linked to its design, as the design sets the baseline for an element's quality, maintenance need, necessity for repair, adaptability, and residual value when removed. To enable adaptability potential during the use stage, it is critical that the building has the ability and resiliency to adapt to a new function to retain its value. Two design principles are considered for adaptability: versatility and convertibility, which are, in turn, related to the required level of system change adaptations.

Design for disassembly aims at enabling the disassembly potential at the end of service life. The useful life of some components in buildings outlast the service life of the system they are part of. It is important to design upfront for the practical disassembly of components, to recover residual value at the end of service life. According to ISO 20887, seven design principles for disassembly should be considered: ease of access, independence, avoidance of unnecessary treatments and finishes, supporting re-use business models, simplicity, standardisation, and safety of disassembly, appropriate for all sites and typologies.

2.3.6 Assessing existing building envelopes (ARUP)

Refurbishing the existing building stock is an essential step in minimising carbon emissions, saving resources, and reducing waste, and is, therefore, a great commitment to climate change. The lifecycle stages (A to D) are set chronologically throughout the typical life of a new building asset. However, the scope of the study for an existing building shall commence with Module C, not Module A. Framing the assessment as described above ensures the emissions associated with the EoL of existing components are most accurately represented. Three emission associations shall be considered:

- emissions of materials sent to landfills
- emissions of re-used materials and components
- emissions of recycled materials and components

2.4 BEST-PRACTICE PROJECTS

People's Pavilion, Eindhoven – The Netherlands (2017)

The temporary People's Pavilion, the centrepiece of the 2017 Dutch Design Week in Eindhoven, was a bold experiment in sustainability and material re-use that has forced the property industry to re-imagine a circular economy-inspired future. With a nearly zero-carbon footprint, the entire structure was made from borrowed materials. The pavilion is a design statement of the circular economy, a 100% circular building where no building materials are lost in construction and decommissioning. The People's Pavilion also served as the central meeting place for the week-long event, holding up to 600 people for a variety of talks, plays, and discussions. It was designed with easily reversible connections without the need for nails or glue, while the glass roof was borrowed from a greenhouse supplier, and the lower glass façade was saved from a demolished office building. Additionally, over nine thousand coloured interlocking plastic tiles served as shingles around the top of the building, which were made from recycled PET bottles donated by local Eindhoven residents. Once it had been dismantled, all borrowed materials used in the construction of the People's Pavilion were returned. Many items were re-used in further construction projects, preserving another key circular economy principle: to ensure the materials are kept in use at their value across the construction supply chain. ("People's Pavillion," n.d.)

1 Triton Square, London – UK (2021)

1 Triton Square was originally designed by Arup for British Land in the 1990s with future regeneration in mind. Twenty years later, British Land saw potential to increase the building's size and transform it for today's workstyle, opting for refurbishment to save time, money and carbon. The philosophy of the project is to retain and re-use as much as possible across every possible area. Through a marginal gain approach, dozens of systems, components and strategies have been refined to deliver a highly sustainable building. The project required the removal, refurbishment, and reinstallation of over 3,000m² façade, comprising over 25,000 separate parts. This approach alone saved 2,400 tonnes of carbon and represented a 66% cost saving compared to a new façade ("1 Triton Square," n.d.).

The Circular Building, London – UK (2016)

Arup collaborated with The Built Environment Trust, Frener & Reifer and BAM, as part of the London Design Festival 2016, to design and construct the Circular Building, which was located outside the Building Centre in September 2016. It was a prototype for a new approach to housing in which all components would be selected for their inherent low levels of embodied energy, and at the end of the building's life, all components would be taken apart and returned to the supply chain for re-use and recovery. The building was designed and constructed out of fully re-useable components and elements that can be disassembled and removed with minimum damage, helping each component to retain its value. Digital technology was used to 'tag' each item, from window framings to individual fixings, with a unique QR code containing information and store the data in a virtual material database, allowing it to be re-used ("The Circular Building: the Most Advanced Reusable Building yet - Arup," 2016).

2.5 GAPS AND OBSTACLES

Despite the advances towards more sustainable façade design and principles, there are still certain gaps and challenges, which can be regarded as obstacles towards a more circular façade design. Some of these are summarised below:

- Clear circular frameworks and waste and re-use hierarchies for the built environment in general, limited knowledge and experience in building envelope or façade-specific applications.
- EU policies, strategies, and targets provide a guideline for best-practice targets; however, no current mandatory requirements for built environment projects.
- Changing legislation and government regulations result in varied international competitiveness. Availability also varies according to each economic scheme.
- Limited façade-specific requirements across EU policies, strategies, guidelines and targets. Discrepancies between material efficiencies and adaptability.

Thematic areas	Macro-objectives	Indicators			
Resource use and environmental performance	1. Greenhouse gas emissions along a building's life cycle	1.1 Use stage energy performance (kWh/m ² /year)	1.2 Life cycle Global warming potential (CO ₂ eq./m ² /year)		
	2. Resource efficient and circular material life cycles	2.1 Bill of quantities, materials and lifespans	2.2 Construction and demolition waste	2.3 Design for adaptability and renovation	2.4 Design for deconstruction
	3. Efficient use of water resources	3.1 Use stage water consumption (m ³ /occupant/year)			
Health and comfort	4. Healthy and comfortable spaces	4.1 Indoor air quality	4.2 Time out of thermal comfort range	4.3 Lighting	4.4 Acoustics
Cost, value and risk	5. Adaption and resilience to climate change	5.1 Protection of occupier health and thermal comfort	5.2 Increased risk of extreme weather	5.3 Sustainable drainage	
	6. Optimised life cycle cost and value	6.1 Life cycle costs (€/m ² /year)	6.2 Value creation and risk factors		

Legend: 5 guided learning journeys

- Circularity
- Sustainable finance
- Resilience and future proofing
- Global warming
- Occupant welfare

FIG. 5 Overview of the Level(s) Framework. Source: European Commission, 2020.

- No targets for increasing the service life of buildings.
- High investment costs, lack of experience and waste infrastructure and insufficiently advanced recycling and recovery technology can pose a major challenge to creating a global circular economy.
- Environmental impact calculations present a gap in the literature. Circular assessments for façade design are required to establish benchmarks for best practice.

3 METHODOLOGY

3.1 CIRCULAR DESIGN FRAMEWORK

Adapting the Ellen MacArthur Foundation circular economy diagram to model a circular façade industry as illustrated in Figure 6, the biological and technical cycles can be identified for façade systems, components, and materials (“How to Build a Circular Economy | Ellen MacArthur Foundation,” n.d.).

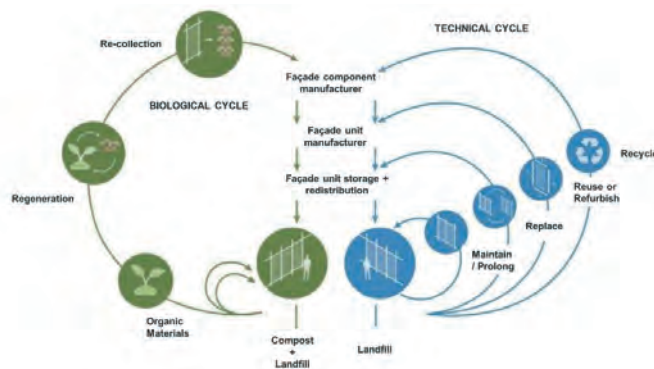


FIG. 6 Proposed Façade Circular Economy Model © Arup. Adapted from Ellen MacArthur Foundation.

3.1.1 Biological resources for façade materials

Biological façade systems use bio-based materials. Current academic research and emerging material technologies investigate the use of hemp-based composites, mycelium, straw and mud for façade construction. Despite the environmental benefits of bio-based facades, the manufacturing limitations, fire, durability, and structural performance requirements have prevented large-scale adoption within the façade industry.

3.1.2 Hybrid biological-technical resources for façade materials

Hybrid biological-technical façade systems use a combination of bio-based and mineral-based resources. Current academic resources and emerging material technologies investigate the use of green walls and roofs, algae façade systems, as well as more experimental bio-composite materials. This category includes, for instance, façade panels made of a hardened carbon-negative thermoplastic compound that makes use of (pyrolysed) wood waste to lock up carbon for long periods ("Made of Air - Carbon-Negative Materials," n.d.). Another example of biobased composite alternatives found in the market are façade panels which consist of natural fibres, a filler from waste streams and a largely biobased resin, which can be further ground and re-used in new bio-composites ("Nabasco Material I," n.d.). However, due to their experimental factor, such façade products are not yet widely encountered in the market and still have limited applications in the façade industry.

3.1.3 Technical resources for façade materials

Technical façade systems use abiotic or mineral-based materials which cover all common façade materials. Technical façade systems are of utmost importance for the transition to the circular built environment and are the focus of this report.

3.2 CIRCULAR HIERARCHY FOR FAÇADE DESIGN DECISION

Adapting the EU Waste Hierarchy diagram and the 9R circular framework to model a circular façade industry, useful tools for design decisions are established for façade systems, components, and materials.

As the EU waste hierarchy echoes the order or re-use preference for the technical cycles of the circular economy, so too does the proposed façade waste and re-use hierarchies – reduce material requirements, maintain products for as long as possible, prepare products for re-use or refurbishment, recycle products, recover products for energy production.

The proposed 9Rs of façade circular design provide a more detailed framework for façade material, components, and system design decisions. The 9Rs of design are classified by three main objectives (Kircherr, Reike, & Hekkert, 2017):

- 1 Smarter façade design
In the first instance, the façade design should be reviewed to reduce the required façade material quantities on projects. This is achieved by refusing non-functional design and designing for minimal material design. To achieve the greatest impact on low-carbon façade design, the brief needs to be challenged from the project onset. Rethinking new façade service models and designing them to suit is also a key consideration.
- 2 Extended life cycle of façade systems and components
In the next instance, the façade design should consider processes to extend the service life of façade materials, components, and systems. This is achieved by re-using, repairing, refurbishing, remanufacturing and repurposing façade materials, components, and systems. Design and EoL considerations.
- 3 Recovery of façade material waste
In the last instance, the façade design should consider processes to recover façade material waste and divert it from landfill. This is achieved by recycling façade materials, components and systems as well as recovering for energy production.

3.3 CIRCULAR DESIGN MECHANISMS

Several circular design mechanisms have emerged on the same framework, addressing one or more of the above objectives. Some of these are briefly explained below:

Design for longevity

This eco-design principle promotes the durability and longer life of products and systems through adaptability, upgradability, and 'timelessness'. To meet these guidelines, features such as modular design and standardised components, which can be easily dismantled for upgrade or repair by their user, can be adopted in the façade design and implementation. It also promotes the implementation of building passports and data management already incorporated in the original design, which will enable specifications and data to be available in case of repair and repair and replacement ("Science for Environment Policy", 2017).

Design for maintenance

From a façade design perspective, maintenance is seen as the prolonged use of components and consists of aspects related to delivering performance for as long as possible in the use phase. This includes cleaning, repair, upgrade and lifetime prognostics, allowing predicting the future performance of a façade product. Such predictive tools can include tracking of use conditions and can be promoted in applications such as the façade-as-a-service business models. An established maintenance regime can also help extend the service life (embodied carbon) and maintain the performance of the façade (operational carbon).

Design for replacement

This design principle promotes extending the useful lifetime of the whole façade element by enabling certain components to be replaced without damaging or disrupting the existing elements. Multiple strategies, including standardisation parts and accessibility, need to be taken into consideration.

Design for disassembly

Here, the design principle calls for the end-of-life options of how the façade components and materials can be deconstructed, enabling them to be repaired, upgraded, recycled or re-used,

prolonging their useful life. Designing for disassembly involves tactics such as minimising the number of parts used in a façade component, reducing the required fasteners, and avoiding glued connections while enabling common and standardised connectors instead. The goal is to simplify the series and speed of the façade build-up, facilitating the reversibility of the assembly (“Design for Disassembly/Deconstruction - Circular Economy Guide,” n.d.).

Design for recovery

Designing for material recovery can be perceived as the possibility for a façade component to be recovered, enabling it to be used as a secondary raw material for use outside of building construction, for the production of a new component. Ideally, a loss-free cycle must be ensured via established logistics; alternatively, this can be replaced by a take-back guarantee or leasing system for the façade component.

4 CASE STUDY

4.1 PROJECT OVERVIEW

In this chapter, the test case will demonstrate how the proposed frameworks for circular low-carbon façade design shall be applied. The selected case is a real-case refurbishment project of both low-rise (4-8 floors) and high-rise (22 floors) commercial buildings located in Europe with a curtain wall construction system. There is a strong drive from the client and the project brief to reduce and minimise carbon emissions, which essentially means an operational upgrade. The buildings were constructed in 2004, and the main technical installation took place in 2005. Thus, most of the installations reach their theoretical lifespan in the next 2-5 years.

Stick curtain walling is used for the low-rise building, and unitised curtain walling is used for the high-rise building. The façade module and components are, however, identical, composed of thermally broken aluminium framing, double glazing unit (vision), opaque glazed panels (spandrels), and decorative aluminium sunshades.

4.2 PROJECT ASSUMPTIONS

In this assessment, key façade performance indicators are reviewed for the existing building envelope and subsequent refurbishment and replacement options.

Thermal performance:

The total U-value for the curtain wall (U_{cw}) on both buildings is considered. U_{cw} includes the area weight average of the glass, opaque spandrel, edge, and framing effects. U_{cw} measures the rate of heat transmission through the façade, directly impacting heating and cooling.

Thermal properties of the glazing part include a U-value of $1.5 \text{ W/m}^2\text{K}$ and the SHGC 0.21 for curtain wall modules.

Façade module:

Façade modules for both low-rise and high-rise buildings are identical.

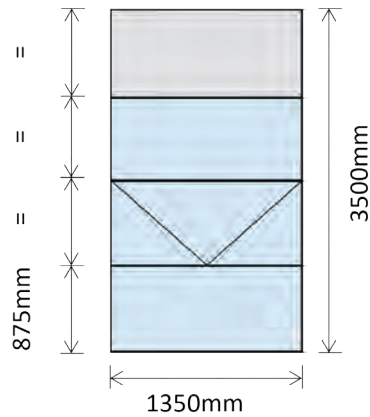


FIG. 7 Existing façade module

Window-to-wall ratio (WWR):

WWR of the existing building is 75%.

Refurbishment measures

In this assessment, two main measures were considered. The first measure is to extend the service life of the façade before any major intervention needs to be carried out. The second measure is to carry out all interventions in the next 2-5 years.

4.3 LCA FOR FAÇADE DESIGN – INPUT PARAMETERS AND BOUNDARY CONDITIONS

Multiple input parameters and boundary conditions for different scenarios were set before the LCA assessments were conducted.

- Only the embodied carbon (Global Warming Potential (GWP)) is assessed in the calculation.
- Functional Unit = /m² façade area
- The estimated service life (ESL) of primary components, such as framing, insulation, concealed supporting elements, and rain-screen cladding material, is 50 years. For the secondary components, such as insulated glazed units (IGUs) and accessible gaskets and sealants, it is 25 years. The client of the project chose these ESL as a more conservative assumption in the industry.
- As a principle, as many life cycle modules as possible shall be included in the assessment; however, it is recognised that considerations of some modules will require data that is not currently available. This assessment follows the minimum life cycle modules in accordance with RICS (RICS, 2017):
 - product stage A1 – A3)
 - construction process stage (A4 – A5)
 - replacement stage (B4)
 - end of life (C4)
- The GWP indicator (Stage A1-A3), recycle rate potential and recycled content rate for each material in this calculation refer to product or manufacturer-specific Environmental Product Declarations (EPDs) and generic EPDs developed by an industry association.
- Transport emissions factors refer to RICS, 2017.
- Waste rates factors refer to the Waste and Resources Action Plan (WRAP, 2020).
- Materials chosen for rain-screen cladding comparison:

- aluminium with 3 mm thickness
- copper with 1.5 mm thickness
- glass fibre reinforced concrete (GFRC) with 13 mm thickness
- natural stone with 30 mm thickness
- terracotta with 30 mm thickness (with cut-out)
- zinc with 0.7 mm thickness

4.4 DESIGN SCENARIOS

An overview of the studied scenarios is shown in Figure 8.

	Remain in Service	Retrofit existing system	Upgrade existing system	Replace system	BAU			
	Scenario A no intervention	Scenario B add component	Scenario C add and replace component	Scenario D new system with reused components	Scenario E new system with regenerative material	Scenario F new system with recycled material	Scenario G new alternative system	Scenario H new system
Input (new)	– n/a	– Opaque glazed spandrel	– Opaque glazed spandrel – Triple glazing unit (incl. gasket)	– Opaque glazed spandrel – Triple glazing unit (incl. gasket)	– Hybrid timber framing – Timber sunshades – Opaque glazed spandrel – Triple glazing unit (incl. gasket)	– Opaque glazed spandrel – Triple glazing unit (incl. gasket)	– Triple glazing unit (incl. gasket) – Opaque rainscreen cladding	– All components
Input (reused/recycled)	– n/a	– n/a	– Reused aluminium framing – Reused aluminium sunshades	– n/a	– n/a	– Recycled aluminium framing – Recycled sunshades – Recycled glass unit – Recycled P1AG6 – Recycled mineral wool	– Recycled aluminium framing – Recycled sunshades – Recycled glass unit – Recycled P1AG6 – Recycled mineral wool	– n/a
Output	– n/a	– All to landfill	– Double glazed unit to be recycled	– Double glazed unit to be recycled	– Existing aluminium framing to be recycled – All glass unit to be recycled	– Existing aluminium framing to be recycled – All glass unit to be recycled	– Existing aluminium framing to be recycled – All glass unit to be recycled	– All to landfill

FIG. 8 Overview of the studied scenarios, which vary with the type of intervention.

4.4.1 Remain in service

This strategy is a short-term opportunity to extend the existing façade service life for another 10 to 15 years. Gaskets and seals of the existing façade have reached their EoL. Therefore, the main challenge in this strategy is to ensure that the airtightness of the existing façade is adequate for another 10 to 15 years.

Scenario A

There is no intervention of the existing façade in this scenario; however, a preliminary investigation to ensure sufficient building airtightness performance through a localised airtightness test and regular façade inspection are within the scope.

4.4.2 Retrofit existing system

In this strategy, minor intervention is considered. The goal is to improve the overall thermal curtain wall performance and reduce solar heat loads.

Scenario B

The scope in this scenario is to retrofit the glass panes of the base curtain wall system with an insulated opaque spandrel. The overall thermal curtain wall performance will be improved ($U_{cw} = 1.35 \text{ W/m}^2\text{K}$), and the solar heat loads will be reduced ($WWR = 50\%$). New material inputs in this scenario are mineral wool insulation retrofitted to the back of the system with a metal backing sheet.

Scenario C

In this scenario, additional opaque spandrel retrofit as in Scenario B is assumed with additional replacement of the existing curtain wall façade double glazed unit (DGU), including material and associated installation work. New material inputs in this scenario are mineral wool insulation, metal backing sheet, triple-glazed unit (TGU), new gaskets, and mechanical fixings. The overall thermal performance will be improved ($U_{cw} = 1.10 \text{ W/m}^2\text{K}$), and the solar heat loads will be reduced ($WWR = 50\%$).

This scenario aims to recycle 98% of the existing DGU. Scenario C only applies to the low-rise building with a stick curtain wall system. Further elaboration on this distinction is provided in section 4.5.1.

4.4.3 Upgrade existing system

Major intervention is considered in the next three different scenarios, which aim to improve the overall thermal curtain wall performance, reduce solar heat loads, and apply a more circular design approach. The approach includes minimum material recycled content, component re-use, minimum embodied carbon targets, bio-regenerative material use, and more circular strategies regarding the EoL of the existing components that are being replaced.

Scenario D

This scenario has the same concept as Scenario C but applies only to the high-rise building with a unitised curtain wall system. Therefore, the methodology of the existing curtain wall replacement is different since it requires the system to be dismantled from the building structure and to be transported from the site to the factory for repair and back to the site for installation. The overall thermal performance will be improved ($U_{cw} = 1.00 \text{ W/m}^2\text{K}$), and the solar heat loads will be reduced ($WWR = 50\%$). The new material inputs in this scenario are the same as in Scenario C.

The existing aluminium framing and sunshade profiles and the glazed spandrel units, including the mineral wool insulation, are to be re-used.

This scenario aims to recycle 98% of the existing DGU.

Scenario E

In Scenario E, a bio-regenerative curtain wall framing system and sunshade element are considered to replace the existing aluminium profiles. Opaque spandrel retrofit and additional replacement of the existing curtain wall façade DGU are assumed, as in the previous scenarios. The overall thermal performance will be improved ($U_{cw} = 1.00 \text{ W/m}^2\text{K}$), and the solar heat loads will be reduced (WWR=50%).

This scenario aims to recycle 98% of the existing DGU and 96% of the existing aluminium framing and sunshade profile.

Scenario F

This scenario aims to replace the existing curtain wall system with highly recycled content materials. This includes aluminium curtain wall framing, aluminium sunshade profile, glazing unit, including the one on the spandrel unit and its associated components, and the mineral wool insulation. The overall thermal performance will be improved ($U_{cw} = 1.00 \text{ W/m}^2\text{K}$), and the solar heat loads will be reduced (WWR = 50%). In this scenario, an upcoming new product of low-carbon glass, which is claimed to have 30% less carbon emission, is used as input.

This scenario aims to recycle 98% of the existing DGU and 96% of the existing aluminium framing and sunshade profile.

4.4.4 Replace system

This strategy is comparable to the upgrade existing system one, but with a major intervention which aims to improve the overall thermal curtain wall performance, reduce the solar heat loads, and applies a more circular design approach as well. Alternative materials and system options are challenged here to understand the impacts on building performance, embodied carbon, and circularity as alternatives to the insulated spandrel glazing. Various alternative materials with different embodied carbon will be compared to the traditional usage of glass in an insulated spandrel unit.

Scenario G

In this scenario, materials with high recycled content are used to replace the existing curtain wall system, including the aluminium curtain wall framing and aluminium sunshade profile. The existing spandrel unit will be replaced with an opaque rear-ventilated rain-screen system with various cladding options. Mineral wool insulation and aluminium sub-structure are assumed as additional material inputs. Various cladding materials are chosen to be demonstrated in the calculation, such as aluminium, copper, GFRC, stone, terracotta, and zinc. The overall thermal performance will be improved ($U_{cw} = 1.00 \text{ W/m}^2\text{K}$), and the solar heat loads will be reduced (WWR = 50%).

This scenario aims to recycle 98% of the existing DGU and 96% of the existing aluminium framing and sunshade profile.

4.4.5 Business as usual

This strategy considers only a conservative refurbishment approach mostly followed in current practice, which aims to improve the overall thermal curtain wall performance and reduce the solar heat loads. A more circular design approach and low-carbon input materials are not considered at all.

Scenario H

In this scenario, all the existing façade components, including the aluminium curtain wall framing, the aluminium sunshade profile, as well as the vision and glazed spandrel units, are replaced with new components with no recycled content or low-carbon material. There is no aim to re-use the existing component. Thus, all the existing components will be sent to landfill.

4.5 OBSERVATIONS

4.5.1 Stick vs unitised curtain wall system

Different construction methods between stick and unitised curtain wall systems affect the feasibility of certain strategies. As described in the above design scenarios, Scenario C is only applied for the low-rise building with a stick curtain wall system. It is theoretically possible to apply this strategy to the high-rise unitised system, but it is not recommended, as it requires more careful disassembly to secure and remove the glazing unit with external access, for instance, by mobile elevated working platform or similar, and generally, it will be quite cost intensive.

However, for the low to medium-rise building with a stick curtain wall system, it is more feasible by externally removing the existing external sunshade features and glazing beads (including mechanical fixing thermal breaks), where the structural glazing is cut out afterwards and then removed. Therefore, in the assessment, Scenario C will only apply to the stick system construction, assuming that the glazing replacement is done on-site, and Scenario D will only apply to the unitised system construction, assuming that the existing framing and glazing unit are brought to the factory, replaced, and then brought back to the site. However, in this project, the team decided that it is not worth the effort to remove the existing framing and glazing components because replacing the components solves the waterproofing issues.

The above distinction also demonstrates that there are different carbon emissions associated with transport and material waste for the stick and unitised curtain wall system. For example, there are advantages and disadvantages associated with the unitised system related to off-site manufacturing. The environment of off-site facilities has better quality control; thus, produces less waste and typically has well-established waste management procedures which improve the utilisation of the material. However, it also requires additional transportation and handling of materials from the manufacturer to the factory before being transported to the site. The different embodied carbon associated with both transport and waste will be part of the assessment.

4.5.2 Organic vs inorganic material

Organic material, such as timber, is currently considered the most favourable framing material where sustainability has a strong drive in the project. As with inorganic materials, timber involves production stage emission. Nevertheless, the use of timber in buildings can be thought of as a 'carbon sink', which means the carbon is kept away for the duration of its service life to delay the emission of the sequestered carbon.

Scenario E is theoretically feasible for both stick and unitised systems. However, there are points to be considered, especially when they are being used in high-rise buildings due to fire restrictions, whereas in low to medium-rise buildings, it possibly meets the fire requirements. Another aspect to be looked at is meeting the structural requirements of the façade; timber profiles generally need a substantial surface area compared to aluminium and, in most cases, will still remain a hybrid aluminium system.

5 RESULT

5.1 UNITISED CURTAIN WALL SYSTEM (HIGH-RISE BUILDING)

Scenario B

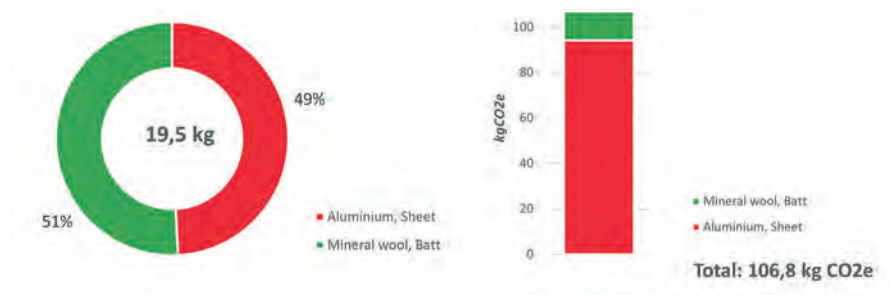


FIG. 9 Total material by weight (left), total embodied carbon by material for stage A1-A3 (right).



FIG. 10 Total embodied carbon by material for stage A-C.

Scenario D

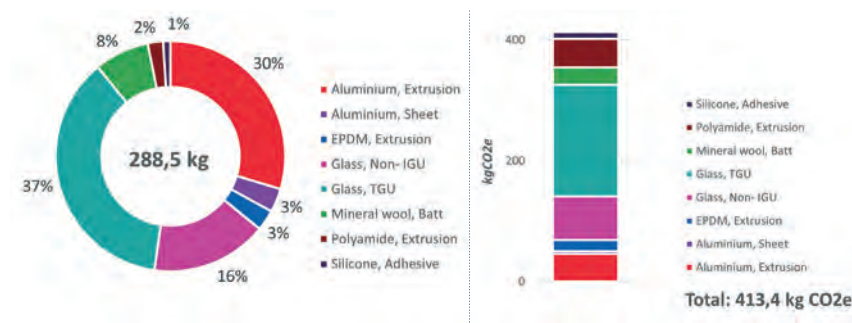


FIG. 11 Total material by weight (left), total embodied carbon by material for stage A1-A3 (right).

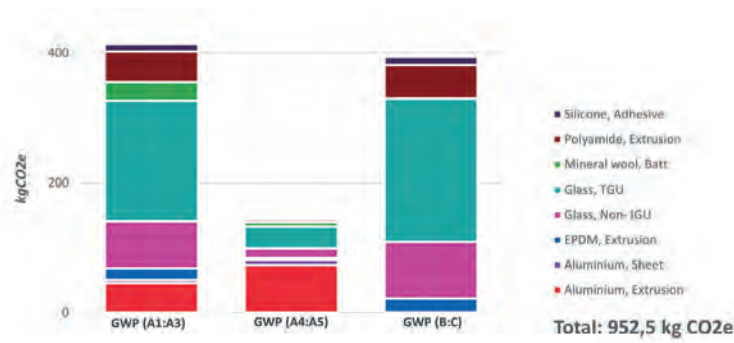


FIG. 12 Total embodied carbon by material for stage A-C.

Scenario E

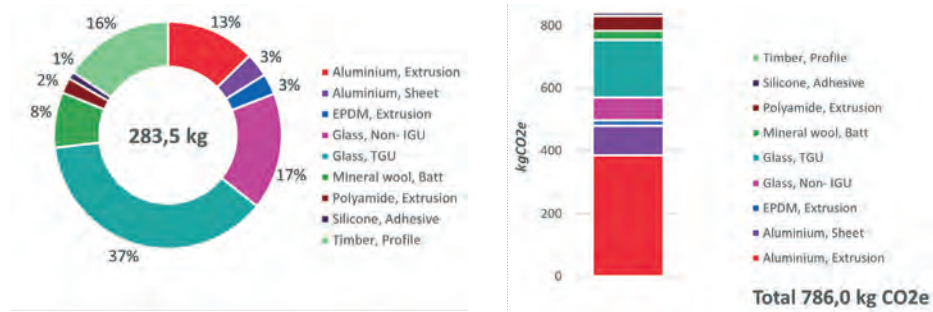


FIG. 13 Total material by weight (left), total embodied carbon by material for stage A1-A3 (right).

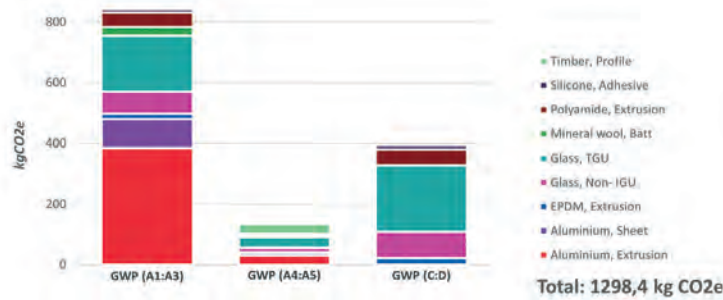


FIG. 14 Total embodied carbon by material for stage A-C

Scenario F

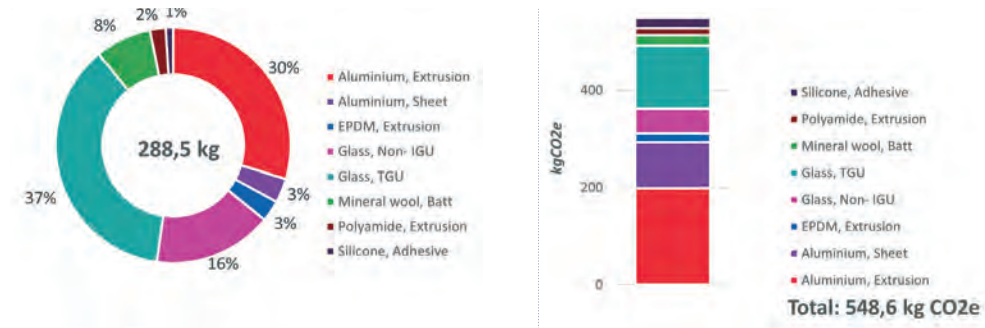


FIG. 15 Total material by weight (left), total embodied carbon by material for stage A1-A3 (right).

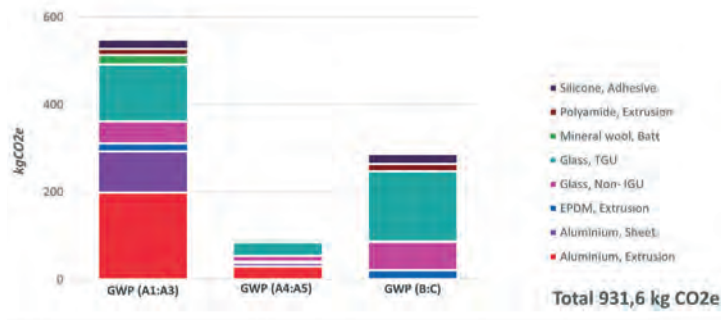


FIG. 16 Total embodied carbon by material for stage A-C.

Scenario G

Aluminium

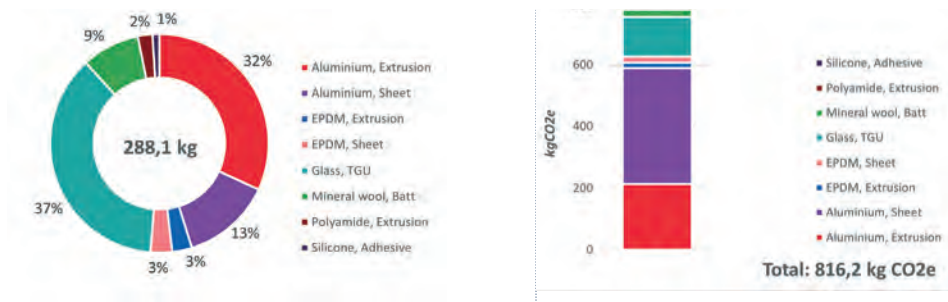


FIG. 17 Total material by weight (left), total embodied carbon by material for stage A1-A3 (right).

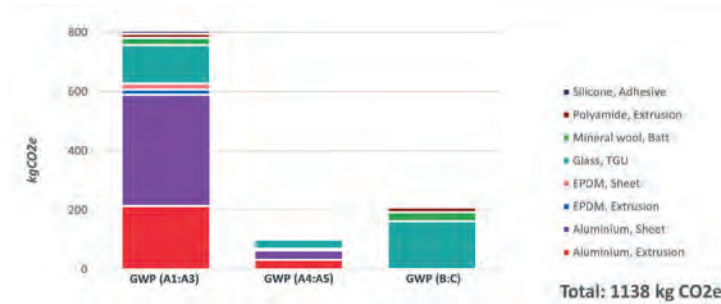


FIG. 18 Total embodied carbon by material for stage A-C.

Copper

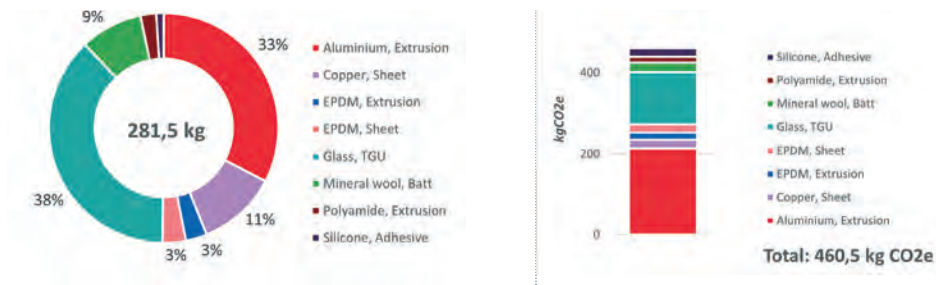


FIG. 19 Total material by weight (left), total embodied carbon by material for stage A1-A3 (right).

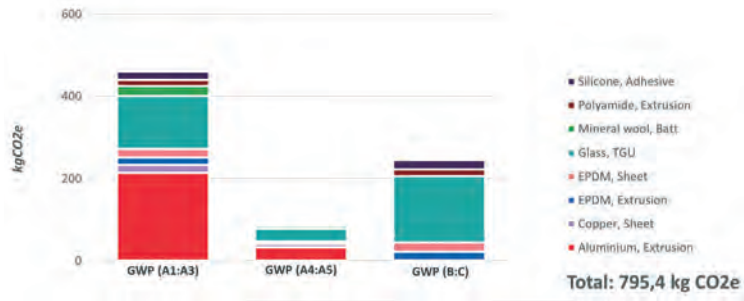


FIG. 20 Total embodied carbon by material for stage A-C.

GFRC

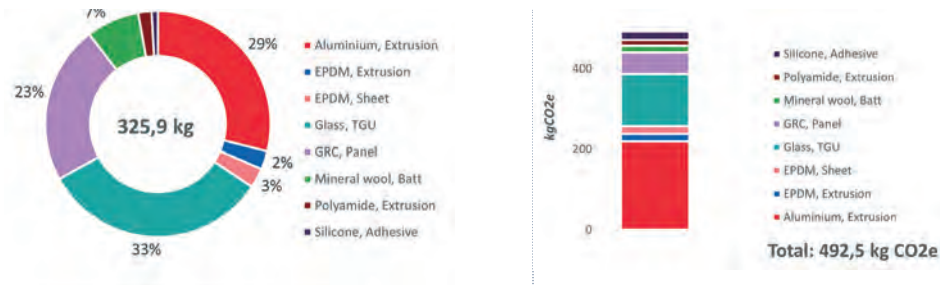


FIG. 21 Total material by weight (left), total embodied carbon by material for stage A1-A3 (right).

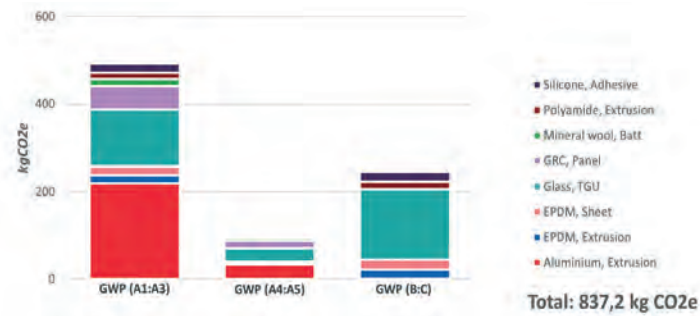


FIG. 22 Total embodied carbon by material for stage A-C.

Natural Stone

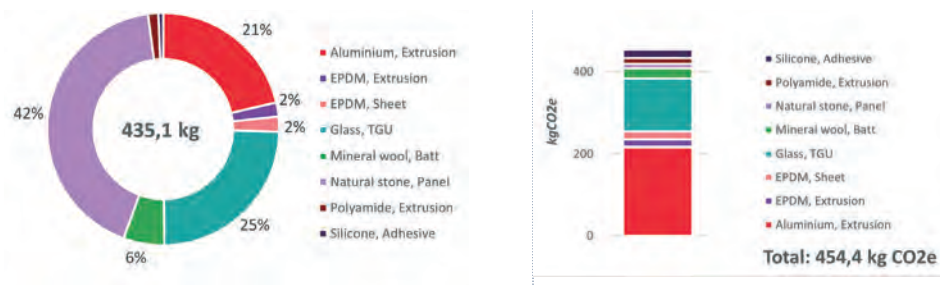


FIG. 23 Total material by weight (left), total embodied carbon by material for stage A1-A3 (right).

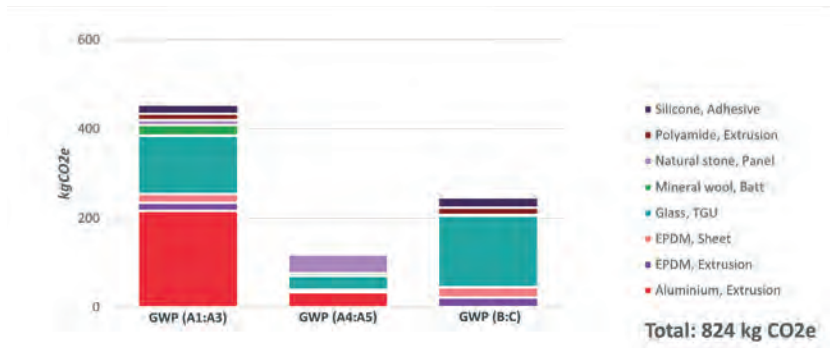


FIG. 24 Total embodied carbon by material for stage A-C.

Terracotta

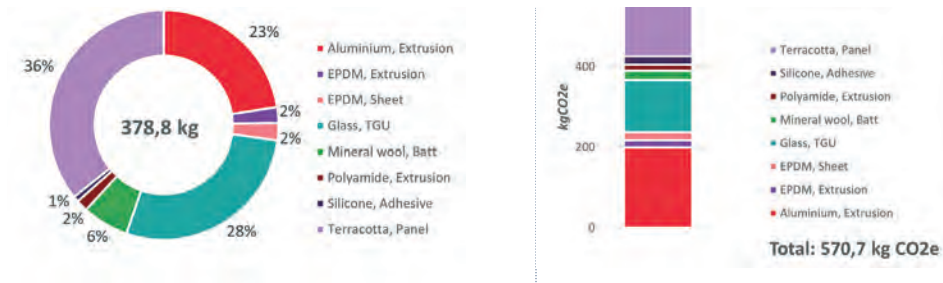


FIG. 25 Total material by weight (left), total embodied carbon by material for stage A1-A3 (right).

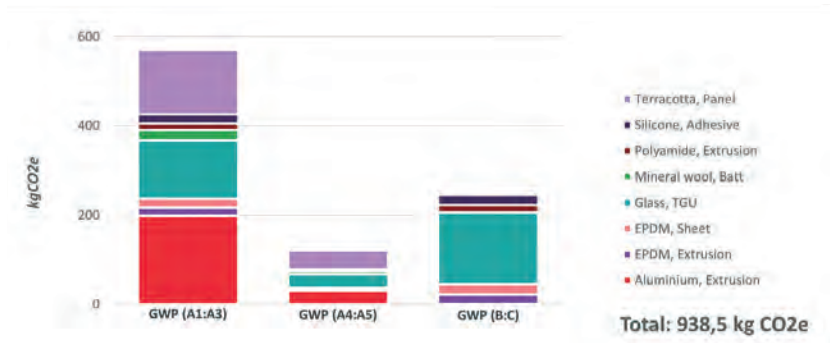


FIG. 26 Total embodied carbon by material for stage A-C.

Zinc

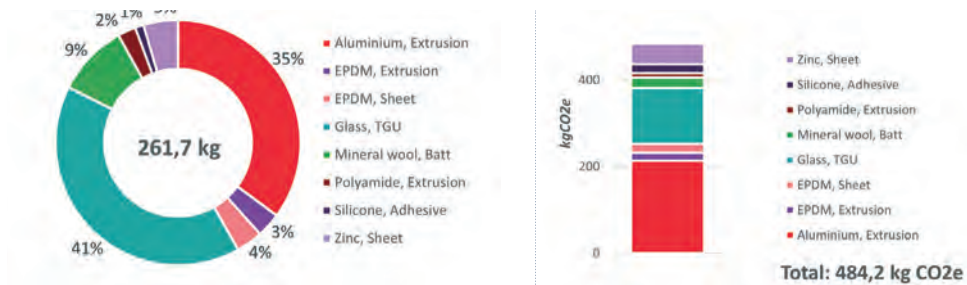


FIG. 27 Total material by weight (left), total embodied carbon by material for stage A1-A3 (right).

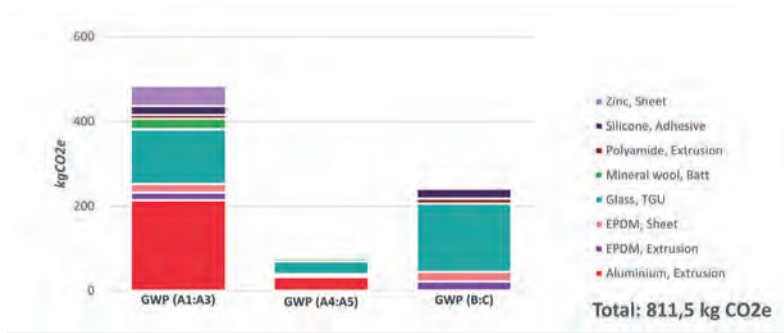


FIG. 28 Total embodied carbon by material for stage A-C.

5.1.1 Scenario H

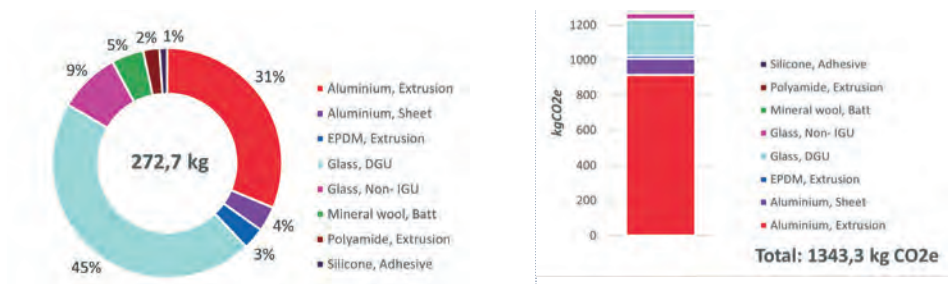


FIG. 29 Total material by weight (left), total embodied carbon by material for stage A1-A3 (right).

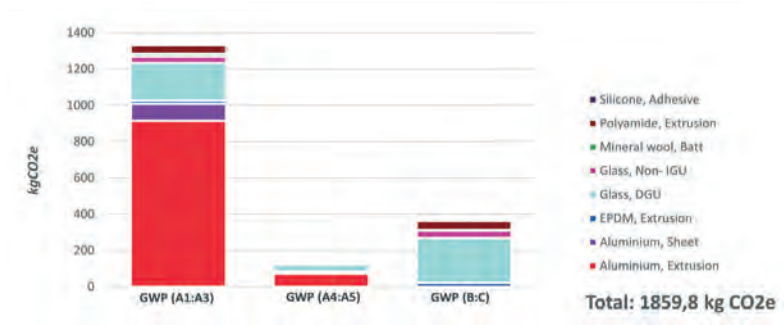


FIG. 30 Total embodied carbon by material for stage A-C.

The results show that when improvement of the operational building performance is necessary, upgrading existing systems or replacing systems would be the recommended strategy.

When comparing the different scenarios for upgrading existing systems, new material inputs without any recycled content contribute significantly to the total carbon emissions even though it is regenerative material, such as timber. Scenario F has slightly better results than Scenario D due to the high recycled content of glass which plays an important role in the total carbon emissions. However, one must also consider the material waste produced in Scenario F shall be higher, as Scenario D aims to re-use as much existing material as possible. Scenario G with different opaque material options generally demonstrates that they all have lower carbon emissions compared to glazing units except aluminium cladding. However, this assessment does not consider the complexity

of replacing partial components of curtain walling to rain-screen systems. Therefore, in practice, Scenario G might be more suitable for new buildings.

5.1.2 Summary

	Remain in Service	Retrofit existing system	Upgrade existing system	Replace system	BAU			
	Scenario A no intervention	Scenario B add component	Scenario C add and replace component	Scenario D new system with reused components	Scenario E new system with regenerative material	Scenario F new system with recycled material	Scenario G new alternative system	Scenario H new system
Total material weight (kg)	-	19,5	-	288,5	283,5	288,5	288,5	272,7
Stage A1-A3 (kgCO ₂ e)	-	106,8	-	413,4	786,0	548,6	result in separate table	1343,3
Stage A4-AS (kgCO ₂ e)	-	10,7	-	145,2	118,6	95,9	result in separate table	140,1
Stage B-C (kgCO ₂ e)	-	0,1	-	383,9	383,8	287,1	result in separate table	376,4
Total (kgCO ₂ e)	-	117,6	-	952,5	1288,4	931,6	result in separate table	1859,8

FIG. 31 Summary - part 1.

Replace system						Scenario G new alternative system (zinc)	Scenario G new alternative system (terracotta)	Scenario G new alternative system (natural stone)	Scenario G new alternative system (GFRC)	Scenario G new alternative system (copper)	Scenario G new alternative system (aluminium)
						261,7	376,8	435,1	325,9	281,5	288,1
						484,2	570,7	454,4	462,5	460,5	816,2
Stage A1-A3 (kgCO ₂ e)	86,2	121,3	122,8	98,5	89,1	111,8					
Stage B-C (kgCO ₂ e)	241,1	246,4	246,8	246,1	246,6	210,0					
Total (kgCO ₂ e)	811,5	938,5	824,0	837,2	795,4	1138,0					

FIG. 32 Summary - part 2.

5.2 STICK CURTAIN WALL SYSTEM (LOW-RISE BUILDING)

This chapter will show the details of Scenario C and the summary results of each scenario.

5.2.1 Scenario C

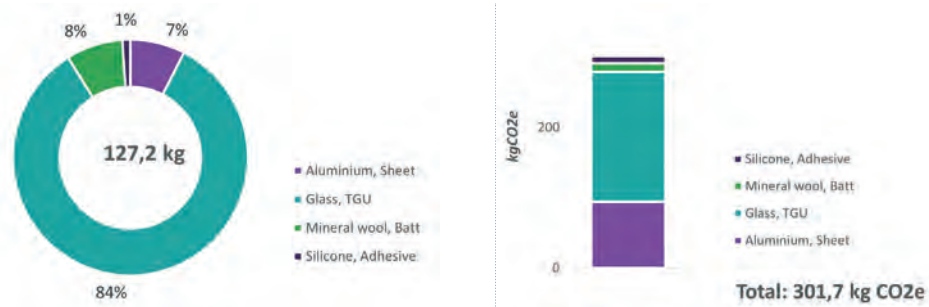


FIG. 33 Total material by weight (left), total embodied carbon by material for stage A1-A3 (right).

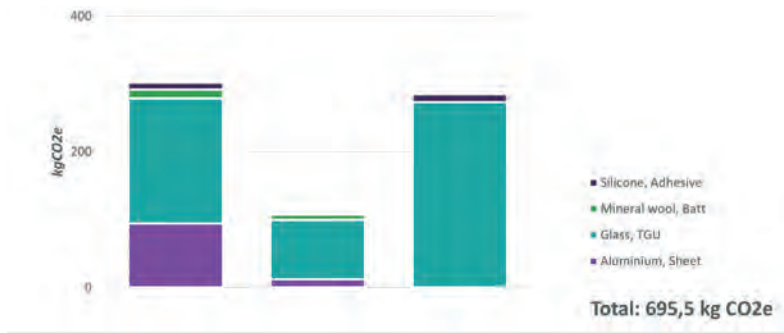


FIG. 34 Total embodied carbon by material for stage A-C.

The results demonstrate that the values from each scenario are comparable to the unitised curtain wall system. The main differences are the material weight, material waste, and transportation of the material.

5.2.2 Summary

	Remain in Service			Retrofit existing system			Upgrade existing system			Replace system		BAU
	Scenario A no intervention	Scenario B add component	Scenario C add and replace component	Scenario D new system with reused components	Scenario E new system with regenerative material	Scenario F new system with recycled material	Scenario G new alternative system	Scenario H new system				
Total material weight (kg)	-	19,5		288,5	283,5	288,5	288,5	272,7				
Stage A1-A3 (kgCO ₂ e)	-	106,8		413,4	786,0	548,6	1343,3					
Stage A4-A5 (kgCO ₂ e)	-	10,7		145,2	118,6	95,9	140,1					
Stage B+C (kgCO ₂ e)	-	0,1		383,9	383,8	287,1	376,4					
Total (kgCO ₂ e)	-	117,6		952,5	1288,4	931,6	1859,8					

FIG. 35 Summary - part 1.

Replace system						
	Scenario G new alternative system (aluminium)	Scenario G new alternative system (copper)	Scenario G new alternative system (GFRC)	Scenario G new alternative system (natural stone)	Scenario G new alternative system (terracotta)	Scenario G new alternative system (zinc)
						
Total material weight (kg)	288,1	281,5	325,9	435,1	378,8	261,7
Stage A1-A3 (kgCO ₂ e)	816,2	460,5	492,5	454,4	570,7	484,2
Stage A4-A5 (kgCO ₂ e)	111,8	89,1	98,5	122,8	121,3	86,2
Stage B+C (kgCO ₂ e)	210,0	246,8	246,1	246,8	246,4	241,1
Total (kgCO ₂ e)	1138,0	795,4	837,2	824,0	938,5	811,5

FIG. 36 Summary - part 2.

6 DISCUSSION

The research shows the different contributions associated with carbon emissions from various façade refurbishment strategies. There are many additional factors to be considered to reach a clear conclusion about which is the best strategy for each curtain wall system. These additional factors include the importance of thoroughly checking the existing façade on-site for the condition of the current gasket, for instance, the complex strategy and process to remove structural silicone glazing, the performance test required in case of re-use, and potential compliance with current building regulations, especially regarding fire. Most importantly, it is crucial to specify the refurbishment measures and the timeline to understand and evaluate the kind of intervention needed and at which moment of the building's lifespan. This defines the point at which it is more sensible to extend the service life of the façade with targeted upgrades, which can increase the building's performance where needed, compared to the point when the components have reached their EoL, and major intervention is inevitably required. The market readiness for some materials is another aspect to be considered. For instance, glass theoretically has a 100% recycling rate potential. However, in reality, not many contractors are willing to go the extra mile to develop a safe methodology needed to separate the laminated glass from the monolithic glass in an IGU. EPDM is also claimed to have up to 98% recycling rate potential; however, in practice, most of it will be downcycled for a different use or recovered for energy. It shows that while these materials are nominated to have a high recycling rate potential, in current practice, both will be downcycled because neither the process nor the

methodology is in place to support the recycling of these materials back into their manufacturing stream. The assessment shows that in refurbishment projects, re-using as many existing materials as possible has the least impact on carbon emissions and waste compared to using new materials, even with recycling content or new regenerative material such as timber. This is in line with the waste hierarchy framework described in the previous chapter. Other small approaches to low-carbon design are reducing, for instance, the weight of the façade, as it is beneficial not only to reduce the material use but also to reduce the demand on the structural support of the building and, ultimately, the foundation system. Visual aspects, such as glass distortions and colour variance, also have a significant impact on the amount of material and energy needed. More relaxed specification requirements would reduce the amount of energy and waste material expended by the supplier.

References

- 14 Triton Square. (n.d.). Retrieved August 30, 2022, from 1 Triton Square - Arup website: <https://www.arup.com/projects/1-triton-square>.
- BREEAM - BRE Group. (2022, February 23). Retrieved August 30, 2022, from BRE Group - Building a better world together website: <https://bregroup.com/products/breeam/>.
- BS EN 15978:2011: Sustainability of construction works. Assessment of environmental performance of buildings. (2011). Calculation method. London: BSI.
- Circular Buildings Toolkit. (n.d.). Retrieved August 30, 2022, from Circular Buildings Toolkit website: <https://ce-toolkit.dhub.arup.com/>.
- Circular ecology (2020). Embodied Carbon — The ICE Database.
- Circular economy action plan. (2022, January 1). Retrieved August 30, 2022, from Environment website: https://environment.ec.europa.eu/strategy/circular-economy-action-plan_en.
- Design for disassembly/deconstruction - Circular Economy Guide. (n.d.). Retrieved August 30, 2022, from Circular Economy Guide website: <https://www.ceguide.org/Strategies-and-examples/Design/Design-for-disassembly-deconstruction>.
- DGNB e.V. – Deutsche Gesellschaft für Nachhaltiges Bauen. (2022, August 31). Retrieved August 30, 2022, from DGNB e.V. – Deutsche Gesellschaft für Nachhaltiges Bauen website: <https://www.dgnb.de/>.
- EU Sustainable Development Strategy - Environment - European Commission. (n.d.). Retrieved August 30, 2022, from EU Sustainable Development Strategy - Environment - European Commission website: https://ec.europa.eu/environment/sustainable-development/strategy/index_en.htm.
- EU taxonomy for sustainable activities. (n.d.). Retrieved August 30, 2022, from Finance website: https://finance.ec.europa.eu/sustainable-finance/tools-and-standards/eu-taxonomy-sustainable-activities_en.
- European Commission (2020). Level(s) – A common EU framework of core sustainability indicators. Retrieved August 30, 2022, from Environment website: https://environment.ec.europa.eu/topics/circular-economy/levels_en.
- How to Build a Circular Economy | Ellen MacArthur Foundation. (2017). Retrieved August 30, 2022, from How to Build a Circular Economy | Ellen MacArthur Foundation website: <https://ellenmacarthurfoundation.org/>.
- Kirchherr, J., Reike, D., & Hekkert, M. (2017) Conceptualising the Circular Economy: An Analysis of 114 Definitions. Resources, Conservation and Recycling, 127, 221-232. <https://doi.org/10.1016/j.resconrec.2017.09.005>.
- LETI. (n.d.). Retrieved August 30, 2022, from LETI website: <https://www.leti.london/>.
- Milieuprestatie Gebouwen (MPG) - Hoe maak je een Milieuprestatieberekening? (2021, May 28). Retrieved August 30, 2022, from Ecochain website: <https://ecochain.com/nl/knowledge-nl/milieuprestatie-gebouwen-berekening/>.
- Made of Air - Carbon-negative materials. (n.d.). Retrieved August 30, 2022, from Made of Air website: <https://www.madeofair.com/>.
- Nabasco materiaal | (n.d.). Retrieved August 30, 2022, from Nabasco materiaal | website: <https://www.npsp.nl/en/nabasco-materiaal/1>.
- Paris Agreement. (2015). Retrieved August 30, 2022, from Climate Action website: https://ec.europa.eu/clima/eu-action/international-action-climate-change/climate-negotiations/paris-agreement_en
- People's Pavillion. (n.d.). Retrieved August 30, 2022, from People's Pavilion, Eindhoven - Arup website: <https://www.arup.com/projects/peoples-pavilion>.
- Potting, J., Hekkert, M.P., Worrell, E., & Hanemaaijer, A. (2017). Circular Economy: Measuring Innovation in the Product Chain.
- RICS (2017). Whole life carbon assessment for the built environment (1st edition). Retrieved August 30, 2022, from RICS website: <https://carbon.tips/rics>.
- Science for Environment Policy: European Commission DG Environment News Alert Service (2017), edited by SCU, The University of the West of England, Bristol:
- The Butterfly Diagram: Visualising the Circular Economy. (n.d.). Retrieved August 30, 2022, from The Butterfly Diagram: Visualising the Circular Economy website: <https://ellenmacarthurfoundation.org/circular-economy-diagram>.
- The Circular Building: the most advanced reusable building yet - Arup. (2016, September 19). Retrieved August 30, 2022, from The Circular Building: the most advanced reusable building yet - Arup website: <https://www.arup.com/news-and-events/the-circular-building-the-most-advanced-reusable-building-yet>.
- Waste Framework Directive. (n.d.). Retrieved August 30, 2022, from Environment website: https://environment.ec.europa.eu/topics/waste-and-recycling/waste-framework-directive_en.
- WRAP (2020). Welcome to the Net Waste Tool. Retrieved August 30, 2022, from WRAP website: <https://carbon.tips/nwtool>.

Additively Manufactured Urban Multispecies Façades for Building Renovation



Iuliia Larikova ¹, Julia Fleckenstein ¹, Ata Chokhachian ¹, Thomas Auer ¹,
Wolfgang Weisser ², Kathrin Dörfler ¹

* Corresponding author, larikova.y@gmail.com

1 TUM School of Engineering and Design, Germany

2 TUM School of Life Sciences

Abstract

This research investigates the potential of additive manufacturing and digital planning tools for the creation of location-specific façade redesigns that can host cavity-dependent animal species and develops methods for their realization. The proposed approach is explored based on a case study of a student dormitory in need of renovation in the urban area of Munich. Based on theoretical knowledge and design experimentations that link the fields of architecture, climate-responsive design, terrestrial ecology, and digital fabrication, a set of design principles for the additive manufacturing of inhabitable ceramic tiles is conceived and transferred into a computational design tool. The conception of single tiles and the overall façade design are developed in terms of their positive climatic impact on both the animal species and humans, their nesting opportunities, their structural feasibility, and their integrability with standard ceramic façade systems. To verify the fabricability of the proposed design, a façade fragment was additively manufactured as a prototype in 1:1 scale. The initial findings presented in this paper provide a glimpse of how emerging digital technologies could provide new ways to expand current habitual architectural planning and fabrication tools, to enable the creation of site-specific solutions, and to bring together human and animal needs.

Keywords

Additive Manufacturing, Computational design, Climate-aware design, Terrestrial ecology, Building renovation

DOI 10.47982/jfde.powerskin.7

Timber-based Façades with Different Connections and Claddings: Assessing Materials' Reusability, Water Use and Global Warming Potential



Miren Juaristi Gutierrez ^{*1}

* Corresponding author, Miren.JuaristiGutierrez@eurac.edu

1 Eurac Research, Austria

Abstract

Timber-based façade technologies have the potential to effectively reduce the carbon footprint, reduce water use in construction, and minimize waste, when their manufacturing process is highly prefabricated. Additionally, avoiding glue parts can enhance the sustainability of the façade as its elements can be replaced (extending the durability of façades and therefore buildings) and separated once that they reach their end of life (to re-use or recycle them). Thus, the connection between materials might have a considerable impact on the façade's sustainability. Moreover, timber-based façades can have different claddings, impacting on the water needed for the technology and their Global Warming Potential (GWP). This paper assesses, through a novel methodological approach, materials' reusability, water use, and GWP for different façade connections and claddings. Four prototypes with different connections (staples, screws, timber nails, and geometrical assembly) were built. Experimental activities representing façade elements' substitution and disassembly provided qualitative and quantitative information about production, extraordinary maintenance, and end-of-life phases. Through these tests, the quantity of material that could be re-used and disposed in such phases was quantified and then inserted in a Life Cycle Analysis (LCA). LCA was conducted using EF v.3.0 impact method and components were modelled with EPD information and Ecoinvent cut-off 3.7 database. According to the results, a timber-based façade with timber nails and wood cladding is the most promising of reusable façade materials, decreasing the water use and GWP.

Keywords

Wood construction, extraordinary maintenance, disassembly, End of Life, Climate Change Potential

DOI 10.47982/jfde.powerskin.5

Mapping and Evaluating External Wall Material Stock in terms of Circularity: a Case Study in Istanbul

Sühan Artuğ^{1*}

1* Istanbul Technical University, Department of Architecture, Turkey, artugs@itu.edu.tr

Abstract

A building system requires the coexistence of elements with different life cycles. Therefore, circular design aims to re-use building elements and/or materials that have not completed their life cycle in a possible renovation scenario. In the construction industry, which plays a large part in using limited natural resources, the circular design approach has an important role. An inventory of the existing building stock should be created to use cities as a resource pool for urban mining. This study aims to map the construction type, exterior wall core and finishing material in Fatih, a district of Istanbul included in the urban renewal process, and evaluate these materials in terms of circularity with the compiled criteria list. The study is based on observation as the data collection method for generating the material inventory in Fatih. The review includes all usage types of buildings. It is also supported by technical documents prepared by the district municipality and other institutions. Based on a literature review, a circularity assessment criteria list is created by compiling and classifying the criteria obtained. As a result of the study, data on the material stock in Fatih, Istanbul is collected. The data is then evaluated with the compiled circularity criteria, serving as a preliminary study to create re-use scenarios for possible urban renewal.

Keywords

Istanbul, exterior wall finishing material, urban mining, building stock, circular design

1 INTRODUCTION

Today, we are faced with the fact that natural resources are decreasing to the point of depletion. Despite this, the construction industry continues to use new materials in most projects for various reasons, such as the ability to supply in bulk, guarantee quality and delivery, etc. (McGinley, 2018). In conjunction with the circular economy, circular design and circular construction try to offer solutions for the potential re-use of the materials before the end of their life. According to the Ellen MacArthur Foundation (2015), the circular economy is based on three principles: elimination of waste and pollution, circulation of products and materials (at their highest value), and regeneration of nature.

The availability of structured information about building stock, material flow, and material identity in a systematic order is critical in supporting the transition of the construction sector with the circular economy model (Munaro & Tavares, 2021). Circular economy strategies such as materials passports, urban mining, and material mapping are used to provide this structured information.

Materials Passport's (MP) definition is: "(Digital) sets of data describing defined characteristics of materials and components in products and systems that give them value for present use, recovery and re-use" (BAMB, 2016). Materials Passports play a key role in gathering data about materials and tracing the materials, applications for organising reverse logistics, and accelerating innovation through information sharing (BAMB, 2016).

The accumulation of materials resulting from continuous consumption in cities has led to urban mining expectations for secondary resources. Urban mining, an approach to the use of materials that are already in use (stock) in the city when the need for materials arises, is an important circular economy strategy for the construction sector (Arora et al., 2020). While Material Passports focus on identifying materials and obtaining their information to reintroduce them into consumption chains, Urban Mining and Material Mapping focus on the location, distribution, and quantities of materials in the city.

Within the framework of the topics mentioned above, the research question is "What are the building material types and re-use potentials to be obtained from the urban renewal process in Fatih, which is planned to be realised in the near future?"

In parallel with the research question, this study aims to map the construction types, exterior wall cores, and finishing materials in Fatih and evaluate these materials in terms of circularity with the compiled criteria list.

Fatih district is selected for the pilot area because:

- Fatih is one of the first settlements in İstanbul; the building stock is quite old and neglected due to the changing demographic structure.
- 18,623 buildings (approximately 85% of the total building stock) were built before the 1999 Great Marmara earthquake; therefore, buildings do not comply with the new building earthquake code reformed after the earthquake.
- According to the Istanbul Earthquake Zones Distribution Map published by the Ministry of Environment, Urbanization and Climate Change, Fatih is located in the first-degree earthquake zone.

The Eminönü region (Figure 1) in the Fatih district is excluded from the study because:

- There are many historic buildings, and buildings that need restoration are excluded from this study as they require different expertise.
- Eminönü was a separate district before 2009.
- The building material information of Eminönü is not found in the Geographical Information System (Url-1) published by Fatih Municipality.

The Akşemseddin, Mevlanakapı, Silivrikapı and Sümbül Efendi neighbourhoods were selected for the detailed and visualised mapping because they are the intersection of the two evaluations in the Spatial Strategy Plan prepared by the Fatih Municipality explained below:

- A building situation analysis was made according to the construction year for buildings constructed after the 1999 Earthquake, which are currently considered earthquake-resistant, excluding historic buildings. According to this, buildings in poor condition and old building stocks are mostly seen in the Mevlanakapı, Şehremini, Sümbül Efendi, Silivrikapı, Akşemseddin, and İskenderpaşa neighbourhoods.
- Neighbourhoods that stand out in terms of many factors as a result of the evaluation made in the urban renewal prioritisation approach: Ayvansaray, Akşemseddin, Zeyrek, Cibali, Mevlanakapı, Sümbül Efendi, Silivrikapı, Nişanca, Mola Gürani.

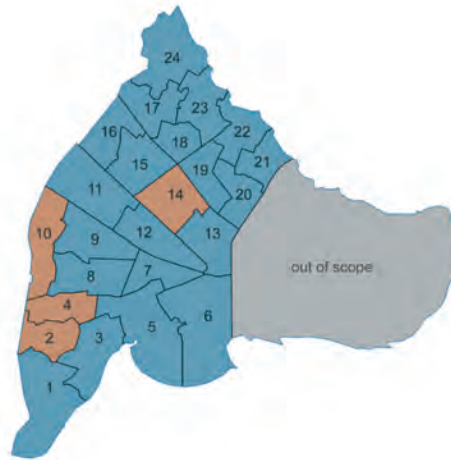


FIG. 1 Fatih district map; the neighbourhoods examined are shown in blue, and the four neighbourhoods that have been mapped are shown in orange.

2 METHODOLOGY

This study was carried out in two-prong. On the one hand, a circularity evaluation criteria list was created by literature review and analysis; on the other hand, materials data from the Fatih district were collected. The methods are explained in Figure 2 and are detailed below.

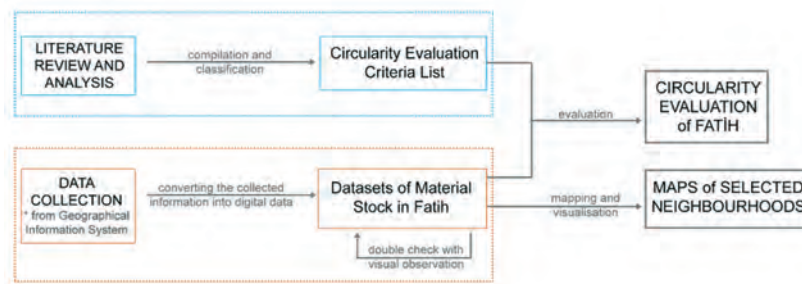


FIG. 2 Flowchart of the study

2.1 LITERATURE REVIEW AND ANALYSIS

The literature review was executed with the keywords “circular design, circular economy, and material circularity assessment” in the Web of Science, Scopus, and Science Direct databases to create a set of criteria and evaluate the circularity assessment of the building. After examining reusability, life cycle, and circularity assessment models, material and connection-oriented ones were chosen since the analysis was made at the scale of the building element. Also, models were chosen to provide a circularity perspective about materials, not deep calculation by using a formula. Therefore, the assessments of Cottafava & Ritzen (2021), Graubner & Reiche (2001), BCIS (2006) and Stephan & Athanassiadis (2018) were analysed and combined as criteria set for this study.

2.2 DATA COLLECTION

The district of Fatih was divided into neighbourhoods, and the information about the construction types, exterior wall core material types, and exterior wall finishing material types of all buildings in each neighbourhood was obtained by using the Geographical Information System (Url-1) published by Fatih Municipality. The information in the Geographic Information System was checked both from Google Maps and through physical observation. Physical observation control was limited to a randomly selected street from each neighbourhood.

3 RESEARCH

3.1 CIRCULARITY EVALUATION CRITERIA LIST

In order to develop the circularity criteria list, different approaches in the sources of the literature review were analysed and compiled into a list. Cottafava & Ritzen (2021) approached the evaluation of circularity in terms of connection type, divided the connections into five categories, and classified them between 1 (max circular) and 0.1 (min circular):

- dry connection (1): dry connection, click connection, elcro connection, magnetic connection
- connection with added elements (0.8): ferry connection, corner connections, screw connection, bolt and nut connection
- direct integral connection (0.6): pin connection, nail connection
- soft chemical compound (0.2): kit connection, foam connection
- hard chemical compound (0.1): glue connection, pitch connection, weld connection, cement bond, chemical anchors, hard chemical connection

From this classification, screw connection (0.8), bolt and nut connection (0.8), nail connection (0.6), and cement bond (0.1) found in buildings in Fatih were selected for the evaluation criteria set.

Another study that approached the evaluation of circularity in terms of the type of connection is that by Graubner & Reiche (2001). This study classifies the connection type as follows:

- separable connection, manual separation possible (elements or components can be re-used)
- separable connection, equipment needed for separation (components must be repaired but can be re-used)
- partly separable connection, equipment needed (elements or components will be reprocessed)
- inseparable connection (extensive reprocessing procedures required or dumping)

From this classification, separable connection–equipment needed and inseparable connection found in the buildings in Fatih were selected for the evaluation criteria set.

The lifetime of material is another selected perspective; BCIS (2006) and Stephan & Athanassiadis (2018) adopted this approach. Stephan & Athanassiadis (2018) also discussed the waste coefficient values of the materials. These values were transferred to the evaluation criteria set according to the material types determined in the buildings in Fatih.

3.2 DATASETS OF MATERIAL STOCK IN FATIH

The Geographical Information System published by Fatih Municipality includes labels for the buildings. By clicking on each building label in the system one by one, the construction type data is counted, compiled, and presented in Table 1. As given in Table 1, there are six construction types: masonry, wooden skeleton, reinforced concrete skeleton, steel skeleton, prefabricated, and a mixed technique of masonry and wooden skeleton.

TABLE 1 Number of buildings with different construction types according to neighbourhoods

NEIGHBOURHOODS	CONSTRUCTION TYPES					
	MASONRY	WOODEN SKELETON	RC SKELETON	STEEL SKEL-ETON	MASONRY+WOODEN S.	PREFABRICATED
1 Yedikule	297	76	967	1	15	4
2 Sömbül Efendi	93	7	716	0	1	0
3 Kocamustafapaşa	486	33	1249	0	12	0
4 Silivrikapı	75	2	856	0	0	0
5 Cerrahpaşa	130	9	562	1	6	0
6 Aksaray	420	28	930	0	6	34
7 Haseki Sultan	110	9	715	0	9	1
8 Seyyid Ömer	232	3	1290	0	0	1
9 Şehremini	101	5	1320	0	0	1
10 Mevlanakapı	261	8	944	0	0	0
11 Topkapı	120	12	769	0	1	0
12 Molla Gürani	84	3	1050	0	0	2
13 İskenderpaşa	169	10	968	0	0	0
14 Akşemseddin	82	0	1463	1	0	0
15 Hırka-i Şerif	297	24	1278	0	2	0
16 Karagümrük	136	4	797	1	5	0
17 Derviş Ali	455	30	948	1	11	2
18 Atikali	167	14	731	0	4	0
19 Ali Kuşçu	168	2	801	0	0	1
20 Zeyrek	284	36	846	0	12	1
21 Cibali	369	44	419	0	114	0
22 Yavuz Sultan Selim	378	23	991	0	34	0
23 Balat	796	34	938	0	46	1
24 Ayvansaray	1614	60	1073	3	34	3
Total number	7324	476	22621	8	312	51
Total %	23.8	1.5	73.5	<0.1	1	0.2

Besides the construction type, the information about exterior walls was recorded and compiled. Seven external wall core materials – brick, stone, briquette, aerated concrete, wooden, and two mixed material of brick+wooden and brick+stone – are presented in Table 2.

TABLE 2 Number of buildings with different external wall core material types according to neighbourhoods

NEIGHBOURHOODS	EXTERNAL WALL CORE MATERIAL TYPES						
	BRICK	STONE	BRI-QUETTE	AERATED CONCRETE	WOODEN	BRICK+WOODEN	BRICK+STONE
1 Yedikule	1253	10	6	0	75	14	2
2 Sümbül Efendi	808	1	0	0	8	0	0
3 Kocamustafapaşa	1739	5	4	0	20	11	1
4 Silivrikapı	906	1	24	0	2	0	0
5 Cerrahpaşa	617	11	64	0	11	5	0
6 Aksaray	1192	8	183	1	24	9	1
7 Haseki Sultan	805	6	11	0	5	17	0
8 Seyyid Ömer	1429	3	82	10	1	1	0
9 Şehremini	1311	2	106	1	4	2	1
10 Mevlanakapı	1185	1	22	0	5	0	0
11 Topkapı	884	6	3	0	6	3	0
12 Molla Gürani	1128	2	5	0	3	0	1
13 İskenderpaşa	1101	2	34	0	10	0	0
14 Akşemseddin	1516	0	30	0	0	0	0
15 Hırka-i Şerif	1485	2	89	0	25	0	0
16 Karagümrük	930	2	2	0	4	5	0
17 Derviş Ali	1392	2	8	0	31	13	1
18 Atikali	891	2	2	0	12	8	1
19 Ali Kuşçu	967	3	1	0	1	0	0
20 Zeyrek	1109	13	25	0	23	9	0
21 Cibali	805	5	6	0	52	78	0
22 Yavuz Sultan Selim	1354	9	7	0	29	24	3
23 Balat	1709	22	14	0	27	40	3
24 Ayvansaray	2654	16	26	1	52	38	0
Total number	29170	134	754	13	430	277	14
Total %	94.7	0.4	2.4	<0.1	1.4	0.9	<0.1

Finally, six exterior wall finishing material types – paint and/or plaster, stone or ceramic tiles, glass mosaic (which has the special name BTB in Turkish), wood siding, PVC siding, and glass – are presented in Table 3.

TABLE 3 Number of buildings with different external wall finishing material types according to neighbourhoods

NEIGHBOURHOODS	EXTERNAL WALL FINISHING MATERIAL TYPES					
	PAINT AND/OR PLASTER	STONE / CERAMIC TILES	GLASS MO-SAIC (BTB)	WOODEN SIDING	PVC SIDING	GLASS
1 Yedikule	812	24	421	83	5	15
2 Sümbül Efendi	337	12	458	9	1	0
3 Kocamustafapaşa	983	34	677	61	12	13
4 Silivrikapı	354	19	548	4	5	3
5 Cerrahpaşa	353	26	291	27	4	7

NEIGHBOURHOODS	EXTERNAL WALL FINISHING MATERIAL TYPES					
	PAINT AND/ OR PLASTER	STONE / CERAMIC TILES	GLASS MO- SAIC (BTB)	WOODEN SIDING	PVC SIDING	GLASS
6 Aksaray	811	73	416	42	7	69
7 Haseki Sultan	302	39	456	27	5	15
8 Seyyid Ömer	584	28	886	5	16	7
9 Şehremini	489	50	858	5	9	16
10 Mevlanakapı	694	13	492	12	2	0
11 Topkapı	544	21	295	23	7	12
12 Molla Gürani	369	40	696	5	12	17
13 İskenderpaşa	393	45	680	19	2	8
14 Akşemseddin	385	89	1030	4	7	31
15 Hırka-i Şerif	712	73	753	43	9	11
16 Karagümrük	399	15	260	264	3	2
17 Derviş Ali	828	46	519	41	4	9
18 Atikali	387	14	476	25	6	8
19 Ali Kuşçu	378	103	450	10	1	30
20 Zeyrek	543	100	443	70	5	18
21 Cibali	628	36	140	126	5	11
22 Yavuz Sultan Selim	807	67	489	48	6	9
23 Balat	1340	104	303	56	5	7
24 Ayvansaray	2131	107	411	99	11	28
Total number	15563	1178	12448	1108	149	346
Total %	50.5	3.8	40.4	3.6	0.5	1.1

3.3 CIRCULARITY EVALUATION OF FATİH

Using the circularity evaluation criteria list, the materials related to the external wall determined in the data collection were evaluated in terms of circularity aspects. The qualitative and quantitative evaluations were made by considering the evaluations in the resources used in the compilation of the criteria list and are given in Tables 4 and 5.

TABLE 4 Circularity evaluations of external wall core materials [1]: (Cottafava & Ritzen, 2021); [2]: (Graubner & Reiche, 2001); [3]:(BCIS, 2006); [4]: (Stephan & Athanassiadis, 2018)

CRITERIA		EXTERNAL WALL CORE MATERIAL TYPES						
		BRICK	STONE	BRIQUETTE	AERATED CONCRETE	WOODEN	BRICK + WOODEN	BRICK+ STONE
types of connection (weights) [1]	screw (0.8)					x	x	
	bolt and nut (0.8)							
	nail (0.6)					x	x	
	cement bond (0.1)	x	x	x	x		x	x
types of connection [2]	separable (with equip- ment)					x	x	
		x	x	x	x		x	x
average typical life expect- ancy (years) [3, 4]		75	100	75	62	50	min 50	min 75
wastage coefficient (1= no waste) [4]		1.05	1	1.05	1.05	1.05	1.05	1.05

TABLE 5 Circularity evaluations of external wall finishing materials [1]: (Cottafava & Ritzen, 2021); [2]: (Graubner & Reiche, 2001); [3]:(BCIS, 2006); [4]: (Stephan & Athanassiadis, 2018)

CRITERIA		EXTERNAL WALL FINISHING MATERIAL TYPES					
		PAINT AND/OR PLASTER	STONE / CERAMIC TILES	GLASS MOSAIC (BTB)	WOODEN SIDING	PVC SIDING	GLASS
types of connection (weights) [1]	screw (0.8)		x		x	x	x
	bolt and nut (0.8)						
	nail (0.6)				x		
	cement bond (0.1)	x	x	x			
types of connection [2]	separable (with equipment)		x		x	x	x
		x	x	x			
average typical life expectancy (years) [3, 4]		10	50	40	30	30	40
wastage coefficient (1= no waste) [4]		1.05	1.05	1.03	1.05	1.05	1.03

3.4 MAPPING AND VISUALISATION OF SELECTED NEIGHBOURHOODS

As a result of this numerical data collection, visual maps were prepared for the four neighbourhoods Akşemseddin, Mevlanakapı, Silivrikapı, and Sümbül Efendi to facilitate an understanding of the distribution of material type and visualise information specific to each building. In the maps, external wall finishing materials are expressed with colour codes, and external wall core materials and construction types are expressed with letter codes in Figures 3 to 7.



FIG. 3 Distribution of material type in Akşemseddin



FIG. 4 Distribution of material type in Mevlanakapı

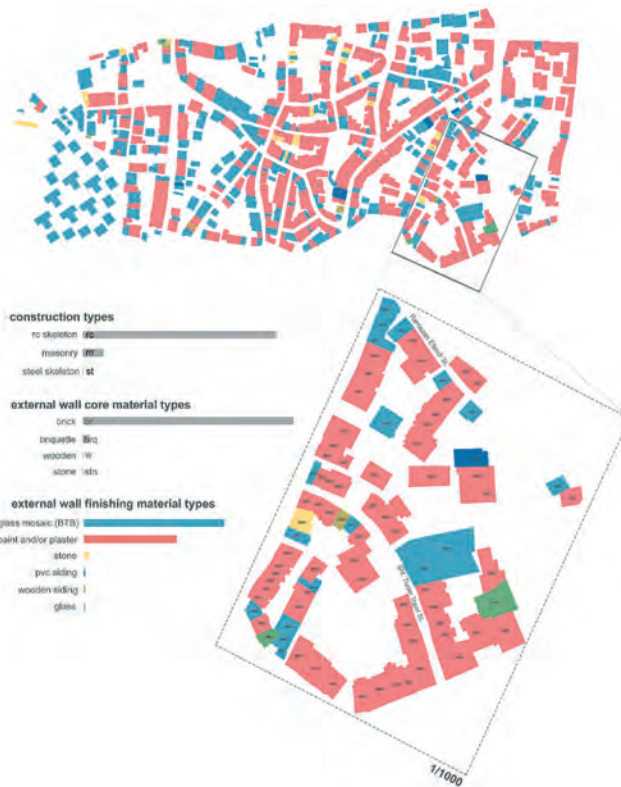


FIG. 5 Distribution of material type in Silivrikapı



FIG. 6 Distribution of material type in Sümbül Efendi

4 RESULTS

4.1 GENERAL DATASET RESULTS:

A total of 30.792 buildings in 24 neighbourhoods were examined. When we look at the results in terms of construction type, the most visible type is reinforced concrete skeleton with 73.5%, followed by masonry with 23.8%, and wooden skeleton with 1.5%. Adobe, steel skeleton and mixed use of masonry + wooden skeleton are at less than 1%.

When we look at the external wall core material type usage ratios, brick is the most used material by far, with 94.7%. Second is briquette with 2.4%, wooden with 1.4%, and brick + wooden with 1%. Stone, aerated concrete, and mixed use of brick + stone were used less than 1%.

Two materials are very close as the external wall finishing material in the buildings examined; paint and/or plaster with 50.5% and glass mosaic (BTB) with 40.4%. Other materials were used at the rates of 3.8% stone/ceramic tiles, 3.6% wooden siding, and 1.1% glass. PVC siding is used less than 1%.

4.2 DATASET RESULTS FOR THE SELECTED NEIGHBOURHOODS

In terms of construction type, in Akşemseddin, 94.6% of buildings have reinforced concrete skeleton construction. In terms of external wall core material, brick was used in almost all buildings with 98%. Finally, the two most used external wall finishing materials are glass mosaic (BTB) with 66.6% and paint and/or plaster with 25%.

Although the use of reinforced concrete skeleton constructions in Mevlanakapı is less than in Akşemseddin, it maintains the first rank with 77.8%. With 21.5%, masonry is another significant construction type. Brick continues to be the most used core material, with 97.7%. In the finishing material, glass mosaic, with 40.6%, is second to paint and/or plaster, with 57.2%.

In Silivrikapı, reinforced concrete skeleton accounts for 91.7% and masonry for 8% in terms of construction type. Brick is the most frequently used wall core material type, with 97.1%. The wall finishing material usage rates are glass mosaic at 58.7%, paint and/or plaster at 37.9% and stone at 2%.

When we look at the construction type of the Sümbül Efendi, 87.6% of the buildings are reinforced concrete skeleton constructions, and 11.4% of the buildings are masonry. As wall core material type, almost all buildings use brick with 98.9%. Wall finishing material usage rates are glass mosaic at 56.1%, paint and/or plaster at 41.2%, and stone at 1.5%.

The comparisons in Table 6 show the relationships between the use of materials in the three building categories per neighbourhood. The first striking aspect is Mevlanakapı, where the use of reinforced concrete skeleton as a construction type is the least, while it is the only neighbourhood where the use of paint and/or plaster for external wall finishing is higher than BTB. Thus, it can be said that masonry leads to the use of paint and/or plaster. On the other hand, in the first two neighbourhoods (Akşemseddin and Silivrikapı), where the use of reinforced concrete skeleton as a construction type is the highest, the use of stone/ceramic tile as a wall finishing material is higher than in other neighbourhoods. This difference can be interpreted such that pre-shaped finishings such as stone/ceramic tile are preferred in reinforced concrete buildings, where the margin of error is considered low (compared to masonry).

TABLE 6 dataların yüzdelik dilimleri for selected neighbours

□	□	Akşemseddin	Mevlanakapı	Silivrikapı	Sümbül-Efendi
		%	%	%	%
construction types	rc-skeleton	94.6	77.8	91.7	87.6
	masonry	5.3	21.5	8	11.4
external-wall-core material types	brick	98	97.7	97.1	98.9
	briquette	2	1.8	2.6	0
	wooden	0	0.4	0.2	1
external-wall-finishing material types	glass-mosaic (BTB)	66.6	40.6	58.7	56.1
	paint-and/or-plaster	25	57.2	37.9	41.2
material types	stone/ceramic-tiles	5.8	1	2	1.5
	wooden-siding /-PVC /-glass	2.6	1.2	1.4	1.2

On the other hand, the use of brick as wall core material is by far the most used material, regardless of the other two building categories. This can be explained by the fact that the use of brick is compatible with many different materials. Finally, when looking at Table 6 in terms of circularity, the rate of use of separable materials is very low; they cannot be fully correlated. For example, although Akşemseddin has the highest use of wooden siding as a wall finishing material, the use of wood as a wall core material is zero. Thus, the material selection is not consistent.

5 CONCLUSION

This study determined and mapped the construction type, exterior wall core, and finishing material datasets in Fatih. External wall core and finishing materials in the Fatih district were evaluated in terms of circularity with a set of criteria compiled by the literature in the context of types of connection, typical average life expectancy, and wastage coefficient. According to these evaluations, brick and briquette, with 97.2%, are the two external wall core materials used the most in the Fatih district. However, when we consider that these two materials are based on “cement bond” and “inseparable” connection types, which are the lowest preferred type of connection in the circularity criteria list, Fatih is not ready for re-use scenarios in possible urban renewal. Although brick and briquette have a long (75 years) typical life expectancy compared to other building materials, this

lifetime is limited to the building's lifetime because they cannot adapt to change. On the other hand, the usage of wood, which has a high circularity rating due to its ability to be disassembled and reassembled, is limited to approximately 1.4%. Considering the four neighbourhoods whose building stock is in poor condition and which are prioritised within the scope of urban renewal, as discussed in detail in this study, it can be seen that they are the same as the results in Fatih – bricks are used between 98-100%.

Secondly, when we look at the external wall finishing materials data, paint and/or plaster (50.5%) and glass mosaic (40.4%) are the most used materials with the inseparable cement bond connection in the district, with a total of 91%. There is a clear difference between the typical life expectancy of these two materials. Glass mosaic has a 40-year lifespan, and paint and/or plaster has a 10-year lifespan, which is much shorter. Although a short lifespan is a negative situation because it requires replacement, it is not necessary to look for disassembly options as the material will consume its life in a shorter time than the building. On the other hand, the usage rates of wood siding, stone/ceramic tile, PVC siding, and glass with separable connections only account for 9% in total. The situation of the four selected neighbourhoods is worse than the district in general, as materials with inseparable connections are used at a rate of up to 97%. Although wall finishing material data is more positive in terms of circularity than wall core material, it is not considered sufficient for Fatih's high renewal process.

In conclusion, within the framework of this study, the answer to the research question "What are the building material types and re-use potentials to be obtained from the urban renewal process in Fatih?" is that the majority of the current material stock cannot participate in the usage circle after the transformation will take place. A solution must be urgently found by developing circular models for the efficient use of the material stock in Fatih, which is undergoing a social and physical transformation and where this transformation will accelerate in the coming days. Otherwise, unnecessary use of limited resources and non-functional wastes will be encountered.

References

- Arora, M., Raspall, F., Cheah, L., & Silva, A. (2020). Buildings and the circular economy: Estimating urban mining, recovery and re-use potential of building components. *Resources, Conservation and Recycling*, 154(December 2019), 104581. <https://doi.org/10.1016/j.resconrec.2019.104581>
- Building As Material Banks (BAMB) (2016), D1 Synthesis of the State-Of-The-Art: Key Barriers and Opportunities for Materials Passports and Reversible Building Design in the Current System, available at: http://www.bamb2020.eu/wp-content/uploads/2016/03/D1_Synthesis-report-on-State-of-the-art_20161129_FINAL.pdf (30 July 2022).
- BCIS (2006). *Life Expectancy of Building Components: Surveyor's Experiences of Building in Use A Practical Guide*. Connelly-Manton (Printing) Ltd., London.
- Cottafava, D., & Ritzén, M. (2021). Circularity indicator for residential buildings: Addressing the gap between embodied impacts and design aspects. *Resources, Conservation and Recycling*, 164(July 2020), 105120. <https://doi.org/10.1016/j.resconrec.2020.105120>
- Ellen MacArthur Foundation, 2015. *Growth Within: A Circular Economy Vision for a Competitive Europe*. Retrieved from <https://emf.thirdlight.com/link/8izw1qhm14ga-404tsz/@/preview/1?o> (accessed 30 July 2022).
- Graubner C. A. & Reiche, K. (2001). Sustainable development in the building industry: an analysis and assessment tool for design of disassembly. *Environmentally Conscious Manufacturing*, Vol. 4193, 372-381. doi: 10.1117/12.417283.
- McGinley, T. (2018). Towards an agile circular economy for the building industry. *Unmaking Waste in Production and Consumption: Towards The Circular Economy*, October, 281-294. <https://doi.org/10.1108/978-1-78714-619-820181022>
- Munaro, M. R., & Tavares, S. F. (2021). Materials passport's review: challenges and opportunities toward a circular economy building sector. *Built Environment Project and Asset Management*, 11(4), 767-782. <https://doi.org/10.1108/BEPAM-02-2020-0027>.
- Stephan, A. & Athanassiadis, A. (2018). Towards a more circular construction sector: Estimating and spatialising current and future non-structural material replacement flows to maintain urban building stocks. *Resources, Conservation and Recycling*, Vol. 129, 248-262. <https://doi.org/10.1016/j.resconrec.2017.09.022>
- Url-1 <https://kentrehberi.fatih.bel.tr/webgis/>

Retrospective Façade LCA: Lessons Learned from a Newly Completed Case Study

Montemayor Javier¹, Li Florence², McGilveray Hugh³

- 1* Façade engineer at Eckersley O'Callaghan, 236 Gray's Inn Road WC1X 8HB, London, +44 20 7354 5402, javier@eocengineers.com
- 2 Senior façade engineer at Eckersley O'Callaghan, 236 Gray's Inn Road WC1X 8HB, London, +44 20 7354 5402, florence@eocengineers.com
- 3 Associate Director at Eckersley O'Callaghan, 236 Gray's Inn Road WC1X 8HB, London, +44 20 7354 5402, hugh@eocengineers.com

Abstract

This paper presents the case study of a façade-focused whole life cycle assessment for a recently completed unitised façade with glass fibre-reinforced concrete rainscreen over a reference period of 60 years. The project, which recently reached practical completion, provides a defined context for the calculations and possible end-of-life scenarios. In the first instance, we carried out an in-depth embodied carbon calculation of the built façade and identified areas where the industry lacks data to improve our knowledge and calculation methods as a practice and as an industry. Based on the Operation and Maintenance Manual (O&M) laid out by the principal contractor and general feedback from the industry, we were able to identify likely replacement and re-life scenarios, which allowed us to carry out a sensible façade-focused Whole Life Cycle Assessment (WLCA). Finally, a comparison was carried out with the original façade with a site-installed, hand-laid brick on a Steel Frame System (SFS) backing wall with precast lintels. This allowed us to compare both façade systems from an embodied carbon perspective and review our original decision-making process in a new light. This speculative whole life carbon assessment stresses the importance of promoting design principles such as design for disassembly for adaptability and reuse early in the conception. These principles are key to facilitating inspection, maintenance and, eventually, replacement. Furthermore, if we are to reduce carbon emissions over building life cycles, it is imperative that the industry has more regard for façades and buildings as highly profitable material banks consisting of materials and components for future use. To that end, compiling comprehensive and robust operation and maintenance information and digital twin records for future generations to understand the systems and how they were built and maintained is essential to promoting circularity.

Keywords

Embodied carbon, façade components design life, unitised, GRC, hand-laid brick, precast

1 INTRODUCTION

1.1 BACKGROUND

Buildings and construction are responsible for up to 30% of annual global greenhouse emissions. Within new buildings, the façade is typically responsible for approximately 15-20% of embodied carbon (Knaack, Klein, Bilow, & Auer, 2014). Carbon emissions are incurred in all stages of a building's life cycle and are generally categorised into operational carbon and embodied carbon.

Embodied Carbon (EC) is the term used to describe the greenhouse gas emissions occurring mainly during the non-operational phases of the life cycle of a building. This includes the emissions occurring during the material extraction, component manufacture, transportation, assembly, replacement, deconstruction, and disposal of building elements. Unlike operational carbon, embodied carbon is not currently regulated. However, as the operational carbon emissions of new buildings decrease due to improved fabric performance and cleaner energy supply, the relative importance of embodied carbon is increasing, making it essential that designers study ways to reduce the embodied carbon emissions of new buildings.

Minimising the embodied carbon of buildings is challenging, and the possible strategies for achieving such reduction vary depending on the systems being considered; however, they can generally be categorised as follows:

- use of low-carbon materials
- use durable materials
- material minimisation and material reduction strategies
- material reuse and recycling strategies
- local sourcing and transport reduction

The life cycle boundaries/stages are the different stages of a product's life and the processes included in an assessment during each stage in accordance with EN 15978. Stages are the Product Stage [A1-A3], Construction Process Stage [A4-A5], Use Stage [B1-B7], End of Life Stage [C1-C4], and additionally Beyond Project Life Cycle Stage [D] as per the diagram below:

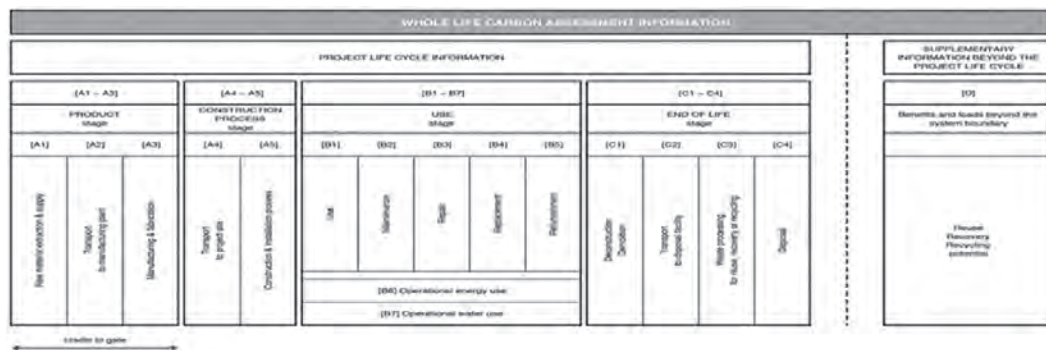


FIG. 1 Modular information for the assessment in accordance with EN 15978

Reference to these modules is made throughout the current paper; as a reminder, each module has the following definition:

A1 – Raw material extraction & supply
A2 – Transport to manufacturing plant
A3 – Manufacturing
A4 – Transport to project site
A5 – Construction & installation process

C1 – Deconstruction / demolition
C2 – Transport to disposal facility
C3 – Waste processing to reuse, recycle
C4 – Disposal

B1 – Use
B2 – Maintenance
B3 – Repair
B4 – Replacement
B5 – Refurbishment
B6 – Operational energy use
B7 – Operational water use
D – Reuse, recovery, recycling potential

1.2 SCOPE OF RESEARCH

EOC was invited to join the design team for a commercial building in Central London in 2017. It was originally designed to respond to its urban context as a hand-laid brick façade with precast lintels and punch windows, a façade system typical of the city. At the time of design, the concept of embodied carbon was relatively new in the industry. The tools for measuring embodied carbon, particularly for façade elements, were not yet established. Whilst the project set out to achieve ambitious sustainability accreditation (BREEAM, LEED, etc.), the focus was primarily on ensuring efficiencies in the operational carbon. Owing to the tight site constraints and ambitious programme, the façade approach took a turn and was ultimately constructed as a lightweight GRC (Glass Fibre Reinforced Concrete) rainscreen on a unitised curtain wall. The main redesign activity was to ensure the unitised façade would perform similarly to the original design. Coordination with the energy model was carried out to ensure there were no significant operational carbon differentiators between the finally engineered systems.

Reflecting on this five-year-long journey, we decided to question our design decisions under a new “sustainability” lens. The aim of the research is, therefore, two-fold.

The project, which recently reached practical completion, provides a defined context and design that gives the calculations and possible scenarios a more grounded foundation. Therefore in the first instance, we carried out an in-depth embodied carbon calculation of the built façade and identified areas where the industry lacks data to complete the life cycle of carbon to improve our knowledge and calculation methods as a practice and as an industry. Based on the Operation and Maintenance Manual (O&M) laid out by the principal contractor and general feedback from the industry, we were able to identify likely replacement and re-life scenarios, which allowed us to carry out a sensible façade-focused Whole Life Cycle Assessment (WLCA).

Finally, and in addition to the embodied carbon figures for the built façade option (off-site manufactured brick-faced unitised system), a comparison was also carried out with the original façade design of a site-installed, hand-laid brick on a Steel Frame System (SFS) backing wall with precast lintels. This allowed us to compare both façade systems from an embodied carbon perspective and review our original decision-making process in a new light.

2 METHODOLOGY

2.1 PROCESS

The methods used to conduct the current calculation are derived from industry guidance, namely the RICS guide (Sturgis, 2017) and the IStructE documents (Gibbons & Orr, 2020). This was done in advance of the upcoming CWCT guidance on embodied carbon, which was in its early stages of development at the time of writing. To get the most accurate representation of the façade EC for the A1-A5 modules, we collected all the information available from the contractors, system suppliers, and parties involved during procurement for A1-A5 modules and construction to inform our EC calculations. Construction costs (relevant for module A5 as explained later), Gross Internal Area (GIA) figures to translate into a comparable metric, total façade areas, product facilities locations, waste facilities, and other parameters were used to form the basis of our study using a custom tool developed by EOC.

An embodied carbon study has been performed to evaluate the emissions associated with all the typical façade systems which are part of the recently completed project. The study considers the types and quantities of materials present within a typical façade bay of the proposed design for each construction type and the embodied carbon emissions from each material.

The basic principle used to quantify the embodied carbon of materials in the façade bay is:

$$\text{Embodied Carbon} = ((\text{Carbon Coefficient} \times \text{Quantity}) / \text{Area}) \quad [\text{Tab}] (1)$$

The embodied carbon coefficient of a material is reported in CO₂eq·kg/FU, in which the Functional Unit (FU) will vary based on the material and type of data (e.g., kg, m², m³, number of pieces, etc.). The carbon emissions of a material (CO₂eq·kg) are determined by multiplying a material's embodied carbon coefficient or Global Warming Potential GWP by the total material quantity in the required functional unit (FU):

$$(\text{CO}_2 \text{ eq} \cdot \text{kg} / \text{FU}) \times \text{FU quantity} = \text{kgCO}_2 \text{ eq} \quad [\text{Tab}] (2)$$

The embodied carbon values for all materials have been added together and divided by the total area of the façade bay to determine the total embodied carbon of the bay. This is then divided by the GIA, resulting in the unit CO₂eq·kg/m² of GIA, which helps establish the embodied carbon contribution of the façade in relation to its building. Where information was unavailable, default material data has been supplemented in the calculation from the following sources or methods:

- ICE Database V.2.0 and V.3.0
- Specific Environmental Product Declarations (EPD)

2.2 BENCHMARK FAÇADE BAY

Inspired by the old Victorian Warehouse, the typical façade bay is composed of three elements, which serve as the basis of the current study:

- a full-height brick pier
- a concrete scallop and stringer element seemingly bearing on the brickwork
- a double window bay with one opening lite

The built system, the first to be analysed, is the unitised aluminium curtain wall system composed of double-glazing units and side-hung and tilt & turn opening vents. An architectural GRC hook-on rainscreen is installed in front of the spandrel panel, and a brick-faced GRC hook-on rainscreen covers the brick pier area. The internal side has a 3 mm aluminium backing panel, and the interiors are lined to achieve the desired thermal performance.

The second analysed system is a hand-laid brickwork façade supported by a boarded SFS system filled with mineral wool insulation. The brick pier consists of masonry supports at each level to restrain the bricks. The window system is a punch element inside the steel studs, and the concrete elements are precast, specifically in the scallops. The interior is lined in the same way as the unitised system.

The details below show how both systems differ considerably in their composition and logic.

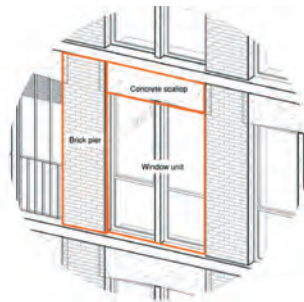


FIG. 2 Typical bay axonometry

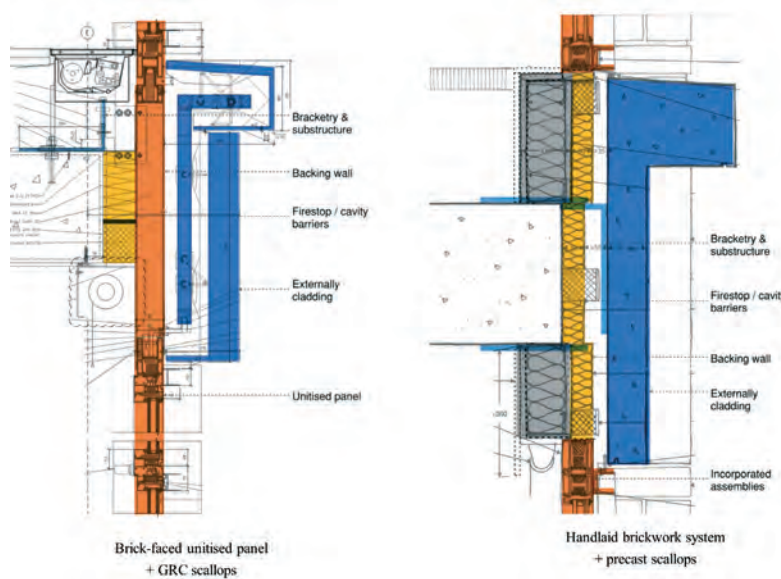


FIG. 3 Components of a typical façade module and the main elements of two systems

Some notes regarding what was excluded from the study:

- slab
- trench heaters
- gaskets and silicone joints
- membranes
- screw fixings
- blind housing and roller blinds

3 RESEARCH

3.1 GENERAL DESIGN CONDITIONS & ASSUMPTIONS

The following two sections focus on each façade system and break down the main modules in the whole life cycle of the analysed product. First is the unitised system, of which more information is available as it was actually built, and the contractors and suppliers provided more Environmental Product Declarations (EPDs). The second system is the hand-laid brick system, which is informed by industry EPDs per material and previous project experiences. For both façade systems, the reference service life of the building is assumed to be 60 years for the purpose of this study.

3.2 AS-BUILT UNITISED CURTAIN WALL

3.2.1 A1-A3 modules assumptions

Given the completed status of the project, the specific Environmental Product Declarations for the unitised system were provided by the specialist trade contractor with the help of their metallic extrusion supplier. The EPDs included all components (aluminium, thermal breaks, gaskets, dead load brackets, glazing, sealant) except for any rainscreen elements in front of the system and associated subframe and bracketry. The latter was incorporated with information from either the specific project supplier or the general material EPD. The breakdown of quantities on the rainscreen was provided by the façade trade contractor. The most relevant embodied carbon coefficients used are the following, omitting the unitised system provided by the contractor:

TABLE 1 EC coefficients

MATERIAL	EC COEFFICIENT [KGCO ₂ EQ/FU]	NOTES
Glass fibre reinforced concrete (GRC)	0.86 / kg	Industry EPD, European manufacturing
Aluminium subframe	6.83 / kg	Industry EPD, European manufacturing
Aluminium sheets	7.47 / kg	Industry EPD, European manufacturing
Stainless steel brackets*	4.41 / kg	Industry EPD, European manufacturing
Facing brickwork	0.21 / kg	Manufacturer EPD
Mortar**	0.14 / kg	Derived from Brick's EPD
Mineral wool (60 kg/m ³)***	2.22 / kg	Manufacturer EPD
Mineral wool (140 kg/m ³)***	5.34 / kg	Manufacturer EPD
Glass****	70 / m ²	Contractor EPD
EPDM****	4.79 / m ²	Contractor EPD
Silicone****	7.08 / kg	Contractor EPD

*Galvanised steel elements were quantified with an embodied carbon coefficient equivalent to that of stainless steel. The additional 0.12 kg CO₂ eq/kg that represents galvanising 1 m² of a steel plate is included in the stainless-steel figure.

**Mortar is considered as proportions of their brick elements.

***Mineral wool of 60 kg/m³ (cladding roll) is considered for all the infill panels and spandrel areas. Mineral wool of 140 kg/m³ is considered for any external grade insulation.

****These components of the unitised façade system were already included in the as-built EPD accounting for the majority of the components within the system; the values shown are just shown for reference, and they are based on industry EPDs.

Mention should be made of the façade being a factory-assembled system. There is currently no distinction in industry guidance between site-assembled façades and off-site manufacture. In this case, transportation of all parts to the system assembler or the A2 module has a low contribution as everything was nationally sourced, including bricks, glass fibre-reinforced concrete cladding, and

frames. Regarding waste occurring during the manufacturing or A3, the project-specific unitised panel EPD accounts for scraps within the factory processes, except for packaging due to its low contribution, as stated in the referenced document (Skonto Plan Ltd SIA, 2019). Furthermore, to account for the wastage driven by the cutting of brickwork into brick slips, an additional 33% of the total volume was included. For carbon emissions due to the actual assembly in the factory, it is accepted that the unitised system EPD does include such contribution.

3.2.2 A4 module assumptions

Based on the documentation of the as-built façade panels provided in the contractor's EPD, all unitised systems have a travelling distance of 2400 km. This is understood to be cumulative between the assembly plant in Latvia and the construction site in London via road transport. Carbon emissions are not included for the glass fibre-reinforced concrete elements installed onto the unitised panels, as the glass fibre-reinforced concrete was preinstalled in the factory and therefore captured in the A2 module. The map below illustrates the flow of materials until the construction site is reached, based on the provided distance from the contractor.



FIG. 4 Main stages of the A modules per available documentation

3.2.3 A5 module assumptions

The construction phase heavily relies on real-time documentation of the resources employed during installation in the form of fuel and energy. Due to the nature of the façade system, it is implied the A5 module is less intensive than a site-assembled system: the system arrives as a panel, is lifted and set with a crane, which is powered from a green tariff energy grid. Complementing this with the construction complexity, a factor of 350 kg CO₂e/ £100,000 of construction is considered, based on the Royal Institution of Chartered Surveyors (RICS) guidance. Such guidance also proposes a 1400 kg CO₂e/ £100,000 factor for the whole building, with the main structure accounting for 40% of this. The façade, in this case, represents 25% of the whole building proportion.

The other component of the A5 module addresses the emissions due to material waste produced during construction. For the unitised solution, the preassembly process avoids most of the usual material cut-off occurring on site. From communication with the design team, the substructures used to transport the panels were brought back to the assembly factory to be reused. Therefore, this contribution was not accounted for.

3.2.4 B1-B3 assumptions

From Modules B and onwards, the embodied carbon calculations become more speculative. As designers, we rarely receive feedback on the operation of the building. Based on our understanding of the built solution and previous experience, we endeavoured to define likely scenarios using the Operation and Maintenance Manual (O&M) that the principal contractor compiled.

The embodied carbon content from a façade perspective is considered negligible for these modules. The reasons that compelled us to make this assumption at this stage are the following:

- Module B1(Use) is negligible for this project as the façade is not motorised except for five automated main entrance doors and pass doors. Therefore the electricity or power needed to operate the façade is very small.
- Module B2 (Maintenance): very few metrics are available to quantify the carbon spent describing a maintenance scenario. The main activity we anticipate is the bi-annual glass cleaning which will be carried out via rope access at a high level and a pole cleaning strategy from the ground and terraces. We envisioned that the carbon emissions from this activity would be negligible.
- Module B3 (Repair): there is no research, information or metric describing a repair scenario. During Stage 4, the design team envisioned that the replacement of the glass, which is widely considered as the most likely large façade item to require replacement, would take place from the inside as the unitised system is designed to be internally beaded, using the goods lift. This supports our assumption that the contribution of this module can be neglected.

3.2.5 B4 module assumptions

B4 module, or replacement, is the most relevant module at this stage, as it dictates which elements would need to be replaced during the building's lifetime. Façade elements are basically divided into primary and secondary components, the latter being elements that need a replacement due to a material that will deteriorate or no longer function as intended. One of the biggest challenges brought on by the switch to the unitised façade system has been reconciling the expected service life of this lightweight façade with the overall design life of the building. During the design process, primary and secondary components were identified within this new system to tease out a possible way of inspecting and replacing "weaker" components in the façade system without the need for a disproportionate whole-scale replacement of the façade.

As stated in the general assumptions, gaskets, sealants, and membranes were not considered as their impact on the overall embodied carbon figure is negligible. However, these elements are critical to the water and airtightness of the façade system and therefore are considered primary components. Since these elements have a shorter life span, they are responsible for the design life of the overall façade system being shorter than the reference period of 60 years. With a curtain wall system, due to the interlocking nature of the construction, failure of gaskets may lead to a whole-scale dismantling of aluminium frames in relatively good condition and, subsequently, significant embodied carbon cost. It is commonly recognised by the industry that gaskets have a service life of approximately 30 years. It is, therefore, reasonable to assume the same for the curtain wall system.

Considering the façade articulation, one high-level, whole-scale replacement strategy at year 30 could consist of a full deconstruction of the unitised façade at year 30; assuming only the gaskets and insulated glazing need to be replaced, it could then be conjectured that the units would be removed and stored off-site for inspection, glass replacement and replacement of hardware and ironmongery before being reinstalled on-site with new gaskets and fire stopping. The glass fibre-reinforced components and the subframe, including the brick-facing elements in the unitised

system, would only undergo a cleaning regime. We have therefore assumed in our calculations that all the glazed unitised panels would be replaced whilst the opaque panels would only be refurbished. Additionally, to consider the demolition and refurbishment activities, we have accounted for two additional A5 modules.

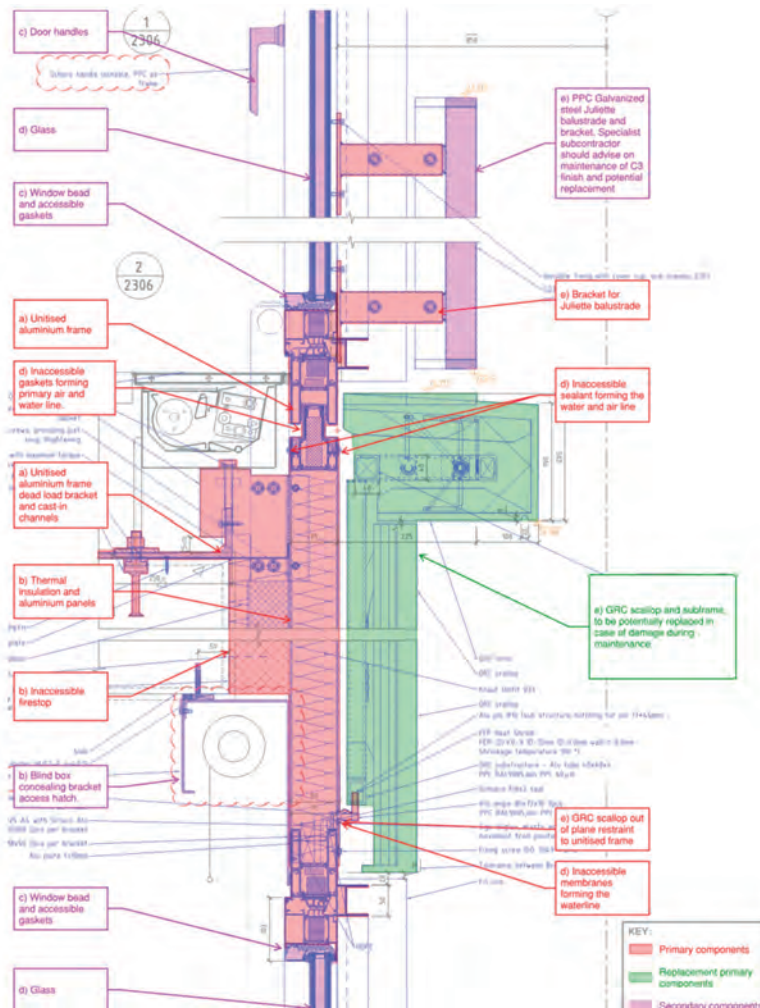


FIG. 5 Primary and secondary components

It should be noted that this scenario relies entirely on the appropriate maintenance and upkeep of the façade by the landlord and the ability to effectively remove and refurbish the façade.

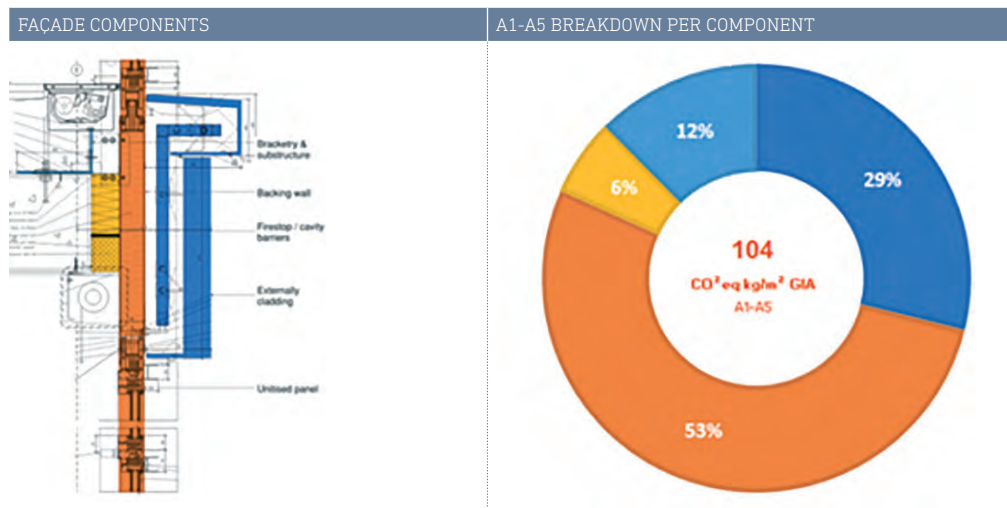
3.2.6 B5-B7 module assumptions

As stated in the assumptions section, the B5 module is not part of the project as no product has been declared as part of a refurbishment plan where a new use for the component is given. Additionally, the B6 & B7 modules do not apply in this study as they refer to operational carbon stages. The monitoring agents of the building should provide figures on how the façade/building generates these carbon emissions.

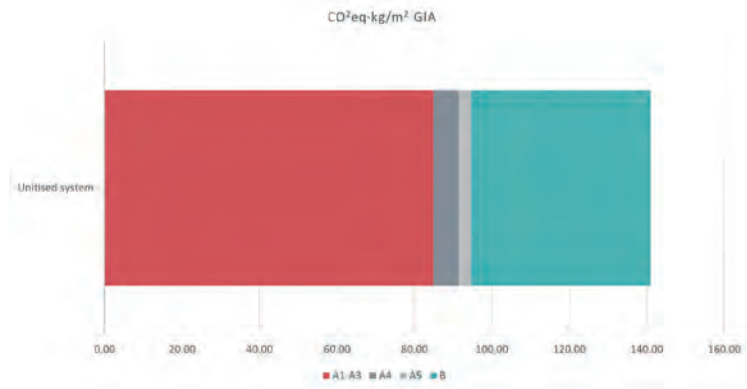
3.2.7 A-B results

The first pie chart outlines the results of the EC calculation for the typical bay for A1-A5 modules. The carbon emissions have been separated into five categories of façade components (external cladding, unitised system or frames, infill panel, firestops and barriers, and others like bracketry). The second chart showcases the contribution per module, taking the façade components as a whole to focus on each module's emissions.

TABLE 2 A-B module breakdown for unitised system



A-B breakdown per module



3.2.8 C-D module assumptions

The C and D modules are the least documented of the whole life cycle and are largely based on potential speculative scenarios based on the façade materials and current state of the art. The following assumptions have been made:

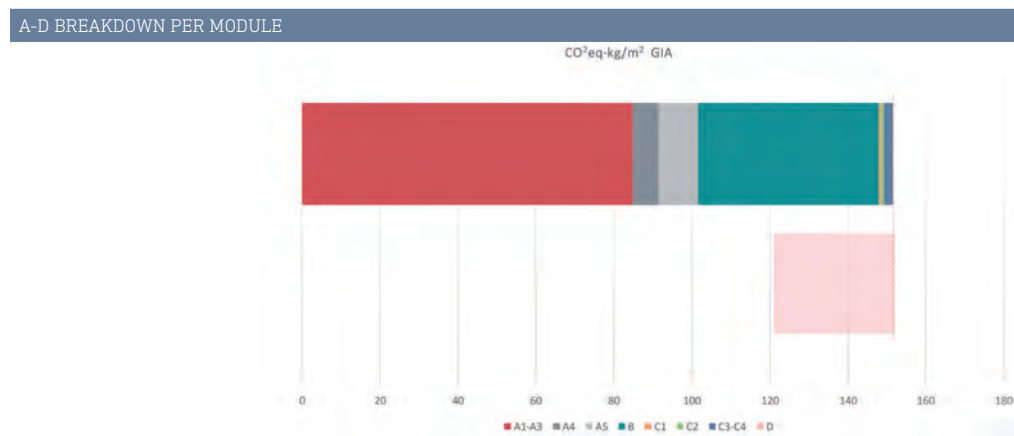
- Investment in a deconstruction scenario for the C1 module would need to be done if the reuse & recycle of materials is to happen. In this sense, the relevant façade materials would be recovered: aluminium frames and substructures, as well as glass panes. Glass fibre-reinforced concrete and bricks could also be disassembled, but their re-life potential is reduced to a downcycle or crushing as

aggregate. Data on carbon emissions for selective deconstruction is unavailable, but a factor of 3.4 kg eq CO₂ / m² GIA (Sturgis, 2017) per the RICS guide was used.

- The C2 module addresses transportation to the recycling facility or the landfill site, which would normally represent local entities. The emissions due to these transportations are low but quantifiable based on a 300 km radius.
- The C3 module refers to the treatment of products prior to reaching the end-of-waste state; any re-looping is included here. Manufacturers provide little information and the industry is still giving generic values per material. The available information was input per the consulted EPDs, or factors based on the mentioned EC guides were used.
- The C4 module would be avoided –emissions due to waste treatment – as no material from the façade system is intended to go untreated.
- Finally, the D module is assumed to develop as follows:
 - Aluminium frames, substructure and sheets: high recycling potential into billets for new products
 - Glass panes: even if there is currently an increasing recycling potential of glass, the construction industry is still progressing on a proper re-loop. No recycling scenario is assumed.
 - Mineral wool insulation: high recycling potential in new insulation products
 - Concrete precast elements (including glass fibre-reinforced concrete and architectural precast): low recycling potential, mostly downcycled to aggregate. Even if the concrete elements are supposed to have a life span of 60 years, reuse is unlikely to happen as shape compatibility with a future use would have to be assured. Metal subframes or reinforcements could be reused.
 - Brick with cement mortar: low recycling potential, mostly downcycled to aggregate

3.2.9 A-D results

TABLE 3 A-D module breakdown for unitised system



In the same way the contribution per module was shown in the previous results section, the whole life cycle is represented here in a chart where the A-C modules are quantified and added together to be then complemented with the potential subtraction of the D module, which accounts for the benefits beyond the system boundary constrained to the current project. This calculation is largely based on assumptions and potential scenarios for every material included in the façade. The intention is to use the end-of-life scenarios representing the most common practices in the market nowadays.

3.3 HAND-LAID BRICKWORK FAÇADE SYSTEM

3.3.1 A module assumptions

An alternative to the built façade was analysed to use as a benchmark, corresponding to a hand-laid brick and precast façade system that would be the most common system used in the London context. The methodology used was the same as the first analysis but based on the drawings and details developed by the design team up to RIBA Stage 4. With such material quantification and industry-wide EPDs, the A1-A3 modules were completed. The rest of the modules are based on assumptions from previous experience.

One of the main differences between the unitised and the hand-laid brick is their method of assembly, the first taking place mostly off-site and the second almost entirely on-site. This would represent meaningful differences in modules A3 & A5. Preassembled façades have their major waste production during the manufacturing/assembly of the panels (A3), while on-site assembled façades would have more wastage during the actual installation module (A5). For this module, the waste rates available in the WRAP Guide (Sturgis, 2017) were used, as shown below.

TABLE 4 Waste rate coefficients

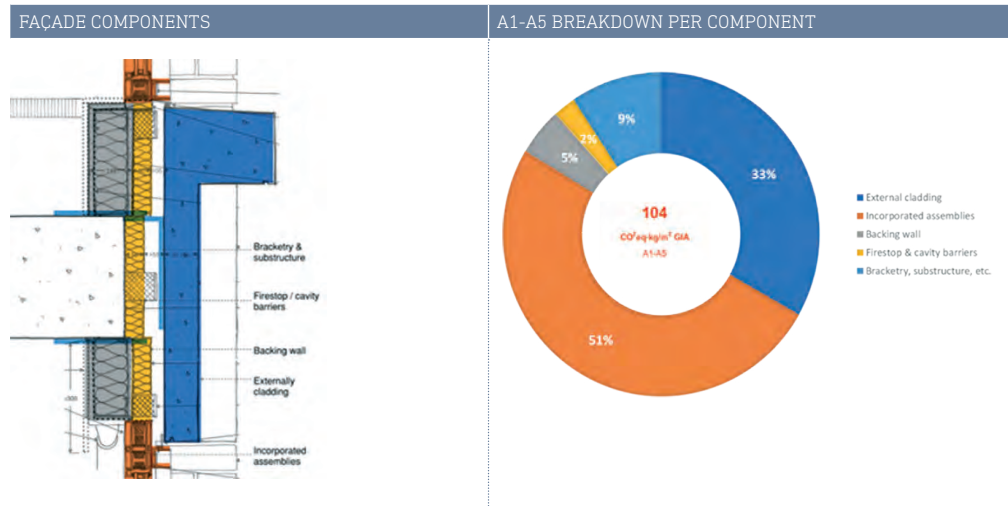
MATERIAL	WASTE RATE (SITE)	NOTES
Concrete in situ	15%	WRAP guide, table 3
Mortar	5%	WRAP guide, table 3
Precast concrete	1%	WRAP guide, table 3
Steel reinforcement	5%	WRAP guide, table 3
Steel frames	1%	WRAP guide, table 3
Brick	20%	WRAP guide, table 3
Aluminium frames	1%	WRAP guide, table 3
Glass	5%	WRAP guide, table 3
Plasterboard	22.5%	WRAP guide, table 3
Mineral wool	10%	WRAP guide, table 3

The A4 module would behave differently, as most of the materials and products would be sourced nationally or even locally, with an approximate distance of 300 km per the RICS guide. The main difference here is that it is not a whole system, but separate products shipped to the site and assembled, where the waste and labour would occur (not in the factory or A3 module, as for the unitised system), resulting in a larger carbon contribution due to waste on site. For the A5 complement on construction activities, the total façade price is assumed to be the same for both design options due to counterbalancing factors. It is expected that the unitised system would be more expensive compared to a hand-laid brick system in terms of installing specialised equipment, and the hand-laid system would be more expensive due to extensive labour hours on-site. This is, however, largely qualitative, and numbers provided by contractors are necessary to inform this stage of the cycle.

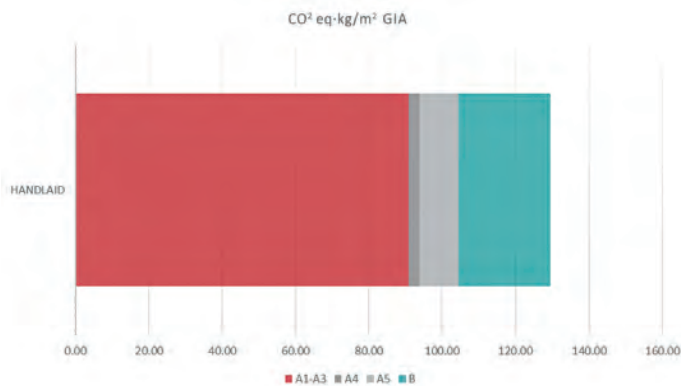
3.3.3 A-B results

Results per façade component for the A modules are shown below, with the referring components colour coded to the left on the markup detail. A breakdown per module is also provided. The comparison of the unitised system and the hand-laid proposal can be found in Section 3.4.

TABLE 5 A-B module breakdown for hand-laid system



A-B breakdown per module



3.3.4 C-D module assumption

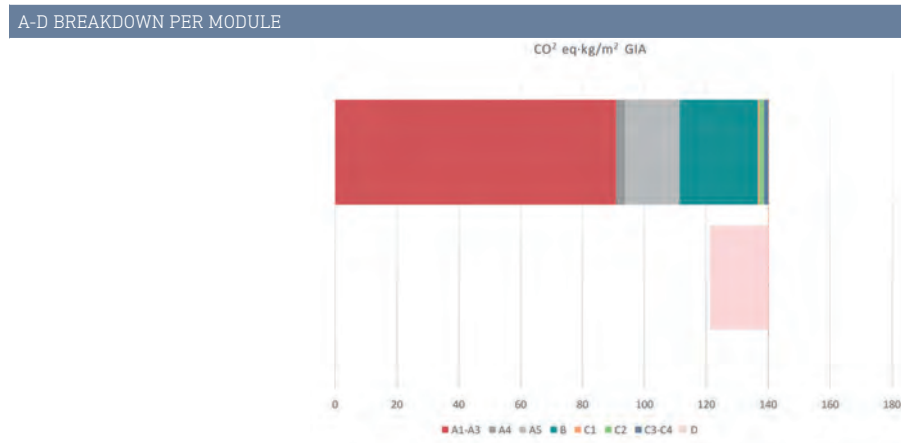
The C-D module assumptions are similar for both façade systems, the hand-laid and unitised, and only potential scenarios on the loops of the materials can be made. It is assumed that the design would facilitate a recovery of products and materials, allowing at least a recycling scenario. Figures on these modules were roughly calculated with the available data from the market; the potential destinations for the relevant materials can be consulted in section 3.2.8. The same re-life scenarios as in the unitised façade system are assumed.

3.3.5 A-D results

By adding the C-D modules to the quantification, the whole life cycle is completed. As explained in previous sections, the benefits beyond the system boundary portrayed in module D show a possible

scenario after the end of life of the façade when the relevant elements are recycled or reused. In this case, the major contribution to the D module is the recycling potential of the metallic elements.

TABLE 6 A-D module breakdown for hand-laid system



3.4 INTERPRETATION OF RESULTS

TABLE 7 Comparison between façade systems

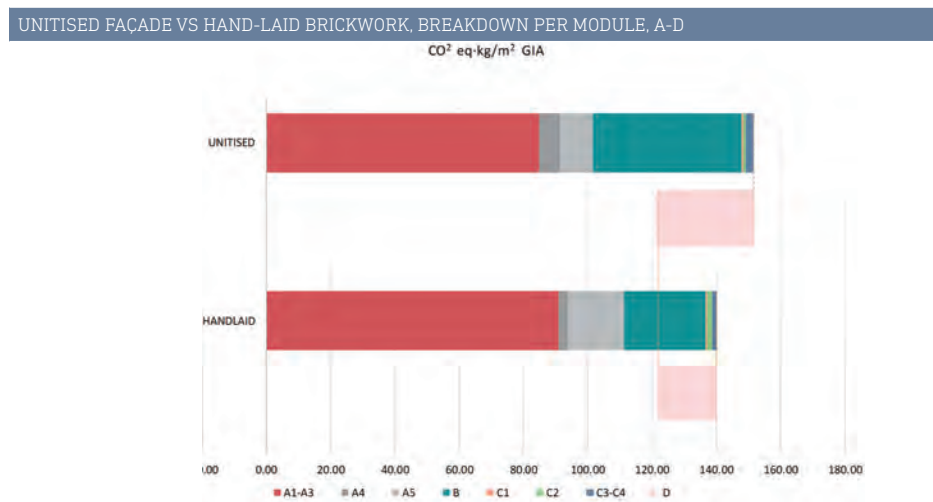


TABLE 8 Embodied carbon breakdown per module in CO₂ eq kg / m²GIA

FAÇADE SYSTEM	A1-A3	A4	A5	B	C1	C2	C3-C4	D	"TOTAL"
Unitised system	94	7	10	47	1	1	2	-36	118
Hand-laid	91	3	18	25	1	2	1	-18	114

When comparing the embodied carbon results for both façade systems, we can make the following observation:

- 1 The upfront embodied carbon cost of the unitised façade is slightly higher than the hand-laid brickwork solution. This appears to be due to the higher embodied carbon coefficients

of the galvanised subframe, which supports the glass fibre-reinforced concrete and the aluminium backing wall.

- 2 Whilst both façades have very different modes of construction and travel distance profiles, we found that the carbon contribution during the construction modules was relatively similar. The rest of the assumptions on how a unitised system is faster to assemble on-site, requires less labour and time, and produces less waste on-site, translate to an amelioration of the EC figure compared to the hand-laid system.
- 3 Considering the shorter service life of the unitised system, the contribution of the unitised. This is in part due to the higher embodied carbon coefficient of aluminium itself but also due to the shorter design life of the unitised system, which leads to the higher cost incurred due to the necessity of deconstructing, replacing, and refurbishing the building halfway through the service life of the building.
- 4 The benefits beyond the system boundary highlight the importance of significant re-life scenarios. In this case, given the predominance of metallic components in the unitised system, a D module with high metallic recycling would lead to a major decrease in carbon emissions, one that would even result in similar carbon emissions compared to the hand-laid system option. However, as stated before, the benefits are just illustrative and should not be subtracted from the overall calculated carbon emissions.

4 CONCLUSIONS AND LESSONS LEARNED

This case study showed that the global warming potential of the lightweight unitised façade system is higher than the more traditional hand-laid brickwork system for this specific project. There were, however, several other key design drivers that led to the selection of the unitised façade for this project, including but not limited to buildability, quality control, programme, health and safety, etc. For instance, considering the project-specific site constraints, hand-laid brickwork with precast would have led to logistical and construction challenges (complex scaffolding adaptations and crane coordination, site storage capacity issues, etc.). Additionally, Design for Manufacture and Assembly (DfMA) brought on by the unitised façade generally ensures better quality and control of the façade, as the system is assembled in a controlled environment in the factory. As site activities are kept to a minimum, this is also a safer option. All of these aspects applied to the analysed project, giving way to a unitised solution.

More importantly, this study demonstrates the importance of considering embodied carbon emissions when weighing different façade construction systems and façade materiality. As we have now learned, selecting low embodied carbon materials in the early days of the design is key to reducing the embodied carbon cost of the façade. Had we implemented these steps during the redesign of this business-as-usual unitised façade, the embodied carbon figures could have been improved.

This speculative, façade-focused whole life carbon assessment also stresses the importance of promoting design principles such as design for disassembly, for adaptability and for reuse early in the conception. These principles are key to facilitating inspection, maintenance and, eventually, replacement. Furthermore, if we are to reduce carbon emissions over building life cycles, it is imperative that the industry has more regard for façades and buildings as highly profitable material banks consisting of materials and components for future use. To that end, compiling comprehensive and robust operation and maintenance information and digital twin records for future generations to understand the systems and how they have been built and maintained is essential to promoting circularity.

Lastly, the present research has identified areas of weakness in the façade industry for WLCA. Major production of documentation is needed to fill in the information gaps that could inform the carbon emissions for activities like installation, repair of a façade, maintenance, deconstruction, or reprocessing of components. Efforts from various entities to produce more literature have been identified in hopes of creating a more grounded façade industry.

Acknowledgements

Caroline Haines and Matt Massey (Derwent), Hugh Queenan (Morris+Company), Neethu Roy (SKANSKA), German Stroganov (SKONTO).

References

- Ferry, J. D. (1980). *Viscoelastic properties of polymers*, 3rd Ed. New York: Wiley.
- Gibbons, O. P., & Orr, J. J. (2020). *How to calculate embodied carbon*. London: The Institution of Structural Engineers.
- Knaack, U., Klein, T., Bilow, M., & Auer, T. (2014). *Façades, Principles of construction*. Basel: Birkhäuser Verlag GmbH.
- Kuntsche, J., & Schneider, J. (2014). Experimental and numerical investigation of the mechanical behaviour of explosion resistant glazing. *Proceedings of engineered transparency 2014*, pp. 219-225.
- Skonto Plan Ltd SIA. (2019). *Environmental product Declaration: Featherstone Building*. Skonto Plan Ltd SIA.
- Sturgis, S. (2017). *Whole life carbon assessment for the built environment*. London: Royal Institute of Chartered Surveyors.
- Young, R. F. (2007). *Crossing boundaries in urban ecology: Pathways to sustainable cities* (Doctoral thesis). Retrieved from ProQuest Dissertations Thesis database. (UMI No. 327681). For more information see: <http://www.library.cornell.edu/resrch/citmanage/apa>

Retrofitting Potential of Building Envelopes Based on Semantic Surface Models Derived From Point Clouds



Edina Selimovic¹, **Florian Noichl**¹, **Kasimir Forth**^{*1}, **André Borrman**¹

* Corresponding author, kasimir.forth@tum.de

¹ Technical University Munich, Germany

Abstract

To meet the climate goals of the Paris agreement, the focus on energy efficiency needs to be shifted to increase the retrofitting rate of the existing building stock. Due to the lack of usable information on the existing building stock, reasoning about the retrofitting potential in early design stages is difficult. Therefore, deconstructing and building new is often regarded as the more reliable and economical option. Digital methods are missing or not robust enough to capture and reconstruct digital models of existing buildings efficiently and automatically derive reliable decision-support about whether demolition and new construction or retrofitting of existing buildings is more suitable. This paper proposes a robust, automated method for calculating existing buildings' life cycle assessments (LCA) using point clouds as input data. The main focus lies in bridging the gap between point clouds and importing semantic 3D models for LCA calculation. Therefore, the automation steps include a geometric transformation from point cloud to 3D surface model, followed by a semantic classification of the surfaces to thermal layers and their materials by assuming the surface elements by building age class.

Keywords

retrofitting potential, LCA, point cloud, semantic enrichment

DOI [10.47982/jfde.2022.powerskin.20](https://doi.org/10.47982/jfde.2022.powerskin.20)

POWERSKIN CONFERENCE

HOSTED BY



FUNDED BY

